Transport thermoélectrique dépendant du temps dans des systèmes quantiques

Adel Kara Slimane

université PARIS-SACLAY

Time-dependent Thermoelectric Transport in Quantum Systems

Transport thermoélectrique dépendant du temps dans des systèmes quantiques

Thèse de doctorat de l'Université Paris-Saclay

École doctorale n° 564, Physique en Île-de-France (EDPIF)
Spécialité de doctorat: Physique

Unité de recherche: Université Paris-Saclay, CEA, CNRS,
Service de physique de l'état condensé (SPEC),
91191, Gif-sur-Yvette, France
Référent: Faculté des sciences d'Orsay

Thèse présentée et soutenue à Paris-Saclay
le 3 décembre 2021, par

Adel KARA SLIMANE

Composition du jury:

Dietmar WEINMANN Directeur de recherche CNRS, Université de Strasbourg	Président
Giuliano BENENTI Professeur associé, Università degli Studi dell'Insubria	Rapporteur & Examinateur
Fabienne MICHELINI Maître de Conférences, HDR, Université Aix-Marseille	Rapportrice & Examinatrice
Anne ANTHORE Professeure, Université de Paris	Examinatrice

Direction de la thèse:

Geneviève FLEURY Chercheur CEA, CEA Saclay	Directrice de thèse
Alexander SMOGUNOV Directeur de recherche CEA, CEA Saclay	Codirecteur de thèse

Membre invité:

Xavier WAINTAL Directeur de recherche CEA, CEA Grenoble	Invité

Thèse de doctorat
NNT: 2021UPASP117

Contents

1. Introduction and summary

This past century has seen the very quick rise to the prominent issue of global warming (see Fig. 1.1a). At its root is the ever growing need for "work" energy in our activities (see Fig. 1.1b), this pressures research into making energy production facilities more efficient while at the same time reducing the ecological footprint of the processes. A fundamental law of physics is conservation of energy: it merely gets transformed from one form to another ; while the second law of thermodynamics states that "work" energy can only be collected from an out of equilibrium system, such as the natural flow of energy from "hot" to "cold", and bounds how much "work" energy can be collected by the universal Carnot efficiency.

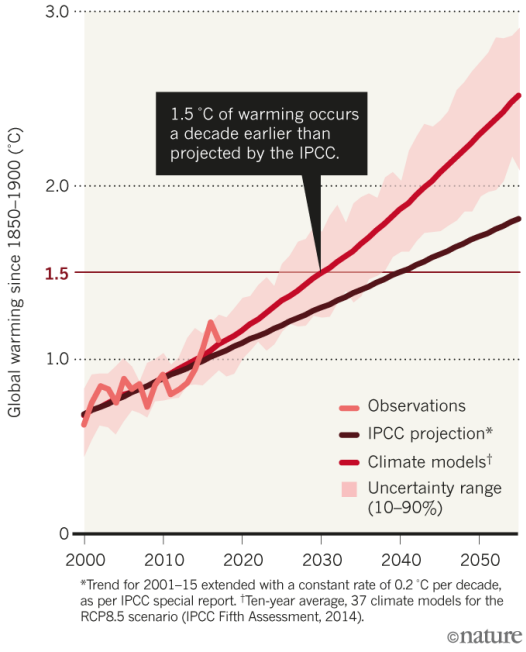

(a) Adapted from [212]: Accelerated warming. "If the planet warms by 2 ℃ — the widely touted temperature limit in the 2015 Paris climate agreement — twice as many people will face water scarcity than if warming is limited to 1.5 ℃. That extra warming will also expose more than 1.5 billion people to deadly heat extremes, and hundreds of millions of individuals to vector-borne diseases such as malaria, among other harms."

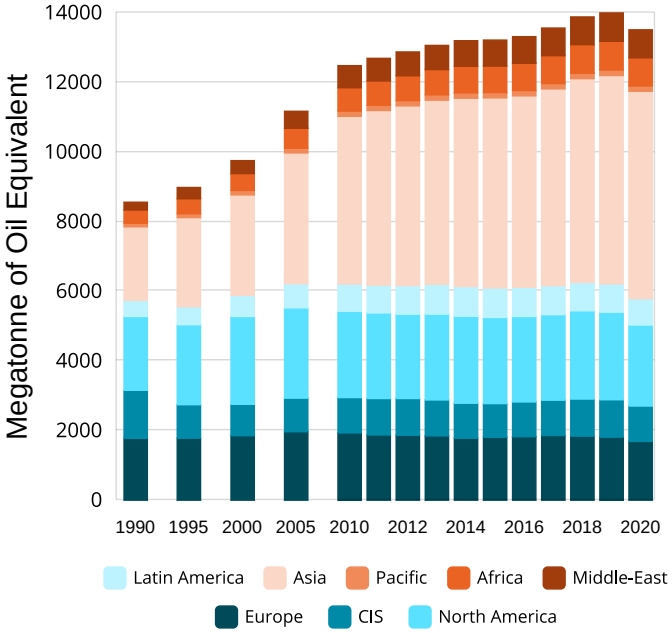

(b) Adapted from [209]. Evolution of energy consumption since 1990. Global energy consumption steadily rose by an average of 2%/year over the 2000-2018 period, a 0.8% slowdown in 2019 and a decline by 4% in 2020 in a context of global pandemic. Consumption increased by more than 50% when compared to 1990.

Figure 1.1. – Accelerated global warming and energy consumption.

Thermoelectricity in this context offers a different way to make or complement heat engines and coolers. Some of the latest research in thermoelectricity is in the mesoscopic field where quantum effects are leveraged such as nano-structuration, band-structure manipulation or defect manipulation. While the vast majority of studies in thermoelectrics have been in the stationary regime, with the well-established Landauer-Buttiker formalism as the main theoretical tool, a new research wave started

investigating time-dependent and far from equilibrium regimes. This joins the ongoing research in building a consistent theory of quantum thermodynamics in all regimes. The field is at its early stages and the published works are mostly theoretical and on simple 'toy' models. Studying more complex systems in the quantum time-dependent regime proves to be analytically difficult and only the simulation road seems to be viable. In particular, `tkwant` [1, 101], the time-dependent extension to `kwant` [2] – the simulation library of reference for quantum transport – has been in the works during the past few years and got recently released. The release of `tkwant` sets an additional milestone in the field of time-dependent quantum transport as it renders possible the investigation of systems previously difficult to tackle. It is however limited to particle transport.

The emerging phenomena in this regime are yet to be fully explored, and some of the already studied phenomena are not well understood: concepts from classical thermodynamics such as 'work' or 'heat' prove difficult to grasp in such regimes, the attempted definitions are still under debate and use different theoretical tools whose equivalence is yet to be outlined. Some recent preliminary theoretical studies [38, 219] even predict an improvement of thermoelectric properties in the transient time-dependent regime. This thesis intervenes in this context with an objective to bring new insights of the role of time-dependent control in mesoscopic quantum thermoelectrics.

We build a gauge-invariant framework for describing energy transport, on top of the current published research on time-dependent particle quantum transport, in an open electronic quantum system under the influence of a time-dependent electromagnetic field. This framework is based on the semi-classical approach where light is described by the (classical) Maxwell equations and electrons are non-interacting and described by the (quantum) Schrödinger equation. We then use this framework to extend `tkwant` to energy transport and further unlock its potential to time-dependent thermoelectric simulation of complex systems, that can model a broad class of mesoscopic devices beyond toy models. We illustrate our numerical approach by investigating briefly the dynamical Peltier effect in a two-dimensional Quantum Point Contact then go back to the extensively studied Resonant Level (toy) Model to be able to grasp a more fundamental understanding of the effects at play : we use our approach, in both its numerical and analytical adaptations, and obtain new insights on the potential of time-dependent thermoelectricity in quantum dots.

1.1. Summary of chapter 3: overview and motivation

In this chapter, we briefly overview the history of thermoelectricity and get to the current developments and challenges in the domain: quantum effects are being investigated and are part of broader early research in building a theory of quantum thermodynamics.

1.1.1. Stationary thermoelectricity

Thermoelectric devices in the stationary regime have been extensively studied in the past seventy years. A characterizing number, called the figure of merit zT, has been introduced to compare the thermoelectric efficiency of different devices and materials, both in the generator and cooler configurations

$$zT = \frac{\sigma S^2}{\kappa_{\mathrm{E}} + \kappa_L} T \tag{1.1}$$

where T is the average absolute working temperature (linear response is assumed for the cold and hot baths), S the Seebeck coefficient, σ the electrical conductivity, κ_{E} and κ_L are respectively the electronic

and lattice thermal conductivities of the material. The expression of the figure of merit highlights the main challenges in creating more performant devices: S, σ and κ are strongly correlated through the material's charge carrier concentration, scattering and band structure [145], and their contributions compete within the figure of merit. The higher the zT, the more performant the device is (see Fig. 1.2):

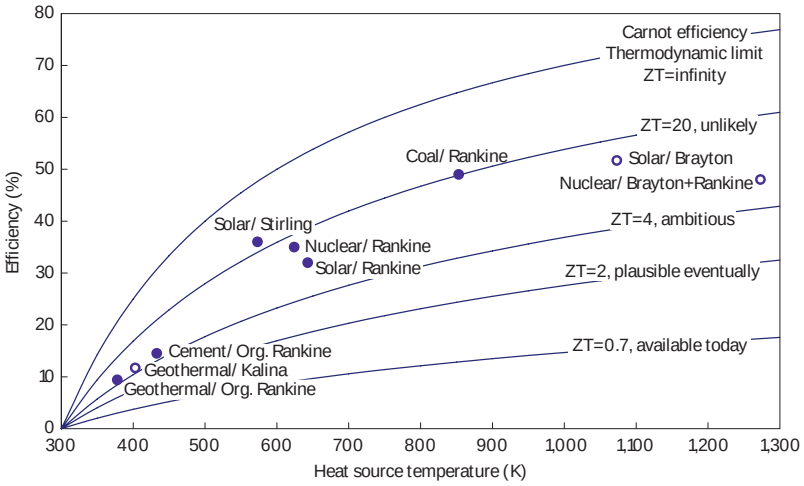

Figure 1.2. – Taken from [197]. Comparing traditional industrial heat engines with thermoelectrics. Current thermoelectrics cannot compete due to their low efficiency, if their figure of merit zT attains ~ 3 they would be a viable alternative for certain applications.

a value of $zT \gtrsim 3$ needs to be reached for thermoelectricity to be broadly used in energy conversion and electricity production [191]. The value of the figure of merit of commercially available thermoelectric generators and coolers is however around $zT \approx 1$ which makes their practical use restricted to niche applications.

1.1.2. Time-dependent mesoscopic thermoelectricity

Near-equilibrium thermoelectricity in the stationary regime is relatively well understood and accurately described by theory [75, 16]. However, the description becomes much more complicated when the system is driven far from equilibrium, with large voltage and temperature biases, or with a dynamical (time-dependent) control. Some of the current endeavors in the field of mesoscopic physics are to iron out thermodynamics in the driven quantum regime: local temperatures and heat current densities can be ill-defined, especially when a 'fast' time-dependent control has to be taken into account. Recent theoretical studies have even reported on an improvement of thermoelectric properties of 'quantum dot' based models [38, 219] (see Fig. 1.3), although the reasons behind this predicted boost, and whether it is realistic, remain unknown. On the other hand, experimentation in high frequency nanoelectronics has made significant progress, which paves the way to future driven (non-adiabatic) thermoelectric experiments.

Theoretical challenges in quantum thermodynamics The theory of thermodynamics aims to describe simply, with a few parameters that are relevant at our scale, systems with a very high number of degrees of freedom. To achieve this simplification, averaging is done over the degrees of freedom, space and time. Thermodynamics revolve around three fundamental laws with regards to the evolution of such a system: *(i)* energy is conserved ; *(ii)* the total entropy of the considered system and its environment can only increase (between two equilibrium configurations); *(iii)* the system cannot reach the absolute zero temperature in a finite-time transformation. The Carnot efficiency $\eta_C = 1 - T_{\mathrm{C}}/T_{\mathrm{H}}$,

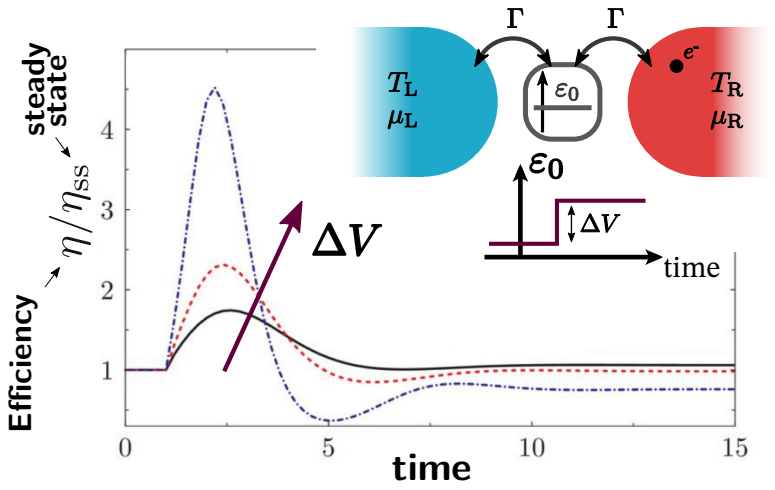

Figure 1.3. – Adapted from [219] "Boosting thermoelectric efficiency using time-dependent control". The Resonant Level Model, a single-energy-level system connected to two thermal baths (with a rate Γ), is reported to see its electric generation efficiency multiplied by a factor of 4, relative to stationary, in the transient regime when the energy level ε_0 (initially at 0.5Γ) undergoes a sudden heaviside jump of $\Delta V = 0.2\Gamma$ (black), 0.3Γ (red) and 0.5Γ (blue).

where T_{H} and T_C are the temperatures of the hot and cold baths, is one of the most known results of thermodynamics: no cyclic heat engine, no matter what its inner workings are, can have an efficiency $\eta = W/Q_{\mathrm{H}}$ that exceeds η_C, where W and Q_{H} are respectively the cycle averaged work produced by the heat engine and the heat lost by the hot reservoir.

Quantum mechanics deals with systems whose size is below the classical thermodynamic limit, where extra quantum effects come into play, such as interference and entanglement. Initial works pointed towards the violation of the classical laws of thermodynamics, such as the aforementioned second law, in the quantum realm [219, 72, 7, 58]. Further research, reviewed in *e.g.* Refs. [107, 68, 198], built upon these first works to recover, within the markovian (quantum) Lindblad master equations approach (see Sec. 3.3.3 below), the quantum equivalent to the classical laws of thermodynamics where no violation occurs and classical finite-time thermodynamics are recovered in some models [70, 71, 156]. The field of quantum thermodynamics is still at its early beginnings: a consensus over the definition of "work" and "heat" is yet to be attained, research is still ongoing on properly building a coherent thermodynamical description where the equivalence or difference between many of the developed approaches is highlighted and understood.

1.1.3. Overview of theoretical approaches

In Chapter 3, we will also briefly overview the main theoretical techniques that are used to describe electronic quantum transport of charge and energy in time-dependent mesoscopic devices. The time dependent drive makes the transport inelastic and complicates considerably the problem. Different techniques have been used to tackle this problem, with different levels of approximation and intrinsic complexity: the Non Equilibrium Green's Function formalism, the (time-dependent) scattering theory, the master equation approaches, or the time-dependent Density Functional Theory. They can be combined with the Floquet theory in case of time-periodic perturbations. In this thesis, we focus on the wavefunction-based scattering theory at the core of `tkwant`.

Scattering theory The scattering theory applies to non-interacting electrons (interaction can still be accounted for at the mean-field level). It describes systems made of a central region, called a scattering region, that is connected to several thermal baths through electronic waveguides, called leads, that lead towards different thermal baths (see Fig. 1.4).

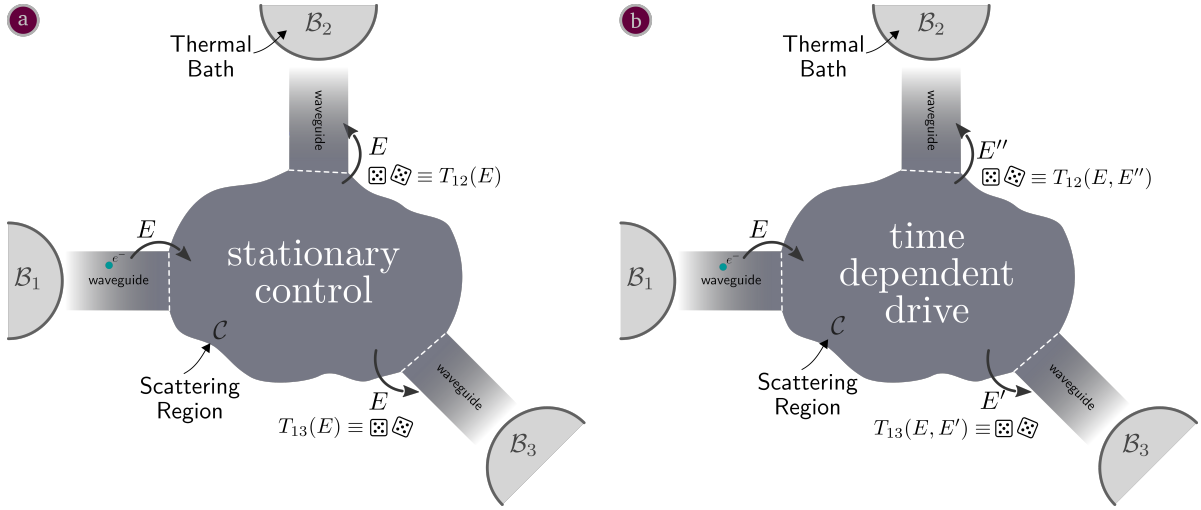

Figure 1.4. – Sketch of the scattering approach. A central system, called a scattering region, is connected to several baths $\mathcal{B}$ through waveguides. Electrons leave each bath $\mathcal{B}_\alpha$, with energies E that follow a thermal distribution, and enter the waveguide till they reach the scattering region where the undertake a first transmission or reflection. Transmitted electrons in the scattering region undergo several reflections and interfere then they eventually leave it to be transmitted in one of waveguides to reach the baths $\mathcal{B}_\beta$ *a)* with the same energy E when in the stationary regime, with a probability $T_{\alpha\beta}$ or *b)* with a different energy E' in the time-dependent regime, due to the drive that causes energy redistribution within the scattering region, with a probability $T_{\alpha\beta}(E, E')$.

Each bath fills the 'incoming modes' of its leads according to a thermal distribution whereas the central system affects the 'outgoing modes' in each lead, although no back action on the baths is considered within this theoretical framework. An electron, described by a wavefunction (see 4.2.1.1), leaves a bath α and enters the central system to eventually be transmitted/reflected in a bath β with a probability $T_{\alpha\beta}$. The probabilities $T_{\alpha\beta}$ can be derived by solving the Schrödinger equation, both in the stationary and time-dependent case, and this enables to write the particle and energy currents that leave each lead α. Note that the calculation of these probabilities can be shortcut in a numerical approach (*e.g.* in `tkwant`) where the working material are a set of wavefunctions. We will use this theory throughout this thesis, a more detailed description is done in Sec. 5.1. A review of the original development for particle transport is done by Ref. [20].

Linear response An orthogonal approach that can be used jointly with the scattering theory is the linear response regime. In a two-bath system, with a "left" L and "right" R bath (see Fig. 1.5), this approach can be undertaken when $\Delta T = T_\mathrm{L} - T_\mathrm{R}$ and $\Delta\mu = \mu_\mathrm{L} - \mu_\mathrm{R}$ are small when compared to their respective average value

In the stationary regime, and without loss of generality, the left particle current I_L^N and the left heat current I_L^Q are related to the displacements $\Delta V/T$ ($\Delta V = \Delta\mu/e$) and $\Delta T/T^2$ through the *Onsager matrix* $\mathbf{L}$[29, 76]

$$\begin{bmatrix} I_\mathrm{L}^\mathrm{N} \\ I_\mathrm{L}^\mathrm{Q} \end{bmatrix} = \underbrace{\begin{bmatrix} L_\mathrm{NN}^\mathrm{L} & L_\mathrm{NQ}^\mathrm{L} \\ L_\mathrm{QN}^\mathrm{L} & L_\mathrm{QQ}^\mathrm{L} \end{bmatrix}}_{\mathbf{L}} \begin{bmatrix} \Delta V/T \\ \Delta T/T^2 \end{bmatrix} \tag{1.2}$$

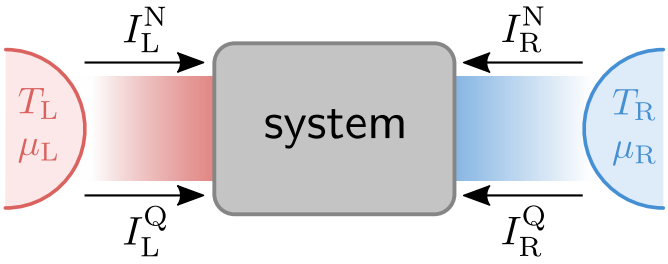

Figure 1.5 – Representation of a two-terminal thermoelectric system. Connected to two thermal baths – left (L) and right (R) – the system is crossed by heat currents I_α^{Q} and particle currents I_α^{N} that go from the bath α =L,R to the other.

where L_{AB} (A,B=N,Q) are the *Onsager coefficients*. This approach has been extended to the time-dependent slow and periodic drive in Ref. [118] where the Onsager coefficients are cycle-averaged quantities. Ref. [219] used the linear response approach in the 'fast' time-dependent regime with time dependent Onsager coefficients that violate some constraints that were followed in the stationary regime. Although, we show in Sec. 6.1 that a time-dependent Onsager matrix is ill-defined and cannot be used for considerations in thermodynamics.

1.2. Summary of chapter 4: theoretical framework

In this chapter, we build a local transport quantum theory of non-interacting electrons and the energy they carry, while under a time-dependent electromagnetic field. First we quickly outline the equivalent classical description from which some main ideas will be ported over to the quantum description. Then, we introduce the quantum transport theory of a single electron described by wavefunctions, in both continuous and discrete space. We finally generalize it to non-interacting many-body transport. This chapter establishes the theoretical framework for time-dependent thermoelectric transport that will be implemented numerically in `tkwant` in Chapter 5.

1.2.1. Classical electrodynamics

The classical approach to charge transport is to describe the motion of the charged particles with classical mechanics – through the equivalent Newton mechanics, Lagrangian mechanics or Hamiltonian mechanics – while the behavior of the electromagnetic field and its interaction with charged matter is described by the Maxwell equations. These describe the interplay between the electric field $\vec{E}(\vec{r},t)$, the magnetic field $\vec{B}(\vec{r},t)$, the local density of charge $\rho(\vec{r},t)$ and the local charge current density $\vec{j}(\vec{r},t)$. The Maxwell equations give rise to local conservation equations of matter

$$\partial_t \rho(\vec{r},t) + \vec{\nabla}\cdot\vec{j}(\vec{r},t) = 0 \tag{1.3}$$

and electromagnetic energy through the Poynting relation

$$\partial_t u_{\mathrm{EM}} + \vec{\nabla}\cdot\vec{\pi} = -\vec{j}\cdot\vec{E} \tag{1.4}$$

where $-\vec{j}\cdot\vec{E}$ is the local power density that is 'lost' to the charged matter, $u_{\mathrm{EM}} = (\varepsilon_0 E^2 + \frac{1}{\mu_0}B^2)/2$ is the electromagnetic energy density and $\vec{\pi} = \vec{E}\times\vec{B}/\mu_0$ is the Poynting vector, *i.e.* the energy current density associated with light. The derivation of the energy conservation equation (1.4) leaves a degree of freedom for the definition of $\vec{\pi}$: the same issue will arise when we will want to define an energy current density carried by quantum particles.

Gauge invariance In Hamiltonian mechanics (classical [141] and quantum [111]), the effect of electromagnetic fields on charged matter is described by the so called 'potentials' : the scalar potential $\phi(\vec{r},t)$ and vector potential $\vec{A}(\vec{r},t)$. Their relationship with the electromagnetic fields is the following

$$\begin{aligned}\vec{E} &= -\vec{\nabla}\phi - \partial_t\vec{A}\\ \vec{B} &= \vec{\nabla}\times\vec{A}\end{aligned} \tag{1.5}$$

This relationship highlights that the potentials are non-unique: given an arbitrary scalar field $\Lambda(\vec{r},t)$, one can add its time partial derivative $\partial_t\Lambda$ to the scalar potential $\phi(\vec{r},t)$ and subtract its gradient $\vec{\nabla}\Lambda$ from the vector potential $\vec{A}(\vec{r},t)$ while leaving the electromagnetic fields defined in Eq. (1.5) remain unchanged.

$$\forall\Lambda(\vec{r},t),\quad \begin{cases}\vec{A}' = \vec{A} - \vec{\nabla}\Lambda\\ \phi' = \phi + \partial_t\Lambda\end{cases} \implies \begin{cases}\vec{E}' = \vec{E}\\ \vec{B}' = \vec{B}\end{cases} \tag{1.6}$$

Since the interaction between electromagnetic fields and charged matter is classically described through fields and not potentials, the physics remains unchanged after such a change. This transformation in the electromagnetic potentials is called a 'gauge transformation'.

Mechanical energy: the issue of time-dependence When considering a classical charged particle under the influence of a time-dependent electromagnetic field. The usual definition of the mechanical energy U, obtained by summing the kinetic energy and the energy associated with the scalar potential ϕ, becomes gauge-dependent

$$\mathrm{d}_t U = \mathrm{d}_t\left[\frac{1}{2}m\dot{\vec{r}}^{\,2}(t) + q\phi(\vec{r}(t),t)\right] = q\partial_t\phi(\vec{r}(t),t) - q\partial_t\vec{A}(\vec{r}(t),t)\cdot\dot{\vec{r}}(t) \tag{1.7}$$

as can be seen in the right hand-side of Eq. (1.7). This makes the originally stationary definition of the mechanical energy non-physical: this issue will appear in the quantum case too, if we consider the Hamiltonian as an energy.

1.2.2. Semi-classical electrodynamics

In the previous section, we did a quick overview to classical electrodynamics of charged particles, with a focus on charge and energy transport. In the scope of this thesis, we describe the behavior of electrons through quantum mechanics. In this field, the particle transport equations are well known and tackled in general physics textbooks, the energy transport equations on the other hand, especially with a gauge invariant conservation equation approach, remains rather marginal: we uncover such an approach then do a more thorough description of energy transport with a gauge-invariant energy conservation point of view.

One-body quantum mechanics In the quantum realm, at each instant t, the physical properties of an electron (energy, position, kinematic momentum, dynamic momentum [56, Chap. 21-3], angular momentum...) can all be computed from a 'wavefunction' $\psi(\vec{r},t)$. Its equation of motion is given by Schrödinger's equation

$$\mathrm{i}\hbar\partial_t\psi(\vec{r},t) = \hat{h}[\psi](\vec{r},t) \tag{1.8}$$

Wavefunctions that abide by Schrödinger's equation are not unique and form a vector space, this is a feature of quantum mechanics as it enables the so called 'quantum superposition': a particle can be in a linear superposition of such solutions.

The Hamiltonian $\hat{h}$ is the equivalent to the classical "mechanical" energy: the sum of the kinetic energy operator $\hat{\kappa}$, the potential energy from the associated electromagnetic scalar potential $q\hat{\phi}[\psi] = q\phi(\vec{r},t)\,\psi$ and an eventual stationary potential energy $V(\vec{r})$.

$$\hat{h}[\psi] = \hat{\kappa}[\psi] + q\,\phi(\vec{r},t)\,\psi + V(\vec{r})\psi \tag{1.9}$$

→ Time-dependent particle transport Once a wavefunction obtained, the local probability current density $\vec{j}(\vec{r},t)$ and probability density $\rho(\vec{r},t)$ obey a conservation law, where both are gauge invariant

$$\partial_t \rho(\vec{r},t) + \vec{\nabla}\cdot\vec{j}(\vec{r},t) = 0 \tag{1.10}$$

This is known text book result [111, Chap. 10.3] [172, Chap. 16.4][56, Chap. 21-2]

→ Time-dependent energy transport Although not considered in textbooks, Ref. [127] defined various energy conservation equations in the quantum regime. For a given wavefunction ψ, they have the following form

$$\partial_t \rho^{\epsilon}_{\psi}(\vec{r},t) + \vec{\nabla}\cdot\vec{j}^{\epsilon}_{\psi}(\vec{r},t) = S^{\epsilon}_{\psi} \tag{1.11}$$

where ρ^{ϵ}_{ψ}, $\vec{j}^{\epsilon}_{\psi}$ and S^{ϵ}_{ψ} are candidates for, respectively, the energy density, the energy current density and the energy source/power density. Unlike the particle number operator, there are several candidates for the energy operator, referred to by the ϵ superscript: it can refer to the Hamiltonian $\hat{h}$, to the Kinetic energy operator $\hat{\kappa}$ or the 'total energy' operator $\hat{\varepsilon}$ (defined bellow). Each density $\rho^{\varepsilon}_{\psi}, \vec{j}^{\varepsilon}_{\psi}, S_{\psi}$, once integrated over space, must give the expectation value of its associated operator on the state ψ. In the context of describing a single non-relativistic particle, the local quantities $(\rho^{\varepsilon}, j^{\varepsilon}, S^{\varepsilon})$ bear no real physical meaning as they are not unique (for a same linked operator), while the expectation value of their associated system-wide operator does [127, 8]. One possible expression for energy density ρ^{ϵ}_{ψ} and the current density $\vec{j}^{\epsilon}$ are the following

$$\rho^{\epsilon}_{\psi} = \mathrm{Re}\Big[\psi^{*}\hat{\epsilon}[\psi]\Big] \tag{1.12}$$

$$\vec{j}^{\epsilon}_{\psi} = \frac{1}{2}\mathrm{Re}\Big[\hat{\epsilon}[\psi]^{*}\,\hat{\vec{v}}[\psi] + \psi^{*}\hat{\vec{v}}[\hat{\epsilon}[\psi]]\Big] \tag{1.13}$$

An additional constraint over the energy operators comes from the time-dependent electromagnetic fields: gauge invariance. Indeed, the electromagnetic potentials $(\phi, \vec{A})$ can be replaced by their gauge changed counterparts Eq. (1.6) while any energy operator candidate must see its expectation value unchanged. Further research [127, 102, 213] on defining a gauge invariant energy operator rules out the Hamiltonian $\hat{h}$ as a potential energy operator and narrows down the possibilities to essentially the kinetic energy $\hat{\kappa}$, or what we call in this thesis the 'total energy' energy operator $\hat{\varepsilon}$

$$\hat{\varepsilon}(t) = \hat{\kappa}(t) + V \tag{1.14}$$

where the stationary potential energy V is taken into account and is considered to not be affected by gauge changes. Its source term S^{ε} recovers the classical power given locally to electrons, by the electromagnetic field, given in Eq. (1.4)

$$S^{\varepsilon}(\vec{r},t) = q\vec{j}\cdot\vec{E} \tag{1.15}$$

While the expressions for the other energy operators have been derived in the main body of the thesis, we use the 'total energy' operator as it is Gauge invariant and recovers results form the literature in the stationary regime (through V).

Non-interacting many-body quantum description When considering a non-interacting many-body quantum system of electrons, many-body states can be written from one-body states but with a strong constraint of total anti-symmetry: electrons are undistinguishable and at most one electron can occupy a one-body state at a time. Many-body states are described by occupation numbers of one-body states, with their associated *creation* $\hat{c}^\dagger_{\lambda_i}$ (and *annihilation* $\hat{c}_{\lambda_i}$) operators. Using a discrete set of spatially localized spinless wavefunctions λ_i on sites i (we use $\hat{c}^\dagger_{\lambda_i} \to \hat{c}^\dagger_i$) to make a *tight-binding* representation, non-interacting operators $\hat{O}$ write

$$\hat{O}(t) = \sum_{ij} o_{ij}(t)\, \hat{c}^\dagger_i \hat{c}_j \quad \text{where} \quad o_{ij}(t) = \langle i |\, \hat{o}\, | j \rangle \tag{1.16}$$

where $o_{ij}(t)$ coefficients can be fitted with experiments, empirically set or derived from '*ab initio*' calculations.

→ Local energy operator In our previous continuous one-body description, we defined local energy densities $\rho^\epsilon_\psi(\vec{r}, t)$ such that their integral over space computes the expectation value of its associated system-wide operator $\hat{\epsilon}$. Then, an energy conservation equation (1.11) is verified for each density, with an associated current density and source density. There is however no unique definition of a *local* energy density nor current [127, 8], both in the one-body approach and in the many-body second quantization approach. This issue also applies to defining the energy of a subsystem, it translates through an apparent arbitrariness in splitting the localized energy at the boundary between the considered subsystem and the rest of the system, with the so called 'coupling term'. This applies when trying to define an energy density operator $\hat{\mathcal{E}}^\epsilon_i$ of a subsystem made of a single site i, when on a tight-binding approach. We take the following definition of the local energy operator

$$\hat{\mathcal{E}}^\epsilon_i = \frac{1}{2} \sum_j \epsilon_{ij}\, \hat{c}^\dagger_i \hat{c}_j + \epsilon_{ji}\, \hat{c}^\dagger_j \hat{c}_i \tag{1.17}$$

The idea of considering half the contribution of the hoppings has already been introduced in Ref. [8] when considering disordered harmonic solids. It has then been used by Ref. [210] in its definition of a local energy operator in a 1D discrete chain. And finally, it got generalized for a generic tight-binding Hamiltonian in Ref. [129] with the same expression as $\hat{\mathcal{E}}^\epsilon_i$ while only considering the Hamiltonian operator $\epsilon = h$. This expression follows the 'natural' splitting [119] as it emerges from the discretization from continuous models (see the derivation that leads to Eq. (4.62)), it was also later endorsed by Refs. [25, 143], while using the Hamiltonian as the energy operator. On our end, we provide one more arguments that justifies this symmetrical splitting: defining the local energy density as the expectation value of the local 'total' energy operator $\hat{\mathcal{E}}^\varepsilon_i$ (with $\epsilon \to \varepsilon$) enables us to recover, for the total energy source term S^ε_i, the classical expression of the power given to electrons (see comment under Eq. (1.4)), just like in Eq. (1.15) in the one-body continuous-space approach. On the other hand, this definition of a local/subsystem energy operator intervenes in a current debate in defining a time-dependent heat current, see Sec. 4.3.4.2.

→ Many-body quantum transport We use the 'lesser Green function' $G^<_{ij}(t)$ to express expectation values of many-body 'single-particle' operators

$$G^<_{ij}(t) = \frac{\mathrm{i}}{\hbar}\left\langle \hat{c}^\dagger_j(t)\hat{c}_i(t)\right\rangle \tag{1.18}$$

It enables writing the non-interacting many-body conservation equations of particle and particle-carried energy. They share the same expression as the discretized one-body conservation equations derived in Sec. 4.2.4 and can be derived by using the Heisenberg equation of motion (an equivalent to the Schrödinger equation) on the expectation value $\rho_i = \langle\hat{\rho}_i\rangle$ of the local many-body energy and particle operators

$$\underbrace{\partial_t\rho_i(t) = \frac{\mathrm{i}}{\hbar}\left\langle\left[\hat{H}(t),\hat{\rho}_i(t)\right]\right\rangle + \langle\partial_t\hat{\rho}_i(t)\rangle}_{\text{Heisenberg equation of motion (4.135)}} \implies \underbrace{\partial_t\rho_i(t) + \textstyle\sum_j I_{ij}(t) = S_i(t)}_{\text{Conservation equation}} \tag{1.19}$$

where I_{ij} is the net current flowing from site i to site j and $S_i(t)$ is the 'source' term. In the well-known case of particle transport, the particle density writes $\rho_i = \left\langle\hat{c}^\dagger_i\hat{c}_i\right\rangle = -\mathrm{i}\hbar G^<_{ii}(t)$, the particle current writes $I^{\mathrm{N}}_{ij} = 2\,\mathrm{Re}[h_{ij}(t)G^<_{ji}(t)]$; the source term is zero as no particles are created or annihilated from the vacuum. For the energy, the local energy density can be expressed as

$$\rho^\epsilon_i(t) = \left\langle\hat{\mathcal{E}}^\epsilon_i(t)\right\rangle = \sum_j \mathrm{Im}\left[\epsilon_{ij}(t)G^<_{ji}(t)\right] \tag{1.20}$$

then we use Eq. (1.19) to derive a generic expression for the local energy current I^ϵ_{ij} flowing from site i to site j

$$I^\epsilon_{ij} = \frac{1}{\hbar}\sum_k \mathrm{Re}\left[\epsilon_{ki}\epsilon_{ij}G^<_{jk} - \epsilon_{kj}\epsilon_{ji}G^<_{ik}\right] \tag{1.21}$$

where ϵ_{ij} is to be replaced by the coefficients of the considered energy operator. As with the continuous one-body approach, the derived expression of the energy current I^ϵ_{ij} is not unique but must give the correct divergence $\sum_j I^\epsilon_{ij}$. The energy source term – the power given to electrons – is dependent on the specified energy operator and write as follows for the 'total energy'

$$S^\varepsilon_i(t) = \sum_j -\frac{1}{2}q\left[\phi_j(t) - \phi_i(t)\right] I^N_{ij}(t) + \sum_j \mathrm{Im}\left[\partial_t\varepsilon_{ij}(t)G^<_{ji}(t)\right] \tag{1.22}$$

from which the interpretation of one term is rather straightforward

$$\sum_j -\frac{1}{2}q\left[\phi_j(t) - \phi_i(t)\right] I^N_{ij}(t) = -q\vec{\nabla}\phi_i\cdot\vec{j}_i \tag{1.23}$$

whereas the second term needs further derivation (done in Appendix. B.3) to show that

$$\sum_j \mathrm{Im}\left[\partial_t\varepsilon_{ij}(t)G^<_{ji}(t)\right] = -\partial_t\vec{A}_i\cdot\vec{j}_i \tag{1.24}$$

so we show that we recover the classical input power $\vec{j}\cdot\vec{E}$ (see Eq. (1.4)), where $\vec{E} = -\vec{\nabla}\phi - \partial_t\vec{A}$ is the time-dependent electric field.

→ Computing lead currents Transport studies consider the following generic systems : a central system, under the influence of a time-dependent electromagnetic field, connected to semi-infinite electron waveguides $\mathcal{L}_\alpha$, called leads. Each lead is filled with incoming electrons that follow a thermal distribution given by a temperature T_α and chemical temperature μ_α (see Fig. 1.6). The main focus is to compute the currents that hop-in and hop-out of the leads. To compute these currents using hopping energy currents I^ϵ_{ij} and particle currents I^{N}_{ij}, we compute the particle current flux $I^{\mathrm{N}}_{\alpha,a}$ and energy flux I^ϵ_α through a section in the lead $\mathcal{L}_\alpha$.

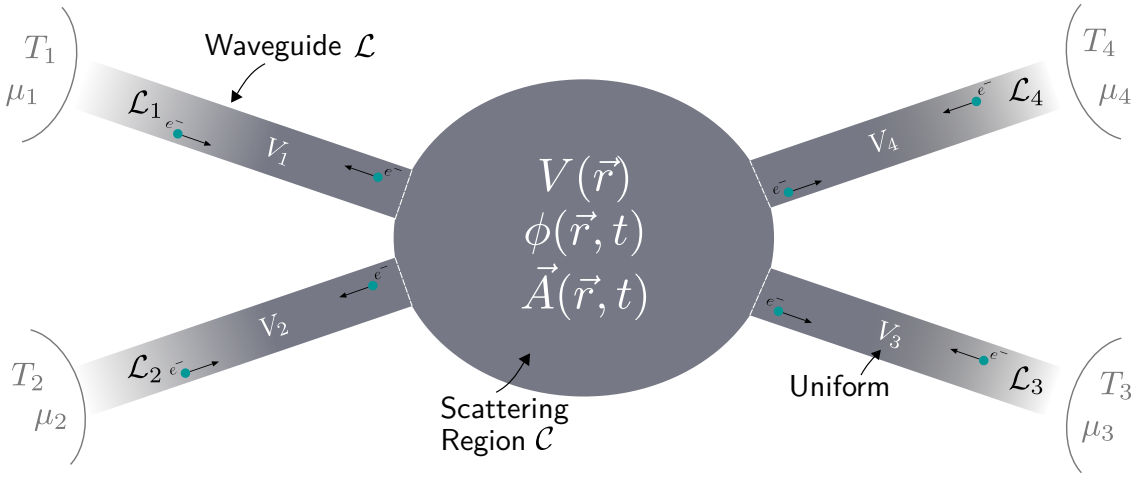

Figure 1.6. – Target system for energy and particle transport. Made of a central area ('scattering region') $\mathcal{C}$ connected to semi-infinite waveguides ('leads'). It is under the influence of an external time dependent electromagnetic field, represented by the scalar potential $\phi(\vec{r},t)$ and the vector potential $\vec{A}(\vec{r},t)$. An additional static potential energy V is considered. Each lead $\mathcal{L}_\alpha$ is filled with incoming electrons that follow a thermal distribution given by the temperature T_α and chemical potential μ_α.

The systems we describe are non-interacting and no relaxation process within the system are taken into account : local temperatures and heat currents cannot be defined within the system. However, a common hypothesis that is made in the stationary regime [16] is that each electron leaving the scattering area $\mathcal{C}$ with an energy E into a lead $\mathcal{L}_\alpha$, will eventually reach the electro-chemical reservoir of temperature T_α and chemical potential μ_α, then undergo thermal relaxation and contribute $E-\mu_\alpha$ in heat to the thermal bath. In terms of currents, this translates to $I^{\mathrm{Q,st}}_\alpha = I^{\epsilon,\mathrm{st}}_\alpha - \mu_\alpha I^{\mathrm{N,st}}_\alpha$ where $I^{\mathrm{Q,st}}_\alpha$ is the stationary heat current going in lead α. Defining a time-resolved lead heat current in the time dependent regime lies within the emerging field of time-dependent non-equilibrium quantum thermodynamics. This field is new with ongoing research over defining a proper and definite theoretical framework. Fundamental issues have arose with respect to the conceptual spatial separation between the central system, the thermal baths and their coupling. In the weak coupling regime, a consistent theory has been established [23, 52, 107, 68] whereas in the strong coupling regime, especially when the coupling is time-dependent, defining a time resolved heat current raises a fundamental issue [31, 54, 44, 25, 143]: the part $\hat{H}_{\mathcal{C}\alpha}$ of the system's total Hamiltonian $\hat{H}$ that couples a lead $\mathcal{L}_\alpha$ to the central system $\mathcal{C}$ is no longer negligible, can be time-dependent, and must be accounted for when one tries to define a time-resolved heat current (the discussion exposed above, in paragraph 'local energy operator' p.15, over the definition of a local energy operator also applies here). An expression to the time-resolved lead heat current has been given by Refs. [119, 121] where the lead's energy current includes half the contribution of the coupling $\hat{H}_{\mathcal{C}\alpha}$

$$I^{\mathrm{Q},h}_\alpha(t) = -\partial_t \left\langle \hat{\tilde{H}}_\alpha + \frac{1}{2}\hat{H}_{\mathcal{C}\alpha} \right\rangle - \mu_\alpha I^{\mathrm{N}}_\alpha(t) \qquad \hat{\tilde{H}}_\alpha = \sum_{i,j\in\mathcal{L}_\alpha} h_{ij}(t)\hat{c}^\dagger_i \hat{c}_j + \mathrm{h.c.} \tag{1.25}$$

This definition recovers the usual one in the stationary case where the coupling Hamiltonian $\hat{H}^{\mathcal{C}\alpha,\mathrm{st}}$ would not contribute ($\partial_t \left\langle \hat{H}^{\mathcal{C}\alpha} \right\rangle = 0$). However, issues have been raised over such a definition [54, 142] and an extra term, that involves the coupling Hamiltonian, has been suggested [81] as a remedy but is zero in our specific description. Given that the Hamiltonian is in general not gauge dependent, we change the Hamiltonian based definition of the heat current $I_\alpha^{\mathrm{Q},h}(t)$ to a 'total energy' based definition $I_\alpha^{\mathrm{Q}}(t) = I_\alpha^{\mathrm{Q},\varepsilon}(t)$ (note that the two definitions coincide on time-*independent* leads and differ otherwise, see Sec. 5.3.2.3)

$$I_\alpha^{\mathrm{Q}}(t) = I_\alpha^{\varepsilon}(t) - S_\alpha^{\varepsilon}(t) - \mu_\alpha I_\alpha^{\mathrm{N}}(t) \tag{1.26}$$

where $I_\alpha^{\varepsilon}(t)$ and $S_\alpha^{\varepsilon}(t)$ are respectively the lead's energy current and input power

$$I_\alpha^{\varepsilon}(t) = \sum_{\substack{i\in\mathcal{L}_\alpha \\ j\in\mathcal{C}}} I_{ij}^{\varepsilon}(t) \qquad\qquad S_\alpha^{\varepsilon}(t) = \sum_{i\in\mathcal{L}_\alpha} S_i^{\varepsilon}(t) \tag{1.27}$$

Computing energy and heat currents farther away in the lead avoids the issue brought up by Ref. [54] with the eventual time-dependent coupling between the central region and the leads. A Landauer-Büttiker scattering approach similar to ours has also been employed in Ref. [24] in the special case of slow time-dependent driving. On the contrary, our approach applies to arbitrary time-dependent perturbations (due to an external electromagnetic field), beyond the adiabatic limit and the single-frequency drive.

Now that the time-resolved lead currents properly defined, we highlight two shortcomings of such an approach: *(i)* due to the travel time and dispersion, time resolved lead currents are dependent on where they are computed; *(ii)* the heat current can theoretically only be accounted for after electrons thermally relax within the bath. The lead is is technically not the heat bath and computing a space and time resolved heat current within the lead is a priori ill-defined, although it can be interpreted differently in terms of bookkeeping [47], *i.e.* "the amount of heat that will eventually be dissipated later on". To workaround these issues, we will also study time integrated lead quantities (following *e.g.* Ref. [44]).

1.3. Summary of chapter 5: numerical simulation with `tkwant`

Our goal is to describe particle and energy (carried by the particles) currents and densities in scattering systems in hopes to better understand mesoscopic thermoelectricity in the time dependent domain. After having drawn up in Chapter 4 the gauge-invariant thermoelectric framework of this thesis (expressed in terms of the lesser Green's $G_{ij}^{<}(t)$ function of the system), we introduce in this Chapter the numerical method (based on wavefunctions) used by `tkwant`, the time-dependent extension to the simulation library of reference (`kwant`) in quantum transport for generic tight-binding systems (see Fig. 1.7). Its development, initiated during the PhD thesis of B. Gaury [63], gave rise to one important equation which links the lesser Green functions $G_{ij}^{<}(t)$ and a specific set of system-wide one-body wavefunctions called 'scattering states'. This last result completes the scattering wavefunction description of non-interacting quantum transport. We extend `tkwant` to energy transport through a module called `tkwantoperator`: we show that this extension enables us to effortlessly recover some of the previous results of the literature on the extensively studied 'Resonant level model' but also opens the doors to simulating complex systems beyond 'toy' models, such as the Quantum Point Contact.

Scattering states Defined as the Eigenstates of the system-wide (central region and leads) Hamiltonian $\hat{h}$ in the stationary regime, the 'scattering states' Ψ^λ can be extended to the time-dependent

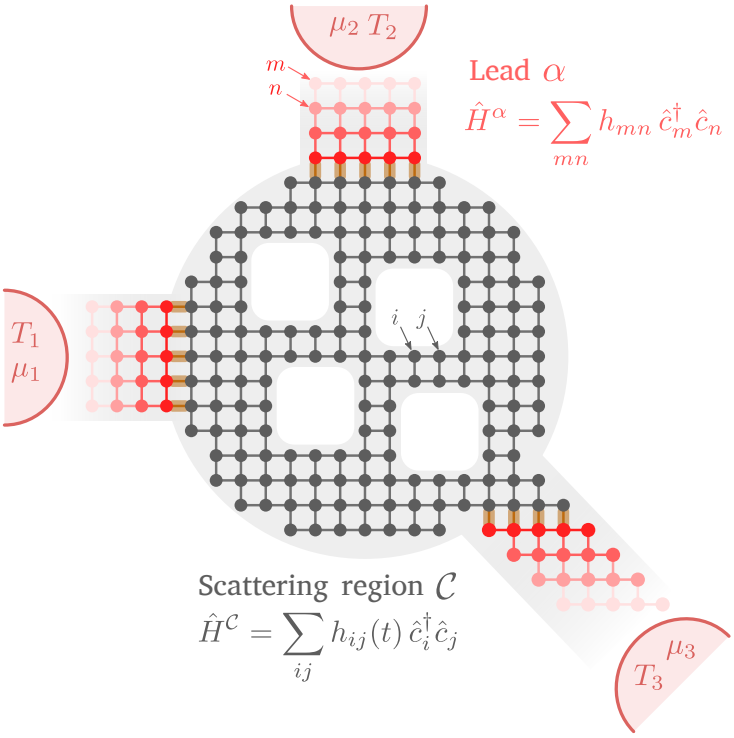

Figure 1.7 – Generic tight-binding system that can be simulated with `tkwant`. It is made of a time-dependent central scattering area $\mathcal{C}$, whose sites are colored in gray, connected to time-independent leads, whose sites are colored in red. A uniform time-dependent scalar potential can be considered in each lead through a time dependent phase in the hoppings (colored in orange) connecting each lead to the central system, through a gauge change (see Eq. (5.23))

non-interacting regime. To achieve, `tkwant` uses a clever approach : the systems that can be simulated are restricted to those that are stationary until a time t_0, then the time-dependence can start. This enables `tkwant` to leverage `kwant`'s stationary computation of the eigenstates of the stationary system, then it time-evolves them separately, one by one thanks to the non-interacting hypothesis, with a modified version of the Schrödinger equation through the 'source-sink' algorithm. Given that the leads (see Fig. 1.7) are semi-infinite, the 'source-sink' algorithm computes only a 'perturbation' over the stationary state. Since the time-dependence only exists in the central region, this perturbation is initially non-zero only in the central region then propagates at finite speed within the leads. As we are not interested by what happens far in the leads, this perturbation is 'absorbed' starting from a certain position in each lead and throughout a finite length, so the practical simulated size of the system remains small, with respect to long simulation times, while keeping an arbitrarily good approximation on the value of the wavefunctions in the main (non-absorbing) region.

Computing currents and densities With the 'scattering states' Ψ^λ now defined, Ref. [66] uses them to express the lesser Green function $G^<_{ij}$ defined in Eq. (1.18), for systems described in Fig. 1.7

$$G^<_{ij} = \mathrm{i} \sum_{\lambda=\alpha,n,E} f_\alpha(E) \Psi^\lambda_j(t)^* \Psi^\lambda_i(t) \tag{1.28}$$

where $\sum_\lambda$ has been used for compactness as an equivalent to $\sum_\alpha \sum_n \int \frac{\mathrm{d}E}{2\pi\hbar}$, which fundamentally expresses a over all the scattering states Ψ^λ, defined by the incoming modes n from the leads α, injected at energies E, where E is a continuous degree of freedom ; $f_\alpha(E) = f_{T_\alpha,\mu_\alpha}(E)$ is a shorthand notation for the Fermi function

$$f_{T,\mu}(E) = \frac{1}{\exp\left(\frac{E-\mu}{k_\mathrm{B}T}\right)+1} \tag{1.29}$$

with k_B being the Boltzmann constant. Eq. (1.28) is the last missing piece to enable computing the energy currents and densities exposed in Sec. 1.2.2 whose expressions have been given in terms of the

lesser Green's function $G^<_{ij}(t)$. Thanks to Eq. (1.28), these can be readily expressed in the wave-function formalism

$$\rho_i^\epsilon(t) = \sum_{\lambda=\alpha,n,E} f_\alpha(E) \sum_j \mathrm{Re}\left[\Psi_i^\lambda(t)^* \epsilon_{ij}(t) \Psi_j^\lambda(t)\right] \tag{1.30}$$

$$I_{ij}^\epsilon = \sum_{\lambda=\alpha,n,E} f_\alpha(E) \sum_k \mathrm{Re}\left[\Psi_k^\lambda(t)^* \epsilon_{ki} \epsilon_{ij} \Psi_j^\lambda(t) - \Psi_k^\lambda(t)^* \epsilon_{kj} \epsilon_{ji} \Psi_i^\lambda(t)\right] \tag{1.31}$$

Both quantities can be computed with `tkwant`, in the same spirit as $\rho_i^{\mathrm{N}}(t)$ and $I_{ij}^{\mathrm{N}}(t)$ but with an additional sum over the system sites. The electric power density $S_i^\epsilon(t)$ can be computed as well for each energy operator, for the total energy operator it writes as the following

$$\begin{aligned} S_i^\varepsilon(t) = &\sum_j -\frac{1}{2}\left[\phi_j(t) - \phi_i(t)\right] q I_{ij}^N(t) \\ &+ \sum_{\lambda=\alpha,n,E} f_\alpha(E) \sum_j \mathrm{Re}\left[\Psi_i^\lambda(t)^* \partial_t \varepsilon_{ij}(t) \Psi_j^\lambda(t)\right] \end{aligned} \tag{1.32}$$

Those local quantities can eventually be summed up over space to deduce for instance subsystem energies or the lead energy currents $I_{\alpha,a}^\epsilon(t)$ and the lead heat currents $I_{\alpha,a}^{\mathrm{Q}}(t)$ as described in the 'Computing lead currents' paragraph p. 17.

1.3.1. `tkwantoperator`: extension to energy transport

To calculate our newly defined energy related quantities, we have implemented a Python package, called `tkwantoperator`: it is open source and freely available, along with a complete documentation that provides install instructions, a tutorial and a technical reference at `gitlab.kwant-project.org/kwant/tkwantoperator`. The code has been published at the same time as our research article [96]. Five Python classes have been implemented : `EnergyDensity`, `EnergySource` and `EnergyCurrentDivergence` can be used for calculating respectively ρ_i^ϵ (given by Eq. (1.30)), S_i^ϵ (given in Eqs. (1.32) for $\epsilon = \varepsilon$), and $\sum_j I_{ji}^\epsilon$ over a given list of sites $\{i\}$; `EnergyCurrent` for calculating the current I_{ji}^ϵ (given by Eq. (1.31)) flowing through a given list of hoppings $\{(j,i)\}$; `LeadHeatCurrent` computes the heat current $I_{\alpha,a}^{\mathrm{Q}}$ (given by Eq. (1.26)) in a given lead $\mathcal{L}_\alpha$. The energy quantity ϵ can either be the total energy $\hat{\varepsilon}$, the Hamiltonian $\hat{h}$ or a 'custom' operator where the user provides the onsite matrix elements ϵ_{ii}. A code snippet showcasing the use of `tkwantoperator`, along with `Kwant` and `tkwant`, is displayed in Fig. 5.7: that relatively small code snippet is sufficient to quickly recover few results from the literature, see Sec. 5.3.2.

The calculation of the many-body expectations values of the various operators involves an integration over all the scattering states Ψ^λ, indexed by the λ parameter (see Eq. (1.28)). Given that the evolution in time of the scattering states $\Psi^\lambda(t)$ is the most time-consuming task of `tkwant`'s algorithm, it is crucial to use as few scattering states as possible to evaluate expectations values, while preserving the accuracy of the computed quantities. For this purpose, a Gauss-Kronrod adaptive scheme [204] is used when integrating the contribution of each scattering state. Moreover, the time evolution of the scattering states can be done in parallel on multi-core computers where each core deals with a subset of the scattering states. Both functionalities, already implemented within `tkwant`, are leveraged to compute the expectation values of our energy operators.

With `tkwantoperator` finalized, we have performed `tkwant` simulations of electronic and heat transport in the paradigmatic time-dependent Resonant Level Model (RLM), in order to validate our

approach and our numerical implementation. We also report on an exploratory investigation of time-dependent heat transport in a Quantum Point Contact (QPC) driven by voltage pulses: without discussing deeply the physics involved, we illustrate the strong potential of the `tkwant`, with our `tkwant-operator` module, in studying dynamical thermoelectricity and caloritronics.

1.3.2. Validation: Resonant Level Model (RLM)

The (non-interacting) time-dependent RLM has been extensively studied in the literature to simulate dynamical charge transport (see *e.g.* Refs. [92, 149, 158]) and more recently dynamical energy transport [38, 116, 55, 121, 120, 219, 44, 215, 113, 37, 51]. In chapter 5 we use this model (described Fig. 1.8) as a test bed to benchmark our numerical approach. We consider two cases: *(i)* when (only) the dot onsite Hamiltonian coefficient $h_0(t)$ is varied in time as $h_0(t) = V_0 + \Delta V \Theta(t)$, Θ being the Heaviside function, and *(ii)* when the time-dependent step-like perturbation is performed in the leads. We calculate the time-dependent energy and heat currents with our numerical approach: we show that we reproduce in the expected limits the results obtained previously in the literature.

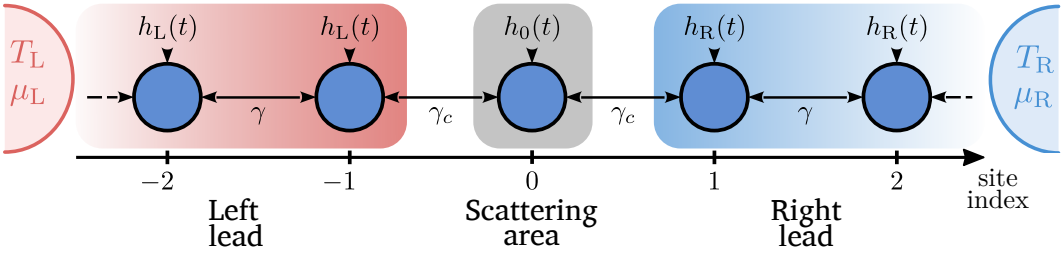

Figure 1.8. – Tight-binding representation of the Resonant Level Model: a one-dimensional (1D) chain made of a central site 0 connected through a nearest-neighbor hopping term γ_c to two semi-infinite left (L, on sites $i \leq -1$) and right (R, on sites $i \geq 1$) leads with uniform on-site Hamiltonian coefficients $h_\mathrm{L}(t)$ and $h_\mathrm{R}(t)$, and a nearest-neighbor hopping term γ. Each lead α is attached from the remote past to an electronic reservoir at equilibrium with static electrochemical potential μ_α and temperature T_α that remain constant.

In particular, we check that we recover in case *(i)* the analytical results obtained within the NEGF technique, in the so-called wide-band limit approximation: it is obtained in `tkwant` by doing the following replacement and limit in the hopping coefficients γ and γ_c [37]

$$\gamma \to \lambda\gamma, \quad \gamma_c \to \sqrt{\lambda}\gamma_c \quad \text{and} \quad \lambda \to \infty \tag{1.33}$$

which keeps the ratio $\Gamma = 2\gamma_c^2/\gamma$ constant. The perfect match between analytics and numerics is illustrated in Fig. 1.9 where we have plotted the time-resolved heat current in *e.g.* the left lead (given by Eq. (1.26))

$$I_L^\mathrm{Q}(t) = -\partial_t \left\langle \hat{H}_L \right\rangle - \mu_L I_L^\mathrm{N}(t) \tag{1.34}$$

and compare it to the one obtained within the NEGF formalism under the wide-band limit approximation (see Appendix C.1 for a derivation). A similar comparison is done for the particle current $I_L^N(t)$ and for an alternative heat current $\tilde{I}_\mathrm{L}^\mathrm{Q}(t)$ with the Hamiltonian $\hat{\tilde{H}}_\mathrm{L}$ that does not include the contribution of the lead-dot tunneling Hamiltonian $\hat{H}_{0L}$ (modified version of Eq. (1.26) without $\hat{H}_{\mathcal{C}\alpha}$)

$$\tilde{I}_L^\mathrm{Q}(t) = -\partial_t \left\langle \hat{\tilde{H}}_\mathrm{L} \right\rangle - \mu_\mathrm{L} I_\mathrm{L}^N(t) \tag{1.35}$$

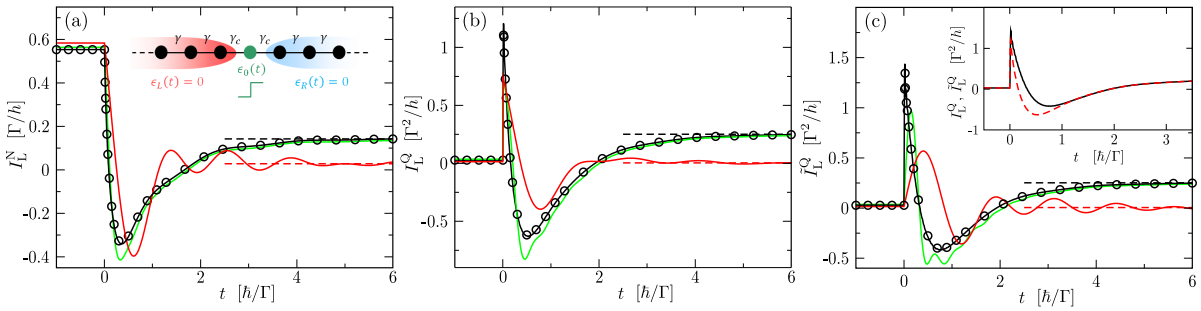

Figure 1.9. – Adapted from our published article [96]: (a) Left particle current I_L^N, (b) left heat currents I_L^Q and (c) $\tilde{I}_L^Q$, as a function of time t, for the 1D RLM defined Fig. 1.8, when the dot energy level is modified as $h_0(t) = V_0 + \Delta V \Theta(t)$ (inset of panel (a)). Units of the x and y axes are indicated in brackets. In all panels, data are computed numerically with `tkwant`+`tkwantoperator` for different values of $\lambda\gamma/\Gamma$ (1 (red lines), 6.25 (green lines), and 100 (black lines). The horizontal dashed lines plotted for $\lambda\gamma/\Gamma = 1$ (in red) and 100 (in black) correspond to the static limits at large times $\Gamma t/\hbar \gg 1$ given by the Landauer-Büttiker formulas (see Sec. 5.2.3.2). When $\lambda\gamma/\Gamma \gg 1$, the `tkwant` results converge to the NEGF results (circles) derived in the wide-band limit (Appendix C.1). Inset of panel (c): comparison of $I_L^Q(t)$ (red dashed line, given by Eq. (1.34)) and $\tilde{I}_L^Q(t)$ (black line, given by Eq. (1.35)) in the wide-band limit. In all panels, $h_0 = 0.5\Gamma$, $\Delta V = 2.5\Gamma$, $h_L(t) = h_R(t) = 0$, $T_L = \Gamma/k_B$, $T_R = 0$, $\mu_L = 0.5\Gamma$, and $\mu_R = -0.5\Gamma$. The NEGF curves are independent of Γ. The `tkwant` curves are functions of $\lambda\gamma/\Gamma$ and not of the three parameters λ, γ, and Γ taken separately.

Such a definition of the heat current was considered in *e.g.* Refs.[38, 219].

We have also benchmarked our numerical results against the ones obtained in Ref. [49] in the case *(ii)* defined above. Finally, we have also checked that in the long time limit $\Gamma t/\hbar \to \infty$, the `tkwant` particle and heat currents converge to the static limits given by the Landauer-Büttiker formulas (horizontal dashed lines in Fig. 1.9), as expected.

1.3.3. Going further: Quantum Point Contact

To illustrate the potential of our `tkwant` based numerical approach, we also report in Chapter 5 on simulations of dynamical (electronic) heat transport in a QPC attached to two reservoirs held at different temperatures. We focus on the possibility of extracting heat from the cold reservoir by Peltier effect and ask whether or not Peltier cooling may be enhanced by applying time-resolved voltage pulses to one of the two electrodes attached to the QPC (instead of a constant voltage bias across the system). We consider a nano-ribbon of length L and width W connected through semi-infinite leads to two left (L) and right (R) electronic reservoirs maintained at temperatures $T_L \lesssim T_R$ and chose the electrochemical potentials $\mu_L \gtrsim \mu_R$ (see Fig.1.10 (a)) so that the stationary transmission $T(E)$ is midway of a step $T(E = \mu_R) \approx 0.6$ and $I_L^Q(t \leq 0) = 0$. The system is discretized on a square lattice (with lattice spacing $a = 1$). For times $t < 0$, no time-dependent perturbation is applied and starting $t \geq 0$, we apply in the left lead a Gaussian voltage pulse $V_L(t)$ of width τ_p, amplitude V_p and center $3\tau_p$. Therefore, the system Hamiltonian becomes $\hat{H}(t > 0) = \hat{H}^0 + \sum_{i \in L} V_L(t) \hat{c}_i^\dagger \hat{c}_i$, where $\hat{H}^0$ is the stationary Hamiltonian.

Using `tkwant` along with our `tkwantoperator` extension [3] we compute the time-resolved particle current $I_L^N(t)$ and heat current $I_L^Q(t)$ in the left lead for different pulse parameters (τ_p, V_p) with a fixed pulse time-integral (to conserve the total number of dynamically injected electrons in the left lead). The `tkwant` currents are compared to the adiabatic currents $I_L^{N,\bar{st}}(V_L(t))$ and $I_L^{H,\bar{st}}(V_L(t))$ given by the Landauer-Büttiker formulas (see Sec.5.2.3.2). For small τ_p (short pulses, see panel (b)), the particle current $I_L^N(t)$ shows a first positive peak centered around $3\tau_p$ corresponding to the injected

pulse and some time later, a second negative peak corresponding to the reflected part of the pulse. They contribute to two main negative peaks in the heat current $I_L^Q(t)$. For long pulses, the `tkwant` currents converge to the adiabatic currents characterized by a single peak centered at $3\tau_p$. We find that heat can be extracted from the cold reservoir ($\int \mathrm{d}t\, I_L^H(t) > 0$) only in the limit of long pulses and, within the set of parameters we chose, the time-integral of non-adiabatic heat current is consistently lower than its adiabatic counterpart $\forall \tau_p \quad \int \mathrm{d}t\, I_L^H(t) \leq \int \mathrm{d}t\, I_L^{H,\bar{st}}(V_L(t))$. Thus, the application of short voltage pulses involving a non-adiabatic response of the quantum system turns out to be detrimental to Peltier cooling, at least for the set of parameters considered here. The present preliminary investigation shows the feasibility of further studies.

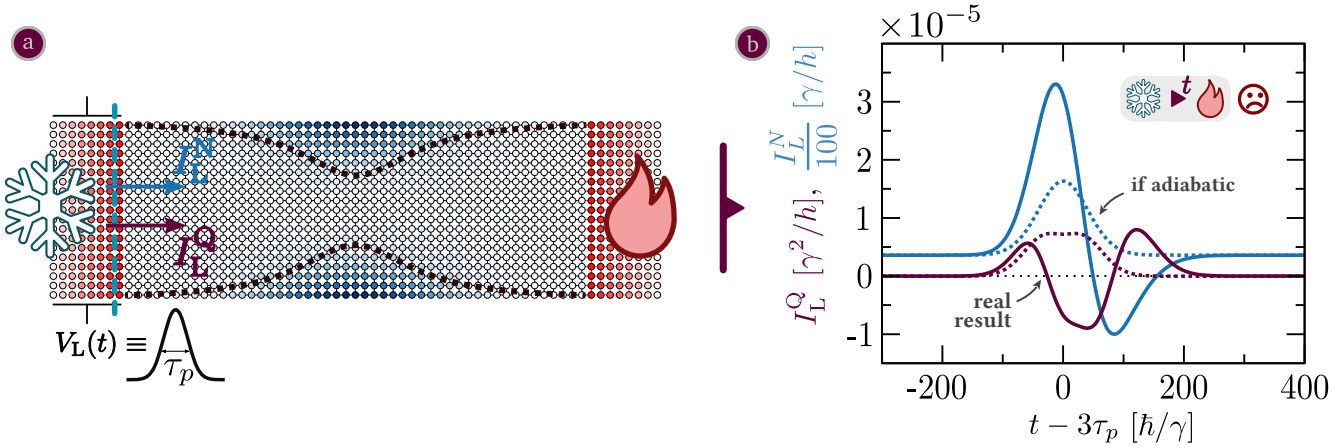

Figure 1.10. – (a) QPC discretized model. The site color in the central region encodes the value of the QPC potential (from 0 (white) to larger values (shades of blue)). A few layers of the left and right semi-infinite leads are shown in red. A voltage pulse $V_L(t)$ is applied in the left lead, currents are evaluated at the interface shown by a dashed blue line. (b) Left particle current I_L^N (in blue, in units of $100\gamma/h$) and left heat current I_L^H (garnet-colored, in units of γ^2/h) as a function of time t (in units of $\hbar/\gamma$), for a voltage pulse of width $\tau_p = 100\,\hbar/\gamma$. Full lines are `tkwant` results, dashed lines are Landauer-Büttiker adiabatic results. Parameters: $W = 18$, $L = 48$, $l_x = 50$, $l_y = 5$, $\mu_L = 0.20607\gamma$, $\mu_R = 0.2\gamma$, $T_L = 0.018\gamma/k_B$, $V_p = 0.2$ and $T_R = 0.02\gamma/k_B$.

The naive approach in trying to 'boost' the Peltier cooling of a QPC by simply adding the time-dependent ingredient is inconclusive and simply highlights that the effects at play are more complex to grasp. Therefore, in the next chapter, we go back to the Resonant Level Model where analytical expressions can be obtained more easily, in an effort to understand better the effects at play.

1.4. Summary of chapter 6: numerical and semi-analytical study of the RLM

This chapter is dedicated to the study of the (non-interacting) time-dependent Resonant Level model. It is a simple system made of a single energy level that can be driven in time, connected to two heat baths, where electrons can hop in and hop out (see Fig. 1.8). Our goal is to achieve a better understanding of the effect of time-dependent drive of the single energy level: Zhou et al. [219] reports a boost of the thermoelectric efficiency of the model, when setup in an electric generator configuration, when the energy level undergoes 'fast' driving. Using the definitions taken in that reference, we reproduce within our own approach the reported results: it enabled us to further validate our approach then to better understand the limitations of the used method and definitions. Then, we use the wavefunction

approach introduced in Chapter 5 to perform an analytical derivation of the transport quantities (the particle/energy/heat current and the driving power) under an arbitrary drive of the dot, in the wideband limit (see Eq. (1.33)). We obtain generic formulas for all the transport quantities, which take the form of integrals over the energy (weighted by the Fermi functions) of various terms written as a function of the transmission amplitude of the model. We follow by a joint semi-analytical (we integrate our analytical formulas) and numerical (using `tkwant+tkwantoperator`) study with a rectangle-like drive of the dot, where we take into account the system-bath coupling term (see Sec. 1.2.2).

To define a heat generator efficiency in the driven regime, one must account for the driving input power, and its effect, in the energy bill. On the other hand, defining an efficiency involves a distinction between what is the 'useful energy' and what is the 'spent energy', and this distinction becomes rather blurry and delicate in the time-dependent regime. We define what we believe is a physically interpretable efficiency, different from that of Ref. [219]. After validating the match between the numerical and the semi-analytical approaches, we use the latter to perform an automated exploration of various parameters in search of an eventual advantage in the driven regime. Among the tested few hundreds of thousands of points in phase space, many show promising behavior with an improved efficiency in the transient regime but converges back to a lower value at long times, close to its stationary value (see left panel of Fig. 1.11). The same behavior can be observed if the rectangular drive is periodically repeated (see right panel of Fig. 1.11).

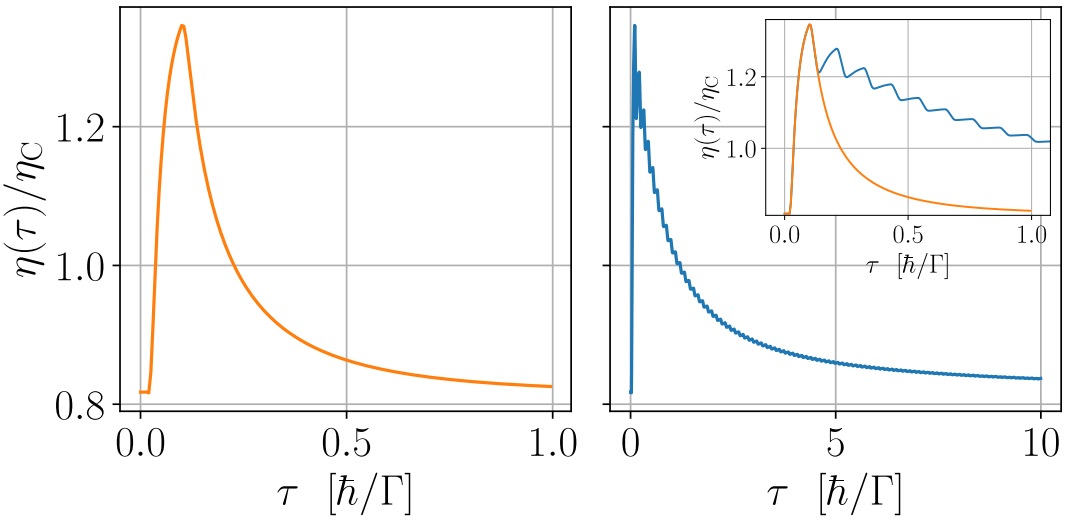

Figure 1.11. – An improved transient efficiency of the RLM. When the dot level is driven by a rectangle function, the particle and heat currents can behave in such a way that the efficiency $\eta(\tau)$ (defined in Eq. (6.74), under the assumptions stated Sec. 6.3.3) is temporarily improved. The left panel is the resulting efficiency of a single pulse whereas the right panel is the resulting efficiency of the same pulse, periodically cycled with a period τ_p. Both curves are plotted in the inset of the right panel to show they coincide till $\tau = \tau_p$. We notice that this has the effect of delaying the return to a lower efficiency but does not seem to maintain a steady-state improvement. Both curves have been obtained through `tkwant+tkwantoperator` simulations. This result is reminiscent of the reported results of Ref. [178] on a Peltier cooler. Simulation parameters (energies are in units of Γ, times are in units of $\hbar/\Gamma$): $T_L = 87, T_R = 25, \mu_L = -26, \mu_R = 26, V_0 = 55, \Delta V = 2, \Delta t = 0.08, t_0 = 0.1, \tau_p = 0.11, wb = 400, \gamma = 1$.

Other limitations of such a behavior are yet to be studied as *e.g.* electronic interaction is not factored in and may change the picture. More complex models can be investigated for which our extension to `tkwant` comes in handy as it renders possible such explorations.

2. Résumé substantiel en français

Ce dernier siècle est marqué par une accélération rapide du réchauffement climatique (voir Fig. 2.1a) et cela est du à nos besoins toujours grandissants en énergie (voir Fig. 2.1b). La recherche actuelle tente d'améliorer le rendement de nos procédés d'extraction et de transformation de l'énergie, tout en réduisant leur empreinte écologique. Une loi fondamentale de la physique est la conservation de l'énergie : elle ne fait que changer de forme ; de plus, le deuxième principe de la thermodynamique stipule que du "travail" ne peut être extrait que de systèmes hors-équilibre, par exemple ceux exhibant un flux naturel de chaleur entre une partie "chaude" vers une partie plus "froide". Ceci impose une borne supérieure à la quantité de "travail" qui peut être extraite de tels systèmes, via le rendement universel de Carnot.

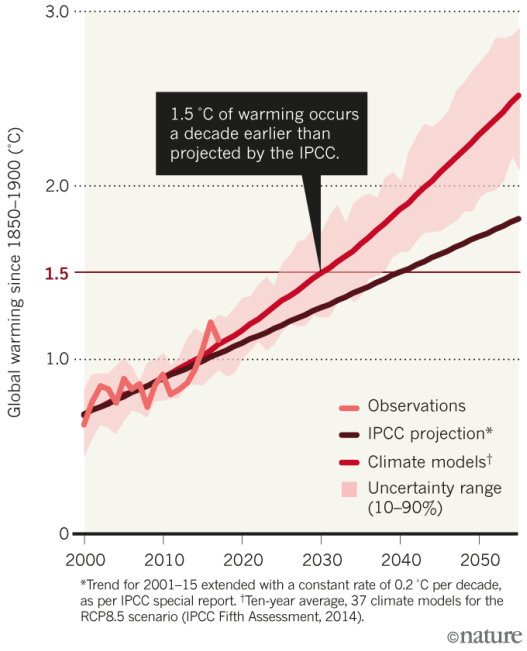

(a) Adapté de [212] : Accélération du réchauffement climatique. "Si la terre chauffe de 2 ℃ — la température limite définie lors de l'accord de Paris sur le climat en 2015 — deux fois plus de personnes subiront les problèmes liés au stress hydrique par rapport à un réchauffement de 1.5 ℃. Ce demi-degré additionnel exposera aussi 1.5 milliard de personnes à des extrema de température mortels, et des centaines de millions feront face à des maladies à transmission vectorielle telles que la malaria, parmi d'autres maladies."

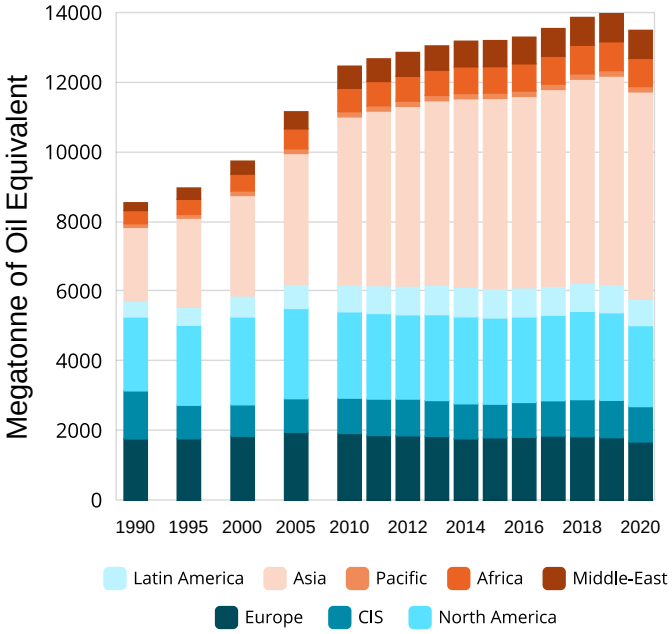

(b) Adapté de [209]. Évolution de la consommation énergétique depuis 1990. La consommation énergétique mondiale a augmenté de manière stable avec une moyenne de 2%/an entre 2000 et 2018. La consommation mondiale a augmenté de plus de 50% par rapport à 1990. Un ralentissement de 0.8% a été enregistré en 2019 et une diminution de 4% en 2020, tous deux attribués à la pandémie de COVID-19.

Fig. 2.1. – Une consommation énergétique et un réchauffement climatique accélérés

La thermoélectricité dans ce contexte offre une façon différente de réaliser des moteurs thermiques et réfrigérateurs. Une partie des recherches actuelles en thermoélectricité s'inscrit dans le domaine

de la physique mésoscopique, où les effets quantiques sont explorés tels que la nano-structuration, la manipulation des défauts ou l'ingénierie la structure de bandes [214]. La vaste majorité des études en thermoélectricité ont été faites dans le régime stationnaire, utilisant le formalisme bien établi de Landauer-Büttiker comme outil théorique. Une nouvelle vague de recherches a commencé à investiguer les régimes dépendant du temps, loin de l'équilibre. Cette vague s'inscrit dans le cadre plus général de la thermodynamique quantique, un domaine encore à ses balbutiements dans lequel on cherche à établir une formulation générale (à tout régime) et unifiée. La littérature dans le domaine de la thermoélectricité mésoscopique hors équilibre s'avère être essentiellement théorique et limitée à des modèles jouets. Étudier analytiquement des systèmes plus complexes dans le régime quantique dépendant du temps s'avère être difficile et seule la simulation semble être viable : les recherches déjà publiées sont principalement théoriques sur des modèles jouets. Sur le plan numérique, la publication en 2021 (après plusieurs années de développement) de la bibliothèque `tkwant` – extension de `kwant`, la librairie de simulation de référence pour le transport quantique – marque une étape importante dans le domaine du transport quantique dépendant du temps car elle ouvre la voie à l'investigation de systèmes complexes, difficiles à explorer auparavant. `tkwant` est cependant seulement limité au transport de particules.

Les phénomènes émergents dans ce régime sont encore pour la plupart inconnus et/ou non maîtrisés théoriquement : les concepts de la thermodynamique classique tels que le "travail" et la "chaleur" s'avèrent être difficiles à appréhender. Les définitions proposées sont encore débattues et utilisent des outils théoriques qui viennent de différents domaines de la physique, si bien que l'équivalence entre ces différentes approches est encore à démontrer. Des études théoriques préliminaires [38, 219] vont jusqu'à prédire une amélioration des propriétés thermoélectriques dans le régime transitoire. Cette thèse intervient dans ce contexte et a pour objectif d'apporter de nouvelles réponses quant au rôle du contrôle dépendant du temps dans les systèmes thermoélectriques mésoscopiques (quantiques).

Pour décrire le transport d'énergie dans des systèmes ouverts d'électrons, de manière quantique et sous l'influence de champs électromagnétiques dépendant du temps, on construit un cadre théorique invariant de jauge qui se base sur la recherche actuelle sur le transport quantique de particules. Notre approche est semi-classique : les champs électromagnétiques sont décrits par les équations (classiques) de Maxwell, tandis que les électrons sont décrits par l'équation (quantique) de Schrödinger, en négligeant l'interaction entre électrons. On utilise ensuite ce cadre pour étendre `tkwant` au transport d'énergie, grâce à un module qu'on a nommé `tkwantoperator`, permettant in fine de traiter des modèles thermoélectriques complexes et dépendant du temps. De tels modèles peuvent modéliser une large gamme de systèmes mésoscopiques qui dépassent les modèles jouets. On illustre alors la puissance de `tkwant`+`tkwantoperator` en investiguant brièvement l'effet Peltier dynamique dans le contact ponctuel quantique bidimensionnel, pour ensuite revenir vers le très étudié modèle (jouet) du niveau résonnant et tenter d'avoir une compréhension plus fondamentale des phénomènes en jeu : on utilise notre approche, dans ses déclinaisons analytique et numérique, pour obtenir une vision plus claire du potentiel de la thermoélectricité dépendante du temps dans des 'points' quantiques.

2.1. Résumé du chapitre 3 : vue d'ensemble et motivations

Dans ce chapitre, on expose une brève vue d'ensemble de l'historique de la thermoélectricité puis des développements et challenges actuels dans le domaine : la question des effets quantiques est discutée ainsi que celle de l'émergence d'un courant de recherche plus général ayant pour but de construire une théorie de thermodynamique quantique.

2.1.1. Thermoélectricité stationnaire

Les dispositifs thermoélectriques dans le régime stationnaire ont été étudiés de façon exhaustive dans les soixante-dix dernières années. Un nombre caractéristique zT, appelé 'facteur de mérite', a été introduit afin de pouvoir comparer différents matériaux et dispositifs thermoélectriques. Ce nombre caractérise aussi bien les réfrigérateurs que générateurs thermoélectriques

$$zT = \frac{\sigma S^2}{\kappa_{\mathrm{e}} + \kappa_{\mathrm{ph}}} T \tag{2.1}$$

où T est la température (absolue) moyenne de fonctionnement (la réponse linéaire est supposée pour les réservoirs chaud et froid), S est le coefficient Seebeck, σ la conductivité électrique, κ_{e} et κ_{ph} respectivement la conductivité thermique due aux électrons et aux phonons. L'expression du facteur de mérite illustre les difficultés liées à sa maximisation : les coefficients S, σ et κ sont fortement liés à la densité de charges, à la diffusion des charges, et à la structure de bandes [145] ; la contribution de chaque coefficient au sein du facteur de mérite est en compétition avec les autres. Plus le facteur de

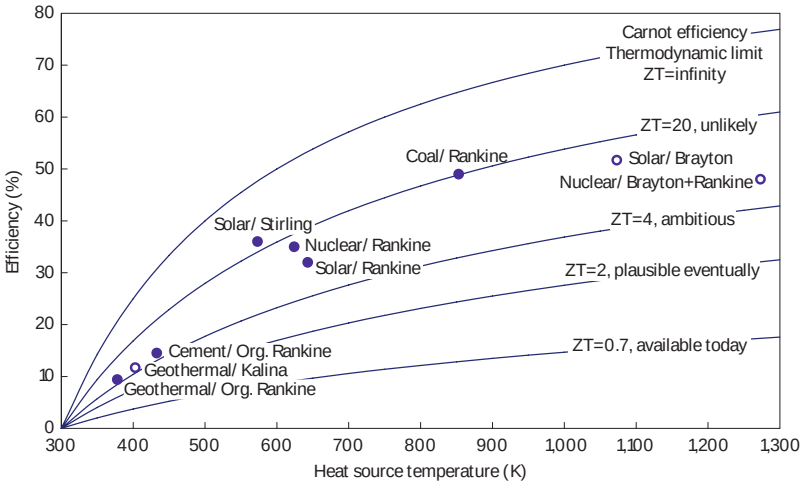

Fig. 2.2. – Extrait de [197]. Comparaison du rendement réel des procédés de conversion utilisés dans les centrales électriques avec les rendement théoriques des thermoélectriques. Les dispositifs thermoélectriques actuellement commercialisés ne sont pas compétitifs, mais si leur facteur de mérite zT arrivait à atteindre ~ 3 alors ils seraient une alternative viable pour certaines applications.

mérite zT d'un dispositif thermoélectrique est haut, plus son rendement est élevé (voir Fig. 2.2) : une valeur $zT \gtrsim 3$ doit être atteinte pour que des dispositifs thermoélectriques soient adoptés à grande échelle pour de la conversion électrique et réfrigération [191]. La valeur du facteur de mérite des réfrigérateurs et générateurs thermoélectriques disponibles à l'achat est actuellement aux alentours de $zT \approx 1$ ce qui restreint leur applicabilité.

2.1.2. Thermoélectricité dépendante du temps à l'échelle mésoscopique

La thermoélectricité proche de l'équilibre, dans le régime stationnaire, est relativement bien comprise et décrite de manière satisfaisante par la théorie [75, 16]. Cependant, la description théorique devient plus complexe quand les systèmes sont poussés loin de l'équilibre par de grandes tensions électrochimiques, températures ou à travers un contrôle temporel 'rapide'. L'un des objectifs des recherches actuelles dans le domaine est d'établir une théorie de la thermodynamique dans les systèmes mésoscopiques (quantiques) dépendant du temps : une description locale en température et courants

de chaleur est difficile voire impossible, en particulier quand un contrôle dépendant du temps non quasi-statique est à prendre en compte. Des études théoriques récentes prédisent une amélioration des propriétés thermoélectriques sur des modèles de 'points quantiques' [38, 219] (voir Fig 2.3), mais la physique sous-jacente reste incomprise. De plus, ces études ne permettent pas de se prononcer sur le cas de systèmes plus réalistes. D'un autre côté, l'expérimentation a fait de grands progrès dans le domaine de la nanoélectronique haute fréquence, ce qui laisse envisager des expériences futures de thermoélectricité dépendante du temps dans ces systèmes.

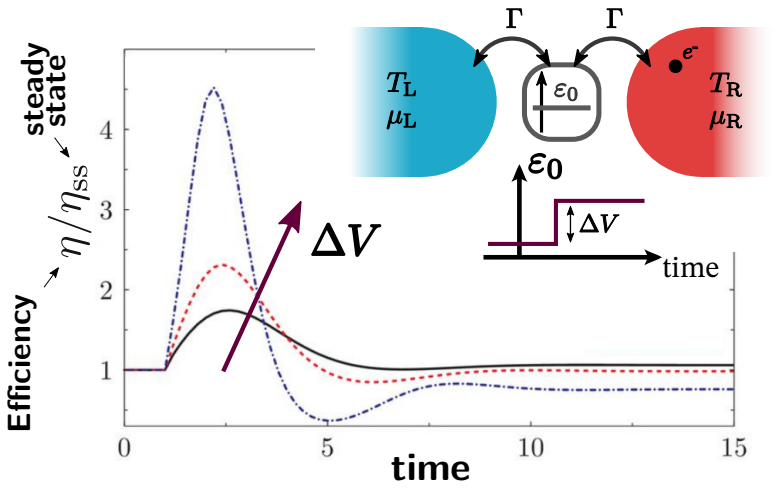

Fig. 2.3. – Adapté de [219] : "Booster le rendement avec un contrôle dépendant du temps". Le modèle du niveau résonnant, un système à niveau unique connecté à deux réservoirs thermiques (avec un taux Γ), voit son rendement en générateur électrique multiplié par 4, par rapport au régime stationnaire, pendant le régime transitoire, quand le niveau d'énergie ε_0 (initialement à 0.5Γ) subit un saut abrupt de $\Delta V = 0.2\Gamma$ (courbe noire), 0.3Γ (courbe rouge) et 0.5Γ (courbe bleue).

Défis théoriques en thermodynamique quantique La théorie de la thermodynamique a pour but de décrire simplement, avec un petit nombre de paramètres physiquement interprétables à notre échelle, des systèmes à grand nombre de degrés de liberté microscopiques. Pour atteindre une telle simplification, une moyenne est effectuée sur les degrés de liberté, le temps et l'espace. La théorie (classique) de la thermodynamique se résume par trois postulats fondamentaux : *(i)* l'énergie est une grandeur qui se conserve ; *(ii)* l'entropie du système considéré et son environment ne peut qu'augmenter (entre deux états à l'équilibre) ; *(iii)* un système ne peut atteindre le zero absolu en température en un temps fini. Le rendement de Carnot $\eta_C = 1 - T_C/T_H$, où T_H et T_C sont les températures respectives du réservoir chaud et froid, est l'une des grandeurs les plus connues en thermodynamique : aucune machine thermique cyclique, quelque soit son fonctionnement interne, ne peut avoir un rendement $\eta = W/Q_H$ supérieur au rendement de Carnot η_C, où W et Q_H sont les moyennes sur un cycle du travail produit par la machine et de la chaleur perdue par le réservoir chaud.

La physique quantique traite les systèmes dont la taille est inférieure à la limite thermodynamique classique, où des effets quantiques entrent en jeu tels que l'interférence et l'intrication. Des premiers travaux ont prédit que les lois classiques de la thermodynamique sont violées dans le monde quantique, comme le second principe cité plus haut [219, 72, 7, 58]. Des recherches ultérieures, discutées (entre autres) dans les références [107, 68, 198], ont construit une première formulation d'une théorie quantique de la thermodynamique, utilisant l'approche des équations maîtresses de Lindblad avec l'hypothèse markovienne (voir Sec. 3.3.3 plus bas) : ces recherches montrent qu'aucune violation n'a lieu et que les lois classiques sont retrouvées dans certains modèles [70, 71, 156]. La thermodynamique

quantique en est encore à ses débuts : un consensus est reste à être atteint sur les définitions du 'travail' et de la 'chaleur', la recherche est en cours pour construire une description cohérente où l'équivalence (ou la différence) des différentes approches théoriques développées est comprise et démontrée.

2.1.3. Revue des approches théoriques

Dans la suite du chapitre 3, on expose brièvement les principales techniques théoriques utilisées pour décrire le transport quantique dépendant du temps des électrons, et de l'énergie qu'ils transportent, dans des systèmes mésoscopiques. Le contrôle dynamique (*i.e.* dépendant du temps) rend le transport inélastique et complexifie considérablement le problème. Plusieurs techniques ont été développées avec différents degrés d'approximation et de complexité (inhérente à chaque outil) : le formalisme des Fonctions de Green Hors-Équilibre, la théorie de la diffusion (dépendante du temps), les approches à équation maîtresse ou la théorie de la fonctionnelle de la densité dépendante du temps. Ces approches peuvent être combinées avec l'approche de Floquet dans le cas d'un contrôle périodique. Dans cette thèse, on se concentre sur la théorie de la diffusion qui se base sur les fonctions d'onde, utilisée dans la bibliothèque `tkwant`.

Théorie de la diffusion La théorie de la diffusion s'applique à des électrons sans interaction (l'interaction à champ moyen peut néanmoins être prise en compte). Elle décrit des systèmes composés d'une région centrale, appelée région de diffusion, connectée à des guides d'onde qui mènent vers différents réservoirs thermiques (voir Fig. 2.4)

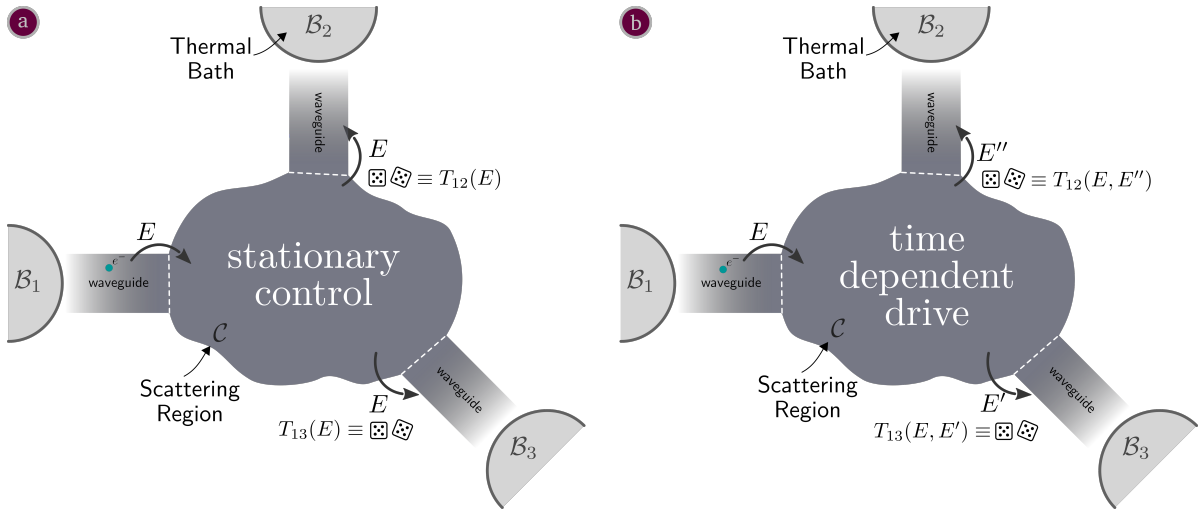

Fig. 2.4. – Illustration de l'approche par diffusion. Un système central, appelé région de diffusion, est connecté à différents réservoirs thermiques $\mathcal{B}$ par des guides d'onde. Des électrons quittent chaque réservoir $\mathcal{B}_\alpha$, avec des énergies E suivant une distribution thermique, pour se diriger vers la région de diffusion à travers les guides d'onde. Les électrons entrant dans la région de diffusion interfèrent et subissent diverses réflexions en son sein puis sont finalement transmis via les guides d'onde vers les divers réservoirs $\mathcal{B}_\beta$, soit *a)* avec la même énergie E dans le régime stationnaire, avec une probabilité $T_{\alpha\beta}(E)$, soit *b)* avec une énergie E' a priori différente dans le régime dépendant du temps, avec une probabilité $T_{\alpha\beta}(E, E')$.

Chaque réservoir thermique remplit les modes incidents (vers la région de diffusion) des guides d'onde suivant une distribution thermique, le système central quant à lui affecte quels modes sortants sont remplis. Dans cet approche les réservoir thermiques ne sont pas affectés par les électrons qui leur

reviennent : leur température et potentiel chimique restent constants. Un électron, représenté par une fonction d'onde (voir 4.2.1.1), quitte un réservoir thermique α pour ensuite entrer dans la région de diffusion, avant d'être finalement réfléchis/transmis dans un réservoir thermique β avec une probabilité $T_{\alpha\beta}$. Les probabilités $T_{\alpha\beta}$ peuvent être calculées en résolvant l'équation de Schrödinger, dans les régimes stationnaire et dépendant du temps, et cela permet d'écrire les courants nets de particules et d'énergie quittant chaque guide d'onde α. Il est à noter que le calcul de ces probabilités peut être omis dans une approche numérique (du type `tkwant`) qui calcule les fonctions d'onde directement. On utilisera cette théorie tout au long de cette thèse, une description plus complète est faite dans la section 5.1 (en anglais). Une revue du développement original de la théorie de diffusion de particules est faite dans la Réf. [20].

Réponse linéaire Une approche complémentaire, qui peut être utilisée conjointement avec la théorie de la diffusion, est celle de la réponse linéaire. Dans un système à deux réservoirs 'gauche' L et 'droit' R (voir Fig. 2.5), cette approche est valide quand le biais en température $\Delta T = T_{\mathrm{L}} - T_{\mathrm{R}}$ et en potentiel chimique $\Delta\mu = \mu_{\mathrm{L}} - \mu_{\mathrm{R}}$ sont petits par rapport à leur valeur moyenne.

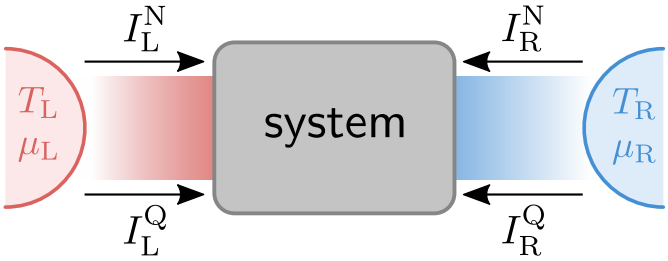

Fig. 2.5 – Représentation d'un système thermoélectrique à deux terminaux. Connecté à deux réservoirs – gauche (L) et droit (R) – le système est traversé par des courants de chaleur I_α^{Q} et de particules I_α^{N} qui partent d'un réservoir α =L,R à l'autre.

Dans le régime stationnaire, on considère sans perte de généralité les courants nets de particules $I_{\mathrm{L}}^{\mathrm{N}}$ et chaleur $I_{\mathrm{L}}^{\mathrm{Q}}$ dans le guide d'onde de gauche. et de chaleur . Ils sont connectés aux biais $\Delta V/T$ ($\Delta V = \Delta\mu/e$) et $\Delta T/T^2$ par la *matrice d'Onsager* $\mathbf{L}$[29, 76]

$$\begin{bmatrix} I_{\mathrm{L}}^{\mathrm{N}} \\ I_{\mathrm{L}}^{\mathrm{Q}} \end{bmatrix} = \underbrace{\begin{bmatrix} L_{\mathrm{NN}}^{\mathrm{L}} & L_{\mathrm{NQ}}^{\mathrm{L}} \\ L_{\mathrm{QN}}^{\mathrm{L}} & L_{\mathrm{QQ}}^{\mathrm{L}} \end{bmatrix}}_{\mathbf{L}} \begin{bmatrix} \Delta V/T \\ \Delta T/T^2 \end{bmatrix} \tag{2.2}$$

où L_{AB} (A,B=N,Q) sont les *coefficients d'Onsager*. Cette approche a été étendue au régime périodique et lentement dépendant du temps (*i.e.* quasi-statique) dans la Réf. [118], l'approche de la réponse linéaire est utilisée dans le régime non quasi-statique et il est observé que les coefficients d'Onsager étendus à ce régime violent des contraintes liées au second principe (vérifiées dans le régime stationnaire). On montre cependant dans la section 6.1 qu'une matrice d'Onsager résolue en temps n'est pas unique et ne peut donc pas être utilisée telle quelle dans des considérations physiques.

2.2. Résumé du chapitre 4 : fondements théoriques

Dans ce chapitre, on construit une théorie locale du transport quantique d'électrons sans interaction et de l'énergie qu'ils transportent, sous l'influence d'un champ électromagnétique dépendant du temps. Premièrement, on passe brièvement en revue l'approche classique équivalente pour exposer certaines idées qu'on transférera vers notre description quantique. Ensuite, on introduit la théorie du transport quantique d'un seul électron, décrit par une fonction d'onde, dans l'espace continu et discret. Finalement, on généralise cette approche à un électron à plusieurs électrons sans interaction. Ce chapitre établit la théorie de transport thermoélectrique quantique, dont la partie énergétique sera implémentée dans `tkwant` dans le chapitre 5.

2.2.1. Électrodynamique classique

L'approche classique du transport de charge sous l'influence d'un champ électromagnétique est de décrire le mouvement de particules chargées par la mécanique classique, en utilisant l'une des approches équivalentes parmi la mécanique Newtonienne, Lagrangienne ou Hamiltonienne ; et de décrire le champ électromagnétique et son interaction avec la matière chargée par les équations de Maxwell. Ces dernières équations décrivent les relations entre le champ électrique $\vec{E}(\vec{r},t)$, le champ magnétique $\vec{B}(\vec{r},t)$, la densité locale de charge $\rho(\vec{r},t)$ et la densité locale de courant de charge $\vec{j}(\vec{r},t)$. Les équations de Maxwell impliquent une relation de conservation de la charge

$$\partial_t \rho(\vec{r},t) + \vec{\nabla}\cdot\vec{j}(\vec{r},t) = 0 \tag{2.3}$$

mais aussi de l'énergie, à travers l'équation de Poynting

$$\partial_t u_{\text{EM}} + \vec{\nabla}\cdot\vec{\pi} = -\vec{j}\cdot\vec{E} \tag{2.4}$$

où $-\vec{j}\cdot\vec{E}$ est la puissance cédée localement aux charges, $u_{\text{EM}} = (\varepsilon_0 E^2 + \frac{1}{\mu_0}B^2)/2$ est l'énergie électromagnétique locale et $\vec{\pi} = \vec{E}\times\vec{B}/\mu_0$ est le vecteur de Poynting, *i.e.* le champ décrivant le flux d'énergie transportée par la lumière. La dérivation de l'équation de conservation d'énergie (2.4) met en avant un degré de liberté intrinsèque quant à la définition de $\vec{\pi}$: un problème analogue sera rencontré quand on tentera de définir le courant d'énergie transportée par des particules quantiques.

Invariance de jauge En mécanique Hamiltonienne (classique [141] et quantique [111]), l'effet du champ électromagnétique sur la matière chargée est décrit à travers des 'potentiels' : le potentiel scalaire $\phi(\vec{r},t)$ et le potentiel vecteur $\vec{A}(\vec{r},t)$. Leur relation au champ électromagnétique $(\vec{E},\vec{B})$ est la suivante

$$\begin{aligned}\vec{E} &= -\vec{\nabla}\phi - \partial_t\vec{A}\\ \vec{B} &= \vec{\nabla}\times\vec{A}\end{aligned} \tag{2.5}$$

Cette relation met en évidence la non-unicité des potentiels : un champ scalaire arbitraire $\Lambda(\vec{r},t)$ peut être utilisé pour définir des potentiels différents. En ajoutant sa dérivée temporelle $\partial_t\Lambda$ au potentiel scalaire $\phi(\vec{r},t)$ et en soustrayant son gradient $\vec{\nabla}\Lambda$ au potentiel vecteur $\vec{A}(\vec{r},t)$, le champ électromagnétique $(\vec{E},\vec{B})$ reste invariant d'après l'Eq. (2.5).

$$\forall\Lambda(\vec{r},t),\quad \begin{cases}\vec{A}' = \vec{A} - \vec{\nabla}\Lambda\\ \phi' = \phi + \partial_t\Lambda\end{cases} \implies \begin{cases}\vec{E}' = \vec{E}\\ \vec{B}' = \vec{B}\end{cases} \tag{2.6}$$

Étant donné que l'interaction entre le champ électromagnétique et la matière chargée est classiquement décrite à travers les champs $(\vec{E},\vec{B})$ et non les potentiels, la physique reste invariante après un tel changement sur les potentiels. La transformation donnée par l'Éq. (2.6) est appelée 'transformation de jauge'.

Énergie mécanique : le problème de la dépendance temporelle Quand on considère une particule chargée classique sous l'influence d'un champ électromagnétique dépendant du temps, la définition usuelle de l'énergie mécanique – la somme de l'énergie cinétique et de l'énergie potentielle associée au potentiel scalaire ϕ – devient dépendante de la jauge considérée comme on peut le voir dans l'équation suivante :

$$\mathrm{d}_t U = \mathrm{d}_t\left[\frac{1}{2}m\dot{\vec{r}}^2(t) + q\phi(\vec{r}(t),t)\right] = q\partial_t\phi(\vec{r}(t),t) - q\partial_t\vec{A}(\vec{r}(t),t)\cdot\dot{\vec{r}}(t) \tag{2.7}$$

Cela rend la définition de l'énergie mécanique, originellement dans le stationnaire, non acceptable dans le cas dépendant du temps : cette problématique apparaît en physique quantique aussi, si l'on considère l'Hamiltonien comme un opérateur d'énergie.

2.2.2. Électrodynamique semi-classique

Dans la section précédente, on a parcouru les bases de l'électrodynamique classique, en nous focalisant sur le transport de charge et d'énergie. Dans le cadre de cette thèse, le comportement des électrons est décrit par la mécanique quantique. Dans ce domaine, le transport de particules est connu et traité dans les livres de référence ; le traitement du transport d'énergie quant à lui reste marginal, en particulier par rapport à l'invariance de jauge : on remet au goût du jour une telle approche à travers une description complète du transport d'énergie avec une équation de conservation invariante de jauge.

Mécanique quantique à un corps En mécanique quantique, à chaque instant t, les propriétés physiques d'un électron (énergie, position, quantité de mouvement [56, Chap. 21-3], moment angulaire...) peuvent toutes être calculées à partir de la 'fonction d'onde' $\psi(\vec{r},t)$. L'équation d'évolution de la fonction d'onde est donnée par l'équation de Schrödinger

$$\mathrm{i}\hbar\partial_t\psi(\vec{r},t) = \hat{h}[\psi](\vec{r},t) \tag{2.8}$$

L'équation de Schrödinger admet plusieurs solutions qui forment un espace vectoriel, cela met en place la description mathématique de la 'superposition quantique' : une particule peut être dans une superposition linéaire de telles solutions.

L'Hamiltonien $\hat{h}$ est l'équivalent quantique de 'l'énergie mécanique' : la somme de l'énergie cinétique $\hat{\kappa}$, de l'énergie potentielle associée au potentiel (scalaire) électrique $q\hat{\phi}[\psi] = q\phi(\vec{r},t)\,\psi$ et d'une éventuelle énergie potentielle additionnelle $V(\vec{r})$

$$\hat{h}[\psi] = \hat{\kappa}[\psi] + q\,\phi(\vec{r},t)\,\psi + V(\vec{r})\psi \tag{2.9}$$

→ Transport dynamique de particules La densité locale de courant $\vec{j}_\psi(\vec{r},t)$ et de particules $\rho_\psi(\vec{r},t)$ (qui s'expriment en fonction de la fonction d'onde ψ) obéissent à une loi de conservation

$$\partial_t\rho_\psi(\vec{r},t) + \vec{\nabla}\cdot\vec{j}_\psi(\vec{r},t) = 0 \tag{2.10}$$

Ce résultat est connu et exposé dans les livres de référence en physique quantique [111, Chap. 10.3] [172, Chap. 16.4][56, Chap. 21-2].

→ Transport dynamique d'énergie Bien que non décrit dans la plupart des livres de référence en physique quantique, la référence [127] introduit des définitions de grandeurs énergétiques locales – l'énergie étant portée par des électrons (quantiques) – qui obéissent à une équation de conservation. Pour une fonction d'onde ψ donnée, l'équation de conservation a la forme suivante

$$\partial_t\rho^\epsilon_\psi(\vec{r},t) + \vec{\nabla}\cdot\vec{j}^\epsilon_\psi(\vec{r},t) = S^\epsilon_\psi \tag{2.11}$$

où ρ^ϵ_ψ, $\vec{j}^\epsilon_\psi$ et S^ϵ_ψ sont des candidats pour respectivement la densité d'énergie, la densité de courant d'énergie et la puissance donnée localement aux électrons. Plusieurs candidats (indexés par l'exposant

ϵ) sont possibles pour chacun de ces termes : ils peuvent être définis en prenant comme opérateur énergie l'Hamiltonien $\hat{h}$, l'énergie cinétique $\hat{\kappa}$ ou bien 'l'énergie totale' $\hat{\varepsilon}$ (définis plus bas). Chaque densité $\rho^{\varepsilon}_{\psi}, \vec{j}^{\varepsilon}_{\psi}, S_{\psi}$, une fois intégrée sur l'espace, doit donner la valeur moyenne de l'opérateur associé, sur l'état ψ. Dans le contexte d'une particule unique non-relativiste, les quantités quantiques locales $(\rho^{\varepsilon}_{\psi}, j^{\varepsilon}_{\psi}, S^{\varepsilon}_{\psi})$ ne portent aucune signification physique car elles sont non uniques (pour un même opérateur associé). En revanche, leur intégrale sur l'espace est bien unique (donnant la valeur moyenne de l'opérateur défini sur le système entier) [127, 8]. Des expressions génériques possibles pour la densité d'énergie ρ^{ϵ}_{ψ} et la densité de courant d'énergie $\vec{j}^{\epsilon}$ sont les suivantes

$$\rho^{\epsilon}_{\psi} = \mathrm{Re}\Big[\psi^* \hat{\epsilon}[\psi]\Big] \tag{2.12}$$

$$\vec{j}^{\epsilon}_{\psi} = \frac{1}{2}\mathrm{Re}\left[\hat{\epsilon}[\psi]^* \, \hat{\vec{v}}[\psi] + \psi^* \hat{\vec{v}}[\hat{\epsilon}[\psi]]\right] \tag{2.13}$$

Une contrainte additionnelle s'applique sur les opérateurs candidats pour représenter une énergie : l'invariance de jauge. En effet, les potentiels électromagnétiques $(\phi, \vec{A})$ peuvent être remplacés par changement de jauge, à travers l'Éq. (2.6), sans changer la valeur moyenne d'un opérateur énergie. La valeur moyenne de l'Hamiltonien ne respecte pas cette invariance : fondamentalement, seule l'énergie cinétique $\hat{\kappa}$ respecte cette invariance, à laquelle on peut ajouter une énergie potentielle stationnaire V – qu'on suppose indépendante du champ électromagnétique – pour définir l'opérateur énergie totale $\hat{\varepsilon}$

$$\hat{\varepsilon}(t) = \hat{\kappa}(t) + V \tag{2.14}$$

qui elle aussi est invariante de jauge [127, 102, 213]. L'expression du terme source S^{ε} associé à cet opérateur coïncide avec l'expression classique de la puissance cédée localement aux électrons par le champ électromagnétique (voir l'Éq. (2.4))

$$S^{\varepsilon}(\vec{r}, t) = q\vec{j} \cdot \vec{E} \tag{2.15}$$

Bien que les expressions pour les autres opérateurs énergie soient dérivées dans cette thèse, on utilisera par défaut 'l'énergie totale' comme opérateur énergie car cet opérateur est invariant de jauge et permet de retrouver les résultats établis dans la littérature dans le cas particulier du régime stationnaire (à travers V).

Description quantique de systèmes à plusieurs électrons sans interaction Quand on considère un système quantique à plusieurs électrons sans interaction, ses états peuvent être écrits à partir des états à un électron mais en imposant la contrainte d'antisymétrie totale : les électrons sont indiscernables et au plus un électron peut occuper un état à un corps donné. Les états à plusieurs électrons sont décrits en dénombrant les occupations des états à un électron, sans dire quel électron occupe quel état, grâce aux opérateurs associés de *création* $\hat{c}^{\dagger}_{\lambda_i}$ et d'*annihilation* $\hat{c}_{\lambda_i}$. Dans une représentation en liaisons fortes utilisant un ensemble discret de fonctions d'onde sans spin λ_i localisées spatialement sur des sites i (on utilisera $\hat{c}^{\dagger}_{\lambda_i} \to \hat{c}^{\dagger}_i$) pour réaliser des représentation en liaison fortes, les opérateurs $\hat{O}$ sans interaction s'écrivent

$$\hat{O}(t) = \sum_{ij} o_{ij}(t)\, \hat{c}^{\dagger}_i \hat{c}_j \;\; \text{où} \;\; o_{ij}(t) = \langle i | \, \hat{o} \, | j \rangle \tag{2.16}$$

où les coefficients $o_{ij}(t)$ peuvent être définis empiriquement, estimés par comparaison aux expériences ou par des calculs '*ab initio*'.

→ Opérateur énergie locale Dans notre description continue à un corps précédente, on a défini des densités locales $\rho^{\epsilon}_{\psi}(\vec{r},t)$ telles que leur intégrale sur l'espace coïncide la valeur moyenne de leur opérateur énergie $\hat{\epsilon}$ associé, défini sur le système entier. Nous avons vu qu'une équation de conservation (2.11) est vérifiée pour chacune des densités, avec une densité locale de courant $\vec{j}^{\epsilon}_{\psi}(\vec{r},t)$ et de puissance délivrée $S^{\epsilon}_{\psi}(\vec{r},t)$ associées. Il n'y a cependant pas d'unique définition de densités *locales* d'énergie ou de courant d'énergie [127, 8], dans les approches à un corps et à plusieurs corps. Ce problème affecte aussi la définition de l'énergie d'une sous-partie d'un système : il se traduit par un arbitraire dans les proportions avec lesquelles 'l'énergie de couplage', qui réside sur la frontière séparant le sous-système considéré et le reste du système, est attribuée à ces deux sous-systèmes. Dans des systèmes en représentation liaisons-fortes, cette problématique intervient quand on veut définir l'opérateur densité d'énergie $\hat{\mathcal{E}}^{\epsilon}_{i}$ d'un unique site i : on adopte la définition suivante

$$\hat{\mathcal{E}}^{\epsilon}_{i} = \frac{1}{2}\sum_{j} \epsilon_{ij}\,\hat{c}^{\dagger}_{i}\hat{c}_{j} + \epsilon_{ji}\,\hat{c}^{\dagger}_{j}\hat{c}_{i} \tag{2.17}$$

L'idée de considérer la moitié de la contribution des termes de couplage a été introduite par la Réf. [8] dans le cadre d'une étude sur des solides harmoniques désordonnées. Cette séparation a été ensuite utilisée par la Réf. [210] pour définir un opérateur d'énergie locale dans une chaîne 1D discrète. Enfin, une définition générique dans un système liaisons-fortes a été introduite dans la Réf. [129] où l'expression donnée est celle donnée par l'Éq. (2.17) mais pour l'opérateur Hamiltonien seulement ($\epsilon = h$). Cette expression est déduite d'une séparation 'naturelle' [119] qui émerge de la discrétisation des définitions originelles dans l'espace continu (voir la dérivation qui aboutit à l'Éq. (4.62)). Elle a aussi été utilisée par les Réfs. [25, 143] mais en utilisant l'Hamiltonien comme opérateur énergie. De notre côté, on apporte un argument additionnel qui soutient cette définition avec un partage symétrique des termes de couplage entre les sites dans $\hat{\mathcal{E}}^{\varepsilon}_{i}$: elle permet d'obtenir une expression pour le terme source S^{ε}_{i} qui concorde avec la version discrète du résultat classique donné à l'Éq. (2.4). D'un autre côté, cette définition d'un opérateur énergie local (ou d'un sous-système) intervient dans un débat, toujours en cours, qui concerne la définition d'un courant de chaleur, voir Sec. 4.3.4.2 (en anglais).

→ Transport quantique à plusieurs corps On utilise la fonction de Green 'lesser' pour exprimer les valeurs moyennes des opérateurs à plusieurs corps sans interaction

$$G^{<}_{ij}(t) = \frac{\mathrm{i}}{\hbar}\left\langle \hat{c}^{\dagger}_{j}(t)\hat{c}_{i}(t)\right\rangle \tag{2.18}$$

Cette fonction permet d'écrire les équations de conservation (particules et énergie) dans le cas à plusieurs corps sans interaction. Ces équations ont la même forme que leurs contreparties à un corps, dérivées à la Sec. 4.2.4 (en anglais). Elles peuvent être dérivées en appliquant l'équation de Heisenberg (équivalente à l'équation de Schrödinger) sur la valeur moyenne $\rho_i = \langle\hat{\rho}_i\rangle$ des opérateurs densité locale de particules et d'énergie

$$\underbrace{\partial_t\rho_i(t) = \frac{\mathrm{i}}{\hbar}\left\langle\left[\hat{H}(t),\hat{\rho}_i(t)\right]\right\rangle + \langle\partial_t\hat{\rho}_i(t)\rangle}_{\text{Équation d'Heisenberg (4.135)}} \quad\Longrightarrow\quad \underbrace{\partial_t\rho_i(t) + \textstyle\sum_j I_{ij}(t) = S_i(t)}_{\text{Équation de conservation}} \tag{2.19}$$

où I_{ij} est le courant net du site i vers le site j et $S_i(t)$ est le terme 'source'. Dans le cas bien connu du transport de particules la densité de particules s'écrit $\rho_i = \left\langle\hat{c}^{\dagger}_{i}\hat{c}_{i}\right\rangle = -\mathrm{i}\hbar G^{<}_{ii}(t)$, le courant a pour expression $I^{\mathrm{N}}_{ij} = 2\,\mathrm{Re}[h_{ij}(t)G^{<}_{ji}(t)]$ et le terme source est nul car aucune particule n'est créée ni détruite du néant. Pour l'énergie, la densité peut s'écrire de la manière suivante

$$\rho^{\epsilon}_{i}(t) = \left\langle\hat{\mathcal{E}}^{\epsilon}_{i}(t)\right\rangle = \sum_{j}\mathrm{Im}\left[\epsilon_{ij}(t)G^{<}_{ji}(t)\right] \tag{2.20}$$

puis on utilise l'Éq. (2.19) pour obtenir une expression générique pour le courant d'énergie

$$I^{\epsilon}_{ij} = \frac{1}{\hbar}\sum_{k} \mathrm{Re}\left[\epsilon_{ki}\epsilon_{ij}G^{<}_{jk} - \epsilon_{kj}\epsilon_{ji}G^{<}_{ik}\right] \tag{2.21}$$

où ϵ_{ij} est à remplacer par les coefficients de l'opérateur énergie considéré. Comme dans le cas continu, l'expression du courant d'énergie I^{ϵ}_{ij} n'est pas unique mais doit donner la bonne divergence $\sum_j I^{\epsilon}_{ij}$. Le terme source – la puissance cédée aux électrons – est dépendant de l'opérateur considéré et s'écrit de la manière suivante pour l'opérateur 'énergie totale'

$$S^{\varepsilon}_{i}(t) = \sum_{j} -\frac{1}{2}q\left[\phi_j(t) - \phi_i(t)\right] I^{N}_{ij}(t) + \sum_{j}\mathrm{Im}\left[\partial_t \varepsilon_{ij}(t) G^{<}_{ji}(t)\right] \tag{2.22}$$

Le premier terme de cette expression a une interprétation simple

$$\sum_{j} -\frac{1}{2}q\left[\phi_j(t) - \phi_i(t)\right] I^{N}_{ij}(t) = -q\vec{\nabla}\phi_i \cdot \vec{j}_i \tag{2.23}$$

alors que le second terme doit être retravaillé (fait en anglais dans l'appendice B.3) pour montrer la réécriture suivante

$$\sum_{j}\mathrm{Im}\left[\partial_t \varepsilon_{ij}(t) G^{<}_{ji}(t)\right] = -\partial_t \vec{A}_i \cdot \vec{j}_i \tag{2.24}$$

pour enfin que l'on retrouve pour $S^{\varepsilon}_{i}(t)$ l'expression classique de la puissance cédée aux électrons $\vec{j}\cdot\vec{E}$ (voir l'Éq. (2.4)), où $\vec{E} = -\vec{\nabla}\phi - \partial_t\vec{A}$ est le champ électrique dépendant du temps.

→ Courants dans les guides d'onde Les études théoriques de transport mésoscopique dynamique considèrent un système générique constitué d'un système central, sous l'influence d'un champ électromagnétique dépendant du temps, qui est connecté à des guides d'électrons $\mathcal{L}_\alpha$ semi-infinis. Chaque guide est rempli d'électrons qui se dirigent vers le système central, suivant une distribution thermique a une température T_α et un potentiel chimique μ_α (voir Fig. 2.6). Le but principal est alors d'obtenir les courants nets de particules et d'énergie qui sortent de chaque guide. Pour les calculer en utilisant les courants locaux d'énergie I^{ϵ}_{ij} et de particules I^{N}_{ij}, un flux est exprimé à travers une section dans chacun des leads $\mathcal{L}_\alpha$.

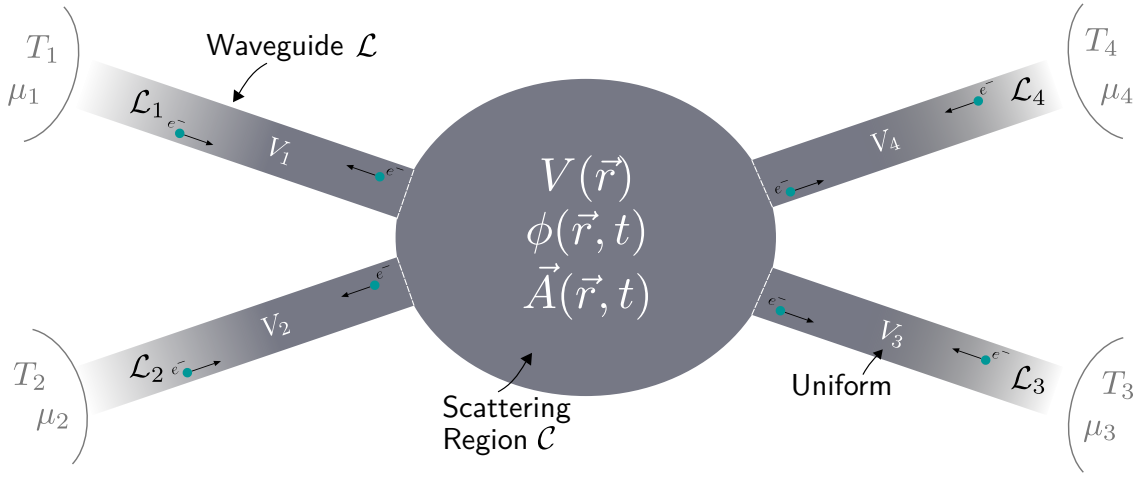

Fig. 2.6. – **Systèmes considérés dans les études de transport**, composés d'une partie centrale ('région de diffusion') $\mathcal{C}$ connectée à des guides d'onde semi-infinis. La partie centrale est sous l'influence d'un champ électromagnétique dépendant du temps, représenté par le potentiel scalaire $\phi(\vec{r},t)$ et potentiel vecteur $\vec{A}(\vec{r},t)$. Une énergie potentielle stationnaire V additionnelle est aussi prise en compte. Chaque guide $\mathcal{L}_\alpha$ est connecté à un réservoir d'électrons à l'équilibre thermodynamique caractérisé par une température T_α et un potentiel chimique μ_α.

Les systèmes qu'on décrit sont sans interaction, ce qui implique qu'aucun mécanisme de relaxation thermique peut être considéré : des températures et les courants de chaleur locaux ne peuvent pas être définis au sein du système. Cependant, une hypothèse usuellement faite dans le régime stationnaire [16] est de considérer que chaque électron quittant la partie centrale $\mathcal{C}$ du système, dans le guide $\mathcal{L}_\alpha$, avec une énergie E, va finalement atteindre le réservoir thermique connecté à ce guide d'onde. Cet électron finira par relaxer au sein de ce réservoir et apportera ainsi une contribution $E-\mu_\alpha$ au terme de chaleur. En termes de courants, cela se traduit en un courant de chaleur stationnaire qui s'écrit $I_\alpha^{\mathrm{Q,st}} = I_\alpha^{\epsilon,\mathrm{st}} - \mu_\alpha I_\alpha^{\mathrm{N,st}}$ où $I_\alpha^{\mathrm{Q,st}}$ est le courant de chaleur net qui traverse le guide α. Définir un courant de chaleur résolu en temps, dans le cas dépendant du temps, fait partie du domaine plus général de la thermodynamique quantique. Ce domaine n'en est qu'à ses débuts et des recherches sont en cours pour définir un cadre théorique solide : des questions fondamentales doivent être résolues quant à la séparation spatiale entre le système central, les réservoirs thermiques et leur couplage. Dans le régime de couplage faible, une théorie robuste a été établie [23, 52, 107, 68]. Dans le régime de fort couplage, en particulier quand ce dernier est dépendant du temps, définir un courant de chaleur résolu en temps soulève une question fondamentale [31, 54, 44, 25, 143] : la partie $\hat{H}_{\mathcal{C}\alpha}$ de l'Hamiltonien total $\hat{H}$, qui couple le réservoir thermique au système central, n'est plus négligeable, peut être dépendante du temps, et doit être prise en compte lors d'une tentative de définition d'un courant de chaleur à cette interface (le problème de définir un opérateur local d'énergie, exposé au paragraphe 'opérateur énergie locale' p.34, s'applique ici). Une expression du courant de chaleur résolu en temps dans un guide a été donné par les Réfs. [119, 121] où le courant d'énergie inclut la moitié de la contribution du terme de couplage $\hat{H}_{\mathcal{C}\alpha}$

$$I_\alpha^{\mathrm{Q},h}(t) = -\partial_t \left\langle \hat{\tilde{H}}_\alpha + \frac{1}{2}\hat{H}_{\mathcal{C}\alpha} \right\rangle - \mu_\alpha I_\alpha^{\mathrm{N}}(t) \qquad \hat{\tilde{H}}_\alpha = \sum_{i,j\in\mathcal{L}_\alpha} h_{ij}(t)\hat{c}_i^\dagger \hat{c}_j + \mathrm{h.c.} \tag{2.25}$$

Cette définition est consistante avec la définition usuelle utilisée dans le régime stationnaire où l'Hamiltonien de couplage $\hat{H}^{\mathcal{C}\alpha,\mathrm{st}}$ n'intervient pas ($\partial_t \left\langle \hat{H}^{\mathcal{C}\alpha} \right\rangle = 0$). Des problèmes ont cependant été soulevés pour une telle définition [54, 142] (dans le cas où $\hat{H}^{\mathcal{C}\alpha}$ dépend du temps) et un terme additionnel, qui implique l'Hamiltonien de couplage, a été suggéré [81] pour y remédier (mais ce terme est nul dans

notre approche dans laquelle la perturbation temporelle provient uniquement d'un champ électromagnétique externe). Étant donné que l'Hamiltonien n'est en général pas invariant de jauge, on modifie cette définition de courant de chaleur $I_\alpha^{\mathrm{Q},h}(t)$ basée sur l'Hamiltonien en une définition $I_\alpha^{\mathrm{Q}}(t) = I_\alpha^{\mathrm{Q},\varepsilon}(t)$ basée sur 'l'énergie totale' (ces deux définitions coincident sur des guides *stationnaires* et diffèrent sinon, voir la Sec. 5.3.2.3 en anglais)

$$I_\alpha^{\mathrm{Q}}(t) = I_\alpha^{\varepsilon}(t) - S_\alpha^{\varepsilon}(t) - \mu_\alpha I_\alpha^{\mathrm{N}}(t) \tag{2.26}$$

où $I_\alpha^{\varepsilon}(t)$ et $S_\alpha^{\varepsilon}(t)$ sont respectivement le courant d'énergie dans le guide et la puissance cédée au guide (entier)

$$I_\alpha^{\varepsilon}(t) = \sum_{\substack{i\in\mathcal{L}_\alpha \\ j\in\mathcal{C}}} I_{ij}^{\varepsilon}(t) \qquad\qquad S_\alpha^{\varepsilon}(t) = \sum_{i\in\mathcal{L}_\alpha} S_i^{\varepsilon}(t) \tag{2.27}$$

Calculer les courants d'énergie et de chaleur plus loin dans les guides évite la problématique du terme de couplage dépendant du temps soulevée par la Réf. [54], les guides étant considérés indépendants du temps[1]. Une approche par diffusion à la Landauer-Büttiker comme la notre à été adoptée par la Réf. [24] dans le cas particulier d'une dépendance temporelle lente. Notre approche quant à elle s'applique à une dépendance temporelle quelconque (due uniquement à un champ électromagnétique), au-delà des régimes quasi-statiques ou périodiques.

Maintenant que les courants résolus en temps dans les guides d'onde sont définis, on relève deux problèmes liés : *(i)* à cause de la dispersion et du temps de propagation, les courants dans les guides dépendent de la position de la section où ils sont calculés ; *(ii)* le courant de chaleur n'existe théoriquement qu'après relaxation des électrons dans les réservoirs thermiques. Les guides ne sont techniquement pas les réservoirs et définir un courant de chaleur résolu en temps, et en espace, en leur sein est a priori physiquement contestable. Un tel courant de chaleur peut cependant être interprété de manière 'comptable' [47], *i.e.* "la quantité de chaleur qui sera dissipée plus tard dans les réservoirs". Pour contourner ces deux problèmes, on étudiera aussi des quantités intégrées en temps (en suivant par exemple la méthode de la Réf. [44]).

2.3. Résumé du chapitre 5 : simulation numérique avec `tkwant`

Notre but est de décrire les courants et densités de particules et d'énergie (transportée par les électrons) dans des systèmes génériques pour tenter de mieux comprendre la thermoélectricité mésoscopique dans le régime dépendant du temps. Après avoir dérivé, dans le chapitre 4, un cadre invariant de jauge au transport thermoélectrique (où les formules sont exprimées à l'aide de la fonction de Green 'lesser'), on introduit dans ce chapitre la méthode numérique (basée sur les fonctions d'onde) utilisée par `tkwant`, l'extension au régime dynamique de la bibliothèque de référence (`kwant`) pour la simulation du transport quantique dans des systèmes dans l'approximation des liaisons fortes (voir la Fig. 2.7). Son développement, initié durant le doctorat de B. Gaury [63], a notamment abouti à l'écriture d'une équation importante qui relie les fonctions de Green 'lesser' $G_{ij}^{<}(t)$ et une base particulière de fonctions d'onde à un corps appelées 'état de diffusion'. Dans le chapitre 5, on étend `tkwant` au transport d'énergie à travers un module appelé `tkwantoperator` : on montre que cette extension permet de retrouver simplement des résultats qui ont été publiés récemment concernant le 'modèle du niveau résonnant' (RLM) ; puis on étudie le cas d'un contact ponctuel quantique bidimensionnel, afin d'illustrer le potentiel de `tkwant` pour la simulation de systèmes complexes, dépassant les modèles simplistes tels que le RLM.

[1] Après un éventuel changement de jauge, voir Sec. 5.2.1 (en anglais).

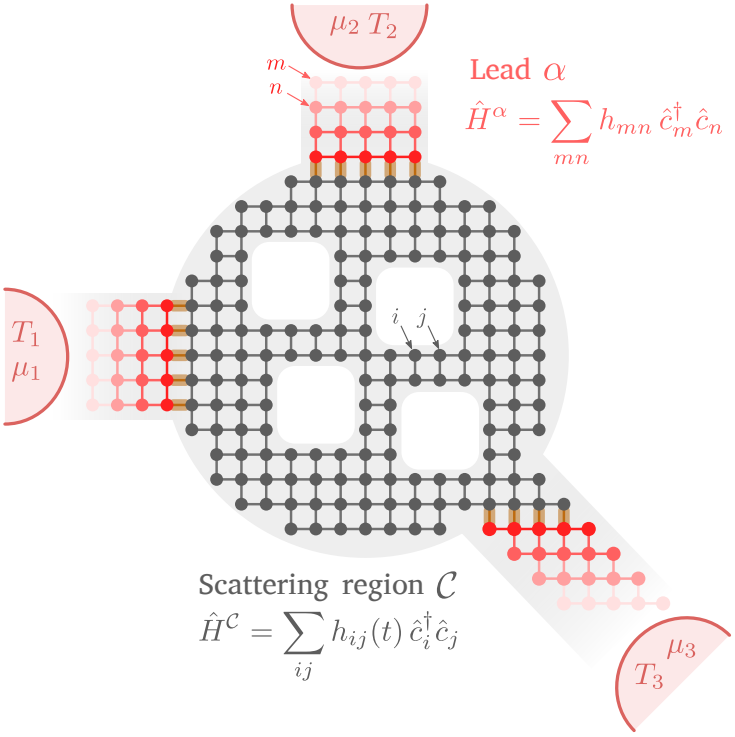

Fig. 2.7 – Système générique en représentation liaisons-fortes que `tkwant` peut simuler. Une région centrale $\mathcal{C}$, dont les sites et couplages sont dépendants du temps (coloriés en gris), est connectée à des guides d'onde dont les sites et couplages sont stationnaires (coloriés en rouge). Un potentiel scalaire uniforme et dépendant du temps peut être considéré dans chacun des guides : un tel potentiel est en pratique inclus après changement de jauge en multipliant les couplages à la frontière avec le système central (couleur orange) par une phase dépendante du temps particulière (voir Éq. (5.23))

États de diffusion Définis comme les états propres de l'Hamiltonien $\hat{h}$ du système entier (région centrale et guides) dans le régime stationnaire sans interaction, les 'états de diffusion' Ψ^λ peuvent être étendus au régime dépendant du temps. Pour ce faire, `tkwant` utilise une approche astucieuse : les systèmes que cette bibliothèque peut simuler sont restreints à ceux qui sont stationnaire jusqu'à un instant t_0, ce n'est qu'après cet instant que le contrôle temporel peut démarrer. Cela permet à `tkwant` d'utiliser `kwant` pour le calcul des états propres du système initialement stationnaire pour ensuite les faire évoluer en temps, un par un (grâce à l'hypothèse de non-interaction), à l'aide d'une version modifiée de l'équation de Schrödinger via l'algorithme 'source-sink'. Cet algorithme ne calcule que la 'perturbation' qui s'ajoute au dessus de l'état stationnaire à cause de la dépendance temporelle et, puisque la dépendance temporelle ne se trouve que dans le système central à des instants $t \geq t_0$, cette perturbation est nulle partout pour $t < t_0$ et est émise à des temps $t > t_0$ à partir de la région centrale ('la source') puis s'étend à vitesse finie dans les guides d'onde, ce qui la rend rend finie dans l'espace et représentable dans un ordinateur. L'algorithme 'source-sink' apporte aussi une optimisation quant au traitement des guides d'ondes qui par définition ne doivent pas réfléchir les ondes sortantes : la perturbation est alors absorbée ('sink') à partir d'une certaine position dans les guides et sur une étendue finie pour ainsi réduire la taille des guides effectivement simulée. Le système simulé est alors de taille finie et cette dernière est gardée petite même à des temps de simulations longs, grâce à l'absorption, tout en gardant la valeur des fonctions d'onde arbitrairement proche de leur valeurs théoriques.

Calcul des courants et densités Une formule essentielle dérivée dans la Réf. [66] permet de relier les états de diffusion résolus en temps $\Psi^\lambda(t)$ (tels que définis au-dessus) à la fonction de Green 'lesser' $G^<_{ij}$ (définie par l'Éq. (2.18)) pour dans systèmes génériques illustrés dans la Fig. 2.7

$$G^<_{ij} = \mathrm{i} \sum_{\lambda=\alpha,n,E} f_\alpha(E) \Psi^\lambda_j(t)^* \Psi^\lambda_i(t) \tag{2.28}$$

où $\sum_\lambda$ a été utilisé comme raccourci pour $\sum_\alpha \sum_n \int \frac{\mathrm{d}E}{2\pi\hbar}$, qui fondamentalement traduit une somme, pondérée par $f_\alpha(E)$, sur tous les états de diffusion Ψ^λ, indexés par les modes incidents n des leads α, injectés à des énergies E, où E est un degré de liberté continue ; $f_\alpha(E) = f_{T_\alpha,\mu_\alpha}(E)$ est aussi une

notation raccourcie pour la fonction de Fermi

$$f_{T,\mu}(E) = \frac{1}{\exp\left(\frac{E-\mu}{k_B T}\right) + 1} \tag{2.29}$$

où k_B est la constante de Boltzmann. Eq. (2.28) est la pièce manquante qui permet de calculer explicitement les courants et densités d'énergie définies dans la Sec. 2.2.2 en termes de fonction de Green 'lesser' $G^<_{ij}(t)$. Grâce à l'Éq. (2.28) ces quantités peuvent être maintenant exprimées en utilisant les états de diffusion

$$\rho_i^\epsilon(t) = \sum_{\lambda=\alpha,n,E} f_\alpha(E) \sum_j \mathrm{Re}\left[\Psi_i^\lambda(t)^* \epsilon_{ij}(t) \Psi_j^\lambda(t)\right] \tag{2.30}$$

$$I_{ij}^\epsilon = \sum_{\lambda=\alpha,n,E} f_\alpha(E) \sum_k \mathrm{Re}\left[\Psi_k^\lambda(t)^* \epsilon_{ki} \epsilon_{ij} \Psi_j^\lambda(t) - \Psi_k^\lambda(t)^* \epsilon_{kj} \epsilon_{ji} \Psi_i^\lambda(t)\right] \tag{2.31}$$

Ces deux quantités peuvent être calculées avec `tkwant`, dans le même esprit que la densité ($\rho_i^N(t)$) et le courant ($I_{ij}^N(t)$) de particules mais avec une somme additionnelle sur les sites du système. La puissance locale moyenne $S_i^\epsilon(t)$ délivrée aux électrons s'écrit quant à elle

$$\begin{aligned} S_i^\varepsilon(t) = &\sum_j -\frac{1}{2}\left[\phi_j(t) - \phi_i(t)\right] q I_{ij}^N(t) \\ &+ \sum_{\lambda=\alpha,n,E} f_\alpha(E) \sum_j \mathrm{Re}\left[\Psi_i^\lambda(t)^* \partial_t \varepsilon_{ij}(t) \Psi_j^\lambda(t)\right] \end{aligned} \tag{2.32}$$

Ces quantités locales peuvent ensuite être sommées sur l'espace pour obtenir par exemple l'énergie d'un sous-système ou bien le courant d'énergie $I_{\alpha,a}^\epsilon(t)$ et de chaleur $I_{\alpha,a}^Q(t)$ dans les leads tels que décrits dans le paragraphe 'Courants dans les guides d'onde' p.35.

2.3.1. `tkwantoperator` : extension au transport d'énergie

Pour calculer nos grandeurs énergétiques nouvellement définies, on a implémenté un module Python, appelé `tkwantoperator` : son code source est libre d'accès, disponible en ligne et accompagné d'une documentation complète (en anglais) qui décrit la procédure d'installation, d'un tutoriel et d'un guide technique, le tout à l'adresse suivante `gitlab.kwant-project.org/kwant/tkwantoperator`. Le code source a été publié en même temps que notre article de recherche [96]. Cinq classes python ont été implémentées : `EnergyDensity`, `EnergySource` et `EnergyCurrentDivergence` peuvent être utilisées pour respectivement calculer ρ_i^ϵ (donné par l'Éq. (2.30)), S_i^ϵ (donné dans l'Éq. (2.32) pour $\epsilon = \varepsilon$), et $\sum_j I_{ji}^\epsilon$ sur une liste donnée de sites $\{i\}$; `EnergyCurrent` calcule les courants I_{ji}^ϵ (donné par l'Éq. (2.31)) sur une liste donnée de couples de sites $\{(j,i)\}$; `LeadHeatCurrent` calcule le courant de chaleur $I_{\alpha,a}^{Q,\epsilon}$ (donné par l'Éq. (2.26)) traversant le lead $\mathcal{L}_\alpha$. La quantité ϵ utilisée en exposant peut faire référence à l'énergie totale $\hat{\varepsilon}$, l'Hamiltonien $\hat{h}$ ou bien un opérateur défini par l'utilisateur en donnant les termes sur sites ϵ_{ii}. Un code illustrant l'utilisation de `tkwantoperator`, en parallèle avec `Kwant` et `tkwant`, est montré en Fig. 5.7 : ce code relativement court est suffisant pour retrouver quelques résultats publiés dans des articles de recherche, voir la Sec. 5.3.2 (en anglais).

Le calcul des valeurs moyennes à plusieurs électrons des différents opérateurs implique une intégration sur tous les états de diffusion Ψ^λ, indexés par le paramètre λ (voir l'Éq. (2.28)). Étant donné que l'évolution en temps de ces fonctions d'onde est l'étape la plus coûteuse en temps de calcul dans

`tkwant`, il est crucial d'utiliser le plus petit nombre de ces états pour évaluer une valeur moyenne des opérateurs, tout en garantissant un degré de précision spécifié en amont par l'utilisateur. Pour cela, une méthode adaptive de Gauss-Kronrod est utilisée [204] pour calculer l'intégrale. De plus, l'évolution en temps des fonctions d'onde peut être faite peut être faite en parallèle sur plusieurs cœurs de calcul, chaque cœur se chargeant d'une sous-partie des fonctions d'ondes. Ces deux fonctionnalités, qui sont déjà implémentées dans `tkwant`, sont utilisées pour calculer les valeurs moyennes de nos opérateurs d'énergie.

Une fois `tkwantoperator` implémenté, on a lancé des simulations `tkwant` de transport électronique et de chaleur pour le modèle jouet du niveau résonnant (RLM), afin de valider notre approche théorique et notre implémentation numérique. On a ensuite exploré le transport de chaleur dépendant du temps dans le contact ponctuel quantique mis hors-équilibre par une impulsion de tension : sans discuter de façon exhaustive la physique des phénomènes en jeu, notre étude nous permet d'illustrer le potentiel de `tkwant`, combiné avec notre module `tkwantoperator`, pour l'exploration de la thermoélectricité dynamique dans des dispositifs quantiques complexes.

2.3.2. Validation : modèle du niveau résonnant (RLM)

Le modèle du niveau résonnant (sans interaction) a été étudié de façon exhaustive dans la littérature scientifique, pour l'étude du transport dynamique de charges (voir par exemple les Réfs. [92, 149, 158]) et plus récemment pour le transport dynamique d'énergie [38, 116, 55, 121, 120, 219, 44, 215, 113, 37, 51]. Dans le chapitre 5 (en anglais), on utilise ce modèle (décrit dans la Fig. 2.8) comme outil de validation de notre implémentation numérique. On considère deux cas : *(i)* quand (seulement) le terme sur site $h_0(t)$ de la 'dot' subit un échelon en temps $h_0(t) = V_0 + \Delta V \Theta(t)$, Θ étant la fonction de Heaviside, et *(ii)* quand l'échelon de potentiel est appliqué à l'un des guides. On calcule les courants résolus en temps d'énergie et de chaleur : on montre qu'on reproduit, dans les limites attendues, les résultats antérieurs de la littérature.

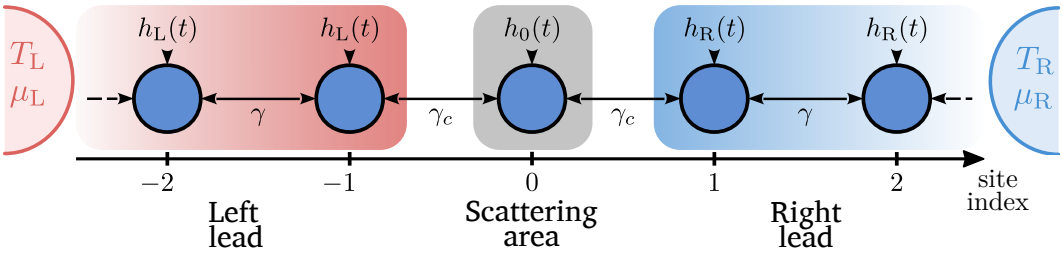

Fig. 2.8. – Représentation en liaisons-fortes du modèle du niveau résonnant. Une chaîne unidimensionnelle (1D) est composée d'un site central 0 connecté, par des termes de couplage γ_c, à des chaînes gauche (L, sites $i \leq -1$) et droite (R, sites $i \geq 1$), semi-infinies et uniformes avec un terme sur site $h_\alpha(t)$ et un couplage inter-sites γ. Chaque guide α est connecté, infiniment loin, à un réservoir d'électrons à l'équilibre, caractérisé par un potentiel chimique μ_α et une température T_α, supposés constants.

En particulier, on vérifie dans le cas *(i)* qu'on retrouve les résultats analytiques obtenus par l'approche des fonctions de Green hors-équilibre, dans la limite 'wide-band' : celle-ci est obtenue dans `tkwant` en modifiant les coefficients de couplage γ et γ_c selon [37] :

$$\gamma \to \lambda\gamma, \quad \gamma_c \to \sqrt{\lambda}\gamma_c \quad \text{et} \quad \lambda \to \infty \tag{2.33}$$

de façon à garder le ratio $\Gamma = 2\gamma_c^2/\gamma$ constant. La concordance parfaite entre l'approche numérique (`tkwant` + `tkwantoperator`) et l'analytique (fonctions de Green hors-équilibre, voir l'Appendice

C.1) est illustrée dans la Fig. 2.9 où l'on compare les courbes du courant de chaleur résolu en temps dans le guide gauche obtenus avec ces deux approches

$$I_L^{\mathrm{Q}}(t) = -\partial_t \left\langle \hat{H}_L \right\rangle - \mu_L I_L^{\mathrm{N}}(t) \tag{2.34}$$

La comparaison est faite également pour les courants de particules gauche $I_L^N(t)$ et pour une définition alternative du courant de chaleur $\tilde{I}_{\mathrm{L}}^{\mathrm{Q}}(t)$

$$\tilde{I}_L^{\mathrm{Q}}(t) = -\partial_t \left\langle \hat{\tilde{H}}_{\mathrm{L}} \right\rangle - \mu_{\mathrm{L}} I_{\mathrm{L}}^N(t) \tag{2.35}$$

considérée notamment dans les Réfs. [38, 219]. Ici, l'Hamiltonian $\hat{\tilde{H}}_{\mathrm{L}}$ utilisé n'inclut pas la contribution du couplage $\hat{H}_{0L}$ entre la 'dot' et le guide d'onde gauche (son expression est une version modifiée de l'Éq. (2.26) sans le terme $\hat{H}_{\mathcal{C}\alpha}$)

$$\tilde{I}_L^{\mathrm{Q}}(t) = -\partial_t \left\langle \hat{\tilde{H}}_{\mathrm{L}} \right\rangle - \mu_{\mathrm{L}} I_{\mathrm{L}}^N(t) \tag{2.36}$$

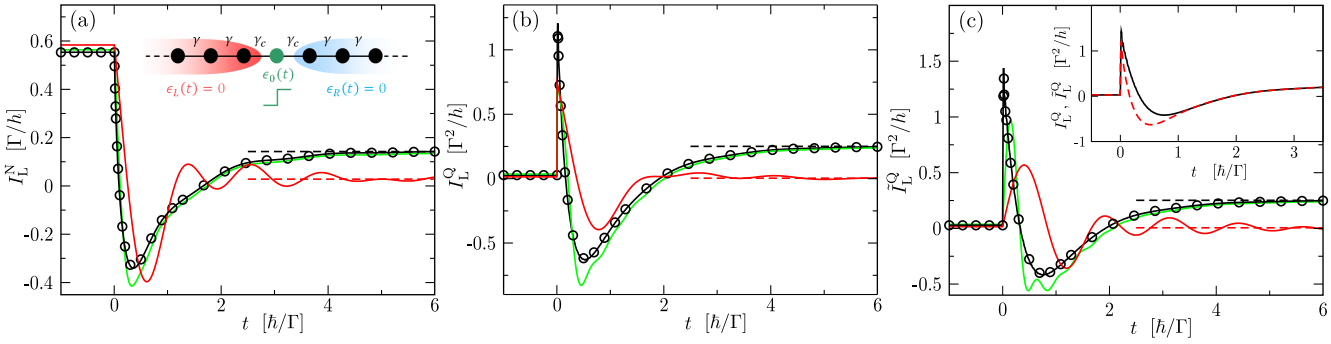

Fig. 2.9. – Adapté de notre article [96] : (a) Courants de particules gauche I_L^N, (b) courants de chaleur I_L^{Q} et (c) $\tilde{I}_L^{\mathrm{Q}}$ gauche, en fonction du temps t, pour le modèle RLM 1D schématisé sur la Fig. 2.8, quand le niveau d'énergie de la 'dot' $h_0(t)$ subit un saut abrupt $h_0(t) = V_0 + \Delta V \Theta(t)$ (voir l'insert dans (a)). Les unités des axes x et y sont indiquées entre crochets. Dans tous les panneaux, les données sont calculées par `tkwant+tkwant-operator` pour différentes valeurs de $\lambda\gamma/\Gamma$ (1 (lignes rouges), 6.25 (lignes vertes), et 100 (lignes noires)). Les lignes horizontales en pointillés, tracées pour $\lambda\gamma/\Gamma = 1$ (en rouge) et 100 (en noir) correspondent à la limite stationnaire à grand temps $\Gamma t/\hbar \gg 1$, données par les formules de Landauer-Büttiker (voir Sec. 5.2.3.2). Quand $\lambda\gamma/\Gamma \gg 1$, les résultats de `tkwant` convergent vers les résultats obtenus par la méthode des fonctions de Green hors-équilibre (cercles) dans la limite 'wide-band' (voir l'appendice C.1, en anglais). Insert dans (c) : comparaison de $I_L^Q(t)$ (lignes en pointillés rouges, données par l'Éq. (2.34)) et $\tilde{I}_L^Q(t)$ (lignes noires, données par l'Éq. (2.36)) dans la limite 'wide-band'. Dans tous les panneaux, $h_0 = 0.5\Gamma$, $\Delta V = 2.5\Gamma$, $h_L(t) = h_R(t) = 0$, $T_L = \Gamma/k_B$, $T_R = 0$, $\mu_L = 0.5\Gamma$, et $\mu_R = -0.5\Gamma$. Les courbes calculées par les fonctions de Green hors-équilibre sont indépendantes de Γ. Les courbes `tkwant` sont des fonctions de $\lambda\gamma/\Gamma$ et non des paramètres λ, γ, et Γ pris séparément.

On a aussi comparé nos résultats numériques à ceux obtenus dans la Réf. [49] dans le cas *(ii)* défini plus haut. Enfin, on aussi vérifié que dans la limite des temps longs $\Gamma t/\hbar \to \infty$, les résultats `tkwant` pour les courants de particules et de chaleur convergent, comme attendu, vers les limites stationnaires données par les formules de Landauer-Büttiker (lignes horizontales en pointillées, dans la Fig. 2.9).

2.3.3. Aller plus loin : contact ponctuel quantique

Pour illustrer le potentiel de notre approche numérique basée sur `tkwant`, on investigue aussi dans le chapitre 5 (en anglais) le transport dynamique de chaleur (transportée par les électrons) dans un

contact ponctuel quantique (QPC), connecté à deux réservoirs maintenus à des températures différentes. On se concentre sur l'effet Peltier permettant d'extraire de la chaleur du réservoir froid et on s'interroge sur la possibilité d'améliorer cet effet à l'aide d'un contrôle temporel, en l'occurrence en appliquant un pulse de tension sur l'une des deux électrodes (guide d'onde) attachées au QPC (à la place d'une tension constante). On considère un nano-ruban de longueur L et largeur W connecté, via des guides d'onde (électrodes) semi-infinies à des réservoirs thermiques gauche (L) et droit (R), maintenus à des températures $T_L \lesssim T_R$. On choisit leurs potentiels chimiques $\mu_L \gtrsim \mu_R$ (voir Fig.2.10 (a)) de sorte que la transmission stationnaire $T(E)$ du QPC soit sur une marche (et non un plateau) de transmission, $T(E = \mu_R) \approx 0.6$ et que $I_{\mathrm{L}}^{\mathrm{Q}}(t \leq 0) = 0$. Le système est discrétisé sur un réseau carré (avec un pas $a = 1$). Le système est stationnaire jusqu'à $t = 0$ puis la dépendance temporelle démarre : on applique sur l'électrode gauche une impulsion gaussienne $V_L(t)$ de largeur τ_p, amplitude V_p et centrée sur $3\tau_p$. Ainsi l'Hamiltonien du système s'écrit $\hat{H}(t > 0) = \hat{H}^0 + \sum_{i \in L} V_L(t) \hat{c}_i^\dagger \hat{c}_i$, où $\hat{H}^0$ est l'Hamiltonien stationnaire.

En utilisant `tkwant` avec notre extension `tkwantoperator` [3], on calcule les courants, résolus en temps, de particule $I_L^N(t)$ et de chaleur $I_{\mathrm{L}}^{\mathrm{Q}}(t)$, dans le guide gauche, pour différentes valeurs des paramètres (τ_p, V_p) de l'impulsion tout en gardant constante son aire sous la courbe (pour maintenir constant le nombre d'électrons dynamiquement injectés à travers le guide gauche). Les courants calculés avec `tkwant` sont ensuite comparés aux courants $I_L^{N,\bar{st}}(V_L(t))$ et $I_L^{H,\bar{st}}(V_L(t))$, qu'on obtiendrait si l'impulsion était quasi-statique, donnés par les formules de Landauer-Büttiker (voir Sec.5.2.3.2, en anglais) à chaque instant. Pour des valeurs petites de τ_p (impulsions courtes, voir Fig. 2.10(b)), le courant de particules $I_L^N(t)$ montre un premier pic positif centré autour de $3\tau_p$, donc du au pulse, puis montre un pic négatif qui provient de la réflexion sur le QPC. Le courant de chaleur $I_{\mathrm{L}}^{\mathrm{Q}}(t)$ quant à lui montre une évolution plus complexe. Dans la limite des longues impulsions, les courbes `tkwant` convergent vers leurs valeurs quasi-statiques, caractérisées par un pic unique centrée sur $3\tau_p$. On trouve, parmi les paramètres testés, que de la chaleur ne peut être extraite du réservoir froid ($\int \mathrm{d}t\, I_L^H(t) > 0$) que dans la limite des impulsions longues et que l'intégrale temporelle du courant de chaleur est systématiquement plus petite que sa contre-partie quasi-statique $\forall \tau_p \quad \int \mathrm{d}t\, I_L^H(t) \leq \int \mathrm{d}t\, I_L^{H,\bar{st}}(V_L(t))$. Ainsi, il semblerait qu'appliquer des impulsions courtes, qui affectent le QPC de manière non quasi-statique, se révèle être néfaste pour la réfrigération Peltier, au moins dans le régime de paramètres exploré ici. Cette investigation préliminaire du QPC montre néanmoins la faisabilité de simulations sur des systèmes complexes.

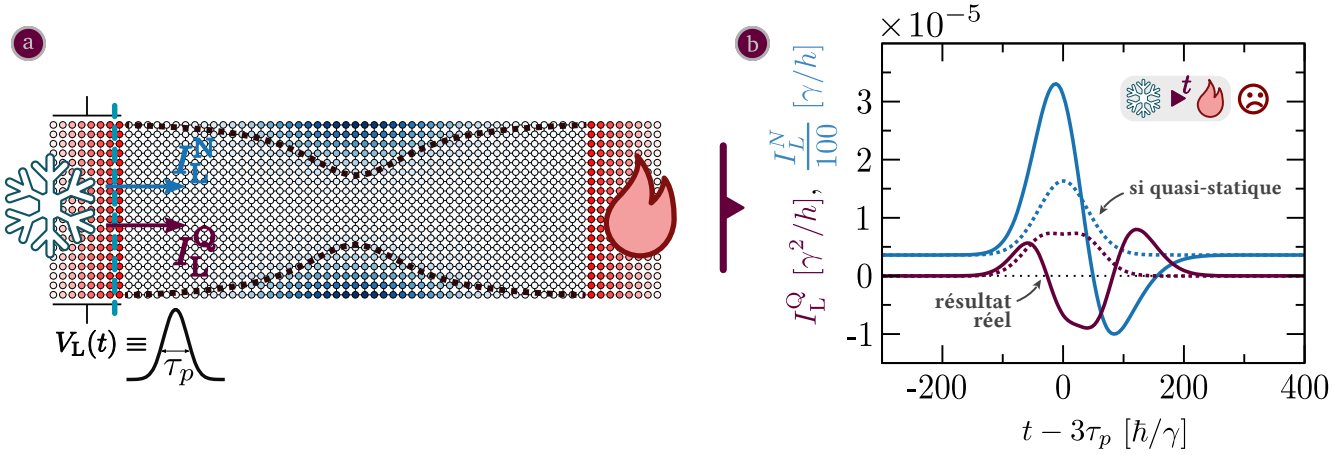

Fig. 2.10. – (a) Modèle discret du contact ponctuel quantique (QPC). La couleur des sites du système central reflète la valeur du potentiel QPC (de 0 (blanc) à des valeurs plus grandes (nuances de bleu)). Quelques couches de sites des guides d'onde semi-infinis gauche et droit sont représentées en rouge. Une impulsion de voltage $V_L(t)$ est appliquée sur le guide gauche, les flux de courants sont évaluées à la frontière indiquée par une ligne verticale discontinue bleue. (b) Courants gauche de particules $I_L^{\mathrm{N}}(t)$ (en bleu, en unités de $100\gamma/h$) et de chaleur I_L^{Q} (en grenat, en unités de γ^2/h) en fonction du temps t (en unités de $\hbar/\gamma$), pour une impulsion de voltage d'une largeur $\tau_p = 100\,\hbar/\gamma$. Les lignes continues sont les résultats `tkwant`, les lignes discontinues sont les résultats quasi-statiques Landauer-Büttiker. Paramètres : $W = 18$, $L = 48$, $l_x = 50$, $l_y = 5$, $\mu_L = 0.20607\gamma$, $\mu_R = 0.2\gamma$, $T_L = 0.018\gamma/k_B$, $V_p = 0.2$ and $T_R = 0.02\gamma/k_B$.

L'approche naïve qui tente d'améliorer la réfrigération Peltier par un contrôle temporel rapide est peu concluante mais montre que la physique en jeu est plus complexe. Ainsi, dans le chapitre suivant, on reprend l'étude du modèle du niveau résonnant où des expressions analytiques peuvent être obtenues, pour tenter de mieux comprendre les effets en jeu.

2.4. Résumé du chapitre 6 : analyse numérique et semi-analytique du RLM

Ce chapitre est dédié à l'étude du modèle du niveau résonnant (RLM) sans interaction et dépendant du temps. Il représente un système simple composé d'un niveau d'énergie unique qui peut être dépendant du temps, connecté à deux réservoirs thermiques, dans lequel des électrons peuvent entrer et sortir. Notre objectif est d'avoir une meilleure compréhension de l'effet d'un contrôle dynamique du niveau d'énergie : Zhou et al. [219] prédisent un 'boost' du rendement thermoélectrique du modèle en configuration Seebeck quand le niveau subit une variation temporelle 'rapide'. En utilisant les définitions prises dans cette référence, on reproduit, en utilisant notre approche, leur résultats : ceci nous permet de valider une fois de plus notre approche mais également d'appréhender les limitations de leur méthode et définitions. Ensuite, on utilise l'approche de diffusion avec des fonctions d'onde, introduite au chapitre 5, pour obtenir des formules génériques semi-analytiques des grandeurs de transport (les courants et densités de particules et d'énergie) pour un contrôle temporel arbitraire du niveau d'énergie, dans la limite 'wide-band' (voir l'Éq. (2.33)). Ces formules génériques sont des intégrales sur l'énergie (pondérées par les fonctions de Fermi de chacun des réservoirs) de plusieurs termes impliquant l'amplitude de transmission dépendante du temps du modèle. On intègre ensuite numériquement ces formules analytiques et les comparons à des simulations `tkwant+tkwantoperator` quand le niveau d'énergie suit un créneau. Comme discuté au paragraphe 'courants dans les guide d'onde' p. 35, on calcule les courants d'énergie en prenant en compte le terme de couplage avec les guides.

Pour définir un rendement Seebeck, on doit prendre en compte la puissance délivrée aux électrons par la dépendance temporelle, et ses effets, dans le bilan énergétique. De plus, définir un rendement implique une différenciation entre 'l'énergie utile' et 'l'énergie dépensée' et elle devient délicate dans le régime dépendant du temps. On définit alors un rendement qu'on pense être physiquement interprétable, différent de celui utilisé par la Réf. [219]. Après avoir validé la concordance entre nos résultats `tkwant` + `tkwantoperator` et semi-analytiques, on utilise notre approche semi-analytique (plus rapide grâce aux formules pré-calculées) pour lancer une exploration automatisée sur les paramètres du problème, et ainsi tenter de trouver une combinaison de paramètres qui améliore le rendement qu'on a défini, par rapport au rendement stationnaire. Parmi les deux cent milles simulations ainsi obtenues, plusieurs montrent des effets prometteurs où le rendement est amélioré de façon transitoire mais converge vers une valeur inférieure, proche de celle stationnaire (voir le panneau gauche de la Fig. 2.11). Ce même comportement peut être observé si le contrôle en créneau est périodiquement répété (voir le panneau droit de la Fig. 2.11).

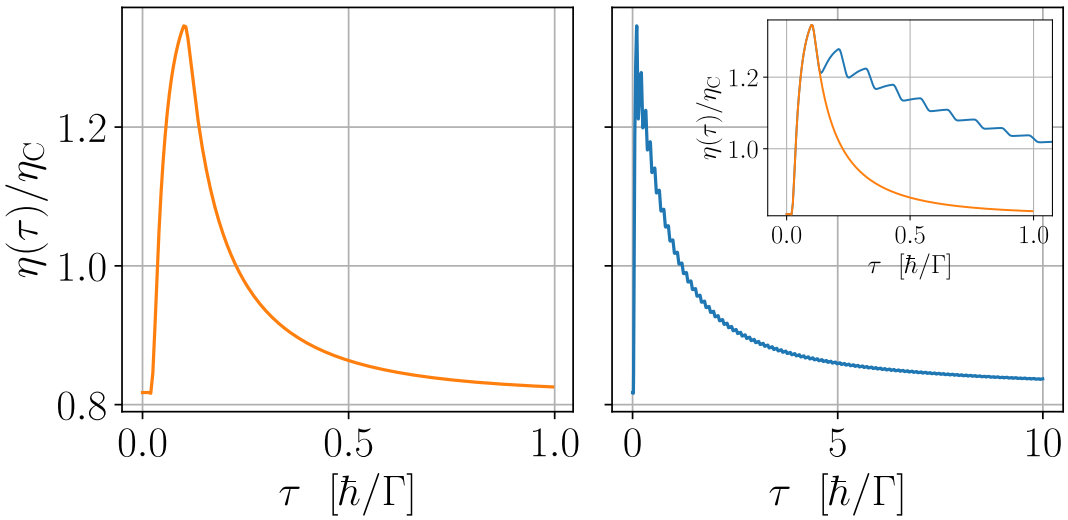

Fig. 2.11. – Un rendement amélioré du modèle du niveau résonnant. Quand le niveau d'énergie suit une fonction rectangle, les courants de particules et de chaleur peuvent se comporter d'une manière telle que le rendement $\eta(\tau)$ (défini dans l'Éq. (6.74), sous les hypothèses exposées en Sec. 6.3.3) est temporairement amélioré. Le panneau gauche est le rendement résultant d'un unique créneau de longueur Δt alors que dans le panneau droit le contrôle est périodiquement bouclé, avec une période τ_p. Les deux courbes sont tracées dans la figure insérée au panneau droit afin de montrer que les deux rendements coïncident jusqu'au moment $\tau = \tau_p$ où le créneau est répété dans le cas périodique. On remarque que boucler périodiquement le contrôle périodique retarde le retour à un rendement inférieur mais ne semble pas aider à obtenir un rendement amélioré, dans le régime permanent. Les deux courbes ont été obtenues par des simulations `tkwant+tkwantoperator`. Ce résultat rappelle le résultat expérimental de la Réf. [178] sur un module Peltier. Paramètres de simulation (les énergies sont en unité de Γ, les temps en unité de $\hbar/\Gamma$) : $T_L = 87, T_R = 25, \mu_L = -26, \mu_R = 26, V_0 = 55, \Delta V = 2, \Delta t = 0.08, t_0 = 0.1, \tau_p = 0.11, wb = 400, \gamma = 1$.

Les limitations d'un tel comportement restent à étudier car par exemple l'interaction électronique n'est pas prise en compte ici et pourrait changer le résultat. D'un autre côté, des modèles plus complexes peuvent être maintenant investigués numériquement avec l'aide de notre extension à `tkwant`.

3. Past and current developments in thermoelectricity

Since its discovery in the late 18th century [75], the use of devices leveraging thermoelectricity remained marginal as their efficiency for energy generation and cooling is a major blocker. The second half of the 20th saw a rebirth of research in thermoelectrics, initiated by the boom in the semi-conductor industry with the development of the transistor and the research made to miniaturize it, resulting in the first experimental realizations of thermoelectric generators and coolers [90, 73]. The efficiency of such devices remained unattractive, compared to traditional machines, and the field saw no further breakthroughs till the early 1990s where the effects of quantum confinement have been theoretically studied [86, 85] and predicted promising improvements. Those initial results started a second wave of research that is still ongoing. Several new leads are being explored, many of which come from the quantum understanding of matter such as band-structure engineering [145] and nano-structuring [95].

One interesting lead in improving thermoelectric conversion efficiency in mesoscopic devices is through a time-dependent drive: initial theoretical works reported an improvement of the efficiency in the transient regime [38, 219]. The field of time-dependent quantum thermoelectricity is at its early stages and is part of the undergoing efforts in building a theory of quantum thermodynamics, where a proper definition of what 'heat' and 'work' are is still under debate and research. Experimentally, the field is still in its infancy [146] although first major developments have been reported in quantum thermometry [201, 97] and in electron manipulation with *e.g.* the realization of a Maxwell demon [36, 106] and single-electron sources [14]. The literature in the field so far is dominated by theoretical works, with multiple goals: investigate the fundamentals of quantum thermodynamics [134, 119, 121, 205, 47] ; assess the applicative potential of high-frequency nanoelectronics for AC-driven thermoelectrics [38, 115, 35, 219, 44, 61, 123], heat pumping [132, 155, 147, 12, 82] or Josephson-effect-based refrigeration [180, 199] ; or use energy current and noise as new probes of mesoscopic electron systems [13, 45]. From a technical point of view, the theoretical tools used to describe dynamical energy and heat transport in driven mesoscopic electron systems are diverse *e.g.* the Floquet theory in the AC regime [13, 134, 119, 121, 120, 61] ; master equation approaches such as Lindblad's [190, 82, 107] or the DLvN method [167, 6, 218, 217, 216, 143] ; or the well-established (but cumbersome) NEGF technique [12, 38, 116, 55, 219, 44, 215] and more recently the wave-function [129] and the auxiliary-mode [113] approaches. The effect of Coulomb interaction has been included within different frameworks, near the adiabatic regime [115, 163, 82, 47] and beyond [35, 34, 205]. Moreover, alternative methods have been developed to describe transient particle and heat currents in response to the application of a temperature gradient [19, 49, 37, 117]. However, to date, the different methods listed above have only been applied to paradigmatic systems ranging mostly from the single site Resonant Level Model (RLM) to the one-dimensional chain.

3.1. Stationary thermoelectricity: a brief overview

Discovered in the end of the 18th century[1], thermoelectricity is a property of certain materials that display an electrostatic potential gradient when under a temperature gradient and inversely. The effect where a temperature difference produces a voltage difference is called the Seebeck effect: its main demonstration is done by connecting the ends of two metallic wires and heating it. The Seebeck effect manifests in a measurable non-zero voltage between the other edges of the wires, see Fig. 3.1. The measurable voltage difference ΔV is related to the temperature difference ΔT, when on an open electric loop (the electric current $I^e = 0$), through a proportionality coefficient S, called the Seebeck coefficient or the thermopower

$$S = -\left.\frac{\Delta V}{\Delta T}\right|_{I^e=0} \tag{3.1}$$

The 'conjugate' effect, where an imposed voltage forces heat to flow from cold to hot, also exists and is called the Peltier effect.

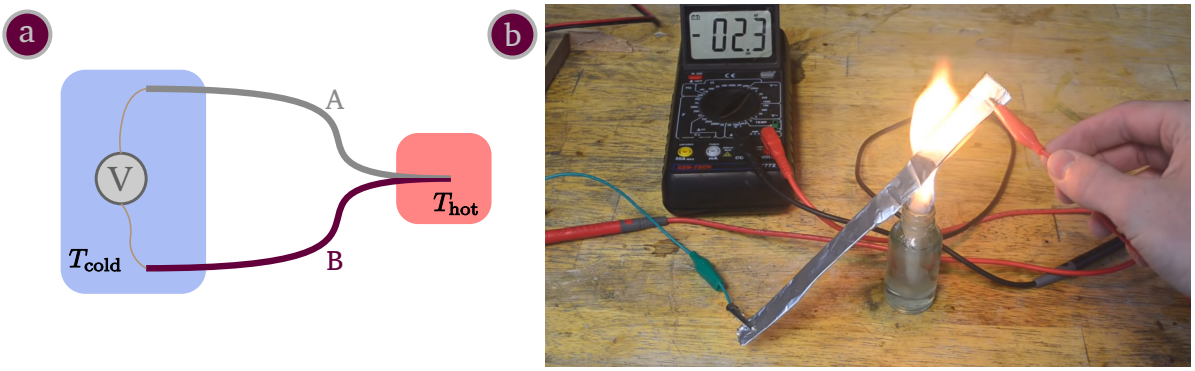

Figure 3.1. – Description of the Seebeck effect. *a)* The ends of two metallic wires are connected then heated, this results in a measurable voltage difference between the other two ends *a)* A practical demonstration of the effect by heating an aluminum foil, screenshot from the Youtube™ video "How to make a ThermoElectric Generator" from the channel "Keystone Science".

3.1.1. Thermoelectricity for energy conversion

The Seebeck effect naturally lent itself to a practical application in making temperature sensors as the voltage depends on the temperature difference. In principle, this first practical implementation could be used for electrical generation but it suffers from a prohibitively low efficiency and remained unused for energy conversion. Starting from the late 1950s, the semi-conductor industry boomed around the manufacturing of micro-processors and new research had been undertaken to make thermoelectric generators based on semi-conductors : a new wave of investigations was initiated by the Russian researcher A. F. Ioffe who introduced a dimensionless parameter, zT [75, 194, 90], later called the 'figure of merit', as a simple but efficient performance indicator of each material he studied as a thermoelectric generator

$$zT = \frac{\sigma S^2}{\kappa_{\text{E}} + \kappa_L} T \tag{3.2}$$

[1]See the first chapter of Ref. [75] for a concise and thorough history of thermoelectricity.

where T is the average absolute working temperature (linear response is assumed for the cold and hot baths), S the Seebeck coefficient, σ the electrical conductivity, κ_{E} and κ_L are respectively the electronic and lattice thermal conductivities of the material. Unfortunately S, σ and κ are strongly correlated through the material's charge carrier concentration, scattering and band structure [145]. One correlation that can be intuitively understood is between the thermal conductivity κ_{E} and the electrical conductivity σ as both are due to electrons and therefore cancel each other's contribution in zT (see Fig. 3.2b for an illustration): the Wiedemann–Franz law for example, an empirical law followed by some materials, states that these two conductivities are proportional [124]. Research has been undertaken to find materials and systems that violate this law (*e.g.* see Refs. [189, 200, 160]) in hopes of improving the efficiency.

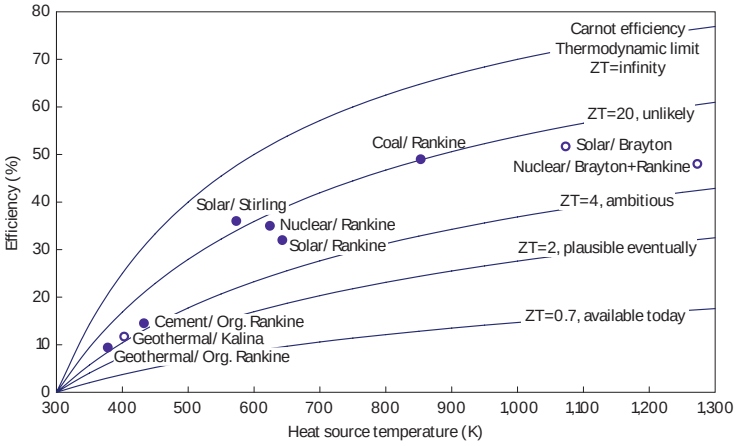

(a) Taken from [197]. Comparing traditional industrial heat engines with thermoelectrics. Current thermoelectrics cannot compete due to their low efficiency, if their figure of merit zT attains ~ 3 they would be a viable alternative.

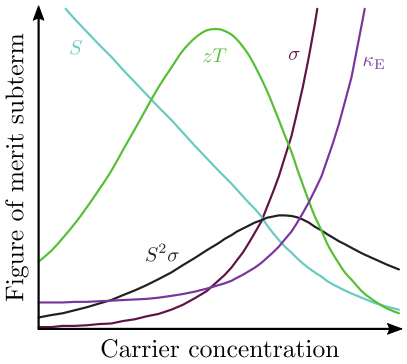

(b) Adapted from [177] : illustration of the effect of changing the carrier concentration on each term of the expression (3.2) of zT

Figure 3.2. – Assessment of the values of the figure of merit zT and its subterms

In the case of a two-terminal system in the linear regime near equilibrium, the highest attainable electrical generation efficiency $\eta_{\max}$ is related to the figure of merit as follows [74]

$$\eta_{\max} = \eta_{\mathrm{C}} \frac{\sqrt{zT+1}-1}{\sqrt{zT+1}+1} \tag{3.3}$$

where $\eta_{\mathrm{C}} = 1 - T_{\mathrm{C}}/T_{\mathrm{H}}$ is called the Carnot efficiency: the theoretical maximum efficiency no system can outperform, where T_{C} and T_{H} are the temperatures of the cold and hot reservoirs. Note that the figure of merit zT also characterizes cooling performance of the same materials, when used in the Peltier configuration. This system also highlights another important issue with any kind of heat engine so far: the power output and the efficiency cannot be simultaneously maximized [9, 16] and a tradeoff has to be made depending on the use cases. In the two-terminal linear response regime, under the time-reversal symmetry hypothesis, the efficiency at maximum power $\eta(P_{\max})$ is the following

$$\eta(P_{\max}) = \frac{\eta_{\mathrm{C}}}{2} \frac{zT}{zT+2} \tag{3.4}$$

One can note that $\eta(P_{\max}) \xrightarrow{zT\to 0} 0$ and $\eta(P_{\max}) \xrightarrow{zT\to\infty} \eta_{\mathrm{C}}/2$. The latter limit coincides with the linear response expansion of the Curzon-Ahlborn efficiency η_{CA}

$$\eta_{\mathrm{CA}} = 1 - \sqrt{\frac{T_{\mathrm{C}}}{T_{\mathrm{H}}}} \tag{3.5}$$

the (non-universal) efficiency at maximum power of a more realistic model of a cyclic Carnot engine [42].

Current status of thermoelectrics When compared to traditional heat engines, thermoelectric generators have the advantage of not having any macroscopic moving parts but suffer from a comparatively low efficiency (see Fig. 3.2a): the mainstream commercially available thermoelectric generators and refrigerators present a $zT \lesssim 1$ and are reserved to niche applications such as radioisotope thermoelectric generators for deep-space exploration [208]. Attempts have been made to use thermoelectric devices for seat cooling and heating in some high-end cars [114] ; to power autonomous low-power devices such as pacemakers [18] or sensors [43] ; for fine-grained heat extraction on computer processors [112] ; with mixed results or still ongoing development. For broad use of thermoelectricity for electricity generation and refrigeration, $zT \sim 2, 3$ needs to be practically reached with low manufacturing costs and low practical parasitic losses [191].

3.1.2. Improving thermoelectric devices

Initial implementations of thermoelectric devices by Ioeffe [90] and Goldsmid [73] in the early 1950s presented a $zT \sim 0.5$ [85], a decade later the figure of merit zT reached a theoretical value of ~ 1 then stalled until the early 1990s. In 1993, Hicks & Dresselhaus [86] published an article where they theoretically predict that a low-zT Bi_2Te_3 bulk material can see its figure of merit boosted by an order of magnitude and reach $zT \sim 14$ when cut down to thin square section ($\sim 0.5 \times 0.5$ nm), showcasing that low dimensionality theoretically improves the figure of merit due to quantum confinement effects. That result initiated a new wave of research where quantum effects are the leading motor in further improvement of thermoelectric generators and refrigerators, see Fig. 3.3.

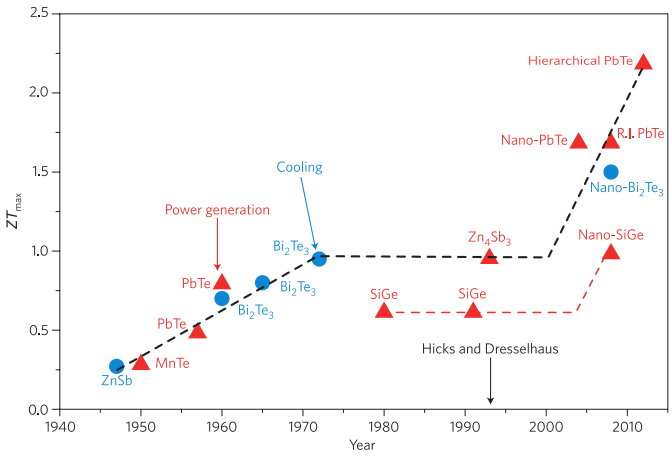

Figure 3.3 – Taken from Ref. [85]: "Evolution of the maximum ZT over time. Materials for thermoelectric cooling are shown as blue dots and for thermoelectric power generation as red triangles. The black dashed line guides the eye. The compound semiconductors (PbTe, Bi2Te3) indicate only the basic constituent; most high ZT materials are alloys or nanocomposites." This graph highlights a first wave of improvements of the figure of merit thanks to the development of the semi-conductor industry, starting the early 1950s ; a second wave of improvements started from the early 1950s thanks to quantum-led nano-engineering. However, the figure of merit has not yet reached the critical value of $zT = 3$ for broad use [191].

Quantum thermoelectrics In traditional thermoelectrics at room temperature and large scale, the charge carrier's relaxation length is relatively negligible when compared to the system's size. This enables describing the transport within the bulk of classical thermoelectrics with smooth local thermodynamical equilibrium at each point in space, such systems are usually well described by Boltzmann transport theory (see Ref. [74]). When the thermal relaxation length becomes similar to the system's size, Boltzmann's transport theory does not apply any longer. Moreover, when the quantum phase

coherence length of the charge carriers is comparable to the size of the system, coherence quantum effects manifest: particles have a (relatively) coherent wavelike behavior that can exhibit interferences or strong correlations. In meso/nanoscale devices, electron-phonon and eventually electron-electron interactions get inhibited when the temperature is lowered. Interactions being the main factor behind relaxation processes and decoherence, transport is elastic and is accurately described within the quantum theory: this opens up new doors to thermoelectricity and can potentially help with improving the performance of thermoelectric devices in the long run. Opportunities offered by mesoscopic physics for thermoelectrics are discussed in the review paper [148].

Current research Several leads are being explored for increasing the figure of merit zT with an end goal to improve one or several of its terms: increase the Seebeck coefficient S or improve the electric conductivity σ while simultaneously lowering/maintaining the thermal conductivities. Many bulk materials have been researched – *e.g.* Skutterudites, Clathrates, Zintls, Half-Heuslers, GeTe, SnTe, PbTe, $Bi_{2-x}Sb_xTe_3$ – where even a $zT \sim 5$ has been predicted [87] but so far no single material stands out as each has their pros and cons [176]. In parallel, optimization techniques are being developed around band-structure manipulation, nanostructuring, superionic conduction and defect manipulation (see Ref. [214] for an overview on the latest developments at the time of writing). In the next paragraphs, we illustrate two of the various benefits of nanostructuring: energy filtering and phonon thermal conduction reduction.

→ Reduce the phonon thermal conductivity In the field of low temperature mesoscopic thermoelectricity, recent theoretical [211] and experimental [22] works highlighted a very effective way in reducing the phonon's contribution κ_L (see Eq. (3.2)) to the thermal conductivity in nanowires by changing the geometry of their surface, which breaks down the mean free path of phonons in the ballistic regime, and therefore reduces the thermal conductivity, see Fig. 3.5. The electrical conductivity in the other hand is unaffected by the geometrical change. The resulting material is an *electron crystal & phonon glass*.

→ Energy filtering for electric generation Quantum dots are a popular test bed in mesoscopic thermoelectric systems for both theoretical and experimental [181, 152, 188] approaches, due to their relatively simple theoretical model and experimental implementation : an isolated 'island', with one or many energy levels, where electrons can hop in and out from different heat baths (see Fig. 3.7 *(a)* for a sketch). Such systems are predicted to be able to reach the Carnot efficiency (although with zero output power), when used as heat engines [137]. Josefsson et al.[93, 94] experimentally showcased the former prediction by measuring an efficiency close to the Carnot efficiency $\eta \approx 70\%\,\eta_C$ (see Fig. 3.4). The experiment is performed at low energies ($\hbar\Gamma \approx 6\mu\text{eV} \approx k_B T/10$), so the Carnot efficiency can be approached, and at ultra-low temperatures ($T \approx 1\text{K}$, $\Delta T \approx 0.5\text{K}$) so only one energy level of the quantum dot is populated but also to freeze the phonons, higher temperatures would otherwise drastically decrease the efficiency. More research is therefore needed for room temperature applications, although efficient experimental techniques have been developed to reduce the phonon's contribution to the thermal conductivity, as noticed in the previous paragraph.

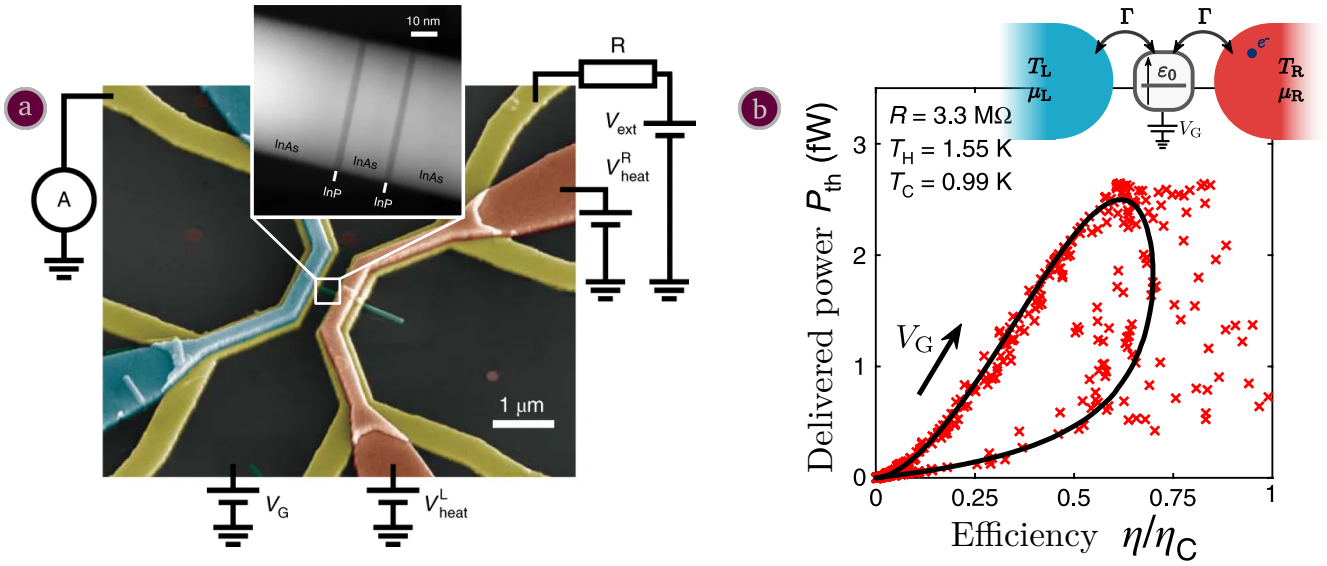

Figure 3.4. – Adapted from [93]: a) "False-coloured SEM image of a nominally identical device to the one used in the experiment. Metallic leads (yellow) make contact to the nanowire (green). Heaters (blue and red) run over the contact leads and are insulated from them by a layer of high-k oxide. One of the heaters (red) is used in the experiment for thermal biasing, and the other (blue) is unused. The resulting $\Delta T = T_H - T_C$ is set by the temperature profile of the phonon bath". b) Plot of the delivered power P_{th} vs the efficiency $\eta = P_{\text{th}}/I^{\text{Q}}$, where I^{Q} is the heat current, at different values of V_{G} (the gate voltage that controls the energy level of the dot, the arrow indicates the direction of increasing values). Data points are based on the measured values of P_{th} and the calculated I^{Q} using experimentally determined parameters. The solid line is the result of a theoretical calculation, using the same parameters. The spread in the data points at high efficiency is due to fluctuations in the measured current as it nears zero (the reversal point in V_{G}).

3.2. Time-dependent mesoscopic thermoelectricity

Classical electric generation and cooling makes use of a heat transfer fluid that undergoes a cyclic transformation for respectively power generation and heat extraction with *e.g.* Carnot and Otto engines. Initial research in classical thermodynamics derived the first theoretical results, *e.g.* the Carnot efficiency, with a hypothesis of an infinitely slow transformation so no extra entropy is generated and the efficiency is the highest, however with a zero power output. Real world implementations need to deliver finite power with finite time cycles, which put the efficiency of practical implementations below the theoretical limit. Extensive literature has been published on the subject of 'finite time' (classical) thermodynamics field, see *e.g.* Ref. [9] for a recent review.

The current thermoelectric devices used for electric generation and refrigeration work autonomously within the steady state regime. This regime of functioning is relatively well understood and accurately described by theory [75, 16] but it differs from the cyclic behavior, where a dynamical (time-dependent) control is needed to drive the system and make its thermodynamical properties (volume, temperature, pressure... etc) follow cycles. Some of the current endeavors in the field of mesoscopic physics are to iron out thermodynamics in the driven quantum regime: local temperatures and heat current densities can be ill-defined, especially when a 'fast' time-dependent control has to be taken into account. Recent theoretical studies have even reported on an improvement of thermoelectric properties of 'quantum dot' based models, although the reasons behind this predicted boost remain unknown. On the other hand, experimentation in driven electron transport has made significant progress, which paves the way to future driven thermoelectric experiments.

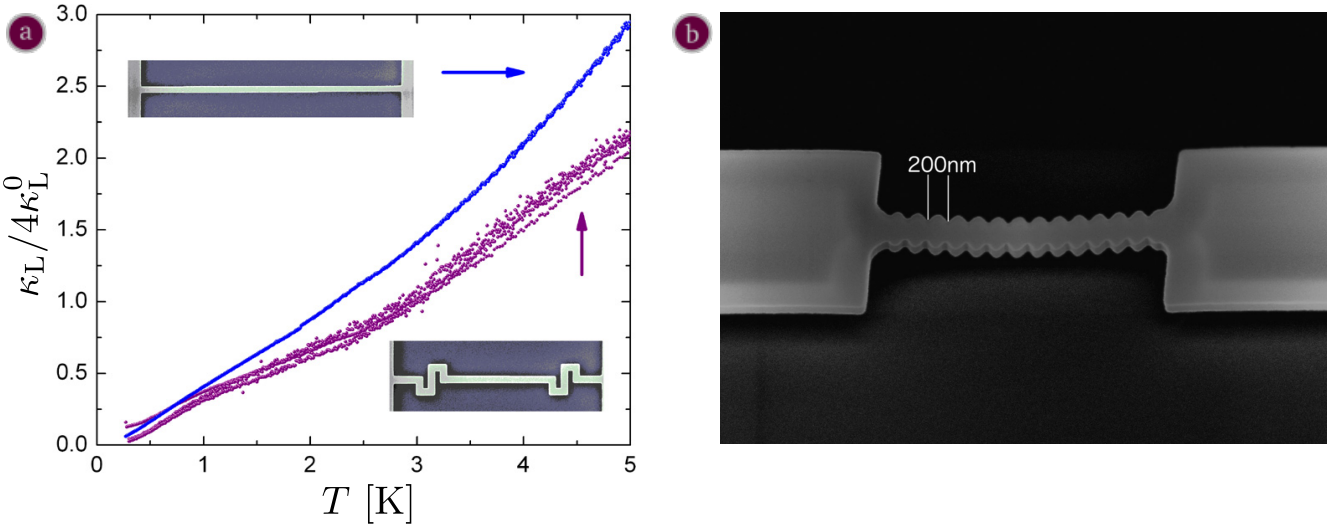

Figure 3.5. – Adapted from [22]: a) "Thermal conductance κ_L of 5 μm long nanowires normalized to four times the universal value of thermal conductance versus temperature. The thermal conductance of the straight nanowire is much bigger than the thermal conductance of the S-shape nanowires" b) Another tested shape of nanowire, it has also been shown to reduce the phonon thermal conductivity.

3.2.1. Theoretical challenges in thermodynamics

The theory of thermodynamics aims to describe simply systems with a very high number of degrees of freedom with a few relevant parameters to our scale. To achieve this simplification over the degrees of freedom, averaging over the degrees of freedom, space and time is done. Thermodynamics revolve around three fundamental laws with regards to the evolution of such a system: *(i)* energy is conserved ; *(ii)* the total entropy of the considered system and its environment can only increase ; *(iii)* the system cannot reach the absolute zero temperature in a finite-time transformation. The Carnot efficiency $\eta_C = 1 - T_C/T_H$, where T_H and T_C are the temperatures of the hot and cold baths, is one of the most known results of thermodynamics: no cyclic heat engine, no matter what its inner workings are, can have an efficiency $\eta = W/Q_H$ that exceeds η_C, where W and Q_H are respectively the cycle averaged work produced by the heat engine and the heat lost by the hot reservoir.

Classical thermodynamics The aim of the original theory of thermodynamics is to describe macroscopically stationary, and in equilibrium, systems [29] with a high number of degrees of freedom like gases, liquids and solids made of $\sim 10^{23}$ atoms/molecules. The Carnot upper limit is obtained within a simple model of piston-and-cylinder in the quasi-static limit, where the transformation (the movement of the piston in the cylinder) is done infinitely slowly so that no extra entropy is produced other than the one that is transferred from the hot reservoir to the cold reservoir. This quasi-static limit is an ideal case that also theoretically results in a zero power output since the period of a cycle is considered to be infinitely long. Even though obtained within a simple model, this limit applies to any practical implementation of a heat engine with the extra constraint that it needs to deliver finite power with finite-time cycles. This makes these realistic engines undergo an irreversible (non quasi-static) transformation that produces extra entropy and result in an efficiency $\eta < \eta_C$. Within this real-life context, the efficiency is not the only quantity of interest as power output, costs and ecology come into play and cannot be simultaneously maximized. See Refs. [42, 10, 166, 98] for more information on classical finite-time thermodynamics.

Quantum thermodynamics Quantum mechanics is the current most accurate description of the behavior of fundamental particles at small scales and/or cold temperatures. Its relationship with classical physics and how the behavior of matter smoothly transitions from the quantum realm to the classical realm has been discussed and debated since the inception of the quantum theory, but this matter is yet to be solved and 'is still in its infancy'[27, p. 530] (see also Ref. [21]). However, from a more pragmatic approach, some systems are accurately described by a classical theory and some others are not. In the latter case quantum or semi-classical models are needed to alleviate the discrepancies between what is observed and the predictions of classical models, see Fig. 3.6 for an example.

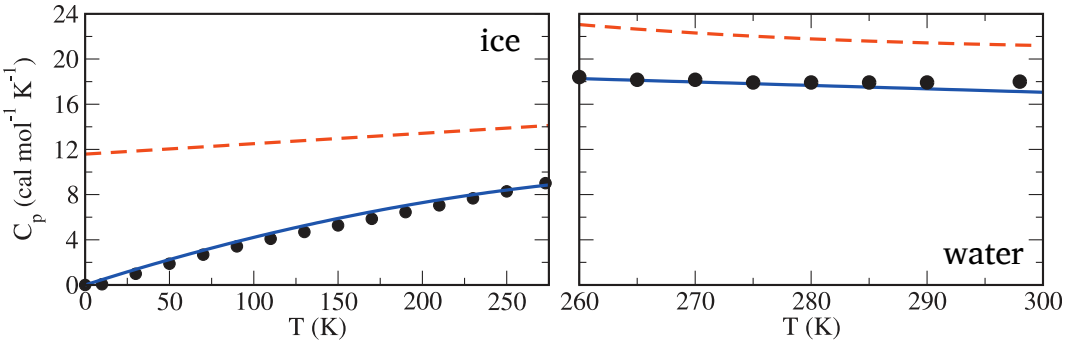

Figure 3.6. – Adapted from [195]: Heat capacity C_p at a pressure $P = 1$bar for liquid water (right graph) and ice (left graph) as obtained from quantum path-integral simulations (solid line) and from classical simulations (dashed line). Experimental results are given by solid black disks. We notice that simulations based on the quantum approach describe precisely the heat capacity of water in both its liquid and solid state whereas the classical simulation fails.

Quantum mechanics chronologically appeared more than a century after the initial development of classical thermodynamics – *e.g.* works by Carnot [32] were published on 1824 – and was developed without consideration for thermodynamics for a few decades before researchers started working towards recovering known results of thermodynamics: the first works in this context highlighted the equivalence between a Carnot engine and a three-level Maser [174, 69]. Quantum mechanics deals with systems whose ensemble size is below the classical thermodynamic limit, in non-equilibrium where extra quantum effects come into play, such as interference and entanglement. Initial hopes were on the emergence of a quantum theory of thermodynamics where classical laws are violated, such as the aforementioned second law. Some results pointing towards such a violation have been published [72, 7, 58] but are only attributed to a derivation with ill-defined quantities. Further research, reviewed in *e.g.* Refs. [107, 68, 198], built upon these first works to recover, within the markovian (quantum) Lindblad master equations approach (see Sec. 3.3.3 below), the quantum equivalent to the classical laws of thermodynamics where no violation occurs and classical finite-time thermodynamics are recovered in some models [70, 71, 156]. Technological advances recently enabled realizing real implementations of the Maxwell demon in both the quantum [30, 36] and classical [162, 105, 196] descriptions, further improving the understanding of thermodynamics and its intimate relationship with theory of (quantum) information. The field of quantum thermodynamics is although far from being a closed subject as it has been approached by scientists from different fields [198] (statistical physics, mesoscopic physics, quantum information theory and other fields) who approached the question with different tools : the Lindblad master equations approach sets up a first complete quantum description of thermodynamics, but it is one approach amongst others and comes with limitations *e.g.* a weak, slowly driven (to remain markovian *i.e.* not depend on previous times), system-bath coupling assumption. A consensus over the definition of "work" and "heat" is yet to be attained, research is still ongoing on properly building a coherent thermodynamical description where the equivalence or difference between each approach is highlighted and understood. In this thesis, we tackle both the strong coupling and the fast driving

regime using the non-interacting scattering approach with wavefunctions. We bring to the table the necessity of electromagnetic gauge invariance of any energy quantity and bring extra elements to the ongoing discussion over the definition of a heat current, see Sec. 4.3.3.3 and Sec. 4.3.4.2.

3.2.2. Exploring the new time-dependent regime

Many thermoelectric experiments have been done, in the stationary regime, in resonant tunnel junctions, molecular junctions [159, 41, 151] and quantum dots. Gate-controlled heat engines [93, 94] and heat valves [48] have been implemented. The theoretical approach used to described these experiments is through the Resonant Level Model: a simple system with a single energy level connected to two heat baths. This model has been extensively studied in the literature in the stationary regime, for both particle and heat transport, in the non-interacting [15, 53, 125] and in the interacting regime where Coulomb interactions [192] are taken into account in different regimes (*e.g.* Coulomb blockade [220] and Kondo [108] regimes).

The Resonant Level Model (RLM) is a simple system and has been used as the test-bed for the current developments around time-dependent quantum thermodynamics (including thermoelectrics). The non-interacting time-dependent RLM has been extensively studied in the literature to simulate dynamical charge transport (see *e.g.* Refs.[92, 150, 158, 79]) and more recently dynamical energy transport: Refs. [116, 119] highlight the complex behavior of the energy currents in the time-dependent domain ; Refs. [51, 121, 24] focus on thermodynamics and entropy, leading to initial developments of a theory of thermodynamics when the time-dependent drive is slow [55, 24, 81, 17], periodic [120, 17] or generic [143, 175] (but with different theoretical approaches) ; Ref. [215] investigate the full-counting statistics (FCS) of energy flow ; Ref. [37] studies the limitations to the usually used wide-band approximation in calculations in the RLM model ; Refs. [44, 51, 40, 80] study the cyclic drive to make heat engines and heat pumps, stochastic cycles have also been studied [128]; Refs. [55, 142] raise issues while trying to define heat currents when the system-bath coupling is also time-dependent.

Improve the thermoelectric efficiency ? Promising results are reported within the non-interacting two-terminal Resonant Level Model, when its energy level undergoes a heaviside jump in time (see Fig. 3.7 *(a)* and *(b)*): Refs. [38] reports in improvement in the calculated Seebeck coefficient S (see Fig. 3.7 *(c)*) whereas Ref. [219] reports a 'boost' of the efficiency of the model when in the generator configuration (see Fig. 3.7 *(d)*), a similar boost is also predicted in the transient regime for a train of square pulses. Those exploratory results hints at a positive impact of time-dependent driving on thermoelectricity. However, it is important to notice that those results depend on the choice of the definition of a time-resolved Seebeck coefficient and a time-resolved efficiency and the used choice in those papers is questionable. Moreover, those studies focus on the transient regime at short times after the quench and do not investigate the contribution at long times. Those two crucial points will be addressed in Chapter 6 of this thesis dedicated to the RLM. Finally, it is clear that those results for the Resonant Level (toy) Model remain to be confirmed (or refuted) in more realistic devices. In Chapter 5, we will report on the numerical method we have implemented to investigate time-dependent thermoelectric transport in generic (non-interacting) systems.

Towards time-dependent thermoelectric experiments The current progress in experimental realizations already enables implementing promising thermoelectric devices in the stationary regime for bulk materials at ambient temperature [89, 84] (see *e.g.* [214] for a review) but also nano-devices at

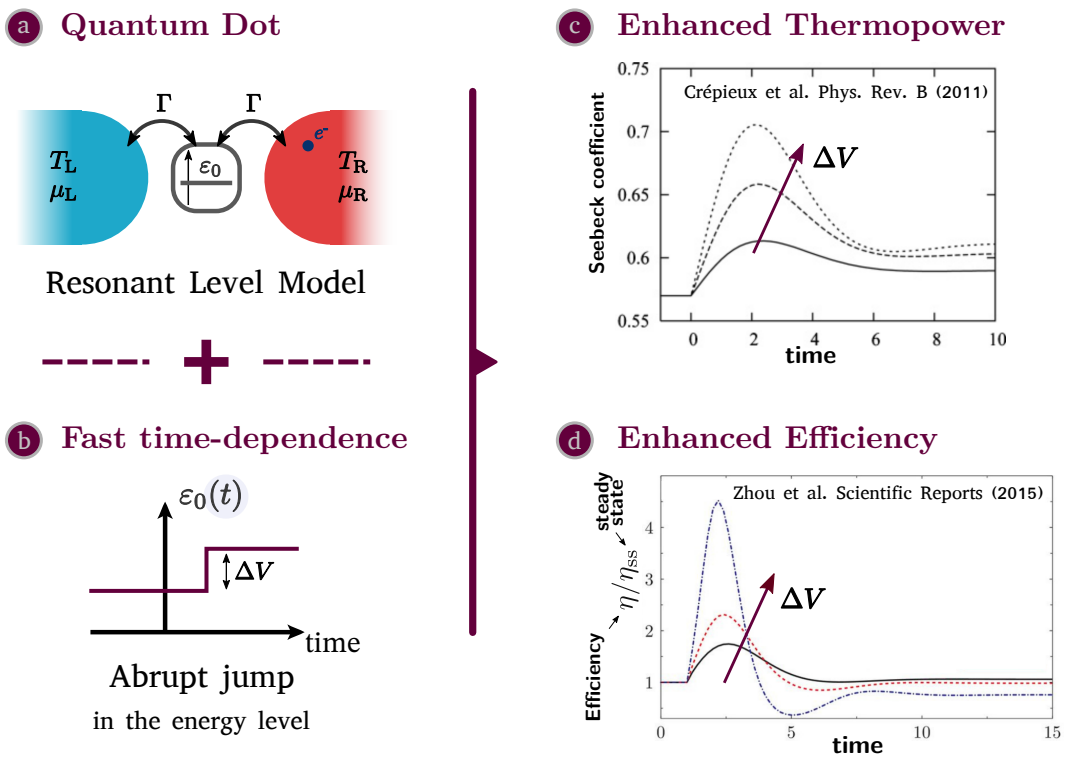

Figure 3.7. – Reported thermoelectric improvements in the driven Resonant Level Model. (a) Representation of the Resonant Level Model, a central single-level system connected to two heat baths via electron tunneling with rate Γ. (b) When the single level of the central 'dot' jumps by an energy ΔV, (c) the calculated Seebeck coefficient of the system is reported to be enhanced [38] while (d) its efficiency is reported to significantly improve in a heat engine configuration [219], in the transient regime. Note that the parameters used in each article are different.

ultra-low temperature that showcase the 'quantum-advantage' in electric generation [93] and thermal conduction inhibition [22]. On the other hand, the field of high frequency nanoelectronics made significant improvements over the past decade and now offers fine time-dependent control over electrons through mesoscopic capacitors / *single-electron boxes* that can emit single electrons on demand with a tunable energy or time resolution tradeoff (see Fig. 3.8 below) or electron pumps that can emit periodically electrons in the gigahertz range (see *e.g.* Ref. [14] for a review). Note that all these experiments need to operate at very low temperature $T \lesssim 0.5K$ and high frequency $\omega \gtrsim 10$GHz to reach the quantum dynamical regime where $k_B T \lesssim \hbar\omega$.

One of the initial main goal of these developments is single-electron quantum optics for quantum information, although it is not far fetched to imagine that they also help shaping experiments in quantum thermodynamics and mesoscopic thermoelectricity. Along with Josephson junction based quantum devices that enable fast, time-resolved measurements of the electronic temperature [201], current experimental progress deepens our understanding of energy and particle transfers at small time and energy scales and paves the way for initial time-resolved thermoelectricity experiments. This thesis intervenes within this context, we provide additional tools for theoretical research, which in turn we hope it will motivate experimentation.

3.3. Theoretical frameworks for quantum transport

In this subsection we shortly highlight two theoretical approaches to describe quantum transport of electrons and energy that we will use within this thesis: the scattering theory and the linear response.

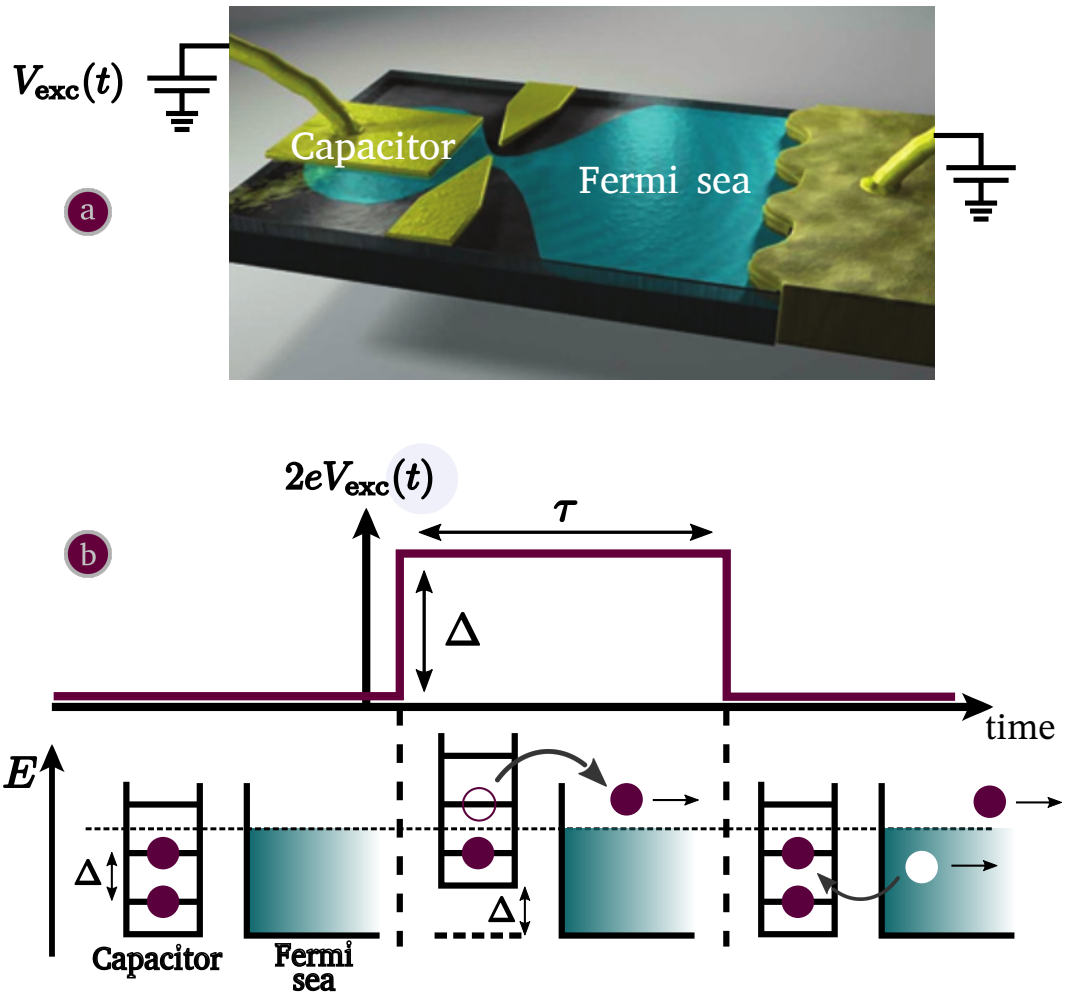

Figure 3.8. – Sketch of the inner workings of a mesoscopic capacitor. (a) Adapted from [131]. 3D representation of a mesoscopic capacitor: an isolated cavity connected to a Fermi sea of electrons, through a quantum point contact. (b) Redrawn from [14]. Energy resolved mesoscopic capacitor: initially, the capacitors levels are filled till the Fermi energy. Then the energy levels of the capacitor are shifted, by the gate potential V_{ext}, by exactly the spacing Δ between two energy levels, this releases an electron with a well defined energy with a tunable uncertainty (through the emission time τ). Finally the gate potential is shifted back to original value, the Fermi sea fills back the empty space left by the previous electron, which creates a hole below the Fermi energy level.

The scattering theory will be extensively described in Chap. 5 whereas the linear response will be used to recover a result from the literature in Sec. 6.1. Other theoretical frameworks for describing transport, both in the stationary and time-dependent regime, will be quickly listed.

For a more complete study of the theoretical descriptions, Ref. [46] describes quantum transport in the stationary regime, Ref. [16] is a review of the methods to describe thermoelectric quantum transport in the stationary regime, Ref. [66] makes an overview of the time-dependent theoretical methods for describing quantum transport and generalizes the non-interacting scattering approach to the time-dependent regime. Ref. [139] describes electronic transport in both the classical and quantum regimes, under stationary and time-dependent drive. For the classical approaches and practical thermoelectric implementations, one can refer to Refs. [75, 74].

3.3.1. Scattering Theory – Landauer-Büttiker formalism

This approach applies to non-interacting electrons (interaction can still be accounted for at the mean-field level) and is based on considering a central system, also called a scattering region, that is connected to several thermal baths through electronic waveguides called leads (see Fig. 3.9). The baths then influence which 'incoming modes' are populated within the leads whereas the system affects the 'outgoing modes' in each lead although no back action on the baths is considered within this theoretical framework. An electron, described by a wavefunction (see 4.2.1.1), leaves a bath α and enters the central system to eventually be transmitted/reflected in a bath β with a probability $T_{\alpha\beta}$. The probabilities $T_{\alpha\beta}$ can be derived by solving the Schrödinger equation, and this enables to write the particle and energy currents that leave each lead α. We will use this theory throughout this thesis, a more detailed description is done in Sec. 5.1. A review of the original development for particle transport is done by Ref. [20], extended to heat and energy transport by Ref. [26].

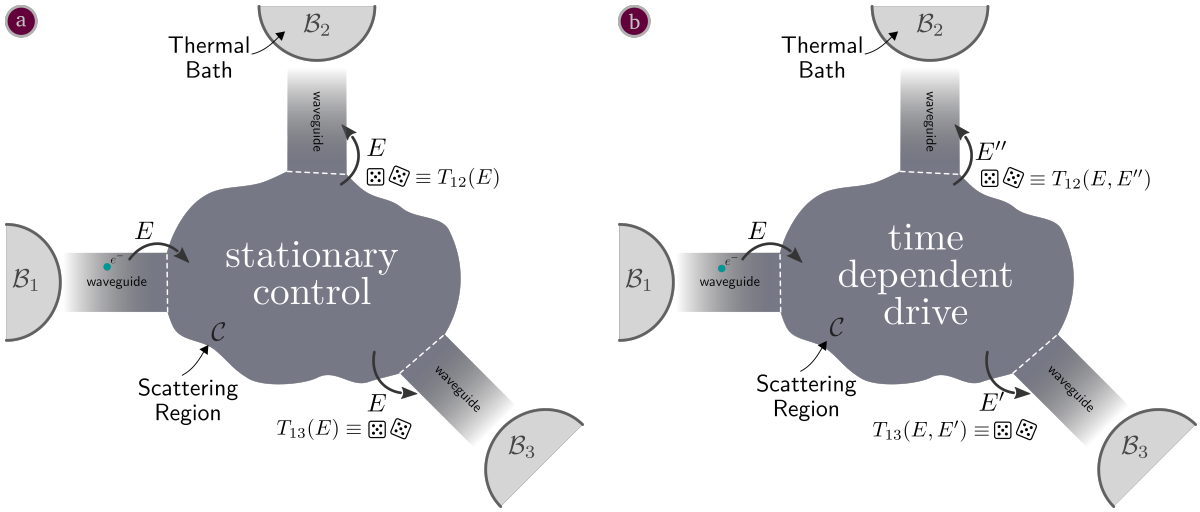

Figure 3.9. – Sketch of the scattering approach. A central system, called a scattering region, is connected to several baths $\mathcal{B}$ through waveguides. Electrons leave each bath $\mathcal{B}_\alpha$, with energies E that follow a thermal distribution, and enter the waveguide till they reach the scattering region where the undertake a first transmission or reflection. Transmitted electrons in the scattering region undergo several reflections and interfere then they eventually leave it to be transmitted in one of waveguides to reach the baths $\mathcal{B}_\beta$ *a)* with the same energy E when in the stationary regime, with a probability $T_{\alpha\beta}$ or *b)* with a different energy E' in the time-dependent regime, due to the drive that causes energy redistribution within the scattering region, with a probability $T_{\alpha\beta}(E, E')$.

Stationary regime An electron leaving a bath $\mathcal{B}_\alpha$ with an energy E gets transmitted to each bath β, at the same energy E (see Fig. 3.9 a), with an amplitude $d^{\alpha\beta}(E)$ whose absolute square $T_{\alpha\beta} = \left|d^{\alpha\beta}(E)\right|^2$ is the probability of getting transmitted to the bath β. The particle current I_α^{N}, the energy current I_α^{E} and the heat current I_α^{Q} leaving a bath α are simply the net sum of the electron number, the energy and the heat carried by each electron leaving the bath minus the one carried by the electrons

entering, weighted by the probability of each event

$$I_\alpha^{\mathrm{N}} = \sum_{\beta\neq\alpha} \int \frac{\mathrm{d}E}{2\pi\hbar} \qquad \left[f_\alpha(E) - f_\beta(E)\right] T_{\alpha\beta}(E)$$

$$I_\alpha^{\mathrm{E}} = \sum_{\beta\neq\alpha} \int \frac{\mathrm{d}E}{2\pi\hbar} \quad E \qquad \left[f_\alpha(E) - f_\beta(E)\right] T_{\alpha\beta}(E)$$

$$I_\alpha^{\mathrm{Q}} = \sum_{\beta\neq\alpha} \int \frac{\mathrm{d}E}{2\pi\hbar} \, (E-\mu_\alpha) \left[f_\alpha(E) - f_\beta(E)\right] T_{\alpha\beta}(E)$$

where $f_\alpha = \left(\exp\left(\frac{E-\mu_\alpha}{k_\mathrm{B}T_\alpha}\right)+1\right)^{-1}$ is the Fermi distribution of the bath $\mathcal{B}_\alpha$ (also given in Eq. (5.28)), see Sec. 5.1.2 for a description of its implementation in the `Kwant` simulation library.

Time-dependent regime The time dependent regime adds one extra ingredient over the stationary approach of scattering: inelastic events due to the time-dependent drive that redistributes the energy of the electrons coming from each bath. Two equivalent approaches can be used to describe quantum transport in scattering systems sketched in Fig. 3.9. Each one with its advantage and drawback over the other.

→ Scattering states – wavefunction approach This approach relies on time evolving a set of one-body wavefunctions, called scattering states, to describe many-body transport in non-interacting tight-binding systems, it does not need the computation of the transmission amplitudes to be able to express transport quantities. One implementation of this idea has been developed by X. Waintal's group [66, 203, 101], at CEA Grenoble, and has been used to implement the `tkwant`[101] simulation library. This implementation is reported to be equivalent to the *partition-free initial condition approach*[109, 182] as the electronic baths are attached to the scattering region from the remote past ; it also is a generalization of the *single-electron approach* [78, 79] used within specific models. Although less useful for analytical studies, the scattering states are extremely efficient for numerical simulation. In this thesis, we will describe the method used by `tkwant` in more details in Sec. 5.1 and generalize it to energy transport: see Sec. 5.2.3.1 for the end result of the generalization. In Sec. 5.2.3.2 we show that it recovers the static limit described above, and Sec. 5.3 we describe its practical implementation within `tkwant`.

→ Two-energy transmission amplitudes Under a time-dependent drive, electrons leaving the bath α with an energy E will get transmitted in the other baths β with a different energy E' due to the time-dependent drive that pumps in/out energy (see Fig. 3.9 b): the transmission happens with an amplitude $d^{\alpha\beta}(E', E)$ whose expression is determined by the drive. The goal of this approach is therefore to express or compute the transmission amplitudes $d^{\alpha\beta}(E', E)$ *e.g.* by solving the Schrödinger equation on a generic scattering state, by combining known subsystem transmission amplitudes (see Fig. 6.6 for an illustration) or, when the time-dependent drive is periodic, Fourier series enable a Floquet approach to quantum transport [133, 135]. Using transmission amplitudes is adapted to an analytical and semi-analytical study of systems as they are interpretable as-is, for example as energy filters [16]. In this thesis, we use this approach and determine the transmission amplitude $d(E', E)$ of the Resonant Level Model (see Sec. 5.3.2.1 for a description of the model), when we use the 'wideband limit'. See Sec. 6.

3.3.2. Linear-Response – Onsager Matrix

To simplify the description, we consider two-terminal systems that are connected to only two, "left" and "right", electrochemical baths characterized by their temperature T_α and electrochemical potential μ_α, $\alpha = \mathrm{L}$ (left), R (right), see Fig. 3.10. A generalization to multi-terminal systems can then be made. The "linear response" approach can be undertaken when $\Delta T = T_\mathrm{L} - T_\mathrm{R}$ and $\Delta\mu = \mu_\mathrm{L} - \mu_\mathrm{R}$ are small when compared to their respective average value ; or when the variation δT of the temperature and $\delta\mu$ of the chemical potential, over the span of the relaxation length, are small with respect to their average value T and μ, in which case local equilibrium can be assumed. Equilibrium transport coefficients – namely the electrical conductance G, the thermal conductance K, the Seebeck coefficient S and the Peltier coefficient Π – can then be derived to predict the behavior of a thermoelectric system.

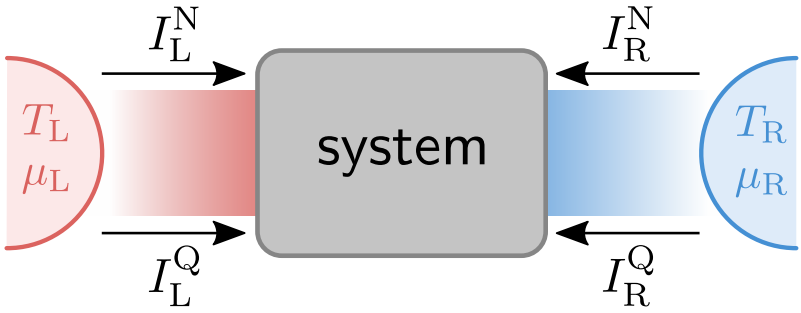

Figure 3.10. – Representation of a two-terminal thermoelectric system. Connected to two thermal baths – left (L) and right (R) – the system is crossed by heat currents I_α^Q and particle currents I_α^N that go from the bath α =L,R to the other.

Stationary regime Under stationary biases ΔT and $\Delta\mu$, the system eventually reaches a steady state characterized by constant particle currents I_α^N and heat currents I_α^Q. Without loss of generality, the left particle current I_L^N and the left heat current I_L^Q are related to the displacements $\Delta V/T$ ($\Delta V = \Delta\mu/e$) and $\Delta T/T^2$ through the *Onsager matrix* $\mathbf{L}$[29, 76]

$$\begin{bmatrix} I_\mathrm{L}^\mathrm{N} \\ I_\mathrm{L}^\mathrm{Q} \end{bmatrix} = \underbrace{\begin{bmatrix} L_\mathrm{NN}^\mathrm{L} & L_\mathrm{NQ}^\mathrm{L} \\ L_\mathrm{QN}^\mathrm{L} & L_\mathrm{QQ}^\mathrm{L} \end{bmatrix}}_{\mathbf{L}} \begin{bmatrix} \Delta V/T \\ \Delta T/T^2 \end{bmatrix} \tag{3.6}$$

where L_AB (A,B=N,Q) are the *Onsager coefficients*. They verify the *Onsager reciprocal relation*

$$L_\mathrm{NQ} = L_\mathrm{QN} \tag{3.7}$$

if the system is invariant with respect to the time-reversal symmetry and is not under the influence of a magnetic field: the second principle of thermodynamics further constrains these coefficients

$$L_\mathrm{NN} \geq 0 \qquad\qquad \det(\mathbf{L}) \geq 0 \tag{3.8}$$

The right currents I_R^N and I_R^Q, with the same sign convention (positive when leaving the bath), are related to the left currents as follows

$$I_\mathrm{L}^\mathrm{N} = -I_\mathrm{R}^\mathrm{N} \qquad\qquad I_\mathrm{L}^\mathrm{Q} + I_\mathrm{R}^\mathrm{Q} = \Delta V\ I_\mathrm{R}^\mathrm{N} \tag{3.9}$$

The Onsager coefficients can either be computed from a lower level approach (see next paragraph)

or from experimentally measuring the transport coefficients, to which they are related as follows [16]

$$\begin{aligned} G = & \left.\frac{I^{\mathrm{N}}}{\Delta V}\right|_{\Delta T=0} = \frac{L_{\mathrm{NN}}}{T} \\ K = & \left.\frac{I^{\mathrm{Q}}}{\Delta T}\right|_{I^{\mathrm{N}}=0} = \frac{1}{T^2}\frac{\det(L)}{L_{\mathrm{NN}}} \\ S = & -\left.\frac{\Delta V}{\Delta T}\right|_{I^{\mathrm{N}}=0} = \frac{1}{T}\frac{L_{\mathrm{NQ}}}{L_{\mathrm{NN}}} \end{aligned} \tag{3.10}$$

Time-dependent regime Ref. [118] developed a consistent theory in the slow and periodic regime where the relations in Eq. (3.8) and Eq. (3.9) are still valid but with cycle-averaged matrix elements. Ref. [219] used the linear response approach in the 'fast' time-dependent regime for a non-interacting two-terminal device: while the biases $[\Delta V, \Delta T]$ are still considered time-independent, the system is driven by *e.g.* a time-dependent gate-voltage. In this article, the considered Onsager coefficients $L^{\alpha}_{\mathrm{AB}}(t)$ are time-dependent: the 'conservation' relations Eqs. (3.9)-(3.8) are reported to be violated which would give hopes for a higher thermoelectric efficiency in the driven regime. In this thesis, we recovered the reported results although we believe that the physical interpretability of a time-dependent Onsager matrix, in the driven regime, is not straightforward: see Sec. 6.1 for a more complete analysis. The Seebeck has also been generalized to the time-dependent regime $S(t)$ [38]. If one wishes to treat the time-dependent control itself in the linear-response regime, *i.e.* as a perturbation over the stationary state, a more fundamental and thorough approach to linear-response theory is described in Ref. [183].

3.3.3. Other theoretical frameworks for time-dependent quantum transport

We succinctly describe few other theoretical frameworks – some will be omitted, such as the Time-dependent Density Functional theory [110, 109] that are out of scope within this thesis – to describe time-dependent transport. Each framework comes with their own advantages, equivalences/similarities and drawbacks when compared with the other frameworks.

Time-dependent quantum master equations Master equations describes the evolution of a quantum open system $\mathcal{S}$ as a part of a global 'total' system $\mathcal{T}$ that is made of $\mathcal{S}$ and the environment $\mathcal{E}$ with whom it interacts and exchanges matter, energy and heat. The practical description relies on writing a 'master equation' of the density operator $\hat{\rho}_{\mathcal{T}}$ of the total system or its reduction $\hat{\rho}_{\mathcal{S}}$ to the system $\mathcal{S}$. The most extensively studied theoretical framework within this approach relies on Lindblad master equations [68, 173, 138] where, initially, two main assumptions are made over the nature of the coupling between the system and the environment : it is assumed to be weak and of markovian nature. The markovian assumption being usually attained by a sufficient condition of slow driving in time. No other assumption in particular is made over the system of interest, it can be time-dependent and involve interactions of arbitrary strength. Further works generalized the Lindblad approach to the strong coupling, non-markovian regime [187, 179, 170, 186] while other studies developed alternative master equation approaches such as the driven Liouville von Neumann (DLvN) method [167, 6, 218, 217, 216, 143] or NEGF-based [47, 175].

Non-equilibrium Green's functions (NEGF) This is a powerful method for describing quantum transport as it can theoretically fully handle electron-electron and electron-phonon interactions in the

time-dependent regime, in the weak and strong coupling regime with the baths. The price to pay is its added complexity both in its theoretical framework and in computation. A quantum system is fully described within this approach with the so called *Green functions*: the *retarted*, *advanced*, *lesser* and *greater* Green functions. Various methods have been developed to derive these Green functions, as the *Nonequilibrium Equation of Motion* method or the *Kadanoff-Baym-Keldysh* method. Practical implementations to simulate electronic transport can be to directly calculate the non-equilibrium green functions from their equations of motion but it is too expensive in terms algorithmic complexity [66] and therefore unpractical. Other methods have been developed such as the Auxiliary-Mode Expansion [39] for charge and energy currents [113]. It has been shown [66] that the NEGF approach is equivalent to the wavefunction scattering approach in the non-interacting case, with a relationship linking the two given in Eq. (5.26). For more information about the NEGF formalism, see *e.g.* [165, 183].

4. Non-interacting time-dependent quantum transport : Theoretical apparatus

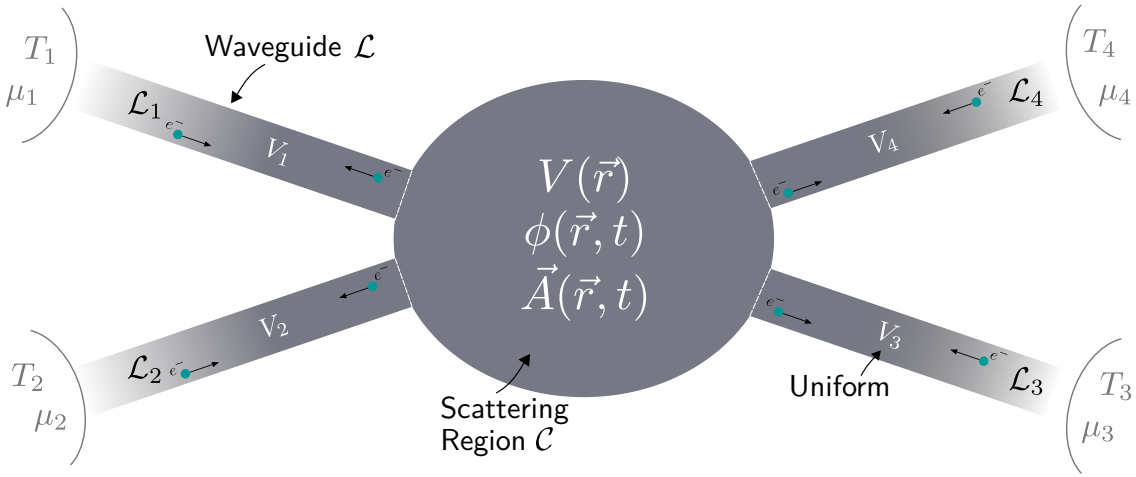

Figure 4.1. – Target system in which energy and particle transport will be considered
Made of a central area $\mathcal{C}$ called 'scattering region'. It is under the influence of an external time dependent electromagnetic field, represented by the scalar potential $\phi(\vec{r},t)$ and the vector potential $\vec{A}(\vec{r},t)$. The scattering region is connected to semi-infinite 'waveguides' $\mathcal{L}_\alpha$. An additional static potential energy V is considered to model any potential created by the system itself e.g. the potential created by the nuclei of atoms. Each lead $\mathcal{L}_\alpha$ is filled with electrons that travel towards the scattering region, according to a thermal distribution given by the temperature T_α and chemical potential μ_α. In our approach, the time dependence only starts after an instant t_0. Note that a time-dependent uniform scalar potential in each lead can be taken into account through a gauge change, see Sec. 5.1.1.

In this chapter, we build a local transport quantum theory of non-interacting electrons and the energy they carry, while under a time-dependent electromagnetic field. The goal is to describe a class of generic scattering systems as described in Fig. 4.1. First, in Sec. 4.1, we briefly go through the classical theory of charge and energy transport to highlight two driving principles that will be ported over to the quantum description, *i.e.* local energy conservation and gauge invariance, but also discuss the case of the ill-defined 'mechanical energy' in the time-dependent regime, the quantum equivalent being the Hamiltonian. Then, in Sec. 4.2, we quickly redraw the well-known quantum theory of single particles described by wavefunctions. We introduce the Schrödinger equation as a means to obtain these wavefunctions, then we use these wavefunctions to expose once again the well-known local particle transport quantities and their less known energy counterpart with a strong focus on gauge invariance and the ongoing debates over defining an energy local operator. These local equations are then re-derived in the discretized space (see Sec. 4.2.4) and in the many-body non-interacting second quantization approach (see Sec. 4.3), after a concise introduction to second-quantization and the constraints coming from considering many-body quantum physics. Finally, we expose in Sec. 4.3.4

how lead currents can be calculated as a flux of local quantities and discuss the ongoing research and debates over the heat current. Note that Sections 4.3.3 and 4.3.4 constitute the main parts of this chapter. They are leveraged in Chapter 5 where we discuss the (wavefunction based) numerical implementation of this theoretical framework.

4.1. Classical electrodynamics

Classical electrodynamics are entirely described by joining classical mechanics – through the equivalent Newton's mechanics, Lagrangian mechanics or Hamiltonian mechanics – the Maxwell equations that uncover the interplay between the electric field $\vec{E}(\vec{r},t)$, the magnetic field $\vec{B}(\vec{r},t)$, the local density of charge $\rho(\vec{r},t)$ and the local charge current density $\vec{j}(\vec{r},t)$. The description is given by the following well-known set of four equations

$$\begin{aligned} \vec{\nabla}\cdot\vec{E} &= \rho/\varepsilon_0 & \vec{\nabla}\cdot\vec{B} &= 0 \\ \vec{\nabla}\times\vec{E} &= -\partial_t\vec{B} & \vec{\nabla}\times\vec{B} &= \frac{1}{c^2}\partial_t\vec{E} + \mu_0\vec{j} \end{aligned} \tag{4.1}$$

where c is the speed of light in the vacuum, ε_0 is the vacuum permittivity, μ_0 is the vacuum permeability[1] and $\vec{\nabla}$ is the gradient operator[2].

4.1.1. Conservation equations

Using solely the equations above, one can derive a local particle conservation equation:

$$\partial_t\rho(\vec{r},t) + \vec{\nabla}\cdot\vec{j}(\vec{r},t) = 0 \tag{4.2}$$

Further derivation [91] enables us to write a local energy conservation equation, called the Poynting relation:

$$\partial_t u_{\text{EM}} + \vec{\nabla}\cdot\vec{\pi} = -\vec{j}\cdot\vec{E} \tag{4.3}$$

where P_{EM} is the local power density that is 'lost' to the charged matter,

$$P_{\text{EM}} = -\vec{j}\cdot\vec{E} \tag{4.4}$$

u_{EM} is the electromagnetic energy density and $\vec{\pi}$ is the Poynting vector, *i.e.* the energy current density associated with light. They are given by

$$u_{\text{EM}} = \frac{1}{2}(\varepsilon_0 E^2 + \frac{1}{\mu_0}B^2) \tag{4.5}$$

$$\vec{\pi} = \frac{1}{\mu_0}\vec{E}\times\vec{B} \tag{4.6}$$

What one can note with the energy conservation equation above, is that its derivation leaves a degree of freedom for the definition of $\vec{\pi}$: one can add to it the curl of an arbitrary vector field $\vec{O}(\vec{r},t)$, i.e. $\vec{\pi}' = \vec{\pi} + \vec{\nabla}\times\vec{O}$ while still having $\vec{\nabla}\cdot\vec{\pi} = \vec{\nabla}\cdot\vec{\pi}'$, therefore leaving equation (4.3) unchanged. Reference [91] reports that relativistic considerations make the definition (4.6) unique. This same problem will happen later on when we will want to define an energy current density carried by quantum particles : the equivalent of the classical kinetic energy current density $\frac{1}{2}mv^2\,\vec{v}/v$

[1] These constants are related by the following relation $\varepsilon_0\mu_0 c^2 = 1$

[2] In cartesian coordinates $\vec{\nabla} = (\partial_x, \partial_y, \partial_z)$

Integral conservation equation Using divergence theorem, the local conservation equations for particles (4.3) and energy (4.2) can be also written in an integral way for a given volume U and its envelope ∂U:

$$\partial_t N_U(t) + \int_{\partial U} \mathrm{d}S\ \vec{j}(\vec{r},t)\cdot\vec{n} = 0 \tag{4.7}$$

$$\partial_t \varepsilon_{\mathrm{EM}} + \int_{\partial U} \mathrm{d}S\ \vec{\pi}(\vec{r},t)\cdot\vec{n} = -\int_U \mathrm{d}^3 r\ \vec{j}\cdot\vec{E} \tag{4.8}$$

$$\text{where}\ \ N_U(t) = \int_U \mathrm{d}^3 r\ \rho(\vec{r},t)\ \ \text{and}\ \ \varepsilon_U(t) = \int_U \mathrm{d}^3 r\ u_{\mathrm{EM}}(\vec{r},t) \tag{4.9}$$

The divergence theorem states that the integral of the divergence $\vec{\nabla}\cdot\vec{E}$ of a vector field $\vec{E}$ over U is equal to its outgoing flux off the envelope ∂U:

$$\int_U \mathrm{d}^3 r \vec{\nabla}\cdot\vec{E}(\vec{r},t) = \int_{\partial U} \mathrm{d}S\ \vec{E}(\vec{r},t)\cdot\vec{n} \tag{4.10}$$

where $\mathrm{d}S$ is an infinitesimal surface on ∂U and $\vec{n}$ is the unit normal to $\mathrm{d}S$. And this translates the intuitive understanding of conservation: the rate of change of the intensive quantity enclosed within a volume can either be changed by an external source or by leaving the volume.

4.1.2. Gauge invariance

A way to theoretically handle the influence of electromagnetic fields on charged particles is to work with the electromagnetic scalar potential $\phi(\vec{r},t)$ and vector potential $\vec{A}(\vec{r},t)$ which substitute the electromagnetic fields in the Hamiltonian approach of classical mechanics [141]. Their relationship with the electromagnetic fields is the following:

$$\begin{aligned} \vec{E} &= -\vec{\nabla}\phi - \partial_t \vec{A} \\ \vec{B} &= \vec{\nabla}\times\vec{A} \end{aligned} \tag{4.11}$$

One caveat with those electromagnetic potentials is that they are not unique: given an arbitrary scalar field $\Lambda(\vec{r},t)$, one can add its time partial derivative $\partial_t\Lambda$ to the scalar potential $\phi(\vec{r},t)$ and subtract its gradient $\vec{\nabla}\Lambda$ from the vector potential $\vec{A}(\vec{r},t)$ while still keeping the relation (4.11) valid. Since the interaction between electromagnetic fields and charged matter is classically described through fields and not potentials, the physics remains unchanged after such a change. This transformation in the electromagnetic potentials is called a gauge transformation.

$$\begin{cases} \vec{A}' = \vec{A} - \vec{\nabla}\Lambda \\ \phi' = \phi + \partial_t\Lambda \\ \Lambda \text{ arbitrary scalar field} \end{cases} \tag{4.12}$$

One can summarize this with the following assertion:

$$\forall\Lambda(\vec{r},t),\quad \begin{cases} \vec{A}' = \vec{A} - \vec{\nabla}\Lambda \\ \phi' = \phi + \partial_t\Lambda \end{cases} \implies \begin{cases} \vec{E}' = \vec{E} \\ \vec{B}' = \vec{B} \end{cases} \tag{4.13}$$

where the electromagnetic fields verify equation (4.11).

4.1.3. Mechanical energy: the issue of time-dependence

In this paragraph, I will explore the issues raised in classical mechanics by time dependent electromagnetic fields. Ref. [103] does a similar but more extensive approach of this matter using the classical Hamiltonian approach. I re-derived here on my own here an equivalent approach using Newton's equation instead.

A particle with a charge q will be under the influence of the Lorentz force [91] $\vec{F} = q(\vec{E} + \dot{\vec{r}} \times \vec{B})$, where $\vec{r}(t)$ is its position at time t and $\dot{\vec{r}}(t)$ is its velocity. For this particle, Newton's equation writes:

$$m\ddot{\vec{r}}(t) = q\left[\vec{E}(\vec{r}(t),t) + \dot{\vec{r}}(t) \times \vec{B}(\vec{r}(t),t)\right] \tag{4.14}$$

We can do the scalar product of both sides with $\dot{\vec{r}}(t)$ and obtain, knowing that $\dot{\vec{r}} \cdot (\dot{\vec{r}} \times \vec{B}) = 0$:

$$m\ddot{\vec{r}}(t) \cdot \dot{\vec{r}}(t) = q\vec{E}(\vec{r}(t),t) \cdot \dot{\vec{r}}(t) \tag{4.15}$$

After noticing that the left hand side is total derivative with respect to time, we end up with the well-known Work-Kinetic energy theorem

$$\mathrm{d}_t\left[\frac{1}{2}m\dot{\vec{r}}^2\right](t) = q\vec{E}(\vec{r}(t),t) \cdot \dot{\vec{r}}(t) \tag{4.16}$$

We can note that the right hand side of (4.16) is the opposite of the right hand side of (4.3) (for a single particle in this case): the energy lost by the electromagnetic fields is won as kinetic energy by the particle.

Knowing that we can write the electric field with the potentials $\vec{E}(\vec{r},t) = -\vec{\nabla}\phi(\vec{r},t) - \partial_t\vec{A}(\vec{r},t)$, we can go further and express the time derivative of $\phi(\vec{r}(t),t)$:

$$\mathrm{d}_t\phi(\vec{r}(t),t) = \dot{\vec{r}}(t) \cdot \vec{\nabla}\phi(\vec{r}(t),t) + \partial_t\phi(\vec{r}(t),t) \tag{4.17}$$

It is useful in rewriting the right hand side of (4.16)

$$\vec{E}(\vec{r}(t),t) \cdot \dot{\vec{r}}(t) = -\mathrm{d}_t\phi(\vec{r}(t),t) + \partial_t\phi(\vec{r}(t),t) - \partial_t\vec{A}(\vec{r}(t),t) \cdot \dot{\vec{r}}(t) \tag{4.18}$$

that we can finally rewrite as

$$\mathrm{d}_t\left[\frac{1}{2}m\dot{\vec{r}}^2\right](t) = \underbrace{-\mathrm{d}_t q\phi(\vec{r}(t),t)}_{\alpha(t)} + \underbrace{q\partial_t\phi(\vec{r}(t),t) - q\partial_t\vec{A}(\vec{r}(t),t) \cdot \dot{\vec{r}}(t)}_{\beta(t)} \tag{4.19}$$

The right hand side of (4.19) can be written as a sum of two terms, $\alpha(t)$ and $\beta(t)$: these two terms are clearly gauge dependent, whose sum is gauge independent by construction (because derived from the gauge independent electric field). The term $\alpha(t)$ has been defined because it is a total time derivative that can be moved to the left hand side of (4.19) and make it part of an alleged Mechanical/Total energy U: it is – strictly speaking – gauge dependent

$$\mathrm{d}_t U = \mathrm{d}_t\left[\frac{1}{2}m\dot{\vec{r}}^2(t) + q\phi(\vec{r}(t),t)\right] = \underbrace{q\partial_t\phi(\vec{r}(t),t) - q\partial_t\vec{A}(\vec{r}(t),t) \cdot \dot{\vec{r}}(t)}_{\beta(t)} \tag{4.20}$$

This makes the usual definition of mechanical energy non-physical and should be in principle avoided, for the time-dependent phenomena at least. In the special case of stationary electromagnetic fields $E(\vec{r})$ and $B(\vec{r})$, one usually takes for them stationary scalar and vector potentials $\phi(\vec{r})$, $\vec{A}(\vec{r})$:

$$\begin{cases} \partial_t\vec{E} = 0 \\ \partial_t\vec{B} = 0 \end{cases} \implies \exists\ \vec{A}(\vec{r}), \phi(\vec{r}) \mid \begin{cases} \vec{E} = -\vec{\nabla}\phi \\ \vec{B} = \vec{\nabla} \times \vec{A} \end{cases} \tag{4.21}$$

Given the definition of the scalar potential and how it behaves through a gauge transformation, this makes the scalar potential unique (among the stationary possibilities, while the vector potential is still not[3] but is time-independent). In this case, equation (4.20) simplifies to:

$$\mathrm{d}_t U = \mathrm{d}_t \left[\frac{1}{2} m \dot{\vec{r}}^2(t) + q\phi(\vec{r}(t)) \right] = 0 \tag{4.22}$$

Which is the usual mechanical energy conservation, which is unique and well defined among the stationary potentials. Although in principle only the kinetic energy has a real physical meaning in that equation.

This issue with time dependence and mechanical energy will appear in the quantum case too, as we will see in our quantum description of particles in sec 4.2.3.

4.2. One-body quantum approach – First quantization

In the previous section, we did a quick introduction to classical electrodynamics. In the scope of this thesis, particle behavior will be described by quantum mechanics. In this section, we will make a minimal introduction to one-body quantum mechanics along with the underlying mathematics that we will use to describe particle and energy transport. The particle transport equations are well known and tackled in general physics textbooks, the energy transport equations on the other hand, especially with a gauge invariant conservation equation approach, remain rather marginal. In this thesis, we uncover such an approach then do a more thorough description of energy transport with a gauge-invariant energy conservation point of view.

4.2.1. An introduction to quantum mechanics of a single particle

We will expose in the following the base concepts and mathematics of quantum mechanics involving a single particle. We will use these mathematical tools all along our approach to describe quantum-mechanically particle and energy transport.

4.2.1.1. The wavefunction

In the quantum realm, at each instant t, physical properties of an electron (energy, position, kinetic momentum, dynamic momentum [56, Chap. 21-3], angular momentum...) do not have a fixed, deterministic, value. Instead, physical properties are fundamentally random, with a deterministic probability distribution that can be probed through repeated same-experiments. For a given single particle, at each time t, probability distributions for any physical property are entirely defined by a complex scalar field $\psi(\vec{r}, t)$, called the wavefunction, that completely characterizes the state of the particle.

Equation of motion The equivalent to Newton's equation to describe the time evolution of the position $\vec{r}(t)$ of a single particle is the Schrödinger's equation

$$\mathrm{i}\hbar\partial_t \psi(\vec{r}, t) = \hat{h}[\psi](\vec{r}, t) \tag{4.23}$$

[3] $\vec{\nabla} \times (\vec{\nabla}\Lambda) = 0$

where the Hamiltonian $\hat{h}$ is a linear operator that acts on wavefunctions[4]. Wavefunctions that describe the evolution of the particle's state must abide by this equation. An equivalent evolution equation can be written with the *evolution operator* $\hat{u}(t, t_0)$

$$\psi(\vec{r}, t) = \hat{u}(t, t_0)\psi(\vec{r}, t_0) \tag{4.24}$$

that time-evolves a wavefunction from an initial state at time t_0 to its state at time t. Its connection with the Hamiltonian $\hat{h}$ is the following

$$\mathrm{i}\hbar\partial_t \hat{u}(t, t_0) = \hat{h}\hat{u}(t, t_0) \tag{4.25}$$

The term "wavefunction" has been used in its plural form here to translate a fundamental aspect of quantum mechanics: there are many wavefunction candidates $\psi(\vec{r}, t)$ that can theoretically describe the evolution of the state of a particle as long as they verify Schrödinger's equation. Given that $\hat{h}$ is a linear operator, any (complex) linear superposition of solutions to Schrödinger's equation is also a solution. A unique wavefunction can be defined with initial boundary conditions.

Given a valid candidate wavefunction $\psi(t)$, the modulus square $|\psi(\vec{r}, t)|^2$ expresses the density of probability $\rho(\vec{r}, t)$ of finding the particle at a point $\vec{r}$ at time t.

$$\rho(\vec{r}, t) = |\psi(\vec{r}, t)|^2 = \psi^*(\vec{r}, t)\,\psi(\vec{r}, t) \tag{4.26}$$

Hilbert space The interpretation of $\rho(\vec{r}, t) = |\psi(\vec{r}, t)|$ as being a spatial density of probability brings an additional restriction to wavefunctions that describe a physically valid states: given that $\rho(\vec{r}, t)$ is a probability density, its integral over space must be 1.

$$\int \mathrm{d}^3 r\ \rho(\vec{r}, t) = \int \mathrm{d}^3 r\ \psi^*(\vec{r}, t)\psi(\vec{r}, t) = 1 \tag{4.27}$$

which means that, at each instant t, wavefunctions that bear a physical meaning live in the space $\mathcal{H}$ of square integrable complex functions[5] with the following inner product between two 'vectors' $\psi(\vec{r})$ and $\phi(\vec{r})$

$$\langle\psi|\phi\rangle = \int \mathrm{d}^3 r\ \psi(\vec{r}, t)^*\phi(\vec{r}, t) \tag{4.28}$$

to define a Hilbert space: a complex vector space with a hermitian inner product, more information in [111, Chap. 4].

→ Orthonormal bases There exist orthonormal bases $\left(\lambda_i(\vec{r})\right)_i$, where each function $\lambda_i \in \mathcal{H}$ and $\forall i, j\ \langle\lambda_i|\lambda_j\rangle = \delta_{ij}$ for the Hilbert space $\mathcal{H}$ of square integrable complex functions of space, where δ is the Kronecker delta

$$\delta_{ij} = \begin{cases} 1 & \text{if} \quad i = j \\ 0 & \text{otherwise} \end{cases} \tag{4.29}$$

Note that i is in general a tuple of integer values $i = (i_1, \ldots, i_k),\ i_n \in \mathbb{Z}$. Examples of such bases are the ones used for wavelet transformation [184]. Any vector $\psi(\vec{r})$ from $\mathcal{H}$ can be written as a linear

[4] it can parametrically depend on the time parameter t but this time dependence will not be made explicit as it will be reserved to writing operators in the Heisenberg representation

[5] a non-normalized, square integrable, wavefunction can always be normalized by a real valued factor

combination of vectors of the given basis, the coefficients are obtained by using the inner-product to perform projections

$$\forall \psi(\vec{r}) \in \mathcal{H} \;\; \psi(\vec{r}) = \sum_i \langle \lambda_i | \psi \rangle \, \lambda_i(\vec{r}) \tag{4.30}$$

The arbitrary basis $(\lambda_i(\vec{r}))_i$ can be time-evolved with the evolution operator $\hat{u}(t, t_0)$ to define a time-dependent basis $(\lambda_i(\vec{r}, t))_i$ of solutions to the Schrödinger equation, where $\lambda_i(\vec{r}, t_0) = \lambda_i(\vec{r})$. At each instant t, the base $(\lambda_i(\vec{r}, t))_i$ remains orthonormal thanks to the Hermitian nature of the Hamiltonian $\hat{h}$. A wavefunction $\psi(\vec{r}, t)$ that verifies Schrödinger's equation defines a vector $\psi_t(\vec{r})$ of $\mathcal{H}$ at each instant t. It can either be expressed in the basis $(\lambda_i(\vec{r}))_i$ with time dependent coefficients or in the basis $(\lambda_i(\vec{r}, t))_i$ with time-independent coefficients

$$\forall \psi(\vec{r}, t) \;\; \mathrm{i}\hbar \partial_t \psi = \hat{h}[\psi] \implies \begin{cases} \psi(\vec{r}, t) = \sum_i \langle \lambda_i | \psi(t) \rangle \, \lambda(\vec{r}) \\ \psi(\vec{r}, t) = \sum_i \langle \lambda_i | \psi(t_0) \rangle \, \lambda(\vec{r}, t) \end{cases} \tag{4.31}$$

When the Hamiltonian doesn't parametrically depend on time, one can use its Eigenstates to define an orthogonal basis thanks to the Hermitian nature of the Hamiltonian operator

$$\hat{h}[\lambda_i^0](\vec{r}) = E_i \lambda_i^0(\vec{r}) \;\; \text{with} \;\; E_i \in \mathbb{R} \tag{4.32}$$

A base of solutions to the Schrödinger equation are then simply obtained from this basis by time evolving it:

$$\lambda_i^0(\vec{r}, t) = \lambda_i^0(\vec{r}) \exp\left(-\mathrm{i}\frac{E_i t}{\hbar}\right) \tag{4.33}$$

While solving the Schrödinger equation, sometimes it is useful to define a base of solutions $(\mu_\alpha(\vec{r}))_\alpha$ that are not square integrable – *i.e.* $\lambda_\alpha \notin \mathcal{H}$ – where α can be a tuple of real and integer variables $\alpha = (\alpha_1, \dots, \alpha_k), \alpha_i \in \mathbb{R}$ or $\mathbb{Z}$. An example of such a basis are the plane waves $||_{\pm,k,E}(\vec{r}, t) = \exp\left(\pm \mathrm{i}(\frac{Et}{\hbar} - \vec{k} \cdot \vec{r})\right)$ that are solution to the free Schrödinger equation.

→ Braket notation A vector $\psi(\vec{r})$ from the Hilbert space $\mathcal{H}$ can also be written like $|\psi\rangle$, called a *ket*. There is a 1-to-1 correspondence between a *ket* $|\psi\rangle$ and the linear form $\langle\psi|$, called *bra*, whose action on a *ket* $|\phi\rangle$ is the inner-product between *ket* $|\psi\rangle$ and *ket* $|\phi\rangle$

$$\begin{aligned} \langle\psi| : \mathcal{H} &\longrightarrow \mathbb{C} \\ |\phi\rangle &\longmapsto \langle\psi|\phi\rangle \end{aligned}$$

To move back to a wavefunction description from a ket $|\psi\rangle$. One can introduce the set of kets $|\vec{r}\rangle$ whose interpretation is "the particle is entirely located at the position $\vec{r}$". The associated 'wavefunction' $\psi_{\vec{r}}$ to the ket $|\vec{r}\rangle$ is the dirac distribution $\psi_{\vec{r}}(\vec{r}') = \delta^{(3)}(\vec{r} - \vec{r}')$ which enables recovering the associated wavefunction $\psi(\vec{r})$ from any given ket $|\psi\rangle$ as an inner product

$$\psi(\vec{r}) = \langle \vec{r} | \psi \rangle = \int \mathrm{d}^3 r' \; \delta^{(3)}(\vec{r} - \vec{r}') \psi(\vec{r}') \tag{4.34}$$

4.2.1.2. Physical properties – Operators

In this Hilbert space $\mathcal{H}$, to each physical property $\mathcal{O}$ corresponds a linear hermitian operator $\hat{o}$ that acts within $\mathcal{H}$. Given a particle describe by a wavefunction $\psi(\vec{r}, t)$ – *i.e.* normalized to 1 and verifies

the Schrödinger equation – the expectation value of the physical quantity $\mathcal{O}$, at a given time t, that we write $\langle\hat{o}\rangle_{\psi(t)}$ [6] can be computed as the hermitian inner product, written as $\langle .|.\rangle$, between ψ and $\hat{o}[\psi]$

$$\langle\hat{o}\rangle_{\psi(t)} = \langle\psi|\hat{o}[\psi]\rangle = \int \mathrm{d}^3r\, \psi^*(\vec{r},t)\hat{o}[\psi](\vec{r},t) \tag{4.35}$$

In braket notation, this expectation value also writes as $\langle\psi(t)|\hat{o}(t)|\psi(t)\rangle$. From the operator $\hat{o}$, the *adjoint operator* $\hat{o}^\dagger$ can be defined as the following

$$\forall\psi,\varphi\in\mathcal{H}\quad \langle\psi|\hat{o}[\varphi]\rangle = \langle\hat{o}^\dagger[\psi]|\varphi\rangle \tag{4.36}$$

An operator $\hat{o}$ is called Hermitian if it's equal to its adjoint operator $\hat{o}^\dagger$

$$\forall\psi,\varphi\in\mathcal{H}\quad \langle\psi|\hat{o}[\varphi]\rangle = \langle\hat{o}[\psi]|\varphi\rangle \tag{4.37}$$

which implies that its expectation $\langle\hat{o}(t)\rangle_{\psi(t)}$ is real valued as any physical quantity must be.

Heisenberg representation So far the described operators $\hat{o}$ act on time-dependent wavefunctions $\psi(\vec{r},t)$ that are solution to the Schrödinger equation, these operators are defined in the *Schrödinger representation*. Given the deterministic evolution of the wavefunctions, one can define operators $\hat{o}_{\mathrm{H}}(t)$, that we will simply write $\hat{o}(t)$ even if the operator $\hat{o}$ already depends parametrically on t, said in the *Heisenberg representation*, that act on wavefunctions $\psi(\vec{r})$ at an initial time t_0: they time evolve the wavefunction first to time t before applying the operator in the Schrödinger representation

$$\hat{o}(t) = \hat{o}_{\mathrm{H}}(t) = \hat{u}^\dagger(t,t_0)\,\hat{o}\,\hat{u}(t,t_0) \tag{4.38}$$

so that the expectation value of operators in the Heisenberg representation remains unchanged[7]

$$\langle\hat{o}(t)\rangle_{\psi(t_0)} = \langle\hat{o}\rangle_{\psi(t)} \tag{4.39}$$

which justifies the 'representation' naming as it is only a different way the describe the same physics. The time-derivative of the expectation value can also written in the Heisenberg representation

$$\frac{\mathrm{d}}{\mathrm{d}t}\langle\hat{o}(t)\rangle_{\psi(t_0)} = \frac{\mathrm{i}}{\hbar}\left\langle[\hat{h}(t),\hat{o}(t)]\right\rangle_{\psi(t_0)} + \langle[\partial_t\hat{o}](t)\rangle_{\psi(t_0)} \tag{4.40}$$

where $\hat{o}(t)$, $\hat{h}(t)$ and $\partial_t\hat{o}(t)$ are obtained by transforming respectively $\hat{o}$, $\hat{h}$ and $\partial_t\hat{o}$ according to Eq. (4.38). The $[\hat{h},\hat{o}]$ operator is called the commutator and is defined as follows

$$[\hat{h},\hat{o}][\psi] = \hat{h}[\hat{o}[\psi]] - \hat{o}[\hat{h}[\psi]] \tag{4.41}$$

The equation of motion (4.40) is also valid if the operators are in the Schrödinger representation if one takes the expectation values with the wavefunction at time t instead of t_0.

[6] Note that the operator itself can depend on time, like the Hamiltonian when it describes a time-dependent electromagnetic field.

[7] $\langle\hat{o}(t)\rangle_{\psi(t_0)} = \langle\psi(t_0)|\hat{u}^\dagger(t,t_0)\,\hat{o}\,\hat{u}(t,t_0)[\psi(t_0)]\rangle = \langle\hat{u}^\dagger(t,t_0)[\psi(t_0)]|\hat{o}\,\hat{u}(t,t_0)[\psi(t_0)]\rangle = \langle\psi(t)|\hat{o}[\psi(t)]\rangle$

Common operators The position operator $\hat{\vec{r}}$ is defined as the following [111, Eq. 8.119]:

$$\hat{\vec{r}}[\psi] = \vec{r}\,\psi \tag{4.42}$$

which leads to the following intuitive expectation value of the position:

$$\left\langle \hat{\vec{r}} \right\rangle_{\psi} = \int \mathrm{d}^3 r\ \psi^*(\vec{r},t)\,\vec{r}\,\psi(\vec{r},t) = \int \mathrm{d}^3 r\ \rho(\vec{r},t)\,\vec{r} \tag{4.43}$$

In the presence of a general electromagnetic field, represented by a scalar potential $\phi(\vec{r},t)$ and vector potential $\vec{A}(\vec{r},t)$, the velocity operator $\hat{\vec{v}}$ is defined as the following [56, Eq. (21.13)]:

$$\hat{\vec{v}}[\psi] = -\frac{\mathrm{i}\hbar}{m}\vec{\nabla}\psi - \frac{q}{m}\vec{A}(\vec{r},t)\,\psi \tag{4.44}$$

The kinetic energy operator $\hat{\kappa}$ is then defined, like its classical counterpart $\hat{\kappa} = \frac{1}{2}m\hat{\vec{v}}^2$ [8]:

$$\hat{\kappa}[\psi] = \frac{1}{2}m\hat{\vec{v}}^2[\psi] = \frac{1}{2m}\left[-\mathrm{i}\hbar\vec{\nabla} - q\vec{A}\right]^2[\psi] = \frac{1}{2m}\left[-\mathrm{i}\hbar\vec{\nabla} - q\vec{A}\right]\cdot\left[-\mathrm{i}\hbar\vec{\nabla}\psi - q\vec{A}\,\psi\right] \tag{4.45}$$

The Hamiltonian $\hat{h}$ is then the equivalent to the classical "mechanical" energy defined in the section above: the sum of the kinetic energy operator $\hat{\kappa}$, the potential energy from the associated electromagnetic scalar potential $q\hat{\phi}[\psi] = q\phi(\vec{r},t)\,\psi$ and an eventual stationary potential energy $V(\vec{r})$ from another physical origin[9]

$$\hat{h}[\psi] = \hat{\kappa}[\psi] + q\,\phi(\vec{r},t)\,\psi + V(\vec{r})\psi = \frac{1}{2m}\left[-\mathrm{i}\hbar\vec{\nabla} - q\vec{A}(\vec{r},t)\right]^2[\psi] + q\,\phi(\vec{r},t)\,\psi + V(\vec{r})\,\psi \tag{4.46}$$

In the scope of this thesis, the time-dependence of the external electromagnetic field is considered to start only after a certain time t_0: the scalar potential ϕ is zero before then and vector potential $\vec{A}$ is stationary

$$\begin{cases} \phi(\vec{r}, t < t_0) = 0 \\ \vec{A}(\vec{r}, t < t_0) = \vec{A}(\vec{r}) \end{cases} \tag{4.47}$$

4.2.1.3. Gauge change

After having a look at the expression of the expectation value $\langle\hat{o}\rangle_{\psi}$ of a physical quantity $\mathcal{O}$ when on a state ψ, one can realize that it is independent from a global fixed phase of ψ: ψ can be replaced by $\psi' = \mathrm{e}^{\mathrm{i}\alpha}\psi$, $\alpha \in \mathbb{R}$ while still preserving any operator's expectation value $\langle\hat{o}\rangle_{\psi} = \langle\hat{o}\rangle_{\psi'}$

In the case of the interaction with electromagnetic fields, described by the Hamiltonian $\hat{h}$ given in (4.46), an additional gauge invariance is respected [111, Chap 10.3][172, Chap. 7.4]: multiplying a wavefunction ψ by a space and time dependent phase $\exp(-\mathrm{i}\frac{q}{\hbar}\Lambda(\vec{r},t))$ does not change the underlying physics of the described system and only leads to a gauge change to the electromagnetic potentials in the Hamiltonian. The expectation value of any operator $\hat{o}$ that bears a physical meaning must remain unchanged:

$$\forall\Lambda(\vec{r},t), \forall\psi, \forall\hat{c}\ \ \psi' = \exp\left(-\mathrm{i}\frac{q}{\hbar}\Lambda(\vec{r},t)\right)\psi \implies \langle\hat{o}\rangle_{\psi} = \langle\hat{o}'\rangle_{\psi'} \tag{4.48}$$

where $\hat{o}'$'s expression is the same as $\hat{o}$ except for the electromagnetic potentials that are changed from $(\vec{A},\phi)$ to $(\vec{A}',\phi')$ according to (4.12). One can check that $\hat{\vec{v}}$ verifies (4.48) and consequently $\hat{\kappa}$ too.

[8] Note that $\vec{\nabla}\cdot\left[\vec{A}\psi\right] = (\vec{\nabla}\cdot\vec{A})\psi + \vec{A}\cdot\vec{\nabla}\psi$

[9] It can be for example the gravitational potential energy.

→ Effect on the Hamiltonian Interestingly enough the Hamiltonian does not abide by Eq. (4.48), one can derive the following relation by replacing $(\vec{A}, \phi)$ with $(\vec{A}', \phi')$ according to (4.12) in (4.46)

$$\hat{h}'[\psi'](\vec{r},t) = \exp\Big(-\mathrm{i}\frac{q}{\hbar}\Lambda(\vec{r},t)\Big)\left[\hat{h}[\psi](\vec{r},t) + q\,\partial_t\Lambda(\vec{r},t)\,\psi(\vec{r},t)\right] \tag{4.49}$$

which leads to the following relation for its expectation value

$$\left\langle \hat{h}' \right\rangle_{\psi'} = \left\langle \hat{h} \right\rangle_{\psi} + \left\langle q\,\partial_t\Lambda \right\rangle_{\psi} \tag{4.50}$$

The Schrödinger equation (4.23) in the other hand remains form-invariant – the same expression with the gauge transformed potentials – due to its left hand-side

$$\mathrm{i}\hbar\partial_t\psi'(\vec{r},t) = \exp\Big(-\mathrm{i}\frac{q}{\hbar}\Lambda(\vec{r},t)\Big)\left[\mathrm{i}\hbar\partial_t\psi(\vec{r},t) + q\,\partial_t\Lambda(\vec{r},t)\,\psi(\vec{r},t)\right] \tag{4.51}$$

and therefore writes

$$\mathrm{i}\hbar\partial_t\psi'(\vec{r},t) = \hat{h}'[\psi'](\vec{r},t) \tag{4.52}$$

→ Covariant derivatives In the next section, we define a particle current density whose value is gauge invariant thanks to writing the space derivative $\vec{D}$ as *covariant* – at least in the sense of being form invariant [111, Chap 7.4] – by involving the electromagnetic vector potential

$$-\mathrm{i}\hbar\hat{\vec{D}}[\psi] = -\mathrm{i}\hbar\vec{\nabla}\psi - q\vec{A}\,\psi \quad\Longrightarrow\quad \hat{\vec{v}} = -\frac{\mathrm{i}\hbar}{m}\hat{\vec{D}} \tag{4.53}$$

One *could* do the same with the time derivative and define a covariant time derivative D_t, inspired by special relativity [91]:

$$\mathrm{i}\hbar\hat{D}_t[\psi] = \mathrm{i}\hbar\partial_t\psi - q\,\phi(\vec{r},t)\,\psi \tag{4.54}$$

then use it to define a new "Schrödinger equation":

$$\mathrm{i}\hbar\hat{D}_t[\psi] = -\frac{\mathrm{i}\hbar}{m}\hat{\vec{D}}^2[\psi] + V\psi \tag{4.55}$$

where each term from both hand sides is form-invariant and whose expectation value is gauge invariant. This elegant form of the Schrödinger equation highlights the operators $\hat{\kappa}$ and V that have the dimension of an energy, a valid gauge invariant energy operator therefore involves these operators. Further development on defining an energy operator is done in Sec 4.2.3.

4.2.2. Time-dependent particle transport

It is a well known textbook approach to define a local probability current density $\vec{j}(\vec{r},t)$ that obeys a conservation law [111, Chap. 10.3] [172, Chap. 16.4][56, Chap. 21-2] with the local probability density $\rho(\vec{r},t)$

$$\partial_t\rho(\vec{r},t) + \vec{\nabla}\cdot\vec{j}(\vec{r},t) = 0 \tag{4.56}$$

where $\rho = \psi^*\psi$ (4.26) and $\vec{j}$ uses the velocity operator $\vec{v}$ given in (4.44)

$$\vec{j} = \mathrm{Re}\Big[\psi^*\hat{\vec{v}}[\psi]\Big] \tag{4.57}$$

The divergence of the current probability density writes

$$\vec{\nabla} \cdot \vec{j} = -\frac{2}{\hbar} \mathrm{Im}\Big[\psi^* \hat{h}[\psi]\Big] \tag{4.58}$$

One can notice the interesting fact that the integral of $\vec{j}$ over space gives the expectation value of the velocity:

$$\left\langle \hat{\vec{v}} \right\rangle_{\psi(t)} = \underbrace{\int \mathrm{d}^3\vec{r}\ \psi^* \hat{\vec{v}}[\psi]}_{\hat{\vec{v}} \text{ hermitian} \implies \in \mathbb{R}} = \int \mathrm{d}^3\vec{r}\ \mathrm{Re}\Big[\psi^* \hat{\vec{v}}[\psi]\Big] = \int \mathrm{d}^3\vec{r}\ \vec{j}(\vec{r}, t) \tag{4.59}$$

Given that $\vec{j}$ depends on $\hat{\vec{v}}$ which itself depends on the vector potential $\vec{A}$, we can prove that $\vec{j}$ is gauge invariant, i.e. that it keeps the same value when the vector potential $\vec{A}$ is changed to $\vec{A}'$ according to (4.12).

4.2.3. Time-dependent energy transport

The conservation equation involving the particle probability density and the probability current density are well known and documented in many textbooks. The same approach for energy would make understanding the underlying physics more intuitive. Although not considered in textbooks, Ref. [127] defined various energy conservation equations. For a given wavefunction ψ, they have the following form

$$\mathrm{d}_t \rho^\epsilon_\psi(\vec{r}, t) + \vec{\nabla} \cdot \vec{j}^\epsilon_\psi(\vec{r}, t) = S^\epsilon_\psi \tag{4.60}$$

where ρ^ϵ_ψ, $\vec{j}^\epsilon_\psi$ and S^ϵ_ψ are candidates for, respectively, the energy density, the energy current density and the energy source/power density. The ϵ superscript is there to indicate the energy quantity that we consider: it can either be the one related to the Hamiltonian $\hat{h}$, to the Kinetic energy operator $\hat{\kappa}$ or the 'total energy' operator $\hat{\varepsilon}$ (that will define further down). Each density $o_\psi = \rho^\varepsilon_\psi, \vec{j}^\varepsilon_\psi, S_\psi$, once integrated over space must give the expectation value (4.35) of its associated operator $\hat{o}$ on the state ψ

$$\int \mathrm{d}^3 r\ o_\psi(\vec{r}, t) = \langle \psi |\, \hat{o}\, | \psi \rangle = \langle \hat{o} \rangle_\psi \tag{4.61}$$

In the context of describing a single non-relativistic particle, the local quantities $(\rho^\varepsilon, j^\varepsilon, S^\varepsilon)$ bear no real physical meaning while the expectation value (4.61) of their associated system-wide operator does [127, 8]. This implies that any density candidate whose integral over space matches with the expectation value of its operator is a valid candidate[10]. We follow [127] to define a candidate for each term of the conservation equation (4.60).

One possible expression for energy density is to take the real part of the integrand whose integral computes the expectation value of the energy operator $\hat{\epsilon}$

$$\rho^\epsilon_\psi = \mathrm{Re}\Big[\psi^* \hat{\epsilon}[\psi]\Big] \tag{4.62}$$

[10] We will tackle further on the many body non-interacting problem where the big number of particles may enable us to interpret the many-body energy density as a "classical" energy density just like with particle transport [56, Chap. 21-4]. Although whether that interpretation is correct remains an open question since we build upon these single body definitions that are not unique.

The energy current density we take is essentially the symmetrized quantum equivalent to the classical energy current density $\rho_\epsilon \vec{v}/|\vec{v}|$, where ρ_ϵ is the associated energy density to the energy quantity ϵ[11]

$$\vec{j}^{\epsilon} = \frac{1}{2}\mathrm{Re}\left[\hat{\epsilon}[\psi]^* \hat{\vec{v}}[\psi] + \psi^* \hat{\vec{v}}[\hat{\epsilon}[\psi]]\right] \tag{4.63}$$

On top of the non-uniqueness of the densities whose integral is unique. The energy current density bears an additional degree of freedom as only its divergence is involved in the conservation equation (4.60): as with the electromagnetic Poynting vector $\vec{\pi}$ defined Eq. (4.6), it is theoretically not unique and an arbitrary curl of a vector field can be added to the energy current vector field while keeping its divergence unchanged.

An additional constraint over the considered energy operators comes into play from considering time-dependent electromagnetic fields: gauge invariance. Indeed, the electromagnetic potentials $(\phi, \vec{A})$ can be replaced by their gauge changed counterparts Eq. (4.12) while each term of the conservation equation (4.60) must remain unchanged. Further research [127, 102, 213] on defining a gauge invariant energy operator rules out the Hamiltonian $\hat{h}$ as a potential energy operator (because of Eq. (4.50)) and narrows down the possibilities to essentially the kinetic energy $\hat{\kappa}$, or the kinetic energy $\hat{\kappa}$ plus the stationary potential energy V which is considered to not be affected by gauge changes. We call the 'total energy' operator $\hat{\varepsilon}$ the sum of the kinetic energy $\hat{\kappa}$ and the stationary potential energy V.

Total energy The total energy operator $\hat{\varepsilon}$ is the sum of the kinetic energy operator $\hat{\kappa}$ and the stationary potential energy V.

$$\hat{\varepsilon}[\psi] = \hat{\kappa}[\psi] + V(\vec{r})\,\psi = \hat{h}[\psi] - q\,\phi(\vec{r},t)\,\psi \tag{4.64}$$

The total energy operator is gauge invariant as we consider the stationary potential V to not be affected by gauge changes. The potential V either originates from another physical interaction like gravity or is still of electromagnetic origin but comes from another source, we discuss this matter further at the end of the section. With this new energy operator, we take the following local densities that verify the conservation equation (4.60)

$$\rho^{\varepsilon} = \mathrm{Re}[\psi^* \hat{\varepsilon}[\psi]] = \mathrm{Re}[\psi^* \hat{\kappa}[\psi]] + V\rho \tag{4.65}$$

$$\vec{j}^{\varepsilon} = \frac{1}{2}\mathrm{Re}\left[\hat{\varepsilon}[\psi]^* \hat{\vec{v}}[\psi] + \psi^* \hat{\vec{v}}[\hat{\varepsilon}[\psi]]\right] \tag{4.66}$$

$$S^{\varepsilon} = q\vec{j}\cdot\vec{E} \tag{4.67}$$

where $\vec{E} = -\vec{\nabla}\phi - \partial_t \vec{A}$ and $\vec{j}$ the particle current given in (4.57). The explicit space and time dependence of each term has been omitted for clarity. We notice here that S^{ε} is the opposite of the classical energy power P_{EM}, given in Eq. (4.4), lost by light to the charged particles: we describe here how that energy is then redistributed in space by matter, through a quantum description.

Kinetic energy The kinetic energy operator $\hat{\kappa}$ proportional to the square of velocity operator $\hat{\vec{v}}$ as shown Eq. (4.45). In Appendix. A.1.1, we re-derive a textbook result which states that the velocity operator $\hat{\vec{v}}$, as defined in Eq. (4.44), is gauge invariant. Therefore the kinetic operator is gauge invariant.

[11] When $\epsilon = \kappa$ is the kinetic energy, we have $\rho^{\kappa} = \frac{1}{2}\rho\vec{v}^2$ for the kinetic energy current, where ρ is the mass density field and $\vec{v}$ is the velocity density field.

We define the following candidates for the energy conservation equation

$$\rho^{\kappa}(\vec{r},t) = \mathrm{Re}[\psi^* \hat{\kappa}[\psi]] \tag{4.68}$$

$$\vec{j}^{\kappa}(\vec{r},t) = \frac{1}{2}\mathrm{Re}\left[\hat{\kappa}[\psi]^* \hat{\vec{v}}[\psi] + \psi^* \hat{\vec{v}}[\hat{\kappa}[\psi]]\right] \tag{4.69}$$

$$S^{\kappa}(\vec{r},t) = \vec{j} \cdot \left[q\vec{E} - \vec{\nabla} V\right] \tag{4.70}$$

where $\vec{E} = -\vec{\nabla}\phi - \partial_t \vec{A}$ and $\vec{j}$ the particle current given in (4.57). The explicit space and time dependence of the wavefunction ψ and the result of applying operators on it have been omitted for clarity.

In the case of a charged particle under a time-dependent electromagnetic field represented by the potentials $(\vec{A}, \phi)$ but also under a *stationary* potential energy field $V(\vec{r})$ from a different physical origin, the Hamiltonian $\hat{h}$ writes, according to Eq. (4.46):

$$\hat{h}[\psi] = \hat{\kappa}[\psi] + q\phi(\vec{r},t)\,\psi + V(\vec{r})\,\psi \tag{4.71}$$

Hamiltonian energy In time-independent systems, the Hamiltonian $\hat{h}$ Eq. (4.46) is considered to be the energy operator. In this stationary regime, the 'total energy' operator and the Hamiltonian can coincide if one merges the scalar potential $\phi(\vec{r})$ with the potential energy $V(\vec{r}) \to V'(\vec{r}) = V(\vec{r}) + q\phi(\vec{r})$. The Hamiltonian can be considered as an energy operator (although with a fundamental issue) in the time-dependent case: one could take the following densities and verify the conservation equation (4.60)

$$\rho^{\mathrm{H}} = \mathrm{Re}\left[\psi^* \hat{h}[\psi]\right] \tag{4.72}$$

$$\vec{j}^{\mathrm{H}} = \frac{1}{2}\mathrm{Re}\left[\hat{h}[\psi]^*\, \hat{\vec{v}}[\psi] + \psi^* \hat{\vec{v}}[\hat{h}[\psi]]\right] \tag{4.73}$$

$$S^{\mathrm{H}} = \mathrm{Re}[\psi^* (\partial_t H)\,\psi] = q\,\vec{j} \cdot (-\partial_t \vec{A}) + q\,\partial_t \phi\,\rho \tag{4.74}$$

where $\rho = \psi^*\psi$ is the particle density and $\vec{j}$ is the particle current density given in (4.57). A more detailed derivation of the explicit expression of the energy source S^{H} is given in Appendix. A.2.2

→ Gauge dependence The Hamiltonian's expectation value is **not** gauge invariant in general (especially when the electromagnetic fields are time dependent). Indeed, we have seen in Sec. 4.2.1.3 that a gauge transformation (4.12) of the electromagnetic fields along with a phase change of the wavefunction $\psi \to \psi'$ must keep the expectation value of operators that bear physical meaning unchanged, as summarized in Eq. (4.48). However, the Hamiltonian's expectation value is not invariant under such a change

$$\langle H' \rangle_{\psi'} = \langle H \rangle_{\psi} + \langle \partial_t \Lambda \rangle_{\psi} \tag{4.75}$$

This makes any Hamiltonian based energy density irrelevant since it bears no particular physical meaning. Note that this result is not specific to quantum mechanics and the Schrödinger equation. Indeed, we have seen in Sec. 4.1.3 that the mechanical energy U from Eq. (4.20) – the classical equivalent of the Hamiltonian – of a particle under a time dependent electromagnetic field is also gauge dependent.

In what follows, we will be using the energy operator $\hat{\varepsilon}$ by default, along with its corresponding densities.

Note: The potential energy V that we will consider can theoretically be of electrostatic origin – *i.e.* $V(\vec{r}) = q\varphi(\vec{r})$ where φ is an electromagnetic scalar potential. This leads to fundamental issues

[185] since φ should also be able to be gauge transformed and still keep the energy operator with an invariant expectation value: the 'total energy' operator $\hat{\varepsilon}$ defined Eq. (4.64) in this case would not be gauge invariant if the gauge change involves a time-dependent gauge function $\Lambda(\vec{r},t)$. The kinetic energy operator $\hat{\kappa}$ in the other hand remains gauge invariant. As stated in Sec. 4.1.3, this issue also applies when one considers the Hamiltonian as an energy operator in the stationary case with a time-dependent gauge-change. Just like with the Hamiltonian $\hat{h}$ in the stationary case, taking $\hat{\varepsilon}$ as the energy operator in the time-dependent case has an experimental meaning since the stationary scalar potential φ would come from another source (*e.g.* the atomic lattice) while the time-dependent control through the electromagnetic potentials $(\vec{A},\phi)$ is generated by an external device. Using the energy operator $\hat{\varepsilon}$ also enables recovering the well-known results from the Landauer-Büttiker scattering theory since it coincides with the Hamiltonian in the stationary regime.

4.2.4. Discretizing the continuous space

In order to better understand energy quantum transport, numerical simulation is a powerful tool that enables prototyping to test more quickly intuitions and ideas. As we will be using Kwant along with tkwant that use a formalism defined on tight-binding systems, a way to derive tight-binding equations is to discretize the continuous equations that we exposed in the previous sections.

4.2.4.1. Discretization process

The discretization process involves moving from describing points by their real space $(x,y,z)\in\mathbb{R}^3$ coordinates to a single integer index $i\in\mathbb{Z}$ that indexes unique points on a lattice. We will describe here the discretization process on a cubic lattice with a lattice parameter a

$$(x,y,z)\in\mathbb{R}^3 \xrightarrow{\text{discretisation}} \left[\begin{array}{l}(ka,la,ma)\\ k,l,m\in\mathbb{Z}\\ a\in\mathbb{R}_+^*\end{array}\right. \xrightarrow[\text{of variables}]{\text{change}} (k,l,m)\in\mathbb{Z}^3 \xrightarrow[\text{map } f]{\text{flattening}} i\in\mathbb{Z} \tag{4.76}$$

Moving from 3D integer coordinates to a single integer coordinate involves a flattening map f

$$\begin{array}{rccc} f: & \mathbb{Z}^3 & \to & \mathbb{Z} \\ & (k,l,m) & \mapsto & i \end{array} \tag{4.77}$$

that makes a 1-to-1 correspondence between $\mathbb{Z}^3$ and $\mathbb{Z}$, or at least in the region where the system is defined. Let us define the maps $n_\alpha(i)$ and $p_\alpha(i)$, $\alpha=x,y,z$, that are respectively the '<u>n</u>ext site' and '<u>p</u>revious site' of a given site i in the direction α:

$$\begin{array}{lll} n_x(i)=f(k+1,l,m) & n_y(i)=f(k,l+1,m) & n_z(i)=f(k,l,m+1) \\ p_x(i)=f(k-1,l,m) & p_y(i)=f(k,l-1,m) & p_z(i)=f(k,l,m-1) \end{array} \tag{4.78}$$

where $(k,l,m)=f^{-1}(i)$. Upon discretization, the continuous wave function $\psi(x,y,z,t)$ becomes a vector $[\psi_i(t)]$ and the Hamiltonian operator $\hat{h}$ becomes a matrix $[h_{ij}(t)]$. The discretized Schrödinger equation writes

$$\mathrm{i}\hbar\partial_t\psi_i=\hat{h}[\psi]_i=\sum_j h_{ij}\psi_j \tag{4.79}$$

To derive the Hamiltonian in discrete space, one needs to write the 'flattened' and discrete counterpart to the gradient operator $\vec{\nabla}$. We use here the previously defined 'neighbor' maps to write it using finite

differences, we therefore assume a to be small enough with respect to all characteristic lengths so the discrete gradient is close to its continuous counterpart

$$\vec{\nabla}[\psi]_i = \frac{1}{2a}\begin{bmatrix}\psi_{n_x(i)} - \psi_{p_x(i)} \\ \psi_{n_y(i)} - \psi_{p_y(i)} \\ \psi_{n_z(i)} - \psi_{p_z(i)}\end{bmatrix} = \frac{1}{2a}\sum_{\alpha=x,y,z}\left(\psi_{n_\alpha(i)} - \psi_{p_\alpha(i)}\right)\vec{e}_\alpha \tag{4.80}$$

This allows us to write down the discrete counterpart of $\hat{h}[\psi]$ given in Eq. (A.5)

$$\begin{aligned}\hat{h}[\psi]_i = \sum_{\alpha=x,y,z}\Bigg[&-\frac{\hbar^2}{2ma^2}\left(\psi_{n_\alpha(i)} - 2\psi_i + \psi_{p_\alpha(i)}\right) \\ &+ \mathrm{i}\frac{\hbar q}{2ma}\left[\left(\psi_{n_\alpha(i)} - \psi_{p_\alpha(i)}\right)A_i^\alpha + \frac{1}{2}\psi_i\left(A^\alpha_{n_\alpha(i)} - A^\alpha_{p_\alpha(i)}\right)\right] \\ &+ \frac{q^2}{2m}A^2\psi_i + V_i\psi_i\end{aligned} \tag{4.81}$$

which gives the following for h_{ij}[12]:

$$h_{ij} = \begin{cases}\sum_{\alpha=x,y,z}\left[\frac{\hbar^2}{ma^2} + \mathrm{i}\frac{\hbar q}{4ma}\left(A^\alpha_{n_\alpha(i)} - A^\alpha_{p_\alpha(i)}\right)\right] + \frac{q^2}{2m}A^2 + q\phi_i + V_i & \text{for} \quad j = i \\ -\frac{\hbar^2}{2ma^2} + \mathrm{i}\frac{\hbar q}{2ma}A_i^\alpha & \text{for} \quad j = n_\alpha(i) \\ -\frac{\hbar^2}{2ma^2} - \mathrm{i}\frac{\hbar q}{2ma}A_i^\alpha & \text{for} \quad j = p_\alpha(i) \\ 0 & \text{otherwise}\end{cases} \tag{4.82}$$

Given that these equations are first order Taylor expansions with respect to the lattice parameter a, we can rewrite the previous Hamiltonian elements in terms of exponentials[13]

$$h_{ij} = \begin{cases}\sum_{\alpha=x,y,z}\frac{\hbar^2}{ma^2}\exp\left[+\mathrm{i}\frac{1}{2}\frac{qa}{\hbar}\frac{1}{2}\left(A^\alpha_{n_\alpha(i)} - A^\alpha_{p_\alpha(i)}\right)\right] + \frac{q^2}{2m}A^2 + q\phi_i + V_i & \text{for} \quad j = i \\ -\frac{\hbar^2}{2ma^2}\exp\left(-\mathrm{i}\frac{qa}{\hbar}A_i^\alpha\right) & \text{for} \quad j = n_\alpha(i) \\ -\frac{\hbar^2}{2ma^2}\exp\left(+\mathrm{i}\frac{qa}{\hbar}A_i^\alpha\right) & \text{for} \quad j = p_\alpha(i) \\ 0 & \text{otherwise}\end{cases} \tag{4.83}$$

which gives rise to the usual Peierls substitution [88] used in tight-binding systems. Now that the Hamiltonian is defined in discrete space, we can derive the discrete equivalent of the conservation equations described in the previous sections.

4.2.4.2. Gauge transformation

We consider the following discrete counterpart to the continuous gauge transformation Eq. (4.12) when we consider a discrete lattice, *e.g.* as described Eq. (4.76)

$$\begin{cases}\vec{A}'_i(t) = \vec{A}_i(t) - \vec{\nabla}[\Lambda]_i \\ \phi'_i(t) = \phi_i(t) + \partial_t\Lambda_i(t) \\ \Lambda_i(t) \text{ arbitrary scalar field}\end{cases} \tag{4.84}$$

[12] One can notice that h_{ii} is not real in general due to the discrete counterpart of $\vec{\nabla}\cdot\vec{A}$ which, in the Coulomb gauge, is taken to be equal to zero [172, Chap. 7.1]. We will assume in what follows that $h_{ii} \in \mathbb{R}$

[13] Since $1 + xa + \mathcal{O}(a^2) = e^{xa} + \mathcal{O}(a^2)$

where $\vec{\nabla}[\Lambda]_i$ is given by Eq. (4.80). When applied to the discrete Hamiltonian $\hat{h}$, it affects its matrix elements in the following way

$$h'_{ij} = \begin{cases} h_{ii}(t) + q\,\partial_t \Lambda_i(t) & \text{for} \quad j = i \\ \\ h_{ij}(t)\exp\Big(\mathrm{i}\frac{q}{\hbar}[\Lambda_j(t) - \Lambda_i(t)]\Big) & \text{for} \quad i \neq j \end{cases} \tag{4.85}$$

This expression can be derived in the same way it has for Eq. (4.83), starting from the action of the Hamiltonian $\hat{h}'$ on a wavefunction ψ_i Eq. (4.81), after having done the replacement $(\vec{A}, \phi) \to (\vec{A}', \phi')$ according to (4.12). In particular, for $t \leq t_0$ when $\phi_i(t) = 0$ and $\vec{A}_i(t) = \vec{A}_i$, the gauge-transformed static Hamiltonian $\hat{h}'$ may become artificially time-dependent: in the rest of this thesis, we fix the gauge when so that no time-dependent electromagnetic field exists for $t \leq t_0$. We choose the 'natural' gauge in which $\Lambda_i(t \leq t_0) = 0$ and the 'initial' (before any gauge change) Hamiltonian is time-independent for $t < t_0$.

4.2.4.3. Particle transport

The discrete equivalent to Eq. (4.56) writes as the following

$$\partial_t \rho_i(t) + \sum_j I^{\mathrm{N}}_{ij}(t) = 0 \tag{4.86}$$

where $\rho_i(t)$ is the discrete equivalent to the continuous density $\rho(\vec{r}, t)$ defined in Eq. (4.26) and I^{N}_{ij} is interpreted as the current density flowing from site i to site j[14]

$$\rho_i(t) = \psi_i^* \psi_i \tag{4.87}$$

$$I^{\mathrm{N}}_{ij}(t) = -\frac{2}{\hbar}\mathrm{Im}\big[\psi_i^* h_{ij} \psi_j\big] \tag{4.88}$$

I^N_{ij} being a scalar value, it is not directly the equivalent to the continuous current density vector field $\vec{j}$ defined in (4.57). The connection between I^N_{ij} and the discrete counterpart $\vec{j}_i$ of $\vec{j}$ is the following

$$\vec{j}_i = \sum_{\alpha=x,y,z} \frac{a}{2}\left[I^N_{i,n_\alpha(i)} - I^N_{i,p_\alpha(i)}\right]\vec{e}_\alpha \tag{4.89}$$

Each component j_i^α of the probability current density vector field $\vec{j}_i$ is the net probability current going through site i in the direction α. A short derivation for Eq. (4.86) and Eq. (4.89) is done in Appendix. A.1.2

4.2.4.4. Energy transport

We showcase here the discrete equivalent to the continuous one-body energy transport approach Sec. 4.2.3. The continuum energy conservation equation (4.60) becomes

$$\partial_t \rho^\epsilon_i(t) + \sum_j I^\epsilon_{ij}(t) = S^\epsilon_i(t) \tag{4.90}$$

[14]Where the necessary condition $I^{\mathrm{N}}_{ij} = -I^{\mathrm{N}}_{ji}$ needs to be met.

where $\rho_i^\epsilon(t)$ is the energy probability density and S_i^ϵ is the input power on site i. $\sum_j I_{ij}^\epsilon(t)$ is the discrete equivalent of the divergence of continuous energy current density $\vec{\nabla}\cdot\vec{j}^\epsilon(\vec{r},t)$, *i.e.* the sum of the currents I_{ij}^ϵ flowing from a site i to its neighboring sites j. The energy quantity ϵ can either be the total energy ε, the kinetic energy κ or the Hamiltonian h.

Such a derivation has been done in the literature without consideration for gauge invariance: Ref. [210] has carried a derivation, in 1D discrete space, for various time-independent Hamiltonians while considering extra degrees of freedom like the spin. Ref. [12] performed the derivation in a 1D chain with a periodic time-dependence. We perform a derivation in a generic system described by the spinless and time-dependent electromagnetic Hamiltonian $\hat{h}$ given in Eq. (4.46). Starting with the discretized version $\rho_i^\epsilon(t)$ of the continuous energy density $\rho_i^\epsilon(t)$ given in Eq. (4.62)

$$\rho_i^\epsilon(t) = \mathrm{Re}[\psi_i^*\hat{\epsilon}[\psi]_i] = \mathrm{Re}\left[\sum_j \psi_i^*\epsilon_{ij}\psi_j\right] \tag{4.91}$$

where $\hat{\epsilon}=\hat{\varepsilon},\hat{\kappa},\hat{h}$, we express its time-derivative with the help of the discrete Schrödinger equation Eq. (4.79) and identify an expression for the energy current I_{ij}^ϵ and the energy source S_i^ϵ

$$\underset{\substack{\text{Energy}\\\text{density}}}{\rho_i^\epsilon(t)} \quad \underset{\substack{\text{Schrödinger}\\\text{equation}}}{\Longrightarrow} \quad \underbrace{\partial_t\rho_i^\epsilon(t) + \textstyle\sum_j I_{ij}^\epsilon(t) = S_i^\epsilon}_{\substack{\text{Conservation}\\\text{equation}}} \tag{4.92}$$

To be interpretable as the energy current flowing from site i to site j, I_{ij}^ϵ must verify $I_{ij}^\epsilon = -I_{ji}^\epsilon$. For the three energy operators we have considered ('total', kinetic and hamiltonian), we could identify a generic expression for the energy currents I_{ij}^ϵ whereas the energy source S_i^ϵ depends on the considered energy operator:

$$I_{ij}^\epsilon(t) = -\frac{1}{\hbar}\mathrm{Im}\left[\hat{\epsilon}[\psi]_i^*\epsilon_{ij}\psi_j - \hat{\epsilon}[\psi]_j^*\epsilon_{ji}\psi_i\right] \tag{4.93}$$

$$= -\frac{1}{\hbar}\sum_k \mathrm{Im}\left[\psi_k^*\epsilon_{ki}\epsilon_{ij}\psi_j - \psi_k^*\epsilon_{kj}\epsilon_{ji}\psi_i\right] \tag{4.94}$$

On top of verifying $I_{ij}^\epsilon = -I_{ji}^\epsilon$, they also verify $h_{ij}=0 \implies I_{ij}^\epsilon = 0$ which makes them better suited for practical calculations and interpretability. Just like with the continuous approach, the expression of the energy current I_{ij}^ϵ is not unique: only the divergence $\sum_j I_{ij}^\epsilon$ seems to carry a real physical meaning, we showcase in Sec. 4.3.3.4 another candidate, used in Ref. [129]. The energy current density vector field $\vec{j}_i^\epsilon$, that is obtained by discretizing its continuous counterpart equation (4.73),

$$\vec{j}_i^\epsilon = \frac{1}{2}\mathrm{Re}\left[\hat{\epsilon}[\psi]_i^*\,\hat{\vec{v}}[\psi]_i + \psi_i^*\hat{\vec{v}}[\hat{\epsilon}[\psi]]_i\right] \tag{4.95}$$

can be expressed with the I_{ij}^ϵ scalars in the same way as with the particle current density:

$$\vec{j}_i^\epsilon = \sum_{\alpha=x,y,z}\frac{a}{2}\left[I_{i,n_\alpha(i)}^\epsilon - I_{i,p_\alpha(i)}^\epsilon\right]\vec{e}_\alpha \tag{4.96}$$

Each component $j_{\alpha,i}^\epsilon$ of the current density vector field $\vec{j}_i^\epsilon$ is the net energy current going through site i in the direction α. A more detailed derivation of Eq. (4.96) is made in Appendix. A.2.1.

Since the Hamiltonian is not gauge invariant, we chose to work with the 'total' energy operator $\hat{\varepsilon}$. In the following sections, we use the discretization process described in Sec. 4.2.4.1 to express the discrete equivalent of the energy densities exposed in Sec. 4.2.3.

Hamiltonian energy To obtain the energy conservation equation (4.90) for the Hamiltonian $\hat{h}$, we follow the derivation process expressed in Eq. (4.92) and develop the time derivative of the Hamiltonian energy density ρ_i^h given Eq. (4.91) (with $\epsilon = h$), using the discrete Schrödinger equation (4.79)

$$\partial_t \rho_i^h = \frac{1}{\hbar}\mathrm{Re}\left[\sum_j \mathrm{i}\hat{h}[\psi]_i^* h_{ij}\psi_j - \mathrm{i}\psi_i^* h_{ij}\hat{h}[\psi]_j\right] + \mathrm{Re}\left[\sum_j \psi_i^*\left(\partial_t h_{ij}\right)\psi_j\right] \tag{4.97}$$

We can already identify the discrete power density S_i^h from its continuous counterpart in Eq. (4.74)

$$S_i^h(t) = \mathrm{Re}\left[\sum_j \psi_i^*\left(\partial_t h_{ij}\right)\psi_j\right] \tag{4.98}$$

By deriving the explicit expression of $\partial_t h_{ij}$ involving the electromagnetic potentials from the expression of h_{ij} given in Eq. (4.82), we show in Appendix. (A.2.3) that the source term writes as follows

$$S_i^h = \partial_t V_i\,\rho_i \;+ \sum_{\alpha=x,y,z} -\partial_t A_i^\alpha\, q j_i^\alpha = q\partial_t\phi_i\,\rho_i - \partial_t\vec{A}_i\cdot q\vec{j}_i \tag{4.99}$$

This expression of the source term S_i^h is the discrete counterpart to the continuous energy source $S^h = q\partial_t\phi\,\rho + q\vec{j}\cdot(-\partial_t\vec{A})$ given in Eq. (4.74).

Just like the particle current, we interpret the first term of the right hand side of Eq. (4.97), with an added minus factor, as the discrete equivalent to the divergence of the continuous energy current density $\vec{\nabla}\cdot\vec{j}^h(\vec{r},t)$, *i.e.* a sum of energy currents I_{ij}^h flowing from the site i to its neighboring sites j

$$\sum_j I_{ij}^h(t) = \sum_j -\frac{1}{\hbar}\mathrm{Re}\left[\mathrm{i}\hat{h}[\psi]_i^* h_{ij}\psi_j - \mathrm{i}\psi_i^* h_{ij}\hat{h}[\psi]_j\right] \tag{4.100}$$

To define I_{ij}^h, one could simply take the term inside the sum $\sum_j$ as a candidate $\bar{I}_{ij}^h$

$$\begin{aligned}\bar{I}_{ij}^h(t) &= -\frac{1}{\hbar}\mathrm{Re}\left[\mathrm{i}\hat{h}[\psi]_i^* h_{ij}\psi_j - \mathrm{i}\psi_i^* h_{ij}\hat{h}[\psi]_j\right]\\ &= \frac{1}{\hbar}\mathrm{Im}\left[\hat{h}[\psi]_i^* h_{ij}\psi_j - \psi_i^* h_{ij}\hat{h}[\psi]_j\right]\end{aligned}$$

But this candidate $\bar{I}_{ij}^h$ verifies $\bar{I}_{ij}^h = \bar{I}_{ji}^h$ and $I_{ii}^h \neq 0$ which does not agree with interpreting I_{ij}^h as the energy current flowing from site i to site j. However, given that term $\mathrm{Im}\left[\hat{h}[\psi]_i^* h_{ij}\psi_j\right]$ vanishes when summed over j[15], we can swap its sign and define another candidate I_{ij}^h

$$I_{ij}^h(t) = -\frac{1}{\hbar}\mathrm{Im}\left[\hat{h}[\psi]_i^* h_{ij}\psi_j - \hat{h}[\psi]_j^* h_{ji}\psi_i\right] \tag{4.101}$$

$$= -\frac{1}{\hbar}\sum_k \mathrm{Im}\left[\psi_k^* h_{ki} h_{ij}\psi_j - \psi_k^* h_{kj} h_{ji}\psi_i\right] \tag{4.102}$$

This candidate verifies $I_{ij}^h = -I_{ji}^h$, $I_{ii}^h = 0$ and its sum over j gives the correct discrete divergence. We show in Appendix. A.2.1 that this energy current density I_{ij}^h is connected to the direct discretization $\vec{j}_i^h(t)$ of $\vec{j}^h(\vec{r},t)$, given in (4.73), through Eq. (4.96)

[15] $\sum_j[\hat{h}[\psi]_i^* h_{ij}\psi_j = \hat{h}[\psi]_i^*\hat{h}[\psi]_i \in \mathbb{R}$

Kinetic energy The kinetic energy matrix elements k_{ij} can be expressed using the Hamiltonian matrix elements h_{ij}, given in Eq. (4.82) the help of Eq. (4.46)

$$\kappa_{ij} = \begin{cases} h_{ii}(t) - q\phi_i(t) - V_i & \text{for} \quad j = i \\ \\ h_{ij}(t) & \text{otherwise} \end{cases} \tag{4.103}$$

The energy conservation equation (4.90) for the kinetic energy operator $\hat{\kappa}$ is obtained following the process described Eq. (4.92). We take the following expression for the kinetic energy source S_i^κ

$$S_i^\kappa(t) = \sum_k -\frac{1}{2}\left[V_k - V_i + q\phi_k - q\phi_i\right] I_{ik}^N + \sum_k \mathrm{Re}[\psi_i^* \partial_t \kappa_{ik} \psi_k] \tag{4.104}$$

while the kinetic energy current I_{ij}^κ is given by Eq. (4.94) with $\epsilon = \kappa$. The kinetic energy source $S_i^\kappa(t)$ is the discrete equivalent to continuous energy source S^κ given in Eq. (4.70). Indeed, $\sum_k -\frac{1}{2}[V_k - V_i + q\phi_k - q\phi_i]I_{ik}^N$ is the discrete equivalent to $\vec{j} \cdot [-q\vec{\nabla}\phi - \vec{\nabla}V]$; showing that $\sum_k \mathrm{Re}[\psi_i^* \partial_t \kappa_{ik} \psi_k]$ is the discrete equivalent to $-q\vec{j} \cdot \partial_t \vec{A}$ is similar to the derivation done for the Hamiltonian source term Eq. (4.99) in Appendix. A.2.3

Total energy operator The energy operator we will be considering is what we call the "total energy operator" $\hat{\varepsilon}$. Defined in the continuous space in Eq. (4.64) as being the kinetic energy plus the stationary potential energy V, its matrix elements in discrete space are the following

$$\varepsilon_{ij}(t) = \begin{cases} h_{ii}(t) - q\phi_i(t) & \text{for} \quad j = i \\ \\ h_{ij}(t) & \text{for} \quad j \neq i \end{cases} \tag{4.105}$$

where $h_{ij}(t)$ are the Hamiltonian's matrix elements given in Eq. (4.82). Following Eq. (4.92), we isolate the discrete equivalent $S_i^\varepsilon(t)$ to the continuous total energy source $S^\varepsilon = \vec{j} \cdot q\vec{E}$ given Eq. (4.67)

$$S_i^\varepsilon(t) = \sum_k -\frac{1}{2}\left[q\phi_k - q\phi_i\right] I_{ik}^N + \sum_k \mathrm{Re}[\psi_i^* \partial_t \varepsilon_{ik} \psi_k] \tag{4.106}$$

while the total energy current I_{ij}^ε is given by Eq. (4.94) with $\epsilon = \varepsilon$. It verifies $I_{ij}^\varepsilon = -I_{ji}^\varepsilon$ and $h_{ij} = 0 \implies I_{ij}^\varepsilon = 0$.

4.3. Non-interacting many-body quantum approach – Second quantization

In the previous section 4.2 we described the mechanics of a single quantum particle under a time-dependent electromagnetic field, described by the one-body Hamiltonian given in Eq. (4.46). To describe realistic systems one needs to consider the many-body case involving the use of statistical physics. In the scope of this thesis, we consider non-interacting systems which simplifies the underlying mathematics and enables us to have more easily a first understanding of our problem: time-dependent energy transport.

4.3.1. The many-body description in first quantization

In Sec 4.2.1 we introduced the base concepts to describe the behavior of a single particle in the quantum regime. We will build upon these first concepts and expose the framework that describes many quantum particles without interaction, *i.e.* each particle does not affect any other particle. We will follow the development done in [171] and adapt it to our scope.

Let us consider N identical non-interacting particles under the influence of the same time-dependent electromagnetic potentials $(\phi(\vec{r},t), \vec{A}(\vec{r},t))$ and the stationary potential energy $V(\vec{r})$. The quantum description of such a system through a wavefunction ψ involves the use of N space variables $\vec{r}_1, \dots, \vec{r}_N$ in its arguments $\psi_N(\vec{r}_1, \dots, \vec{r}_N, t)$.

In the non-interacting regime, the N-body operators $\hat{O}_N$ simply involve a sum over the one-body operators $\hat{o}$. The N-body Hamiltonian $\hat{h}_N$ can thus be written using the one-body Hamiltonians $\hat{h}_p$ given in Eq. (4.46)

$$\hat{h}_N = \sum_{p=1}^{N} \hat{h}_p \tag{4.107}$$

where the p index denotes that the involved space variable in the potentials is $\vec{r}_p$

$$\hat{h}_p[\psi_N](\vec{r}_1, \dots, \vec{r}_N, t) = \frac{1}{2m}\left[-\mathrm{i}\hbar\vec{\nabla}_{\vec{r}_p} - q\vec{A}(\vec{r}_p,t)\right]^2[\psi_N] + q\,\phi(\vec{r}_p,t)\,\psi_N + V(\vec{r}_p)\psi_N \tag{4.108}$$

The N-body Schrödinger equation therefore writes:

$$\mathrm{i}\hbar\partial_t\psi_N(\vec{r}_1, \dots, \vec{r}_N, t) = \hat{h}_N[\psi_N](\vec{r}_1, \dots, \vec{r}_N, t) \tag{4.109}$$

and the expectation value of an N-body operator $\hat{O}_N$ writes

$$\langle\psi_N(t)|\hat{O}_N|\psi_N(t)\rangle = \int \mathrm{d}^3r_1 \dots \mathrm{d}^3r_N\, \psi_N(\vec{r}_1, \dots, \vec{r}_N, t)\hat{O}_N[\psi_N](\vec{r}_1, \dots, \vec{r}_N, t) \tag{4.110}$$

Given the simple relationship between N-body and one-body operators in the non-interacting case, one can use a time-independent one-body basis $|\lambda\rangle$[16] of the one-body Hilbert space $\mathcal{H}$ to define an N-body basis $(|\lambda_1, \dots, \lambda_N\rangle)$ of the N-body Hilbert space $\mathcal{H}_N$ whose wavefunction is defined as

$$\langle\vec{r}_1, \dots, \vec{r}_N|\lambda_1, \dots, \lambda_N\rangle = \prod_{p=1}^{N}\lambda_p(\vec{r}_p) \tag{4.111}$$

This ket $|\lambda_1, \dots, \lambda_N\rangle$ amounts to describing the N-body system as N numbered and discernable particles where each particle $p = 1 \dots N$ is in the one-body state $|\lambda_p\rangle$.

Fermions, Bosons Quantum particles are fundamentally undiscernible and the N-body ket $|\lambda_1, \dots, \lambda_N\rangle$ described above does not reflect a physical state: one can only tell that the one body-state $|\lambda_p\rangle$ is involved without particle distinction within the N-body state. A physical N-body ket therefore needs to respect a certain symmetry when swapping one-body states λ_i and λ_j, this amounts to swapping

[16] We will use here ket notations as it makes writing N-body states from one-body states simpler. The basis is time-independent therefore Schrödinger equation solutions write on this basis with time-dependent coefficients

the space coordinates $\vec{r}_i$ and $\vec{r}_j$ in the N-body wavefunction. Let's define the permutation operator $\hat{P}_{ij}$ that acts in $\mathcal{H}_N$

$$\hat{P}_{ij} \left| \dots, \lambda_i, \dots, \lambda_j, \dots \right\rangle = \left| \dots, \lambda_j, \dots, \lambda_i, \dots \right\rangle \tag{4.112}$$

There are two types of particles [171, Part. 1.1], bosons and Fermions, the state of the former must be totally symmetric whereas the state of latter must be totally antisymmetric. This means that for bosons, in a given physical state ψ, any permutation $\hat{P}_{ij}$ leaves the N-body wavefunction unchanged. For Fermions, any permutation $\hat{P}_{ij}$ swaps the sign of the N-body wavefunction ψ

$$\text{for Fermions} \quad \forall i,j \;\; \hat{P}_{ij}[\psi] \left| \dots, \lambda_i, \dots, \lambda_j, \dots \right\rangle = - \left| \dots, \lambda_i, \dots, \lambda_j, \dots \right\rangle \tag{4.113}$$

In the scope of this thesis, we are going to work with electrons, therefore with Fermions. To write a physical N-body state for Fermions from a given basis ket $|\lambda_1, \dots, \lambda_N\rangle$ we need to perform all the possible permutations between the one-body states $\lambda_i, i = 1 \dots N$ while respecting the complete anti-symmetry constraint and create the ket $\hat{S}_- |\lambda_1, \dots, \lambda_N\rangle$, where $\hat{S}_-$ is the anti-symmetrization operator . These permutations that create a totally antisymmetric state are what a determinant does, used in this specific case it is called the *Slater determinant*

$$\langle \vec{r}_1, \dots, \vec{r}_N | \, \hat{S}_- \, | \lambda_1, \dots, \lambda_N \rangle = \frac{1}{\sqrt{N!}} \begin{vmatrix} \lambda_1(\vec{r}_1) & \lambda_1(\vec{r}_2) & \cdots & \lambda_1(\vec{r}_N) \\ \lambda_2(\vec{r}_1) & \lambda_2(\vec{r}_2) & \cdots & \lambda_2(\vec{r}_N) \\ \vdots & \vdots & \ddots & \vdots \\ \lambda_N(\vec{r}_1) & \lambda_N(\vec{r}_2) & \cdots & \lambda_N(\vec{r}_N) \end{vmatrix} \tag{4.114}$$

If any of the one-body states are the same, *i.e.* $\phi_{\lambda_i} = \phi_{\lambda_j}$, then the result of this determinant is zero, which means that there cannot be a non-zero N-body totally antisymmetric wavefunction where two quantum particles share the same one-body state: this constraint is also called the Pauli exclusion principle.

$$\lambda_i = \lambda_j \implies \hat{S}_- |\lambda_1, \dots, \lambda_N\rangle = 0 \tag{4.115}$$

As with the one-body approach described Sec. 4.2.1.1, one can build a base of solutions to the N-body Schrödinger equation by time-evolving the base $(|\lambda_1, \dots, \lambda_N\rangle)$ using the N-body evolution operator $\hat{U}_N(t, t_0)$: it is written using the one-body evolution operator $\hat{u}(t, t_0)$ to evolve each one-body wavefunction according to Eq. (4.24)

$$\psi_N = \langle \vec{r}_1, \dots, \vec{r}_N | \, \hat{U}_N(t, t_0) \, | \lambda_1, \dots, \lambda_N \rangle = \prod_{p=1}^{N} \hat{u}(t, t_0)[\lambda_p](\vec{r}_p) \tag{4.116}$$

One can easily verify that the N-body wavefunction ψ_N defined above abides by the N-body Schrödinger equation given in (4.109). To make it respect the anti-symmetry constraints for Fermions and define a basis of "physical" states, the anti-symmetrization operator $\hat{S}_-$ can be applied

$$\langle \vec{r}_1, \dots, \vec{r}_N | \, \hat{S}_- \hat{U}(t, t_0) \, | \lambda_1, \dots, \lambda_N \rangle = \frac{1}{\sqrt{N!}} \begin{vmatrix} \lambda_1(\vec{r}_1, t) & \lambda_1(\vec{r}_2, t) & \cdots & \lambda_1(\vec{r}_N, t) \\ \lambda_2(\vec{r}_1, t) & \lambda_2(\vec{r}_2, t) & \cdots & \lambda_2(\vec{r}_N, t) \\ \vdots & \vdots & \ddots & \vdots \\ \lambda_N(\vec{r}_1, t) & \lambda_N(\vec{r}_2, t) & \cdots & \lambda_N(\vec{r}_N, t) \end{vmatrix} \tag{4.117}$$

to define a base of totally anti-symmetric states $(\hat{S}_- \hat{U}(t, t_0) \, |\lambda_1, \dots, \lambda_N\rangle)$ that are solution to the N-body Schrödinger equation. Note that the anti-symmetrization operator $\hat{S}_-$ commutes with the evolution operator $\hat{U}(t, t_0)$ by construction.

4.3.2. The many-body approach in second quantization

In an N-body non-interacting quantum system of Fermions written from one-body states, a strong constraint of total anti-symmetry must be followed by the wavefunction. The basis $(\hat{S}_- |\lambda_1, ..., \lambda_N\rangle)$ respects this constraint and can be used to write any physical N-body state by linear combination. One can take one step further and define a general many-body state where the number of particles N is not fixed but finite: the associated Hilbert space for such description is called *Fock space*. A basis for this many-body Hilbert space can then be described by a series of occupation numbers $(n_\lambda) \in \mathbb{N}$ on a given one-body orthonormal basis $(|\lambda\rangle)$

$$\left|n_{\lambda_1}, n_{\lambda_2}, ..., n_{\lambda_i}, ...\right\rangle \tag{4.118}$$

where the occupation numbers n_{λ_i} can only be 0 or 1 because of the total anti-symmetry – the Pauli exclusion principle – constraint. The occupation numbers n_{λ_i} also vanish above a certain index to make the state describe a finite number of particles.

$$\exists k \mid \forall i > k \;\; n_{\lambda_i} = 0$$

The number of particles N of a given many-body state $|\Phi\rangle$ is therefore the sum of the occupation numbers

$$N = \sum_i n_{\lambda_i} \tag{4.119}$$

The state $|0\rangle$ that describe a many-body system with no particles – $N = 0$ – plays a special role in defining the *annihilation* and *creation* operators.

4.3.2.1. Operators in second quantization

Given a one-body basis $(|\lambda\rangle)$, we define the non-hermitian[17] creation operators $\hat{c}^\dagger_{\lambda_i}$ that act on kets in the Fock space. Their action is to 'create' the totally antisymmetric ket $\hat{S}_- |\lambda_1, \lambda_2, ..., \lambda_N\rangle$ defined Eq. (4.114) from the empty state $|0\rangle$ as follows

$$\hat{S}_- |\lambda_1, \lambda_2, ..., \lambda_N\rangle = \hat{c}^\dagger_{\lambda_1} \hat{c}^\dagger_{\lambda_2} ... \hat{c}^\dagger_{\lambda_N} |0\rangle \tag{4.120}$$

Given this general property of determinants

$$\hat{S}_- |\lambda_1, \lambda_2, ..., \lambda_N\rangle = -\hat{S}_- |\lambda_2, \lambda_1, ..., \lambda_N\rangle \tag{4.121}$$

we deduce the anti-commutation relation between creation operators

$$\{\hat{c}^\dagger_{\lambda_i}, \hat{c}^\dagger_{\lambda_j}\} = \hat{c}^\dagger_{\lambda_i} \hat{c}^\dagger_{\lambda_j} + \hat{c}^\dagger_{\lambda_j} \hat{c}^\dagger_{\lambda_i} = 0 \tag{4.122}$$

and therefore $\left(\hat{c}^\dagger_{\lambda_i}\right)^2 = 0$ which translates Pauli's exclusion principle: two particles cannot occupy the same state. The state $\left|n_{\lambda_1}, n_{\lambda_2}, ..., n_{\lambda_i}, ...\right\rangle$ given by occupation numbers, where the order between one-body states λ must be arbitrarily fixed, can be defined using these operators

$$\left|n_{\lambda_1}, n_{\lambda_2}, ..., n_{\lambda_i}, ...\right\rangle = \left(\hat{c}^\dagger_{\lambda_1}\right)^{n_{\lambda_1}} \left(\hat{c}^\dagger_{\lambda_2}\right)^{n_{\lambda_2}} ... \left(\hat{c}^\dagger_{\lambda_N}\right)^{n_{\lambda_N}} |0\rangle \tag{4.123}$$

[17] They do not define physical quantities as-is but are used as mathematical tools to simplify the writing of other operators.

Further development can be read on [171]. We will state here useful results and definitions that will be useful in our scope. These operators abide by the following anti-commutation relationships, for Fermions

$$\{\hat{c}_{\lambda_i}, \hat{c}^\dagger_{\lambda_j}\} = \delta_{ij} \qquad \{\hat{c}_{\lambda_i}, \hat{c}_{\lambda_j}\} = 0 \qquad \{\hat{c}^\dagger_{\lambda_i}, \hat{c}^\dagger_{\lambda_j}\} = 0 \tag{4.124}$$

They are used to define the number operator n_{λ_i}

$$\hat{n}_{\lambda_i} = \hat{c}^\dagger_{\lambda_i} \hat{c}_{\lambda_i} \tag{4.125}$$

that gives the density of particles in the one-body state $|\lambda_i\rangle$ within a given general many-body state $|\Phi\rangle$ that is a linear combination of the basis vectors $\left|\dots, n_{\lambda_i}, \dots\right\rangle$. Its effect on a vector of the same basis is the following

$$\hat{n}_{\lambda_i} \left|\dots, n_{\lambda_i}, \dots\right\rangle = n_{\lambda_i} \left|\dots, n_{\lambda_i}, \dots\right\rangle \tag{4.126}$$

where n_{λ_i} is either or zero due to Pauli's exclusion principle. The total particle number operator $\hat{N}$ is the sum of the former operator on all possible one-body states λ_i.

$$\hat{N} = \sum_i \hat{c}^\dagger_{\lambda_i} \hat{c}_{\lambda_i} \tag{4.127}$$

Note that this sum can be formally infinite but computing its expectation value on physical states truncates it.

One-body basis change So far our many-body description relied on the use of a given fixed one-body orthonormal basis ($|\lambda\rangle$). We can do a basis change and move to another stationary basis ($|\mu\rangle$) that can be expressed with the old basis according to Eq. (4.30)

$$|\mu\rangle = \sum_\lambda \langle\lambda|\mu\rangle \, |\lambda\rangle \tag{4.128}$$

The operator $\hat{c}^\dagger_\lambda$ adds a particle in the state $|\lambda\rangle$. Given the above relation between the ($|\lambda\rangle$ basis and the ($|\mu\rangle$) basis, the superposition $\sum_\lambda \langle\lambda|\mu\rangle \, \hat{c}^\dagger_\lambda$ creates a particle in the state $|\mu\rangle$ and therefore

$$\hat{c}^\dagger_\mu = \sum_\lambda \langle\lambda|\mu\rangle \, \hat{c}^\dagger_\lambda \tag{4.129}$$

Single-particle operators The non-interacting many-body counterpart $\hat{O}$, that we will call "single particle operator", to the one-body operator $\hat{o}$, can be expressed with the creation and annihilation operators and the matrix elements of $\hat{o}$

$$\hat{O} = \sum_{ij} o_{ij}(t) \, \hat{c}^\dagger_{\lambda_i} \hat{c}_{\lambda_j} \quad \text{where} \quad o_{ij} = \langle\lambda_i| \, \hat{o} \, |\lambda_j\rangle \tag{4.130}$$

An operator is therefore hermitian when its 'matrix elements' o_{ij} verify the following relation

$$\hat{O} \text{ hermitian} \quad \Leftrightarrow \quad o_{ij}(t) = o^*_{ji}(t) \tag{4.131}$$

which is the case when one-body operator $\hat{o}$ is Hermitian, *i.e.* verifies Eq. (4.37). The non-interacting many-body counterparts, that we will write in capital letters, to the one-body operators defined in Sec.

4.2.1.2 can therefore be expressed. The many-body counterpart $\hat{H}(t)$ to the one-body Hamiltonian $\hat{h}$ Eq. (4.46) writes

$$\hat{H} = \sum_{ij} \int \mathrm{d}^3 r \left[\frac{1}{2m} \phi^*_{\lambda_i} \left[-\mathrm{i}\hbar\vec{\nabla} - q\vec{A}(t) \right]^2 [\phi_{\lambda_j}] + q\,\phi(t)\,\phi^*_{\lambda_i}\phi_{\lambda_j} + V\phi^*_{\lambda_i}\phi_{\lambda_j} \right] \hat{c}^\dagger_{\lambda_i}\hat{c}_{\lambda_j} \tag{4.132}$$

where the parametric time-dependence has been made explicit and the space dependence with respect to the integration variable $\vec{r}$ has been omitted for readability.

Heisenberg representation One can define the many-body evolution operator $\hat{U}(t, t_0)$ by summing over the N-body evolution operators $\hat{U}_N(t, t_0)$. This enables writing many-body operators in the Heisenberg representation, introduced Sec. 4.2.1.2. Where the many-body equivalent to the one-body Heisenberg representation of operators given Eq. (4.38) becomes

$$\hat{O}(t) = \hat{U}^\dagger(t, t_0)\,\hat{O}\,\hat{U}(t, t_0) \tag{4.133}$$

where we have followed the convention where writing explicitly writing the time dependence of operators means that they are written in the Heisenberg representation. Single particle operators in the Heisenberg representation write similarly to Eq (4.130)

$$\hat{O}(t) = \sum_{ij} o_{ij}(t)\,\hat{c}^\dagger_{\lambda_i}(t)\hat{c}_{\lambda_j}(t) \tag{4.134}$$

where the creation and annihilation operators are replaced with their Heisenberg representation according to Eq (4.133). The expectation value of many-body operators also follow the Heisenberg equation of motion defined for one-body operators in Eq. (4.40)

$$\frac{\mathrm{d}}{\mathrm{d}t}\left\langle \hat{O}(t) \right\rangle = \frac{\mathrm{i}}{\hbar}\left\langle [\hat{H}(t), \hat{O}(t)] \right\rangle + \left\langle [\partial_t \hat{O}](t) \right\rangle \tag{4.135}$$

4.3.2.2. Field operators

By formally using the non-physical one-body basis $(|\vec{r}\rangle)$ defined Sec. 4.2.1.1 one can define the *field operators* using Eq. (4.129) for changing the basis

$$\hat{\psi}^\dagger(\vec{r}) = \sum_{\lambda_i} \phi^*_{\lambda_i}(\vec{r})\,\hat{c}^\dagger_{\lambda_i} \tag{4.136}$$

$$\hat{\psi}(\vec{r}) = \sum_{\lambda_i} \phi_{\lambda_i}(\vec{r})\,\hat{c}_{\lambda_i} \tag{4.137}$$

As with any creation and annihilation operators, $\hat{\psi}^\dagger_{\vec{r}}$ and $\hat{\psi}_{\vec{r}}$ verify the anti-commutation relations given in Eq. (4.124). In this case, we will not write many-body states in the $(\hat{S}_- |\vec{r}_1, \ldots, \vec{r}_i, \ldots\rangle)$ basis since the one-body state "the particle is at the position $\vec{r}$" is not physical but a continuous linear combination, *i.e.* an integral over space, can be used to describe a physical normalized state. The associated particle number operator $\hat{n}_{\vec{r}}$ defined through Eq. (4.126)

$$\hat{\rho}_{\vec{r}} = \hat{\psi}^\dagger(\vec{r})\hat{\psi}(\vec{r}) \tag{4.138}$$

acts as the particle density operator at position $\vec{r}$ on states $\left|n_{\lambda_1}, \dots, n_{\lambda_i}, \dots\right\rangle$ defined on the physical one-body basis ($|\lambda\rangle$). The total particle number operator $\hat{N}$ defined through Eq. (4.127) writes intuitively as the integral over space of the particle density operator

$$\hat{N} = \int \mathrm{d}^3 r \; \hat{\psi}^\dagger(\vec{r})\hat{\psi}(\vec{r}) \tag{4.139}$$

which is an expression equal[18] to the one given in Eq. (4.127). Single-particle operators can also be written in terms of field operators, the Hamiltonian $\hat{H}$ writes

$$\hat{H} = \int \mathrm{d}^3 r \; \frac{1}{2m}\, \hat{\psi}^\dagger(\vec{r}) \left[-\mathrm{i}\hbar\vec{\nabla} - q\vec{A}(t)\right]^2 \hat{\psi}(\vec{r}) + q\,\phi(\vec{r},t)\,\hat{\psi}^\dagger(\vec{r})\hat{\psi}(\vec{r}) + V(\vec{r})\,\hat{\psi}^\dagger(\vec{r})\hat{\psi}(\vec{r}) \tag{4.140}$$

where the gradient operator $\vec{\nabla}$ acts on the space dependent coefficients of the creation and annihilation operators

$$\vec{\nabla}\hat{\psi}(\vec{r}) = \sum_{\lambda_i} \vec{\nabla}\phi_{\lambda_i}(\vec{r})\; \hat{c}_{\lambda_i} \tag{4.141}$$

The formal analogy between these expressions of the many-body operators in terms of field operators and the expectation value of the associated one body operators Eq. (4.35) gives rise the naming *second quantization* where the one-body wavefunction becomes an operator that is used formally in the same way. The *first quantization* referring to what happens to the mathematical description of physical quantities when moving from the classical context to the quantum one: from scalars to operators. We will use these field operators to derive our many-body, non-interacting, formulas in the second-quantization formalism.

Many-body expectation values – Lesser Green Functions To compute expectation values of the relevant operators in our scope we will use the *lesser Green function* $G^<(\vec{r},t,\vec{r}',t')$[165]. It is defined as the expectation value, on a given many-body state $|\Phi(t_0)\rangle$, of a specific combination of the field operators written in the Heisenberg representation (described Sec. 4.2.1.2)

$$G^<(\vec{r},t,\vec{r}',t') = \frac{\mathrm{i}}{\hbar}\left\langle \hat{\psi}^\dagger(\vec{r}',t')\hat{\psi}(\vec{r},t)\right\rangle \tag{4.142}$$

The state $|\Phi(t_0)\rangle$ will be made more explicit, but not properly defined, in Sec. 5.2.3. The lesser Green function verifies the following relationship

$$G^<(\vec{r},t,\vec{r}',t') = -G^<(\vec{r}',t',\vec{r},t)^* \tag{4.143}$$

4.3.3. Time-dependent quantum transport in tight-binding models

The transport equations we are about to derive are not analytically tractable for realistic systems, we therefore resort to numerical simulation. To perform simulations, the one-body basis ($|\lambda\rangle$) has to be restricted to a discrete subset $(|i\rangle)_i$. In this case, operators are said to have a 'tight-binding' representation. The non-interacting operators write

$$\hat{O}(t) = \sum_{ij} o_{ij}(t)\, \hat{c}_i^\dagger \hat{c}_j \;\text{ where }\; o_{ij}(t) = \langle i|\,\hat{o}\,|j\rangle \tag{4.144}$$

[18] $\int \mathrm{d}^3 r\; \psi^\dagger(\vec{r})\hat{\psi}(\vec{r}) = \sum_{ij} \underbrace{\int \mathrm{d}^3 r\; \phi^*_{\lambda_i}(\vec{r})\phi_{\lambda_j}(\vec{r})}_{\langle\lambda_i|\lambda_j\rangle=\delta_{ij}}\; \hat{c}^\dagger_{\lambda_i}\hat{c}_{\lambda_j} = \sum_i \hat{c}^\dagger_{\lambda_i}\hat{c}_{\lambda_i}$

where the $o_{ij}(t)$ coefficients can be obtain through different means: from the finite element method [83], from finite differences [99], from atomic orbitals in empirical tight-binding or Kohn-Sham orbitals within the density functional theory [126, Chap. 14-15]. In this thesis, explicit expressions of the coefficients $h_{ij}(t)$, given Eq. (4.82), have ben derived Sec. 4.2.4 with the finite difference method. In this case the creation $\hat{c}_i^\dagger$ and annihilation operators $\hat{c}_j$ correspond to the discrete counterpart to the field operators – defined Eq. (4.136) and (4.137) – on the discrete lattice points i and j as defined in Eq. (4.76). These per-site field operators follow the discrete counterpart to the (anti)commutation relations given Eq. (4.124). We use (4.142) to define its discrete counterpart at the same time t:

$$G_{ij}^<(t) = \frac{\mathrm{i}}{\hbar}\left\langle \hat{c}_j^\dagger(t)\hat{c}_i(t)\right\rangle \tag{4.145}$$

The property it verifies in Eq. (4.143) writes

$$G_{ij}^<(t) = -G_{ji}^<(t)^* \tag{4.146}$$

With the required mathematical tools now exposed to describe non-interacting many-body transport of Fermions, we will derive in what follows the many-body counterpart to the particle and energy transport described in Sec 4.2.2 and Sec. 4.2.3 in tight-binding systems.

4.3.3.1. Gauge transformation

A gauge transformation (4.84) can be applied to the many-body Hamiltonian $\hat{H} \to \hat{H}'$ according to Eq. (4.85) when its coefficients h_{ij} are obtained by the finite difference method (see Sec. 4.2.4.1). The electromagnetic gauge transformation can also be understood [104] as a change of basis of the one-body orbitals on sites i associated with the operators $\hat{c}_i$: under Eq. (4.84) a unitary transformation $\hat{U}$

$$\hat{U} = \exp\left(\mathrm{i}\frac{q}{\hbar}\sum_i \Lambda_i(t)\hat{c}_i^\dagger\hat{c}_i\right) \tag{4.147}$$

is made on the annihilation operator

$$\hat{c}_i' = \hat{U}\hat{c}_i\hat{U}^\dagger = \exp\left(-\mathrm{i}\frac{q}{\hbar}\Lambda_i(t)\right)\hat{c}_i \tag{4.148}$$

so that the transformed Hamiltonian $\hat{H}'$ can be written as [57]

$$\hat{H}' = \hat{U}\hat{H}\hat{U}^\dagger - \mathrm{i}\hbar\,\hat{U}\partial_t\hat{U}^\dagger \tag{4.149}$$

after having noticed that

$$\mathrm{i}\hbar\hat{U}\partial_t\hat{U}^\dagger = q\sum_i \partial_t\Lambda_i\hat{c}_i^\dagger\hat{c}_i = q\sum_i(\phi_i - \phi_i')\hat{c}_i^\dagger\hat{c}_i \tag{4.150}$$

The Schrödinger equation

$$\mathrm{i}\hbar\partial_t\left|\Psi(t)\right\rangle = \hat{H}\left|\Psi(t)\right\rangle \tag{4.151}$$

written here for an arbitrary solution $|\Psi(t)\rangle$ is form invariant under the local gauge transformation when the wavefunction $|\Psi(t)\rangle$ is transformed as follows

$$\left|\Psi(t)'\right\rangle = \hat{U}\left|\Psi(t)\right\rangle \tag{4.152}$$

and the Hamiltonian is transformed according to Eq. (4.149)

$$\mathrm{i}\hbar\partial_t \left|\Psi'(t)\right\rangle = \hat{H}' \left|\Psi'(t)\right\rangle \tag{4.153}$$

While any Hermitian operator $\hat{O} = \sum_{ij} o_{ij}\hat{c}_i^\dagger \hat{c}_j$ that transforms as

$$\hat{O}' = \hat{U}\hat{O}\hat{U}^\dagger \tag{4.154}$$

under Eq. (4.84) – or Eq. (4.12) if the matrix elements are computed according to Eq. (4.144) – has a gauge invariant expectation value

$$\left\langle\Psi\right| \hat{O} \left|\Psi\right\rangle = \left\langle\Psi'\right| \hat{O}' \left|\Psi'\right\rangle \tag{4.155}$$

the Hamiltonian does not (see Eq. (4.149)): its expectation value is in general not gauge invariant

$$\left\langle\Psi\right| \hat{H} \left|\Psi\right\rangle \neq \left\langle\Psi'\right| \hat{H}' \left|\Psi'\right\rangle \tag{4.156}$$

and thus we show here with another approach that it cannot be considered as the energy operator.

4.3.3.2. Time-dependent particle transport

We derive here the well known many-approach of particle transport in tight-binding systems. The derivation is very similar to what have been done in the one-body approach of for particle transport Sec. 4.2.4.3 where we obtain the particle conservation equation

$$\partial_t \rho_i + \sum_j I_{ij}^{\mathrm{N}} = 0 \tag{4.157}$$

where ρ_i is the expectation value of the particle density operator $\hat{\rho}_i(t) = \hat{c}_i^\dagger(t)\hat{c}_i(t)$ (from Eq. (4.138)) at site i, it expression is straightforward using the lesser Green function (given in Eq. (4.145))

$$\rho_i(t) = \left\langle\hat{\rho}_i(t)\right\rangle = -\mathrm{i}\hbar G_{ii}^<(t) \tag{4.158}$$

The time derivative of its expectation value is given by the Heisenberg equation of motion (4.135) where the commutator $\frac{\mathrm{i}}{\hbar}\left\langle\left[\hat{H}(t), \hat{\rho}_i(t)\right]\right\rangle$ writes, using the lesser Green function, as follows

$$\frac{\mathrm{i}}{\hbar}\left\langle\left[\hat{H}(t), \hat{\rho}_i(t)\right]\right\rangle = -\sum_j 2\,\mathrm{Re}\left[h_{ij}(t)G_{ji}^<(t)\right] \tag{4.159}$$

which enables us to write

$$\partial_t \rho_i(t) + \sum_j \underbrace{2\,\mathrm{Re}\left[h_{ij}(t)G_{ji}^<(t)\right]}_{I_{ij}^N(t)} = 0 \tag{4.160}$$

from which we identify the particle current flowing from site i to site j

$$I_{ij}^N(t) = 2\,\mathrm{Re}\left[h_{ij}(t)G_{ji}^<(t)\right] \tag{4.161}$$

The small derivation of the particle's conservation equation is done in Appendix. B.1.1

4.3.3.3. Local energy operator

In Sec. 4.2.3, we defined local energy densities $o_\psi(\vec{r},t)$ such that their integral over space computes the expectation value of the associated system-wide operator $\hat{o}$ in Eq. (4.61), then an energy conservation equation is verified for that density, with an associated current density and source density. There is however no unique definition of a local energy density nor current [127, 8], both in the one-body approach and in the many-body second quantization approach. This arbitrariness also applies when defining the energy of a spatial sub-region of the system, it translates through an apparent arbitrariness in splitting the localized energy at the boundary between the considered subsystem and the rest of the system with the so called 'coupling term'.

To define the 'coupling' energy, let's spatially split the system in two parts $\mathcal{A}$ and $\mathcal{B}$ and then try to define the energy $\hat{\mathcal{E}}_\mathcal{A}$ and $\hat{\mathcal{E}}_\mathcal{B}$ for each subsystem. Given the expression of an operator in tight-binding Eq. (4.144), where the summation indexes indicate position in space, we can restrict the summation to the indexes that refer to positions in space that belong respectively to $\mathcal{A}$ and $\mathcal{B}$

$$\hat{\tilde{\mathcal{E}}}^\epsilon_\mathcal{A} = \sum_{i,j\in\mathcal{A}} \epsilon_{ij}\hat{c}_i^\dagger\hat{c}_j \qquad\qquad \hat{\tilde{\mathcal{E}}}^\epsilon_\mathcal{B} = \sum_{i,j\in\mathcal{B}} \epsilon_{ij}\hat{c}_i^\dagger\hat{c}_j \tag{4.162}$$

However, the sum of these two subsystem energy operator does not give the system's original energy operator

$$\hat{\mathcal{E}}^\epsilon - (\hat{\tilde{\mathcal{E}}}^\epsilon_\mathcal{A} + \hat{\tilde{\mathcal{E}}}^\epsilon_\mathcal{B}) = \sum_{ij} \epsilon_{ij}\hat{c}_i^\dagger\hat{c}_j - \sum_{i,j\in\mathcal{A}} \epsilon_{ij}\hat{c}_i^\dagger\hat{c}_j - \sum_{i,j\in\mathcal{B}} \epsilon_{ij}\hat{c}_i^\dagger\hat{c}_j \tag{4.163}$$

$$= \sum_{\substack{i\in\mathcal{B}\\ j\in\mathcal{A}}} \epsilon_{ij}\hat{c}_i^\dagger\hat{c}_j + \sum_{\substack{i\in\mathcal{A}\\ j\in\mathcal{B}}} \epsilon_{ij}\hat{c}_i^\dagger\hat{c}_j \tag{4.164}$$

An extra hermitian term $\hat{\tilde{\mathcal{E}}}_\mathrm{C}$ that is made of the matrix elements that cross the boundary between $\mathcal{A}$ and $\mathcal{B}$ – which justifies the naming 'coupling term' – is needed to give the system's total energy operator $\hat{\mathcal{E}}$

$$\hat{\mathcal{E}}^\epsilon_\mathrm{C} = \sum_{\substack{i\in\mathcal{A}\\ j\in\mathcal{B}}} \epsilon_{ij}\hat{c}_i^\dagger\hat{c}_j + \epsilon_{ji}\hat{c}_j^\dagger\hat{c}_i \tag{4.165}$$

$$\hat{\mathcal{E}}^\epsilon = \hat{\tilde{\mathcal{E}}}^\epsilon_\mathcal{A} + \hat{\mathcal{E}}^\epsilon_\mathrm{C} + \hat{\tilde{\mathcal{E}}}^\epsilon_\mathcal{B} \tag{4.166}$$

One can define the subsystem energy operators $\hat{\mathcal{E}}_\mathcal{A}$ and $\hat{\mathcal{E}}_\mathcal{B}$ differently where there is no 'coupling' energy. They can be defined using the previous operators by splitting the 'coupling' term $\hat{\tilde{\mathcal{E}}}_\mathrm{C}$ symmetrically between $\hat{\tilde{\mathcal{E}}}_\mathcal{A}$ and $\hat{\tilde{\mathcal{E}}}_\mathcal{B}$

$$\hat{\mathcal{E}}^\epsilon_\mathcal{A} = \hat{\tilde{\mathcal{E}}}^\epsilon_\mathcal{A} + \frac{1}{2}\hat{\mathcal{E}}^\epsilon_\mathrm{C} \qquad\qquad \hat{\mathcal{E}}^\epsilon_\mathcal{B} = \hat{\tilde{\mathcal{E}}}^\epsilon_\mathcal{B} + \frac{1}{2}\hat{\mathcal{E}}^\epsilon_\mathrm{C} \tag{4.167}$$

These operators simply add up to form the system's energy operator

$$\hat{\mathcal{E}}^\epsilon_\mathcal{A} + \hat{\mathcal{E}}^\epsilon_\mathcal{B} = \hat{\mathcal{E}}^\epsilon \tag{4.168}$$

The definition of $\hat{\mathcal{E}}_\mathcal{A}$ given Eq. (4.167) can be obtain by a bottom-up approach where one first defines the local site-wise energy operator $\hat{\mathcal{E}}_i$. It must be Hermitian and its sum over all sites must give the energy operator $\hat{\mathcal{E}}$. An expression can be obtained by analogy to its one-body discrete counterpart Eq.

(4.91) or by bringing the argument that it must be isotropic as there's no reason to favor a site over any other, this leads to writing the system energy operator $\hat{\mathcal{E}}$ as

$$\hat{\mathcal{E}}^{\epsilon} = \sum_{ij} \epsilon_{ij} \hat{c}_i^{\dagger} \hat{c}_j = \sum_i \underbrace{\left[\frac{1}{2} \sum_j \epsilon_{ij} \hat{c}_i^{\dagger} \hat{c}_j + \epsilon_{ji} \hat{c}_j^{\dagger} \hat{c}_i \right]}_{\hat{\mathcal{E}}_i^{\epsilon}} = \sum_i \hat{\mathcal{E}}_i^{\epsilon} \tag{4.169}$$

which gives the following expression for $\hat{\mathcal{E}}_i^{\epsilon}$

$$\hat{\mathcal{E}}_i^{\epsilon} = \frac{1}{2} \sum_j \epsilon_{ij} \hat{c}_i^{\dagger} \hat{c}_j + \epsilon_{ji} \hat{c}_j^{\dagger} \hat{c}_i \tag{4.170}$$

where ϵ refers to the considered one-body energy operator: 'total energy' $\hat{\varepsilon}$ Eq. (4.64), kinetic energy $\hat{\kappa}$ Eq. (4.45) or the Hamiltonian $\hat{h}$ Eq. (4.46). The energy of the subsystem $\mathcal{A}$ is then simply the sum of the energy of each of its sites. This recovers the previous definition that includes the 'coupling' term Eq. (4.167)

$$\hat{\mathcal{E}}_{\mathcal{A}}^{\epsilon} = \sum_{i \in \mathcal{A}} \hat{\mathcal{E}}_i^{\epsilon} = \hat{\tilde{\mathcal{E}}}_{\mathcal{A}}^{\epsilon} + \frac{1}{2} \hat{\tilde{\mathcal{E}}}_{\mathrm{C}}^{\epsilon} \tag{4.171}$$

The idea of considering half the contribution of the hoppings within the definition of a local energy density operator, as we did with $\hat{\mathcal{E}}_i^{\epsilon}$ in Eq. (4.170), has already been introduced in Ref. [8] when considering disordered harmonic solids. It has then been used by Ref. [210] in its definition of a local energy operator in a 1D discrete chain. And finally, it got generalized for a generic tight-binding Hamiltonian in Ref. [129] with the same expression as $\hat{\mathcal{E}}_i^{\epsilon}$, given in Eq. (4.170), while only considering the Hamiltonian operator $\epsilon = h$.

When considering the equivalent problem of defining an energy operator of a sub-system, for example the Hamiltonian energy $\mathcal{E}_{\alpha}^{h}$ of a lead $\mathcal{L}_{\alpha}$ in a system described Fig. 4.1, Ref. [119] justifies the half-half split of the 'coupling' term $\hat{\mathcal{E}}_{\mathrm{C}}^{h}$, given Eq. (4.166), between both sub-systems to define subsystem energy operators as described Eq. (4.167), with several arguments

- It is the 'natural' splitting as it emerges from the discretization from continuous models. We performed a different derivation than the one described in Ref. [119] through Eq. (4.91), which results from the discretization of Eq. (4.62).
- This definition admits an energy conservation equation, and therefore abides by the first law of thermodynamics. As we show in the following paragraphs.

This definition was also later endorsed by Refs. [25, 143], while using the Hamiltonian as the energy operator. On our end, we provide a few more arguments that justify this symmetrical splitting, that rose through our derivations

- The hopping/coupling Hamiltonian coefficients $h_{ij}, i \neq j$ (given in Eq. (4.82)) are the discrete representation of the continuous Kinetic energy part $\hat{\kappa}$ (defined in Eq. (4.45)) part of the Hamiltonian $\hat{h}$ (defined in Eq. (4.46)). It is usual to take into account the local kinetic energy in a local energy density.
- Defining the local energy density as the expectation value of the local 'total' energy operator $\hat{\mathcal{E}}_i^{\varepsilon}$ (given in Eq. (4.170) with $\epsilon \to \varepsilon$) enables us to recover, for the total energy source term S_i^{ε} (given Eq. (4.188)), the classical expression of the power given to electrons in Eq. (4.4)

In the following, we will use this 'natural' definition of the local energy operator $\hat{\mathcal{E}}_i^\epsilon$, given in Eq. (4.170), to define a local energy density and subsystem energies. However, this definition of a local/subsystem energy operator rises issues while trying to define a time-dependent heat current and is still under debate, see Sec. 4.3.4.2.

4.3.3.4. Time-dependent energy transport

The same energy conservation equation (4.90) derived Sec. 4.2.3 in the one-body approach can be done in the many-body approach and obtain the same energy conservation equation

$$\partial_t \rho_i^\epsilon(t) + \sum_j I_{ij}^\epsilon(t) = S_i^\epsilon \tag{4.172}$$

where the ϵ superscript is indicates the considered the energy quantity: the 'total energy' operator $\hat{\varepsilon}$, to the Kinetic energy operator $\hat{\kappa}$ or the Hamiltonian $\hat{h}$. Note that these operators differ only through onsite potentials, therefore we have

$$i \neq j \implies h_{ij} = \varepsilon_{ij} = \kappa_{ij} \tag{4.173}$$

$\rho_i^\epsilon(t)$ is the many-body expectation of the local energy operator $\hat{\mathcal{E}}_i(t)$ written in the Heisenberg picture, it can be further expressed using the lesser green functions defined Eq. (4.142)

$$\rho_i^\epsilon(t) = \left\langle \hat{\mathcal{E}}_i^\epsilon(t) \right\rangle = \sum_j \mathrm{Im}\left[\epsilon_{ij}(t) G_{ji}^<(t)\right] \tag{4.174}$$

An energy conservation equation for the operator $\hat{\mathcal{E}}_i(t)$ is then obtained by interpreting the energy divergence $\sum_j I_{ij}^\epsilon$ and the energy source S_i^ϵ from the expansion of the Heisenberg equation of motion Eq. (4.135) (See Sec. 4.3.2.1) of $\hat{\mathcal{E}}_i(t)$

$$\underbrace{\partial_t \rho_i^\epsilon(t) = \frac{\mathrm{i}}{\hbar}\left\langle \left[\hat{H}(t), \hat{\mathcal{E}}_i^\epsilon(t)\right]\right\rangle + \left\langle \partial_t \hat{\mathcal{E}}_i^\epsilon(t)\right\rangle}_{\text{Heisenberg equation of motion (4.135)}} \implies \underbrace{\partial_t \rho_i^\epsilon(t) + \textstyle\sum_j I_{ij}^\epsilon(t) = S_i^\epsilon}_{\text{Conservation equation}}$$

As we will see in the following sections, and as shown Eq. (4.94) in the discrete one-body approach, the expression we derive for the local energy current, for each energy operator, has the generic following form

$$I_{ij}^\epsilon = \frac{1}{\hbar}\sum_k \mathrm{Re}\left[\epsilon_{ki}\epsilon_{ij} G_{jk}^< - \epsilon_{kj}\epsilon_{ji} G_{ik}^<\right] \tag{4.175}$$

where ϵ_{ij} is to be replaced by the coefficients of the considered energy operator: ε_{ij} for the 'total energy', κ_{ij} for the kinetic energy and h_{ij} for the Hamiltonian energy.

Total energy operator The total energy one-body operator $\hat{\varepsilon}$ is defined in Eq. (4.64) as the being the Hamiltonian $\hat{h}$ without the energy term associated with the time-dependent scalar potential

$$\hat{\varepsilon} = \hat{h} - q\phi(\vec{r}, t)\hat{I} \tag{4.176}$$

where $\hat{I}$ is the identity operator and $\phi(\vec{r},t)$ is the electromagnetic scalar potential. The associated second quantization many-body operator $\hat{\mathcal{E}}^{\varepsilon}$ is a single-particle operator, therefore follows Eq. (4.130) in its second quantization expression

$$\begin{aligned}\hat{\mathcal{E}}^{\varepsilon}(t) &= \sum_{ij} \varepsilon_{ij}(t)\, \hat{c}_i^{\dagger}(t)\hat{c}_j(t) \\ \varepsilon_{ij}(t) &= \langle i|\, \hat{\varepsilon}\, |j\rangle = h_{ij}(t) - q\, \langle i|\, \phi(\vec{r},t)\, |j\rangle\end{aligned} \tag{4.177}$$

where

$$\langle i|\, \phi(\vec{r},t)\, |j\rangle = \int \mathrm{d}^3 r\; \lambda_i(\vec{r})^* \phi(\vec{r},t) \lambda_j(\vec{r}) \tag{4.178}$$

given that the one-body states $|i\rangle$ are orthogonal due their separate spatial localization, the dot product $\langle i|\, \phi(\vec{r},t)\, |j\rangle$ is non zero only when $i=j$, therefore

$$\langle i|\, \phi(\vec{r},t)\, |j\rangle = \phi_i(t)\delta_{ij} \qquad\qquad \phi_i(t) = \int \mathrm{d}^3 r\; \left|\lambda_i(\vec{r})\right|^2 \phi(\vec{r},t) \tag{4.179}$$

This enables us to establish the following connection between the energy operator $\hat{\mathcal{E}}^{\varepsilon}$ and the Hamiltonian $\hat{H}$

$$\hat{\mathcal{E}}^{\varepsilon}(t) = \hat{H}(t) - q\, \hat{\Phi}(t) \tag{4.180}$$

where $\hat{\Phi}(t)$ is the associated many-body (single-particle) operator associated to the electromagnetic scalar potential $\phi(\vec{r},t)$

$$\hat{\Phi}(t) = \sum_i \phi_i(t)\, \hat{\rho}_i(t) \tag{4.181}$$

where $\hat{\rho}_i(t) = \hat{c}_i^{\dagger}\hat{c}_i$ is the number operator at site i. The operator $\hat{\mathcal{E}}_i^{\varepsilon}(t)$ represent the energy density on site i. Its expectation value $\rho_i^{\varepsilon}(t) = \left\langle \hat{\mathcal{E}}_i^{\varepsilon}(t) \right\rangle$, where $\hat{\mathcal{E}}_i^{\varepsilon}$ is given by Eq. (4.170), writes using the lesser green functions defined with Eq. (4.142) as

$$\rho_i^{\varepsilon} = \left\langle \hat{\mathcal{E}}_i^{\varepsilon}(t) \right\rangle = \rho_i^h - q\phi_i(t)\rho_i = \sum_j \mathrm{Im}\left[\varepsilon_{ij}(t) G_{ji}^{<}(t)\right] \tag{4.182}$$

The time derivative of this expectation value follows Heisenberg's equation of motion (4.135)

$$\partial_t \left\langle \hat{\mathcal{E}}_i^{\varepsilon} \right\rangle = \frac{\mathrm{i}}{\hbar} \left\langle \left[\hat{H}(t), \hat{\mathcal{E}}_i^{\varepsilon}(t)\right] \right\rangle + \left\langle \partial_t \hat{\mathcal{E}}_i^{\varepsilon} \right\rangle \tag{4.183}$$

$$= \frac{\mathrm{i}}{\hbar} \left\langle \left[\hat{\mathcal{E}}^{\varepsilon}(t) + q\hat{\Phi}(t), \hat{\mathcal{E}}_i^{\varepsilon}(t)\right] \right\rangle + \left\langle \partial_t \hat{\mathcal{E}}_i^{\varepsilon} \right\rangle \tag{4.184}$$

One can notice when summing over i that the commutator part vanishes partially:

$$\sum_i \left\langle \left[\hat{\mathcal{E}}^{\varepsilon}(t) + q\,\hat{\Phi}(t), \hat{\mathcal{E}}_i^{\varepsilon}(t)\right] \right\rangle = \left\langle \left[\hat{\mathcal{E}}^{\varepsilon}(t) + q\,\hat{\Phi}(t), \hat{\mathcal{E}}^{\varepsilon}(t)\right] \right\rangle = \left\langle \left[q\,\hat{\Phi}(t), \hat{\mathcal{E}}^{\varepsilon}(t)\right] \right\rangle \tag{4.185}$$

The local energy current I_{ij}^{ε} should vanish when summed over all sites j and i as it should verify $I_{ij}^{\varepsilon} = -I_{ji}^{\varepsilon}$ to be interpretable as the net energy current flowing from i to j. This gives a hint to write the continuity equation where we identify $-\frac{\mathrm{i}}{\hbar}\left\langle [\hat{\mathcal{E}}^{\varepsilon}, \hat{\mathcal{E}}_i^{\varepsilon}] \right\rangle$ as the local current divergence $\sum_j I_{ij}^{\varepsilon}$. This former identification leaves a unique possibility for the source term $S_i^{\varepsilon}(t)$

$$\partial_t \rho_i^{\varepsilon}(t) \underbrace{- \frac{\mathrm{i}}{\hbar} \left\langle [\hat{\mathcal{E}}^{\varepsilon}(t), \hat{\mathcal{E}}_i^{\varepsilon}(t)] \right\rangle}_{\sum_j I_{ij}^{\varepsilon}(t)} = \underbrace{\frac{\mathrm{i}}{\hbar} \left\langle [q\,\hat{\Phi}(t), \hat{\mathcal{E}}_i^{\varepsilon}(t)] \right\rangle + \left\langle \partial_t \hat{\mathcal{E}}_i^{\varepsilon}(t) \right\rangle}_{S_i^{\varepsilon}(t)} \tag{4.186}$$

and we therefore obtain the conservation equation (4.172) for the 'total energy' operator

$$\partial_t \rho_i^\varepsilon(t) + \sum_j I_{ij}^\varepsilon(t) = S_i^\varepsilon \tag{4.187}$$

We can show that the source term S_i^ε is the many-body equivalent of the continuous energy source $\vec{j}(\vec{r},t)\cdot\vec{E}(\vec{r},t)$ given in Eq. (4.67). Expanding the term $\frac{\mathrm{i}}{\hbar}\left\langle[q\,\hat{\Phi}(t),\hat{\mathcal{E}}_i^\varepsilon(t)]\right\rangle$ enables us to identify a part of the continuous energy source $-\vec{\nabla}\phi_i(t)\cdot q\vec{j}_i(t)$. Then, using the explicit expression of $\varepsilon_{ij}(t)$ coefficients in Eq. (4.105) and h_{ij} in Eq. (4.82), we show that $\left\langle\partial_t\hat{\mathcal{E}}_i^\varepsilon(t)\right\rangle$ corresponds to $-\partial_t\vec{A}_i(t)\cdot q\vec{j}_i(t)$

$$S_i^\varepsilon(t) = \underbrace{\sum_j -\frac{1}{2}\left[\phi_j(t)-\phi_i(t)\right]qI_{ij}^N(t)}_{-\vec{\nabla}\phi_i(t)\cdot q\vec{j}_i(t)} + \underbrace{\sum_j \mathrm{Im}\left[\partial_t\varepsilon_{ij}(t)G_{ji}^<(t)\right]}_{-\partial_t\vec{A}_i(t)\cdot q\vec{j}_i(t)} \tag{4.188}$$

where $I_{ij}^N(t)$ is the many-body particle current flowing from site i to site j, given in Eq. (4.161), and $\vec{j}_i$ is the particle current density vector whose relation with I_{ij}^{N} is given by (4.89). A complete derivation of Eq. (4.188) has been done in Appendix. B.3 where an explicit expression of h_{ij} has been taken from Eq. (4.82). When the hopping Hamiltonian coefficients $h_{ij}(t), i\neq j$ are written in terms of exponentials, as in Eq. (4.83), or more generally with a Peierls substitution approach [122]

$$h_{ij}(t) = h_{ii}(t)\delta_{ij} + h_{ij}^0 \mathrm{e}^{\mathrm{i}\frac{q}{\hbar}\varphi_{ij}(t)}(1-\delta_{ij}) \tag{4.189}$$

where $\varphi_{ij}(t) = \int_{\vec{r}_i}^{\vec{r}_j}\vec{A}(\vec{r},t)\cdot\mathrm{d}\vec{r}$ is a Peierls phase ($A(\vec{r},t)$ is supposed to have a slow spatial variation between $\vec{r}_i$ and $\vec{r}_j$), the source term $S_i^\varepsilon(t)$ simplifies to

$$S_i^\varepsilon(t) = \sum_j -\frac{1}{2}\left[\phi_j(t)-\phi_i(t)-\partial_t\varphi_{ij}(t)\right]qI_{ij}^N(t) \tag{4.190}$$

To define the energy current however, just like in the one-body derivation done in Sec. 4.2.3 there is no unique way to write the expression of an energy current $I_{ij}^\varepsilon(t)$ flowing between two sites i and j, given an energy current divergence $\sum_i I_{ij}^\varepsilon$ at site i. A possible candidate that we derived, that verifies $h_{ij}=0 \implies I_{ij}^\varepsilon = 0$ on top of $I_{ij}^\varepsilon = -I_{ji}^\varepsilon$ and whose divergence gives the correct result, is the following

$$I_{ij}^\varepsilon = \frac{1}{\hbar}\sum_k \mathrm{Re}\left[\varepsilon_{ki}\varepsilon_{ij}G_{jk}^< - \varepsilon_{kj}\varepsilon_{ji}G_{ik}^<\right] \tag{4.191}$$

A complete derivation of this energy current has been done in Appendix. B.2.1.

The approach followed by [129] to define a Hamiltonian based local energy current can be used here too to define another candidate $\tilde{I}_{ij}^\varepsilon$ for the local "total" energy current

$$\tilde{I}_{ij}^\varepsilon = \frac{\mathrm{i}}{\hbar}\left\langle[\hat{\mathcal{E}}_i^\varepsilon,\hat{\mathcal{E}}_j^\varepsilon]\right\rangle = \frac{1}{2\hbar}\sum_k \mathrm{Re}\left[\varepsilon_{ik}\varepsilon_{kj}G_{ji}^< + \varepsilon_{ij}\varepsilon_{jk}G_{ki}^< + \varepsilon_{ki}\varepsilon_{ij}G_{jk}^<\right] \tag{4.192}$$

For a complete derivation, please refer to Appendix. B.2.2

Kinetic energy operator The kinetic energy one-body operator $\hat{\kappa}$ is defined in Eq. (4.45). It is equal to the Hamiltonian $\hat{h}$ without the energy terms associated with the time-dependent scalar potential $q\phi(\vec{r},t)$ and the potential energy $V(\vec{r})$

$$\hat{\varepsilon} = \hat{h} - [q\phi(\vec{r},t) + V(\vec{r})]\hat{I} \tag{4.193}$$

where $\hat{I}$ is the identity operator. The derivation for this kinetic operator is mathematically equivalent to the previous derivation for the 'total energy' operator $\hat{\mathcal{E}}^{\varepsilon}$ by doing the following symbolic replacement in all the derived expressions

$$q\phi \to q\phi + V \quad \text{and} \quad \varepsilon \to \kappa \tag{4.194}$$

we obtain the following expressions for the kinetic energy density ρ_i^{κ}, energy current I_{ij}^{κ} and energy source S_i^{κ}

$$\rho_i^{\kappa} = \left\langle \hat{\mathcal{E}}_i^{\kappa}(t) \right\rangle = \sum_j \mathrm{Im}\left[\kappa_{ij}(t) G_{ji}^{<}(t)\right] \tag{4.195}$$

$$I_{ij}^{\kappa} = \frac{1}{\hbar} \sum_k \mathrm{Re}\left[\kappa_{ki}\kappa_{ij} G_{jk}^{<} - \kappa_{kj}\kappa_{ji} G_{ik}^{<}\right] \tag{4.196}$$

$$S_i^{\kappa}(t) = \underbrace{\sum_j -\frac{1}{2}\left[q\phi_j(t) + V_j - q\phi_i(t) - V_i\right] I_{ij}^{N}(t)}_{-[q\vec{\nabla}\phi_i(t) + \vec{\nabla}V_i]\cdot \vec{j}_i(t)} + \underbrace{\sum_j \mathrm{Im}\left[\partial_t \kappa_{ij}(t) G_{ji}^{<}(t)\right]}_{-\partial_t \vec{A}_i \cdot \vec{j}_i} \tag{4.197}$$

Hamiltonian energy operator As with the one-body approach Sec. 4.2.3, and even though the Hamiltonian is not gauge invariant, we can interpret the expectation value of the onsite Hamiltonian density operator $\rho_i^h = \left\langle \hat{H}_i \right\rangle$, where $\hat{H}_i$ is given by Eq. (4.170), as an energy density this time in the many-body case. Its time derivative is given by the Heisenberg equation of motion (4.135)

$$\partial_t \rho_i^h(t) = \frac{\mathrm{i}}{\hbar}\left\langle \left[\hat{H}(t), \hat{H}_i(t)\right]\right\rangle + \left\langle \partial_t \hat{H}_i(t)\right\rangle \tag{4.198}$$

One can notice when summing over i that the commutator part vanishes. This gives a hint to write the energy conservation equation:

$$\partial_t \rho_i^h(t) \underbrace{-\frac{\mathrm{i}}{\hbar}\left\langle [\hat{H}(t), \hat{H}_i(t)]\right\rangle}_{\sum_j I_{ij}^h(t)} = \underbrace{\left\langle \partial_t \hat{H}_i(t)\right\rangle}_{S_i^h(t)} \tag{4.199}$$

where the energy current vanishes when summed over i. The energy current should be real and verify $I_{ij}^h = -I_{ji}^h$ to be interpretable as the net energy flowing from i to j per unit of time. However, there is no unique definition of a current flowing between two neighboring sites i and j, we only have a unique definition of total energy leaving a site, *i.e.* $\sum_i I_{ij}^h$. Further derivation, similar to the one performed in Appendix. B.2.1, leads to the following expressions for the Hamiltonian based energy current and energy source

$$I_{ij}^h(t) = \frac{1}{\hbar}\sum_k \mathrm{Re}\left[h_{ki}(t)h_{ij}(t)G_{jk}^{<}(t) - h_{kj}(t)h_{ji}(t)G_{ik}^{<}(t)\right] \tag{4.200}$$

$$S_i^h(t) = \sum_j \mathrm{Im}\left[\partial_t h_{ij}(t) G_{ji}^{<}(t)\right] = q\,\rho_i(t)\,\partial_t\phi_i(t) + \underbrace{\sum_j \mathrm{Im}\left[\partial_t[h_{ij}(t) - q\delta_{ij}\phi_i(t)]G_{ji}^{<}(t)\right]}_{-\partial_t \vec{A}_i \cdot \vec{j}_i} \tag{4.201}$$

The current respects the extra constraint that the current is zero for sites that are not "connected" by the Hamiltonian $h_{ij} = 0 \implies I_{ij}^h(t) = 0$. Another candidate $\bar{I}_{ij}^h$ for a Hamiltonian based energy current has been defined in [210, 129]

$$\bar{I}_{ij}^h = \frac{\mathrm{i}}{\hbar}\left\langle [\hat{H}_i, \hat{H}_j]\right\rangle = \frac{1}{2\hbar}\sum_k \mathrm{Re}\left[h_{ik}h_{kj}G_{ji}^{<} + h_{ij}h_{jk}G_{ki}^{<} + h_{ki}h_{ij}G_{jk}^{<}\right] \tag{4.202}$$

that has the correct divergence but does not does not respect $h_{ij} = 0 \implies I^h_{ij}(t) = 0$ which makes it more complex. The derivation has been done for the total energy operator in Appendix. B.2.2. That same derivation could be done for the Hamiltonian operator.

4.3.4. Computing lead currents

4.3.4.1. Particle and energy

Transport studies aim to compute the currents that hop-in and hop-out of the leads, in systems sketched in Fig. 5.5. To do so using our hopping energy currents I^ϵ_{ij} and particle currents I^{N}_{ij}, for which expression have been derived in Sec. 4.3.3, we simply compute the current flux through the section that separates the lead α from the central system $\mathcal{C}$ (see Fig. 4.1). This amounts to summing the currents over all the hoppings that connect the lead to the central system

$$I^{\mathrm{N}}_\alpha = \sum_{\substack{n\in\mathcal{L}_\alpha \\ i\in\mathcal{C}}} I^{\mathrm{N}}_{ni} \qquad\qquad I^\epsilon_\alpha = \sum_{\substack{n\in\mathcal{L}_\alpha \\ i\in\mathcal{C}}} I^\epsilon_{ni} \tag{4.203}$$

Given that we explicitly consider the spatial span of the leads within our approach, currents can also be computed through a section that is taken further away in the leads (see Sec. 5.2.2 for the practical definition we use within `tkwant`). This is a generalization with respect to the usual approach taken by previous works in the literature. The latter defines the lead's particle and energy current as being the time derivative of the expectation value of the lead's particle operator $\hat{N}_\alpha$ and the lead's Hamiltonian $\hat{H}_\alpha = \hat{\tilde{H}}_\alpha + \frac{1}{2}\hat{H}_{\mathcal{C}\alpha}$[19]

$$\bar{I}^{\mathrm{N}}_\alpha = -\partial_t \left\langle \hat{N}_\alpha \right\rangle \qquad\qquad \bar{I}^h_\alpha = -\partial_t \left\langle \hat{H}_\alpha \right\rangle \tag{4.204}$$

where the operators $\hat{N}_\alpha$ and $\hat{\tilde{H}}_\alpha$ are written with creation and annihilation operators in k space instead of real space, which prevents writing spatially resolved currents within the leads. In our approach, we write the lead particle number operator $\hat{N}_\alpha$ and energy operator $\hat{\mathcal{E}}^\epsilon_\alpha$ as a sum of the local operators $\hat{\rho}_i = \hat{c}^\dagger_i \hat{c}_i$ and $\hat{\mathcal{E}}^\epsilon_i$ (given in Eq. (4.170)) over the sites i in $\mathcal{L}_\alpha$ (c.f. Sec. 4.3.3.4)

$$\hat{N}_\alpha = \sum_{i\in\mathcal{L}_\alpha} \hat{\rho}_i \qquad\qquad \hat{\mathcal{E}}^\epsilon_\alpha = \sum_{i\in\mathcal{L}_\alpha} \hat{\mathcal{E}}^\epsilon_i \tag{4.205}$$

Summing the local particle conservation equation (4.157) and the local energy conservation equation (4.172) over the sites i of the lead $\mathcal{L}_\alpha$ enables us to link our lead current definitions, given in Eq. (4.203), with the usual definition taken in the literature, given in Eq. (4.204)

$$\bar{I}^{\mathrm{N}}_\alpha = I^{\mathrm{N}}_\alpha \qquad\qquad -\bar{I}^\epsilon_\alpha + I^\epsilon_\alpha = S^\epsilon_\alpha \tag{4.206}$$

where $\bar{I}^\epsilon_\alpha$ is the generalization of $\bar{I}^h_\alpha$, given in Eq. (4.204), to the other energy quantities ϵ (see Sec. 4.3.3.4). A few remarks:

- Each lead is considered to be time-independent. The term S^ϵ_α is non-zero only due the sites that are at the boundary between the lead and the central system that make up for either a time-dependent hopping or have a time-dependent onsite Hamiltonian coefficient $h_{ii/jj}(t)$ (See *e.g.* Eq. (4.188)). If one chooses the arbitrary boundary that separates the lead $\mathcal{L}_\alpha$ from the central system $\mathcal{C}$ further away in the lead, we would have $S^\epsilon_\alpha = 0$

[19] We consider directly here that the lead's Hamiltonian $\hat{H}_\alpha$ that contains half the contribution of the coupling Hamiltonian $\hat{H}_{\mathcal{C}\alpha}$, that links the central system $\mathcal{C}$ with the lead $\mathcal{L}_\alpha$. See Sec. 4.3.3.3 for a more complete discussion over this choice.

- We write the lead's energy operator $\hat{\mathcal{E}}^{\epsilon}_{\alpha}$, given by Eq. (4.205), as a sum of local energy operators $\hat{\mathcal{E}}^{\epsilon}_{i}$ defined in Eq. (4.170). The latter include surrounding hoppings terms in their definition and therefore Eq. (4.167) applies here. When the considered energy quantity ϵ is either the 'total energy' ($\epsilon = \varepsilon$) or the Hamiltonian ($\epsilon = h$), which both coincide when considered in the lead as it is time-independent, the lead's energy operator $\hat{\mathcal{E}}^{\epsilon}_{\alpha}$ writes as the following

$$\hat{\mathcal{E}}^{\varepsilon}_{\alpha} = \hat{\mathcal{E}}^{h}_{\alpha} = \hat{H}_{\alpha} = \hat{\tilde{H}}_{\alpha} + \frac{1}{2}\hat{H}_{\mathcal{C}\alpha} \tag{4.207}$$

  where $\hat{H}^{\mathcal{C}\alpha}$ contains the hoppings that connect the sites of the lead $\mathcal{L}_{\alpha}$ to the scattering region $\mathcal{C}$, See Sec. 5.2.1 for more information.

- Within our approach, we can compute current fluxes further away in the leads. In the time-dependent case, this raises some fundamental questions as the values of the computed currents will depend on the position on the lead. Indeed, the time-dependent perturbation that originates from the scattering region travels at a finite speed in the leads. Also, the lead's dispersion relation produces modes at different energies, which travel at different speeds. When considering lead-related quantities in the time-dependent regime, it is therefore more physical to work with time integrated quantities to avoid the arbitrariness of choosing where to compute the time-resolved quantities in the lead.

4.3.4.2. Heat

The systems we describe are non-interacting and no relaxation process within the system are taken into account. We therefore cannot define a local temperatures nor local heat currents within the system, from first principles. However, a common hypothesis that is made in the stationary regime [16] is that each electron leaving the scattering area $\mathcal{C}$ with an energy E into a lead $\mathcal{L}_{\alpha}$, will eventually reach the electro-chemical reservoir of temperature T_{α} and chemical potential μ_{α}, then undergo thermal relaxation and contribute $E - \mu_{\alpha}$ in heat to the thermal bath. In terms of currents, this translates as the following expression for the heat current stationary $I^{\mathrm{Q,st}}_{\alpha}$

$$I^{\mathrm{Q,st}}_{\alpha} = I^{\epsilon,\mathrm{st}}_{\alpha} - \mu_{\alpha} I^{\mathrm{N,st}}_{\alpha} \tag{4.208}$$

where $I^{\epsilon,\mathrm{st}}_{\alpha}$ and $I^{\mathrm{N,st}}_{\alpha}$ are respectively the stationary lead $\mathcal{L}_{\alpha}$ energy current and particle currents, as defined in Eq. (4.203) while in the stationary regime. The equation (4.208) has then been used in a system with a periodic time-dependent drive over cycle-averaged quantities [12]. Note that in the stationary and periodic case (for cycle-averaged quantities), the coupling Hamiltonian $H^{\mathcal{C}\alpha}$ has no contribution to the lead's energy current $I^{\epsilon,\mathrm{st}}_{\alpha}$ and is not considered in the literature: $I^{\epsilon,\mathrm{st}}_{\alpha}$ is simply defined as the opposite of the total time derivative of the lead's Hamiltonian $\hat{\tilde{H}}_{\alpha}$ without consideration for the coupling Hamiltonian $\hat{H}^{\mathcal{C}\alpha}$

$$I^{\epsilon,\mathrm{st}}_{\alpha} = -\partial_t \left\langle \hat{\tilde{H}}_{\alpha,\mathrm{st}} \right\rangle \tag{4.209}$$

Defining a time-resolved lead heat current in the time dependent regime lies within the emerging field of time-dependent non-equilibrium quantum thermodynamics. This field is new with ongoing research over defining a proper and definite theoretical framework. Fundamental issues have arisen with respect to the conceptual spatial separation between the central system, the thermal baths and their coupling. In the weak coupling regime, a consistent theory has been established [23, 52, 107,

68] whereas in the strong coupling regime, especially when the coupling is time-dependent, defining a time resolved heat current raises a fundamental issue [31, 54, 44, 25, 143]: the part $\hat{H}^{\mathcal{C}\alpha}$ of the system's total Hamiltonian $\hat{H}$ that couples a lead to the central system is no longer negligible, can be time-dependent, and must be accounted for when one tries to define a time-resolved heat current. Following our discussion in Sec. 4.3.3.3 over the definition of a local energy operator that also applies for a subsystem, an expression to the time-resolved lead heat current in has been given by Refs. [119, 121] where the lead's energy includes half the contribution of the coupling $\hat{H}^{\mathcal{C}\alpha}$

$$I_\alpha^{\mathrm{Q},h}(t) = -\partial_t \left\langle \hat{H}_\alpha \right\rangle - \mu_\alpha I_\alpha^{\mathrm{N}}(t) = -\partial_t \left\langle \hat{\tilde{H}}_\alpha + \frac{1}{2}\hat{H}^{\mathcal{C}\alpha} \right\rangle - \mu_\alpha I_\alpha^{\mathrm{N}}(t) \tag{4.210}$$

This definition recovers equation (4.208) that gives the heat current in the stationary case as the coupling Hamiltonian $\hat{H}^{\mathcal{C}\alpha,\mathrm{st}}$ would not contribute $\partial_t \left\langle \hat{H}^{\mathcal{C}\alpha} \right\rangle = 0$. Ref. [54] raised two issues with time resolved heat current $I_\alpha^{\mathrm{Q},h}(t)$ given in Eq. (4.210), within a particular model[20]: *(i)* while slowly driven, the evolution is reversible and the heat current is expected to be a state function. $I_\alpha^{\mathrm{Q},h}(t)$ is reported to not be a state function in this case because of the coupling Hamiltonian $\hat{H}^{\mathcal{C}\alpha}$ has been added in its definition. *(ii)* Whether the coupling Hamiltonian is considered in $I_\alpha^{\mathrm{Q},h}(t)$ or not, the heat current $I_\alpha^{\mathrm{Q},h}(t)$ is reported to not abide by the third law of thermodynamics, *i.e.* $I_\alpha^{\mathrm{Q},h}(t)/T_\alpha$ does not converge to zero when $T \to 0$ and diverges instead, T_α being the temperature of the (single) reservoir. In the other hand, Ref. [142] reports that the symmetrical splitting of the coupling fails to describe energy fluctuations. Finally, Ref. [81] proposes a remedy to these issues by proposing adding an extra term $\dot{W}_{\mathrm{B}}(t)$ to the heat current $I_\alpha^{\mathrm{Q},h}(t)$. $\dot{W}_{\mathrm{B}}(t)$ is non zero only when the modulus of coupling strength is time-dependent: in our approach where the time-dependence comes solely from a time-dependent electromagnetic field, the coupling Hamiltonian $\hat{H}^{\mathcal{C}\alpha}$ can only be time-dependent to account for a uniform time-dependent scalar potential in the lead $\mathcal{L}_\alpha$ after a gauge change (*c.f.* Sec. 5.2.1). The coupling strength involves only a time-dependent phase, its modulus remains time-independent and $\dot{W}_{\mathrm{B}}(t)$ is therefore zero.

Given that the Hamiltonian is in general not gauge dependent, we change the Hamiltonian based definition of the heat current $I_\alpha^{\mathrm{Q},h}(t)$, given in Eq. (4.210), to a 'total energy' based definition $I_\alpha^{\mathrm{Q}}(t) = I_\alpha^{\mathrm{Q},\varepsilon}(t)$ (note that the two definitions coincide on time-*independent* leads and differ otherwise, see Sec. 5.3.2.3)

$$I_\alpha^{\mathrm{Q}}(t) = I_\alpha^{\varepsilon}(t) - S_\alpha^{\varepsilon}(t) - \mu_\alpha I_\alpha^{\mathrm{N}}(t) \tag{4.211}$$

where we used the lead's energy current $I_\alpha^{\varepsilon}(t)$ and the lead's input power $S_\alpha^{\varepsilon}(t)$ instead of $-\partial_t \left\langle \hat{\mathcal{E}}_\alpha^{\epsilon} \right\rangle$ to facilitate defining the heat current it farther away in the lead (see Sec. 5.2.2). Computing energy and heat currents farther away in the lead avoids the issue with the eventual time-dependent coupling and circumvents the issues brought up by Ref. [54], just like it has been done by Ref. [24] through its scattering Landauer-Büttiker approach in the special case of slow time-dependent driving while still in the strong coupling regime. In Sec. 5.2.3 we expose the final pieces where we extend the approach of Ref. [24] to the arbitrary time-dependent regime, although we do not tackle the entropy transport problem but can be planned for future research.

Now that the time-resolved lead currents properly defined, we highlight two shortcomings of such an approach: *(i)* due to the travel time and dispersion, time resolved lead currents are dependent on where they are computed; *(ii)* the heat current can theoretically only be accounted for after electrons thermally relax within the bath. The lead is is technically not the heat bath and computing a space

[20] The Resonant Level model (*c.f.* Sec. 5.3.2.1) with a single lead where both the 'dot' and its coupling with the lead are slowly driven.

and time resolved heat current within the lead is a priori ill-defined, although it can be interpreted differently in terms of bookkeeping [47], *i.e.* "the amount of heat that will eventually be dissipated later on". To workaround these issues, we also study time integrated lead quantities (following *e.g.* Ref. [44]), thanks to conservation. Time integrals fit better with what an experimentalist can measure by probing temperature changes, over the course of an experiment, to detect a potential signature of the time-dependent drive

$$Q(\tau) = \int_{t_0}^{\tau} \mathrm{d}t \; I_\alpha^{\mathrm{Q}}(t) \tag{4.212}$$

Given that we consider that electrons leaving the scattering region in the leads only reach the thermal bath infinitely away in the bath, the quantity $Q(\tau)$ is to be taken with a relative origin of time when it is considered experimentally, where leads have a finite length. This definition of $Q(\tau)$ also supposes that the relaxation time-scale within the bath is orders of magnitude faster than the variation of $Q(\tau)$ so one could consider the temperature of the finite and realistic bath T_α to evolve according to the classical equation that links the incoming heat current in a system to its temperature variation

$$C_\alpha \left[T_\alpha(\tau + t_{\text{offset}}) - T_\alpha(t_{\text{offset}})\right] = Q(\tau) \tag{4.213}$$

where C_α is the thermal capacity of the realistic electrochemical bath α.

5. Transport simulations of open quantum systems

Our goal is to describe particle and energy currents and densities in scattering systems, in hopes to better understand thermoelectricity in the time dependent domain. In the previous chapter we outlined the theoretical framework that enables calculating local electron currents and densities and their associated energy currents and densities, given a one-body wavefunction $\psi(\vec{r}, t)$ (or its discretized version $\psi_i(t)$) or a many-body lesser Green function $G^<_{ij}(t)$. Here, we briefly review the approach behind `Kwant`, a simulation library of reference in quantum transport, and its extension `tkwant` to the time-dependent regime. The development of the latter package, initiated during the PhD thesis of B. Gaury [63], exposed one important equation (5.26) which links the many-body lesser Green function $G^<_{ij}(t)$ and a specific set of system-wide one-body wavefunctions, the 'scattering states', defined in systems described by Fig. 5.1. This last result completes the scattering wavefunction description of energy transport. We use it to extend `tkwant` to energy transport through a module called `tkwant.operator`: we show that `tkwant` + `tkwantoperator` enables us to more easily recover previous results of the literature on the extensively studied 'Resonant level model'. The main strength of this simulation tool is that it enables simulating bigger and more complex systems, beyond that 'toy' model: we illustrate this aspect by simulating the Quantum Point Contact.

5.1. A scattering approach to time-dependent quantum transport

The theoretical framework to describes entirely particle and energy transport, for non-interacting spinless particles in tight-binding systems without phonons, has been exposed in Sec. 4.3.3. To be able to compute the transport quantities, the last step is to define more precisely the one-body basis to use to compute the transport quantities on the specific class of systems described in Fig. 5.1, whose tight-binding representation is done in the next section. We will rely on the `Kwant` and `tkwant` simulations libraries for numerical computation. These libraries use a wavefunction approach to quantum transport, they compute a specific one-body basis of wavefunctions called the 'scattering states'. Defined as the eigenstates of the system's total Hamiltonian $\hat{H}(t < t_0) = \hat{H}_0$ in the stationary regime, the 'scattering states' are the building blocks of the scattering theory in its stationary [28, 26] and time-dependent [20] formulation. Following `tkwant`'s theoretical framework [101], the systems we consider are stationary until a given time t_0. This enables using `Kwant` for computing the scattering states in the stationary regime for $t \leq t_0$. Starting $t > t_0$, they are time-evolved one by one (thanks to the non-interacting hypothesis) by `tkwant` according to Schrödinger's equation (4.23).

In this section, we adopt a continuous description of transport for a more intuitive understanding of the concepts at play (the discretized case will be dealt with in the next section 5.2). First, we write down the generic Hamiltonian that describe our target systems. This enables us to define the stationary scattering states, whose discrete version is computed by `Kwant`. Then, we summarize how these

scattering states are time-evolved by `tkwant`'s algorithm.

5.1.1. Writing the Hamiltonian

We describe here more precisely the generic systems that `tkwant` is able to simulate (see Fig. 5.1). They are made of a central area $\mathcal{C}$ under a static potential energy $V(\vec{r})$ and time-dependent electromagnetic fields, represented by the vector potential $\vec{A}(\vec{r},t)$ and scalar potential $\phi(\vec{r},t)$. The central area $\mathcal{C}$, also called scattering region, is connected to 'waveguides', indexed by α. The role of the probes is to lead in incoming 'hot' electrons at a given electrochemical potential μ_α and temperature T_α ; but also transport out electrons from the scattering region. These probes, also called leads, are semi-infinite and periodic along one direction, with a period $\vec{e}_\alpha$.

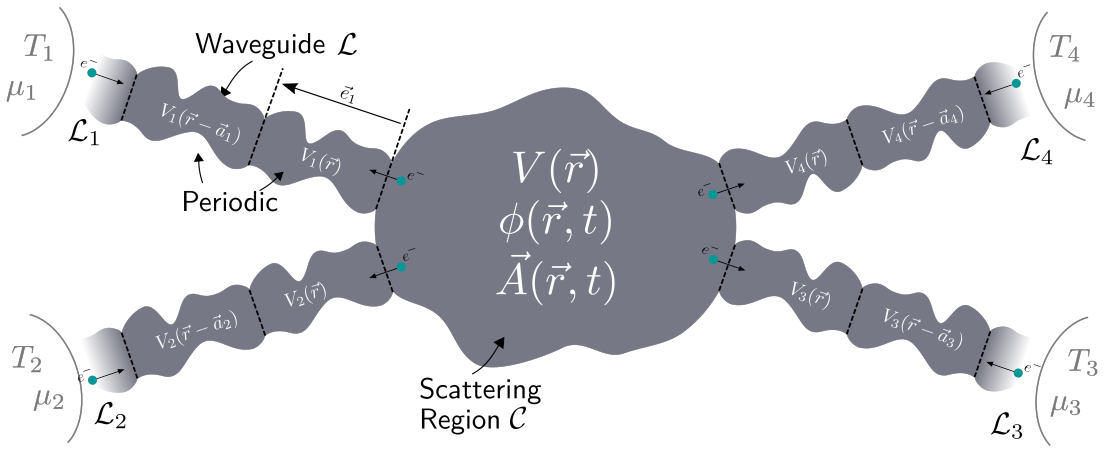

Figure 5.1. – Continuous representation of a generic system that can be simulated by `tkwant`: a central area $\mathcal{C}$ – called scattering region – connected to semi-infinite 'waveguides' $\mathcal{L}_\alpha$, called leads. The leads can have an arbitrary periodic shape along their infinite direction $\vec{e}_\alpha$, where a static and spatially periodic potential energy $V_\alpha(\vec{r})$ resides. The scattering area $\mathcal{C}$ is under a time dependent electromagnetic field, represented by the potentials $(\vec{A},\phi)$, and an additional static potential energy $V(\vec{r})$. Each lead $\mathcal{L}_\alpha$ is attached to an electronic reservoir in thermodynamic equilibrium, at temperature T_α and chemical potential μ_α, from which electrons leave and travel towards the scattering region. In our approach, the time-dependent electromagnetic field is only switched on after an instant t_0.

A stationary potential $V_\alpha(\vec{r})$ can be considered in each lead $\mathcal{L}_\alpha$ and follows its periodicity $V_\alpha(\vec{r}+\vec{e}_\alpha)=V_\alpha(\vec{r})$ (a stationary vector potential can also be considered but is omitted in our considerations). The incoming electrons in each lead α follow the Fermi thermal distribution f_α

$$f_\alpha(E)=\frac{1}{\mathrm{e}^{(E-\mu_\alpha)/k_BT}+1} \tag{5.1}$$

where μ_α and T_α are respectively the chemical potential and the temperature of the connected reservoir to the lead α. In our approach, the time dependence only starts after an instant t_0

$$\begin{cases}\vec{A}(\vec{r},t<t_0)=\vec{A}(\vec{r})\\ \phi(\vec{r},t<t_0)=0\end{cases} \tag{5.2}$$

For this particular system, the general Hamiltonian $\hat{h}$ can be written as a piecewise function of space,

using the general definition from Eq. (4.46)

$$\hat{h}[\psi] = \begin{cases} -\frac{\hbar^2}{2m}\vec{\nabla}^2\psi + V_\alpha(\vec{r})\psi \quad \text{with} \quad V_\alpha(\vec{r}+\vec{e}_\alpha) = V_\alpha(\vec{r}) \quad \text{for} \quad \vec{r} \in \mathcal{L}_\alpha \\ \frac{1}{2m}\left[-\mathrm{i}\hbar\vec{\nabla} - q\vec{A}(\vec{r},t)\right]^2[\psi] + q\,\phi(\vec{r},t)\,\psi + V(\vec{r})\,\psi \quad \text{for} \quad \vec{r} \in \mathcal{C} \end{cases} \tag{5.3}$$

Time-dependence in the leads It is theoretically possible to have an additional spatially uniform time-dependent scalar potential $\phi_\alpha(t)$ in each lead $\mathcal{L}_\alpha$. Indeed, its effect can be accounted for through a gauge transformation, given by Eq. (4.12), with a gauge function Λ that takes the following expression in each lead

$$\Lambda(\vec{r} \in \mathcal{L}_\alpha, t) = -\int_{t_0}^{t} \mathrm{d}u\ \phi_\alpha(u) \tag{5.4}$$

This will bring the leads back to being time-independent but changes the scattering region's Hamiltonian $\hat{h} \to \hat{h}'$[1] while leaving our quantum (particle and energy) description invariant

$$\hat{h}'[\psi] = \begin{cases} -\frac{\hbar^2}{2m}\vec{\nabla}^2\psi + V_\alpha(\vec{r})\psi + \underbrace{(\phi_\alpha(t) + \partial_t\Lambda)}_{=0} \ \text{ for } \vec{r} \in \mathcal{L}_\alpha \\ \frac{1}{2m}\left[-\mathrm{i}\hbar\vec{\nabla} - q(\vec{A} - \vec{\nabla}\Lambda)\right]^2[\psi] + q\,(\phi + \partial_t\Lambda)\,\psi + V(\vec{r})\,\psi \ \text{ for } \vec{r} \in \mathcal{C} \end{cases} \tag{5.5}$$

In an actual device, a time-dependent voltage driving in the leads may induce a variation of the chemical potential μ_α in the affected electronic reservoir, in addition to a variation of the electric potential. This is not taken into account in our non-interacting approach as it requires modeling relaxation inside the reservoirs. A qualitative discussion of the role of electrostatics in realistic devices (reported in Sec. 8.4 of Ref. [66]) shows that this approach already has a broad applicability in the field of time-dependent quantum nanoelectronics.

5.1.2. $t < t_0$: stationary scattering states – `kwant`

In this subsection we define the stationary scattering states. Given our assumption that the time-dependence only starts after a time t_0, we consider here $t < t_0$ so that the system is entirely stationary. The usual approach to solving the Schrödinger equation with a time-independent Hamiltonian is to diagonalize it as described in Eq. (4.32)

$$\hat{h}^{\mathrm{st}}[\Psi^\lambda_{\mathrm{st}}](\vec{r}) = E_\lambda \Psi^\lambda_{\mathrm{st}}(\vec{r}) \tag{5.6}$$

where $\hat{h}^{\mathrm{st}} = \hat{h}(t < t_0)$ is the Hamiltonian before the time dependence starts. This eigenstate equation, within the specific class of systems we consider, with a finite central region connected to semi-infinite periodic leads is solved by the `Kwant` library [77] by computing an orthogonal basis of wavefunctions called 'scattering states'. A scattering state is the system-wide wavefunction that results from an incoming conducting eigenstate of a specific lead that travels towards the system.

Given the periodicity and the semi-infinite nature of each lead, the eigenstate problem, when spatially restricted to a lead, is solved with the Bloch theorem:

$$\psi^{\alpha,\mathrm{in/out}}_{E,n}(\vec{r} \in \mathcal{L}_\alpha) = \xi^\alpha_n(\vec{r})\exp\left(\mathrm{i}k^{\mathrm{in/out}}_{nE} z_\alpha\right) \quad \text{where} \quad \xi^\alpha_n(\vec{r}+\vec{e}_\alpha) = \xi^\alpha_n(\vec{r}) \tag{5.7}$$

[1] The gauge function Λ has been intentionally left undefined in the scattering region $\mathcal{C}$. It can be essentially zero but needs to be differentiable in space (and in time): it needs to smoothly decrease from its value at the boundary with each lead α, to zero within $\mathcal{C}$

where E is the energy, n is the transverse mode and z_α is the z-coordinate in the lead-specific axis parallel to the lead's infinite and periodic direction $\vec{e}_\alpha$. $k_{nE}^{\text{in/out}}$ is the wave vector along that axis and is linked to E and n through a dispersion relation that comes from solving the Schrödinger equation. $k_{nE}^{\text{in/out}}$ can be real, in which case $\psi_{E,n}^{\alpha,\text{in/out}}$ is a conducting/traveling mode: the 'in' superscript in $k_{nE}^{\text{in/out}}$ indicates that the wave travels towards the central system whereas the 'out' superscript indicates the opposite. $k_{nE}^{\text{in/out}}$ can also be imaginary, in which case the mode is evanescent and can only exist at the boundary with the scattering region.

An explicit set of solutions can for example be written for the waveguide of constant rectangular section $[0, L_x] \times [0, L_y]$, represented in Fig. 5.2

$$\psi_{E,n,m}^{\alpha,\text{in/out}}(x, y, z) = \sin\left(n\pi\frac{x}{L_x}\right)\sin\left(m\pi\frac{y}{L_y}\right)\exp(\pm \mathrm{i}kz)$$

where E, V_α, p, q and k are connected through the following dispersion relation

$$E = V_\alpha + \frac{\hbar^2 k^2}{2m} + \frac{\hbar^2 p^2 \pi^2}{2mL_x^2} + \frac{\hbar^2 q^2 \pi^2}{2mL_y^2}$$

An eigenstate $\psi_{E,n}^{\alpha,\text{in}}$ in the lead α that travels towards the scattering region will, in the stationary

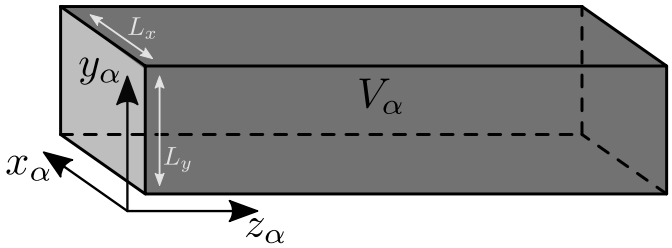

Figure 5.2 – Illustration of a waveguide lead with a rectangular constant section $L_x \times L_y$

regime, cause reflected modes $r_{nn'}^{\alpha}(E)\psi_{E,n'}^{\alpha,\text{out}}$ in the same lead, a specific wavefunction $\Psi_{\text{st}}^{\lambda}|_{\mathcal{C}}$ in the scattering region and transmitted modes $d_{nn'}^{\alpha\beta}(E)\psi_{E,n'}^{\beta,\text{out}}$ in the other leads β. The resulting system-wide wavefunction $\Psi_{\text{st}}^{\lambda}$ is called a 'scattering state' and is fully characterized by the incoming mode $\psi_{E,n}^{\alpha,\text{in}}$ in lead α, therefore $\lambda = \alpha, E, n$. It is an eigenstate of the total one-body Hamiltonian $\hat{h}$

$$\Psi^{\lambda=(\alpha,E,n),\text{st}} = \underbrace{\left[\underbrace{\psi_{E,n}^{\alpha,\text{in}}}_{\substack{\text{incoming}\\\text{mode}}} + \sum_{n'} \underbrace{r_{nn'}^{\alpha}(E)}_{\substack{\text{reflection}\\\text{amplitude}}} \underbrace{\psi_{E,n'}^{\alpha,\text{out}}}_{\substack{\text{reflected}\\\text{mode}}}\right]}_{\text{Lead } \alpha} + \underbrace{\Psi^{\lambda,\text{st}}\Big|_{\mathcal{C}}}_{\substack{\text{Central}\\\text{region}}} + \underbrace{\left[\sum_{\beta}\sum_{n'} \underbrace{d_{nn'}^{\alpha\beta}(E)}_{\substack{\text{transmission}\\\text{amplitude}}} \underbrace{\psi_{E,n'}^{\beta,\text{out}}}_{\substack{\text{transmitted}\\\text{mode}}}\right]}_{\text{Lead } \beta} \tag{5.8}$$

where $\psi_{E,n}^{\alpha,\text{in/out}}$ and $\Psi^{\lambda,\text{st}}|_{\mathcal{C}}$ are respectively non-zero only in the lead $\mathcal{L}_\alpha$ and the scattering region $\mathcal{C}$. Note that the stationary scattering states $\Psi^{\lambda,\text{st}}$ are time dependent but follow a trivial time evolution with $\exp(\mathrm{i}Et/\hbar)$ as a global pre-factor, as shown in Eq. (4.33). The stationary transmission amplitudes $d_{nn'}^{\alpha\beta}(E)$ and the reflection amplitudes $r_{nn'}^{\alpha}(E)$ can be computed by the `Kwant` simulation library [206, 77, 168] as part of the 'scattering matrix' that contains both the transmission and reflection amplitudes. In practice, scattering states are computed in two steps in `kwant`: first, the conducting modes in the leads are computed by diagonalizing the lead hamiltonians ; second, the scattering state in the central region and the scattering amplitudes are calculated by solving a large linear system (corresponding to Eq. (5.6) truncated to the central part $\mathcal{C}$ of the system).

obtained by solving the linear eigenstate stationary problem. An illustration of a scattering state and how it is computed by `Kwant` is illustrated in Fig. 5.3

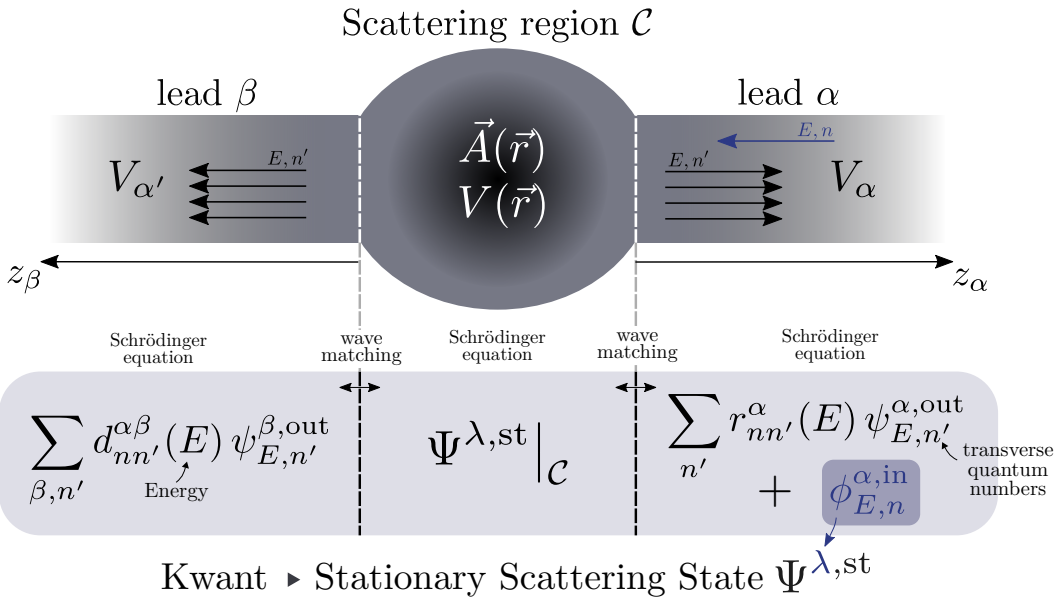

Figure 5.3. – Illustration of a scattering state and how it is in theory computed by `Kwant`: an incident eigenstate $\psi^{\alpha,\text{in}}_{E,n}$ in a mode n and energy E, in the lead $\mathcal{L}_\alpha$, is considered as an initial boundary condition to the eigenstate equation (5.6). The whole scattering state is calculated by `kwant`: it solves the Schrödinger equation in each part of the system and imposes that the wavefunctions match of at the boundaries between the scattering region and the leads, see comments bellow Eq. (5.8).

5.1.3. Time-evolving the scattering states – `tkwant`

After the time t_0 the central part $\hat{H}_\mathcal{C}(t)$ of the system's Hamiltonian $\hat{H}$ becomes time-dependent. In what follows, we consider that $t_0 = 0$ without loss of generality as it can be recovered with a translation of the time t parameter.

$$\text{Time translation:}\quad t - t_0 \to t \tag{5.9}$$

The orthogonal basis formed by the stationary scattering states Ψ^λ_{st} defined in the section above (see Eq. (5.8)) can be time evolved according to the Schrödinger equation (4.23) while remaining an orthogonal basis

$$\begin{cases} \mathrm{i}\hbar\partial_t \Psi^\lambda(t) = \hat{h}[\Psi^\lambda](t) \\ \Psi^\lambda(t=0) = \Psi^\lambda_{\text{st}} \end{cases} \tag{5.10}$$

Given that the leads are still time independent, the time-dependent scattering states $\Psi^\lambda(t)$ in each lead $\mathcal{L}_\alpha$ can still be decomposed as a linear combination of eigenstates of the lead. However, the time dependence redistributes the energies within the system: the transmitted and reflected modes can have a different energy E' than the initial incoming mode [66].

$$\begin{aligned} \Psi^{\lambda=\alpha,E,n}(t) = &\underbrace{\Bigg[\underbrace{\psi^{\alpha,\text{in}}_{E,n}\mathrm{e}^{-\mathrm{i}Et/\hbar}}_{\text{incident mode}} + \sum_{n'}\int\frac{\mathrm{d}E'}{2\pi}\underbrace{r^{\alpha}_{nn'}(E,E')}_{\text{reflection amplitude}}\underbrace{\psi^{\alpha,\text{out}}_{E',n'}\mathrm{e}^{-\mathrm{i}E't/\hbar}}_{\text{reflected mode}}\Bigg]}_{\text{Lead }\alpha} \\ &+ \underbrace{\psi^{\mathcal{C}}_\lambda(t)}_{\text{Central region}} + \underbrace{\Bigg[\sum_\beta\sum_{n'}\int\frac{\mathrm{d}E'}{2\pi}\underbrace{d^{\alpha\beta}_{nn'}(E,E')}_{\text{transmission amplitude}}\underbrace{\psi^{\beta,\text{out}}_{E',n'}\mathrm{e}^{-\mathrm{i}E't/\hbar}}_{\text{transmitted mode}}\Bigg]}_{\text{Lead }\beta} \end{aligned} \tag{5.11}$$

The transmission $d^{\alpha\beta}_{nn'}(E, E')$ and reflection $r^{\alpha}_{nn'}(E, E')$ amplitudes now express the probability amplitude for being transmitted/reflected from energy E to energy E'. The time-dependence of each lead stationary eigenstate needs to be added, using Eq. (4.33). Note that this equation (5.11) is equal to Eq. (5.8) when $t \leq 0$ but does not simplify to the same stationary expression, as the former must also describe the time dependent regime $t > 0$ while Eq. (5.8) does not. `tkwant` does not compute these complex transmission and reflection coefficients but time evolves the stationary scattering states Ψ^{st} for $t > 0$ instead, using the 'source-sink' approach.

Source-Sink algorithm Solving numerically equation (5.10) for $t > 0$ ($t_0 = 0$) is difficult as the scattering states span, with non-trivial behavior, over the entire *infinite* system. The deviation from the stationary state $\bar{\Psi}^{\lambda}$, defined as [203]

$$\Psi^{\lambda}(\vec{r}, t) = \mathrm{e}^{-\mathrm{i}E_{\lambda}t/\hbar}\left[\bar{\Psi}^{\lambda}(\vec{r}, t) + \Psi^{\lambda}_{\text{st}}(\vec{r})\right] \tag{5.12}$$

exhibits more interesting properties for numerical solving

$$\begin{cases} \mathrm{i}\hbar\partial_t\bar{\Psi}^{\lambda} = \left[\hat{h}(t) - E_{\lambda}\right][\bar{\Psi}^{\lambda}] + S^{\lambda}(t) \\ \bar{\Psi}^{\lambda}(t=0) = 0 \end{cases} \tag{5.13}$$

where $S^{\lambda}(t)$ is a 'source' term in the previous Schrödinger-like equation

$$S^{\lambda}(t) = [\hat{h} - \hat{h}^{\text{st}}][\Psi^{\lambda}_{\text{st}}](\vec{r}, t) \tag{5.14}$$

The Hamiltonian being time-dependent only within the central scattering region, the 'source' term $S^{\lambda}(t)$ is zero in the leads. For this reason and as (i) the wave function $\bar{\Psi}^{\lambda}(t)$ vanishes at $t = 0$ and (ii) is only composed of outgoing modes in each lead, it is sufficient to solve Eqs. (5.13)-(5.14) in a finite system around the scattering region $\mathcal{C}$; i.e., it is possible to truncate the leads[2] yet still describe exactly the scattering states on the remaining sites. Given that the time-dependence in the scattering region $\mathcal{C}$ creates outgoing modes that propagates in the leads at finite speed, it is necessary to truncate the leads far enough so they do not reach the border. For long simulation times, this approach can become untractable and a different one is needed [203]: 'absorb' the outgoing modes when nearing the end of the lead while keeping the calculated scattering state accurate outside of the absorption area. The practical implementation of this idea is to add an imaginary on-site potential $\Sigma_{\alpha,a}$, the 'sink'/'absorbing' term, over the last lead units cells $a = a_{\text{abs}}, \ldots, a_{\text{truncation}}$. It is diagonal and uniform in each lead cell a and varies smoothly with a in order to absorb the outgoing waves, it has a caveat of producing spurious back-reflections but they can be arbitrarily minimized (*i.e.* smaller than a target precision). The exact expression for $\Sigma_{\alpha,a}$ is given in Ref. [203] and is more thoroughly studied in Appendix B of Ref. [101]. The equation of motion of $\bar{\Psi}^{\lambda}$ that is solved within the absorbing region is the following

$$\mathrm{i}\hbar\partial_t\bar{\Psi}^{\lambda} = \left[\hat{h}(t) - E_{\lambda} - \mathrm{i}\Sigma\right][\bar{\Psi}^{\lambda}] + S^{\lambda}(t) \tag{5.15}$$

Using `kwant`'s output of the stationary scattering states $\Psi^{\lambda}_{\text{st}}$ as a starting point, `tkwant` uses $\bar{\Psi}^{\lambda}(t = 0) = 0$ and Eq. (5.12) to time-evolve them into the time-dependent scattering states $\Psi^{\lambda}(t)$, described in Eq. (5.11). `tkwant` uses for that purpose a Dormand-Prince method of the Runge-Kutta family of ordinary differential equation solvers. Contrary to `Kwant`, reflection and transmission amplitudes are not computed. Using the source-sink approach theoretically reduces the complexity of the time-evolution algorithm from $O(Nt^2_{\text{max}})$ to $O(Nt_{\text{max}})$, where N is the number of sites in the central system $\mathcal{C}$ and t_{max} is the maximum simulated time, but in practice the exact sink term $\Sigma_{\alpha,a}$ is not computed and a rougher approximation is used, leading to a practical complexity $O(Nt^{1.5}_{\text{max}})$ (see Appendix. B of [101]).

[2] $\Psi^{\lambda}_{\text{st}}$ in the leads is computed beforehand by `Kwant` with other means, more information in Ref. [207].

5.2. Practical tight-binding simulation with tkwant

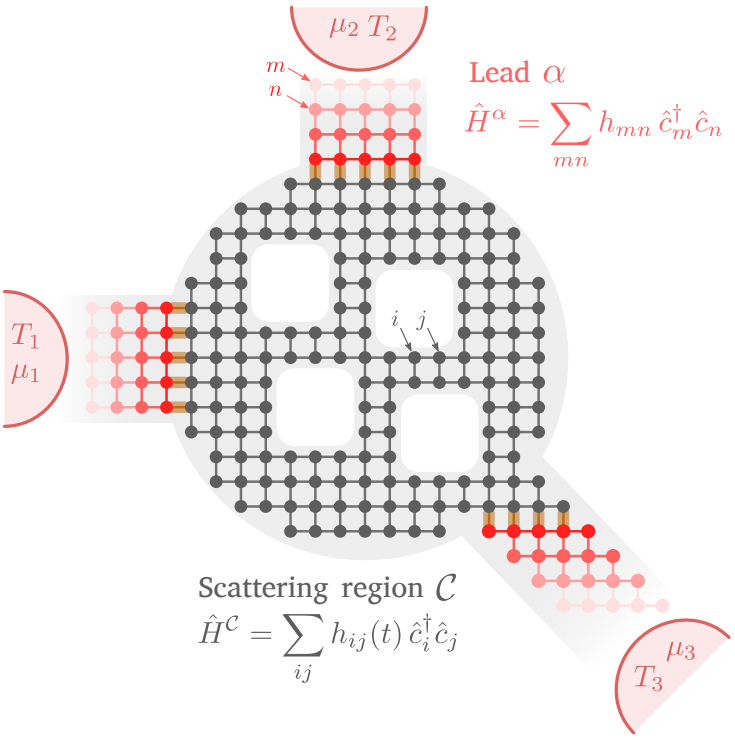

Figure 5.4 – Generic tight-binding system that can be simulated with `tkwant` (the discrete equivalent of Fig. 4.1). It is made of a time-dependent central scattering area $\mathcal{C}$, whose sites are colored in gray, connected to time-independent leads, whose sites are colored in red. A uniform time-dependent scalar potential can be considered in each lead although in practice it is gauged out into an additional time dependent phase: it is added to the hoppings connecting each lead to the central system (colored in orange), according to Eq. (5.23)

`Kwant` [77] is a free and open source Python simulation library, available at `kwant-project.org`. It describes quantum transport in general non-interacting tight-binding systems in the stationary regime. It enables simulating a wide range of phenomena: superconductivity [154, 59, 193], quantum Hall effect [144, 169], topological insulators [67, 130], graphene [62, 33], spintronics [136]. It has become the numerical tool of reference for quantum transport in mesoscopic systems as hundreds of publications have made use of the tool given its wide range of applicability and its flexibility. `tkwant` extends `Kwant` to the time domain and enables computing time-resolved electronic quantities, in generic systems described Fig. 5.4, and uses a wavefunction approach that is strictly equivalent to the NEGF approach (see. Sec. 3.3.3) but faster [66]. Its development has been led by X. Waintal's group at CEA Grenoble and has been iteratively developed for the past years – by B. Gaury [66], J. Weston [203] and T. Kloss [101] – while being internally used at the same time to study time-dependent systems [65, 202, 60, 5, 164], till a first public release in 2021 [101]. `tkwant` is free and open source and is available at `tkwant.kwant-project.org`.

5.2.1. Tight-binding model

The practical tight-binding systems that `tkwant` simulates are the discretized version of the continuous system described in Fig. 5.1. The tight-binding systems `tkwant` handles are represented diagrammatically in Fig. 5.5: a central system, whose Hamiltonian is $\hat{\tilde{H}}_\mathcal{C}$[3], is connected to each lead α with a coupling Hamiltonian $\hat{H}_{\mathcal{C}\alpha}$. Each lead Hamiltonian $\hat{\tilde{H}}_\alpha$ is entirely characterized by a Hamiltonian $\hat{\tilde{H}}_\alpha^{\text{cell}}$ of one of its repeated unit cells and a coupling Hamiltonian $\hat{W}_\alpha$ that connects each unit cell to its next neighbor (expressed in Eq. (5.19)).

[3]The tilde notation indicates that subsystem operators do not include coupling terms with other subsystems, see Sec. 4.3.3.3.

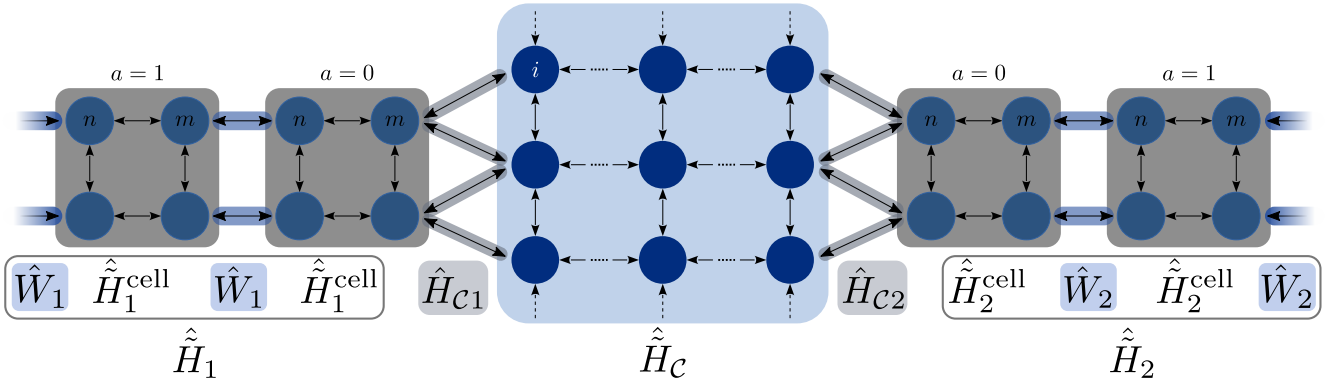

Figure 5.5. – Generic representation of a `tkwant` tight-binding system. A central system $\mathcal{C}$, described by a Hamiltonian $\hat{\tilde{H}}_{\mathcal{C}}$, is connected to semi-infinite leads through a coupling Hamiltonian $\hat{H}_{\mathcal{C},\alpha}$. Each lead α is considered to be periodic, its Hamiltonian $\hat{\tilde{H}}$ is defined by a unit cell Hamiltonian $\hat{\tilde{H}}^{\text{cell}}{}_{\alpha}$ and an inter-cell coupling Hamiltonian W_{α}.

The system's total tight-binding Hamiltonian $\hat{H}$ therefore writes as sum of three terms that illustrate the spatial separation we have made to the system [101]:

$$\hat{H} = \hat{\tilde{H}}_{\mathcal{C}} + \sum_{\alpha} \hat{\tilde{H}}_{\alpha} + \sum_{\alpha} \hat{H}_{\mathcal{C}\alpha} \tag{5.16}$$

The scattering region Hamiltonian $\hat{\tilde{H}}_{\mathcal{C}}$ is a generic second quantization non-interacting Hamiltonian that follows Eq. (4.144)

$$\hat{\tilde{H}}_{\mathcal{C}} = \sum_{ij\in\mathcal{C}} h_{ij}(t)\, \hat{c}_i^{\dagger} \hat{c}_j \tag{5.17}$$

$$h_{ij}(t < t_0) = h_{ij}^0 = \text{cst.} \tag{5.18}$$

The lead α Hamiltonian $\hat{\tilde{H}}_{\alpha}$ is stationary and describes the periodicity of the lead

$$\hat{\tilde{H}}_{\alpha} = \sum_{a=0}^{\infty} \sum_{nm} h_{nm}^{\alpha} \hat{c}_{an}^{\dagger} \hat{c}_{am} + w_{nm}^{\alpha} \hat{c}_{an}^{\dagger} \hat{c}_{a-1,m} + \text{h.c.} \tag{5.19}$$

where $\hat{c}_{a,n}^{\dagger}$ and $\hat{c}_{a,n}$ are the creation and annihilation operators of an electron at the site indexed by n in the unit cell a of the lead α (see Fig. 5.5). h_{nm}^{α} and w_{nm}^{α} are the matrix elements of respectively the unit cell Hamiltonian $\hat{\tilde{H}}_{\alpha}$ and the inter-cell coupling Hamiltonian W_{α}, in the lead α (see Fig. 5.1). The Hamiltonian $\hat{\tilde{H}}_{\mathcal{C}\alpha}$ connects the lead α to the scattering region $\mathcal{C}$

$$\hat{\tilde{H}}_{\mathcal{C}\alpha} = \sum_{i\in\mathcal{C}, n\in\mathcal{L}_{\alpha}} h_{i,n}^{\mathcal{C}\alpha}\, \hat{c}_i^{\dagger} \hat{c}_{a=0,n} + \text{h.c.} \tag{5.20}$$

Time-dependence in the leads A prerequisite for `tkwant` is the absence of time dependence in the leads. However, as we did in Sec. 5.1.1 in the continuous case, we can account for a uniform time-dependent scalar potential $\phi_{\alpha}(t)$ in each lead $\mathcal{L}_{\alpha}$ by means of a gauge transformation (see Sec. 4.2.4.2 and Sec. 4.3.3.1): given an initial Hamiltonian $\hat{H}$ given by Eq. (5.16), that does not have the extra scalar potential $\phi_{\alpha}(t)$, it can be changed to $\hat{H}'$ to account for it

$$\hat{H}' = \hat{\tilde{H}}_{\mathcal{C}} + \hat{\tilde{H}}_{\alpha} + \sum_{\alpha} \hat{\tilde{H}}'_{\mathcal{C}\alpha} \tag{5.21}$$

according to Eq. (4.85) with the following gauge function $\Lambda_i(t)$

$$\Lambda_i(t) = \begin{cases} -\int_{t_0}^{t} \mathrm{d}u\ \phi_\alpha(u) & \text{for} \quad i \in \mathcal{L}_\alpha \\ 0 & \text{for} \quad i \in \mathcal{C} \end{cases} \tag{5.22}$$

where $\hat{\tilde{H}}'_{\mathcal{C}\alpha}$ is related the original $\hat{\tilde{H}}_{\mathcal{C}\alpha}$ given by Eq. (5.20) through Eq. (4.84)

$$\hat{\tilde{H}}'_{\mathcal{C}\alpha} = \sum_{i\in\mathcal{C}, n\in\mathcal{L}_\alpha} h^{\mathcal{C}\alpha}_{i,n} \exp\Big(\mathrm{i}\frac{q}{\hbar}\Lambda_n(t)\Big)\, \hat{c}^\dagger_i \hat{c}_{a=0,n} + \text{h.c.} \tag{5.23}$$

Equation (5.23) assumes setting the gauge function $\Lambda_i(t)$ to zero in the scattering region $\mathcal{C}$ although it is only a matter of choice and it can be chosen arbitrarily: the particle and (non-hamiltonian) energy currents remain invariant no matter the gauge change.

5.2.2. Expressing lead currents

In Sec. 4.3.4, we exposed how we define lead currents given a generic tight-binding system that contains "leads", as described in Fig. 4.1. The structure of the tight-binding Hamiltonian has been described in more details right above in Sec. 5.2.1 and it includes in particular the spatially periodic lead Hamiltonian $\hat{H}_\alpha$, given in Eq. (5.19) (represented in Fig. 5.5). We define time and spatially resolved lead currents as fluxes at the coupling interface between each unit cell of a given lead (see Fig. 5.6):

$$I^{\mathrm{N}}_{\alpha,a}(t) = \sum_{\substack{n\in\mathcal{L}^a_\alpha \\ m\in\mathcal{L}^{a-1}_\alpha}} I^{\mathrm{N}}_{nm}(t) \qquad I^{\epsilon}_{\alpha,a}(t) = \sum_{\substack{n\in\mathcal{L}^a_\alpha \\ m\in\mathcal{L}^{a-1}_\alpha}} I^{\epsilon}_{nm}(t) \tag{5.24}$$

where $I^{\mathrm{N}}_{\alpha,a}$ and $I^{\epsilon}_{\alpha,a}$ are respectively the particle and energy current flowing from the lead's $\mathcal{L}_\alpha$ unit

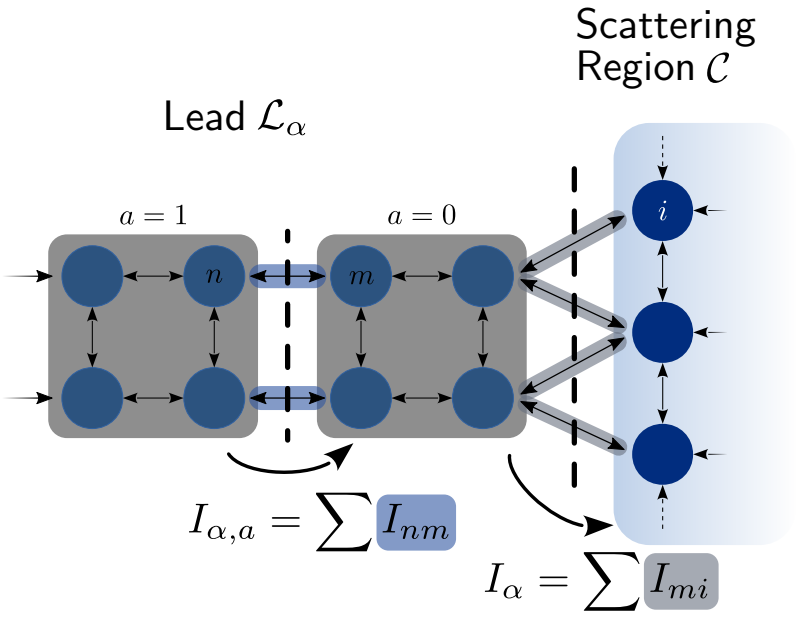

Figure 5.6 – Representation of the spatially resolved lead currents $I_{\alpha,a}$ and $I_\alpha = I_{\alpha,0}$ in a lead $\mathcal{L}_\alpha$, with respect to the scattering region $\mathcal{C}$. $I_{\alpha,a}$ is either the particle current $I^{\mathrm{N}}_{\alpha,a}$ or the energy current I^{ϵ}_{α}, as defined in Eq. (5.24).

cell a to its unit cell $\alpha - 1$, which enable having spatially resolved currents within the lead. $I^{\mathrm{N}}_\alpha = I^{\mathrm{N}}_{\alpha,0}$ and $I^{\epsilon}_\alpha = I^{\epsilon}_{\alpha,0}$ are the currents that flow from the lead $\mathcal{L}_\alpha$ to the scattering region $\mathcal{C}$, as defined in Eq. (4.203). For the lead heat current I^{Q}_α defined in Eq. (4.211), its generalization $I^{\mathrm{Q}}_{\alpha,a}$ to further sections of the lead is simply the following

$$I^{\mathrm{Q}}_{\alpha,a} = I^{\varepsilon}_{\alpha,a} - \mu_\alpha I^{\mathrm{N}}_{\alpha,a} \quad \text{with} \quad a \geq 1 \tag{5.25}$$

Indeed, since the leads we consider are time-independent, once away from the potentially time-dependent coupling $\hat{H}_{\mathcal{C}\alpha}$, *i.e.* for $a \geq 1$, there is no local input power and $S_n^\epsilon = 0$ for sites n that are in unit cells $a \geq 1$ of the lead $\mathcal{L}_\alpha$. This explains why $I^{\mathrm{Q}}_{\alpha,a}$, given in Eq. (4.211), differs from I^{Q}_α in Eq. (5.25)

5.2.3. Computing currents and densities

With the one-body basis of 'scattering states' defined in Sec. 5.1, we can introduce an important result from Ref. [66] that expresses the lesser Green function $G^<_{ij}$ (defined in Eq. (4.145)) using these scattering states, for systems described in Fig. 5.1

$$G^<_{ij}(t,t') = \mathrm{i} \sum_{\lambda=\alpha,n,E} f_\alpha(E) \Psi^\lambda_j(t')^* \Psi^\lambda_i(t) \tag{5.26}$$

Here, $\sum_\lambda$ has been used for compactness as an equivalent to

$$\sum_{\lambda=\alpha,n,E} \equiv \sum_\alpha \sum_n \int \frac{\mathrm{d}E}{2\pi\hbar} \tag{5.27}$$

which fundamentally expresses a sum over all the scattering states λ, where E is a continuous degree of freedom. $\Psi^\lambda_i(t)$ is the scattering state λ computed at site i and time t ; $f_\alpha(E) = f_{T_\alpha,\mu_\alpha}(E)$ is a shorthand notation for the Fermi function

$$f_{T,\mu}(E) = \frac{1}{\exp\left(\frac{E-\mu}{k_{\mathrm{B}}T}\right)+1} \tag{5.28}$$

with k_{B} being the Boltzmann constant. Note that some of the scattering states λ may be evanescent in some leads but they do not contribute to the currents. Eq. (5.26) is the last missing piece to enable computing the densities and the currents exposed in Sec. 4.3.3, it reflects that the incident modes $\psi^{\alpha,\mathrm{in}}_{E,n}$ (appearing in Eq. (5.11)) have been filled according to Fermi statistics in each lead $\mathcal{L}_\alpha$. The core version of `tKwant` (already available at the beginning of this thesis) the calculation of the particle related quantities: the local particle density $\rho_i(t) = -i\hbar G^<_{ii}(t,t)$, given in Eq. (4.158), is directly given by Eq. (5.26)

$$\rho^N_i(t) = \hbar \sum_{\lambda=\alpha,n,E} f_\alpha(E) \left|\Psi^\lambda_i(t)\right|^2 \tag{5.29}$$

while the hopping particle current $I^N_{ij}(t)$ is given by Eq. (4.161)

$$I^N_{ij}(t) = -2 \sum_{\lambda=\alpha,n,E} f_\alpha(E) \,\mathrm{Im}\left[\Psi^\lambda_i(t)^* h_{ij}(t) \Psi^\lambda_j(t)\right]. \tag{5.30}$$

Both quantities are computed with `tkwant` by integrating over the scattering states which were initially occupied at $t < t_0$. In practice, the integration is preferably done in momentum instead of energy, to avoid divergent behavior of the integrand in the vicinity of band openings. This integration over the scattering states is one of the central points of `tkwant`'s implementation as a compromise between precision and computation time needs to be attained: if too many scattering states are taken, the computation time becomes prohibiting; on the other hand, if too few scattering states are considered, the computed results are not accurate. One of the main issues are that the accuracy of the computed operators may decrease at longer simulated times $t > t_0$: the already computed scattering states may no longer form a dense sampling in the relevant integration region or the number of scattering states is simply not enough anymore. When that happens, new stationary scattering states need to be computed at t_0 then evolved to the currently working time t, resulting in a stall in `tkwant`'s parallel algorithm till these new states reach the time t. For more information, see Ref. [101].

5.2.3.1. Generalizing to energy transport

One of the sub-goals of this thesis is to extend tkwant to energy transport. In Sec. 4.3.3.4, explicit expressions for each energy quantity and operator have been derived. The 'generic' local energy density $\rho_i^\epsilon = \left\langle \widehat{\mathcal{E}}_i^\epsilon \right\rangle$ and local energy current $I_{ij}^\epsilon(t)$, written as a function of the lesser Green's function $G_{ij}^<(t,t)$ in Eqs. (4.174) and (4.175) respectively, can be readily expressed in the wave-function formalism with the help of Eq. (5.26)

$$\rho_i^\epsilon(t) = \sum_{\lambda=\alpha,n,E} f_\alpha(E) \sum_j \mathrm{Re}\left[\Psi_i^\lambda(t)^* \epsilon_{ij}(t) \Psi_j^\lambda(t)\right] \tag{5.31}$$

and

$$I_{ij}^\epsilon = \sum_{\lambda=\alpha,n,E} f_\alpha(E) \sum_k \mathrm{Re}\left[\Psi_k^\lambda(t)^* \epsilon_{ki} \epsilon_{ij} \Psi_j^\lambda(t) - \Psi_k^\lambda(t)^* \epsilon_{kj} \epsilon_{ji} \Psi_i^\lambda(t)\right] \tag{5.32}$$

Both quantities can be computed with tkwant, in the same spirit as $\rho_i^\mathrm{N}(t)$ and $I_{ij}^\mathrm{N}(t)$ but with an additional sum over the system sites. The electric power density $S_i^\epsilon(t)$ can be computed as well for each energy operator: it is given by Eq. (4.188) for the 'total energy' ($\epsilon = \varepsilon$)

$$\begin{aligned} S_i^\varepsilon(t) = &\sum_j -\frac{1}{2}\left[\phi_j(t) - \phi_i(t)\right] q I_{ij}^N(t) \\ &+ \sum_{\lambda=\alpha,n,E} f_\alpha(E) \sum_j \mathrm{Re}\left[\Psi_i^\lambda(t)^* \partial_t \varepsilon_{ij}(t) \Psi_j^\lambda(t)\right] \end{aligned} \tag{5.33}$$

by Eq. (4.197) for the kinetic energy ($\epsilon = \kappa$)

$$\begin{aligned} S_i^\kappa(t) = &\sum_j -\frac{1}{2}\left[q\phi_j(t) + V_j - q\phi_i(t) - V_i\right] I_{ij}^N(t) \\ &+ \sum_{\lambda=\alpha,n,E} f_\alpha(E) \sum_j \mathrm{Re}\left[\Psi_i^\lambda(t)^* \partial_t \kappa_{ij}(t) \Psi_j^\lambda(t)\right] \end{aligned} \tag{5.34}$$

and Eq. (4.201) for the Hamiltonian ($\epsilon = h$)

$$S_i^h(t) = \sum_{\lambda=\alpha,n,E} f_\alpha(E) \sum_j \mathrm{Re}\left[\Psi_i^\lambda(t)^* \partial_t h_{ij}(t) \Psi_j^\lambda(t)\right] \tag{5.35}$$

Those local quantities can eventually be summed up over space to deduce for instance the lead energy currents $I_{\alpha,a}^\epsilon(t)$ and the lead heat currents $I_{\alpha,a}^\mathrm{Q}(t)$ as described in Sec. 5.2.2 in Eqs. (5.24) and (5.25) respectively. We notice here that these non-interacting many-body expectation values, for particle and energy currents and densities, are linked to their one-body counterparts, described in Sec. 4.2.4, by simply summing the aforementioned one-body contributions according to Fermi statistics in each lead.

We have implemented an additional Python package, tkwantoperator[3], as an extension to the tkwant package [101] to compute these quantities and have shown that the extra CPU time needed for computing these quantities is small in comparison to the time needed for calculating the scattering states.

5.2.3.2. Static limit – Landauer-Büttiker

Note: this section is adapted from our published article [96]

When $t \leq t_0$ and no external time-dependent electromagnetic field is applied, the system Hamiltonian is time independent *i.e.* $\hat{H}(t \leq t_0) = \hat{H}^{\mathrm{st}}$. Within the static Landauer-Büttiker formalism, the particle, energy, and heat currents in the lead $\mathcal{L}_\alpha$ read (see Sec. 3.3.1 and Refs. [26, 16])

$$I_\alpha^{\mathrm{N,st}} = \sum_{\beta\neq\alpha} \int \frac{\mathrm{d}E}{h} \left[f_{\mu_\alpha,T_\alpha}(E) - f_{\mu_\beta,T_\beta}(E)\right] T_{\alpha\beta}(E) \tag{5.36a}$$

$$I_\alpha^{h,\mathrm{st}} = \sum_{\beta\neq\alpha} \int \frac{\mathrm{d}E}{h} \left[f_{\mu_\alpha,T_\alpha}(E) - f_{\mu_\beta,T_\beta}(E)\right] E\, T_{\alpha\beta}(E) \tag{5.36b}$$

$$I_\alpha^{\mathrm{Q,st}} = I_\alpha^{h,st} - \mu_\alpha I_\alpha^{N,st} \tag{5.36c}$$

where $f_{\mu,T}(E) = [1+\exp\left(\frac{E-\mu}{k_B T}\right)]^{-1}$ is the Fermi function (k_B being the Boltzmann constant), the sum over β is a sum over leads $\mathcal{L}_\beta$ and $T_{\alpha\beta}(E)$

$$T_{\alpha\beta}(E) = \sum_{n_\alpha}\sum_{n_\beta} \left|d^{\alpha\beta}_{n_\alpha n_\beta}(E)\right|^2 \tag{5.37}$$

is the probability for an electron at energy E to be transmitted from the lead $\mathcal{L}_\beta$ into the lead $\mathcal{L}_\alpha$, $d^{\alpha\beta}_{m_\alpha m_\beta}(E)$ being the scattering amplitude from the mode n_β at energy E in $\mathcal{L}_\beta$ to the mode n_α at energy E in $\mathcal{L}_\alpha$, as defined in Eq. (5.8).

In Appendix B.1.2 and B.2.3, we show that the initial $t < t_0$ lead particle current I_α^{N}, energy current I_α^{ε}, as defined in Eqs.(4.203) and (4.208), are equal to the standard static Landauer-Büttiker current formulas

$$I_\alpha^{\mathrm{N}}(t \leq t_0) = I_\alpha^{N,st} \tag{5.38a}$$

$$I_\alpha^{\varepsilon}(t \leq t_0) = I_\alpha^{E,st} \tag{5.38b}$$

even in the 'artificial' time-dependent gauge (see the comment below Eq. (4.85)). The equality for the heat current I_α^{Q} becomes straightforward

$$I_\alpha^{\mathrm{Q}}(t \leq t_0) = I_\alpha^{\mathrm{Q,st}} \tag{5.39}$$

On the other hand, if the external time-dependent electromagnetic field converges to a static limit at long times $t \to \infty$, *i.e* $\hat{h}(t\to\infty) = \hat{h}^{\bar{st}}$, the static currents are also given by the Landauer-Büttiker formulas (5.36). Although this time with $\mu_\alpha \to \mu_\alpha + q\phi_\alpha^{\bar{\mathrm{st}}}$ and $T_{\alpha\beta} \to \bar{T}_{\alpha\beta}$, where $\phi_\alpha^{\bar{\mathrm{st}}}$ is the limit of the uniform scalar potential $\phi_\alpha^{\bar{\mathrm{st}}} = \phi_\alpha(t\to\infty)$ applied in the lead $\mathcal{L}_\alpha$ while $\bar{T}_{\alpha\beta}$ denote the Landauer-Büttiker transmissions with $\hat{h}^{\bar{st}}$, given by Eq. (5.37). In Appendix B.1.2 and B.2.3 we show

$$I_\alpha^{\mathrm{N}}(t\to\infty) = I_\alpha^{N,\bar{st}} \tag{5.40a}$$

$$I_\alpha^{\varepsilon}(t\to\infty) = I_\alpha^{E,\bar{st}} - q\phi_\alpha^{\bar{\mathrm{st}}} I_\alpha^{N,\bar{st}} + S_\alpha^E(t\to\infty) \tag{5.40b}$$

The relation for the heat current, as defined in Eq. (4.211), ensues

$$I_\alpha^{\mathrm{Q}}(t\to\infty) = I_\alpha^{E,\bar{st}} - (\mu_\alpha + eV_\alpha^{\bar{\mathrm{st}}}) I_\alpha^{N,\bar{st}} = I_\alpha^{H,\bar{st}}\,. \tag{5.41}$$

Thus, in the static limit $t\to\infty$, the energy currents $I_\alpha^{\varepsilon}(t\to\infty)$ in the leads $\mathcal{L}_\alpha$ differ from the usual static energy currents $I_\alpha^{E,\bar{st}}$. This is due to the fact that $I_\alpha^{E,\bar{st}}$ is calculated by defining the energy operator $\hat{\mathcal{E}}^{\epsilon}$ as being the Hamiltonian $\hat{H}^{\bar{st}}$ while $I_\alpha^{\varepsilon}(t\to\infty)$ is calculated using $\hat{\mathcal{E}}^{\varepsilon}(t\to\infty) = \hat{H}^{\bar{st}} -$

$q\hat{\Phi}(t \to \infty)$ (see Eq. (4.180)). The discrepancy $I^{\varepsilon}_{\alpha}(t \to \infty) \neq I^{E,\bar{st}}_{\alpha}$ is the price to pay for a gauge-invariant energy current $I^{\varepsilon}_{\alpha}(t)$ that also satisfies $I^{\varepsilon}_{\alpha}(t \leq t_0) = I^{E,st}_{\alpha}$. It stems from the definition of $\hat{\varepsilon}$ in Eq. (4.64) as the sum of the kinetic energy and of the static potential that is present on the system from the remote past. In the peculiar case where the external electromagnetic field converges to a static limit (and then varies again), it might be relevant to redefine the energy operator with respect to this new static configuration and forget the past. More importantly, the heat currents $I^{Q}_{\alpha}(t)$ which are written as a difference of energy currents are not affected by this choice of the reference static potential. We find that $I^{Q}_{\alpha}(t)$ converges to the usual static heat current in the static limit (see Eq. (5.41)).

5.3. tkwantoperator: tkwant extension to energy transport

Note: parts of this section have been adapted from our published paper [96].

To calculate our newly defined energy related quantities, we have implemented a Python package, `tkwantoperator`[3], as an extension to `tkwant`[101] to energy transport. It is open source and freely available at `gitlab.kwant-project.org/kwant/tkwantoperator` along with a complete documentation, available at `kwant-project.org/extensions/tkwantoperator`, that provides install instructions, a tutorial and a technical reference. The code has been published at the same time as our research article [96], with Philipp Reck and Geneviève Fleury.

5.3.1. Overview

A first implementation[4] has been done by Philipp Reck (postdoctoral researcher in the group) at the early stage of this thesis. At that time, the local conservation equation approach (c.f. 4.3.3.4) described within this thesis had not been properly and entirely formalized, the initial work started off the usual approach in the literature by defining only lead currents (see Sec. 4.3.4) through the time derivative of the lead's Hamiltonian $\hat{H}$ or $\hat{\tilde{H}}$ (see comments above Eq. (4.207)) ; while still considering the Hamiltonian as the energy operator. I wrote another implementation from scratch to undertake a more fitting approach where the local, site-wise, energy quantities are implemented first: related code has been written for the energy densities $\rho^{\epsilon}_{i}(t)$, the hopping energy currents $I^{\epsilon}_{ij}(t)$ and the energy sources $S^{\epsilon}_{i}(t)$. It can compute these quantities for the Hamiltonian ($\epsilon = h$), the total energy operator ($\epsilon = \varepsilon$, called `kinetic+` within the code) and a 'custom' energy operator where its onsite terms ϵ_{ii} are provided by the user to offer more flexibility. Since the two extra energy operators, namely the kinetic energy $\hat{\kappa}$ and the total energy $\hat{\varepsilon}$, share their matrix coefficients with the hamiltonian $\hat{h}$ on hoppings (see Eq. (4.173)), the code has been optimized to share code between energy operators, thus the equations (5.31) and (5.32) in the beginning of Sec. 5.2.3.1 using ϵ as a 'generic' energy operator. Lead quantities have then been defined, and implemented, as fluxes through a given section within the lead, as described in Sec. 5.2.2. `tkwant`'s code was also receiving updates by Thomas Kloss (postdoctoral researcher in X. Waintal's group at CEA Grenoble) with whom I was regularly in contact so I could coordinate my development with his changes[5] but also contribute back speed optimizations to `tkwant`[6]

[4] This 'legacy' code is available at [4] in the `energy-args-legacy` branch. This branch also contains a generalization for computing generic operators that could be re-used in future works to implement additional operators.

[5] Development history is available in [4]. A first implementation has been made in the `energy-args` branch, then got updated to accommodate `tkwant`'s changes in the `energy-params` branch

[6] Namely, faster initialization time and reduced memory footprint, available at `gitlab.kwant-project.org/AdelKS/tkwant` in the `faster-init` and `memory-saving-v2` branches, respectively.

In `tkwantoperator`, five Python classes have been implemented to compute energy related quantities : `EnergyDensity`, `EnergySource` and `EnergyCurrentDivergence` can be called for calculating respectively ρ_i^ϵ (given by Eq. (5.31)), S_i^ϵ, and $\sum_j I_{ji}^\epsilon$ over a given list of sites $\{i\}$; `EnergyCurrent` for calculating the current I_{ji}^ϵ (given by Eq. (5.32)) flowing through a given list of hoppings $\{(j,i)\}$; `LeadHeatCurrent` for calculating the heat current $I_{\alpha,a}^{\mathrm{Q}}$ (given by Eq. (5.25)) in a given lead $\mathcal{L}_\alpha$. The energy quantity ϵ can either be the total energy $\hat{\varepsilon}$, the Hamiltonian $\hat{h}$ (more information in Sec. 4.3.3) or a 'custom' operator where the user provides the onsite matrix elements ϵ_{ii}. A code snippet showcasing the use of `tkwantoperator`, along with `Kwant` and `tkwant`, is displayed in Fig. 5.7: that relatively small code snippet is sufficient to quickly recover several results from the literature dealing with the time-dependent Resonant Level Model (see Sec. 5.3.2).

The calculation of the many-body expectations values of the various operators involves an integration over all the scattering states Ψ^λ indexed by the λ parameter (see Eq. (5.27)). The resolution of the Schrödinger-like differential equation (5.13), that gives the evolution in time of the scattering states $\Psi^\lambda(t)$, is the most time-consuming task of `tkwant`'s algorithm (see below). In practice, it is crucial to use as few scattering states as possible to evaluate expectations values. For this purpose, a Gauss-Kronrod adaptive scheme [204] is used when integrating the contribution of each scattering state. It determines the needed number N_{scat} of scattering states for a given precision on the expectation value of a given quantity (controlled by the argument `error_op` when instancing the `tkwant.manybody.State` class, see Fig. 5.7). Moreover, the time evolution of the scattering states can be done in parallel on multi-core computers where each core deals with a subset of the scattering states. Both functionalities, implemented within `tkwant`, are leveraged to compute the expectation values of our energy operators.

```python
#!/usr/bin/env python3

import kwant
import tkwant
import tkwantoperator

import numpy as np
import matplotlib.pyplot as plt

import functools

from mpi4py import MPI
rank = MPI.COMM_WORLD.Get_rank()

γ  = 1.0            # nearest-neighbor hopping term in the leads
γc = 0.2            # nearest-neighbor hopping term between the
                    # central site and the leads
a = 1.0             # lattice constant
Γ = 4 * γc*γc / γ   # Energy scaling unit
V  = 0.5 * Γ        # initial dot energy level
ΔV = 2.5 * Γ        # change in dot energy level at t>0
tmax = 6. / Γ       # Maximum simulation time
dt = 0.01 / Γ       # Simulation time step

def qdot_potential(site, time, V, ΔV):
    if time > 0:
        return V + ΔV
    else:
        return V

lat = kwant.lattice.chain(a, norbs = 1)
builder = kwant.Builder()

# lat(0) is the dot, the rest belongs already formally to the leads
builder[(lat(-1))] = 0
builder[(lat(0))] = qdot_potential
builder[(lat(1))] = 0
builder[lat.neighbors()] = - γc

# Define the right lead
lead = kwant.Builder(kwant.TranslationalSymmetry((-a,)))
lead[lat(0)] = 0
lead[lat.neighbors()] = - γ

# Attach the lead to the central site from the right
# add one site to the central system
added_sites_left = builder.attach_lead(lead, add_cells=1)
# Append lat(-1) to the list
# to calculate the heat current between lat(-1) and lat(0)
added_sites_left.append(lat(-1))


# Attach a reversed copy of the same lead to the left
# add one site to the central system
builder.attach_lead(lead.reversed(), add_cells=1)

# Create finalized system
syst = builder.finalized()

# Define the occupation for each lead
μL =  0.5 * Γ # Chemical potential in the left lead
μR = -0.5 * Γ # Chemical potential in the right lead
TL =  1.0 * Γ # Temperature in the left lead
TR =  0.0 * Γ # Temperature in the right lead

occupation = [None] * len(syst.leads)
occupation[0] = tkwant.manybody.lead_occupation(chemical_potential=μL,
                                                temperature=TL)
occupation[1] = tkwant.manybody.lead_occupation(chemical_potential=μR,
                                                temperature=TR)

# Create list of all time steps
times = np.arange(0, tmax, dt)

# Instance the lead heat current operator
heat_current_left_op = tkwantoperator.LeadHeatCurrent(syst,
                                          chemical_potential=μL,
                                          added_lead_sites=added_sites_left)

# Instance empty list that wil be filled with values
# of the energy current at each time
heat_current_left = []

# Initialize the solver (to solve t-dep SEQ)
# with workaround for our time-discontinuous potential
onebody_wavefunction_type = functools.partial(
            tkwant.onebody.WaveFunction.from_kwant,
            perturbation_type=tkwant.onebody.kernels.PerturbationExtractor)
scattering_state_type = functools.partial(tkwant.onebody.ScatteringStates,
                                wavefunction_type=onebody_wavefunction_type)
solver = tkwant.manybody.State(syst, tmax, occupation,
                               params={'V': V, 'ΔV': ΔV},
                               error_op=heat_current_left_op,
                               scattering_state_type=scattering_state_type)

# Have the system evolve forward in time
# while calculating the operator values at each time step
for time in times:
    # evolve scattering states in time
    solver.evolve(time)
    solver.refine_intervals()

    # Evaluate operators at the specific time then save the values
    heat_current_left.append(solver.evaluate(heat_current_left_op))

if rank == 0:
    # Rescale results
    times = np.array(times) * Γ
    heat_current_left = np.array(heat_current_left) / Γ**2

    # Plot the results
    plt.plot(times, heat_current_left, 'r-', label = "Left")

    plt.xlabel('Time [ħ / Γ]')
    plt.ylabel('Heat current [Γ² / h]')
    plt.legend()
    plt.show()
```

Figure 5.7. – Code example using `tkwantoperator`[3], along with `Kwant` and `tkwant`, to compute the heat current in the left lead of the Resonant Level Model, as described in Fig. 5.9, where the dot level performs a Heaviside jump at $t = 0$, given by Eq. (5.50). This code snippet outputs the green curve of the graph `(b)` in Fig. 5.10. The simulation can be sped up by running the code snippet on N cores with MPI. This code snippet takes 22s to complete when run on 8 cores with an `AMD Ryzen 5950X`™ processor at 4.6GHz.

Hereafter, we analyze the extra CPU time cost due to the evaluation of the energy operators. Given that the computation times for evolving the scattering states (between times t_{n-1} and t_n) and for calculating a many-body expectation value (at a time t_n) grow linearly with the total number N_{scat} of scattering states, we compare these two computation times for only one wave function Ψ. The wave function is initialized (at $t_0 = 0$) with uniformly distributed random complex values on each system site, in the $[-1, 1] \times [-\mathrm{i}, \mathrm{i}]$ complex square. The computation time for the stationary problem, done once for a given system, is not considered here. Investigations of the `tkwant` CPU times are done for a closed (*i.e.* without leads) square system with $N = L^2$ sites lying on a square lattice. The onsite potential h_{ii} is disordered and shifted by a time-dependent perturbation for $t \geq t_1$ as

$$h_{ii}(t > 0) = w_i + \Theta(t - t_1)[\sin(\alpha t)\, \mathrm{e}^{-\beta t^2} + \eta(1 + \tanh(\delta t))] \tag{5.42}$$

where $t_1 = 0.8, \alpha = 8, \beta = 15, \eta = 0.3, \delta = 10$, and w_i are random values that are normally distributed around zero with a standard deviation of 0.025. Hopping terms between sites $i \neq j$ are fixed to $h_{ij} = \gamma(= 1)$ up to the z-th nearest neighbors and are zero beyond. Each site i thus has M_i^z connected neighbors. We note $M_z = \sum_i M_i^z$. In Fig.5.8, we compare the computation times used for making the wave function $\Psi(t)$ evolve by a time step and for calculating its contribution to the various particle and energy operators. Its contribution reads for instance $\sum_j \mathrm{Re}[\Psi_i^* \epsilon_{ij} \Psi_j]$ for the energy density operator evaluated on site i (see Eq. (5.31)). Each point in Fig. 5.8 is obtained by averaging the computation times of 200 measurements performed at times t_n (or over the intervals $[t_n, t_{n+1}]$ for the evolution of $\Psi(t)$) evenly spaced between $t_0 = 0$ and $t_{max} = 2$. CPU times are expressed in seconds and result from simulations run on a single core (Intel Xeon Silver 4114™ CPU at 2.2GHz).

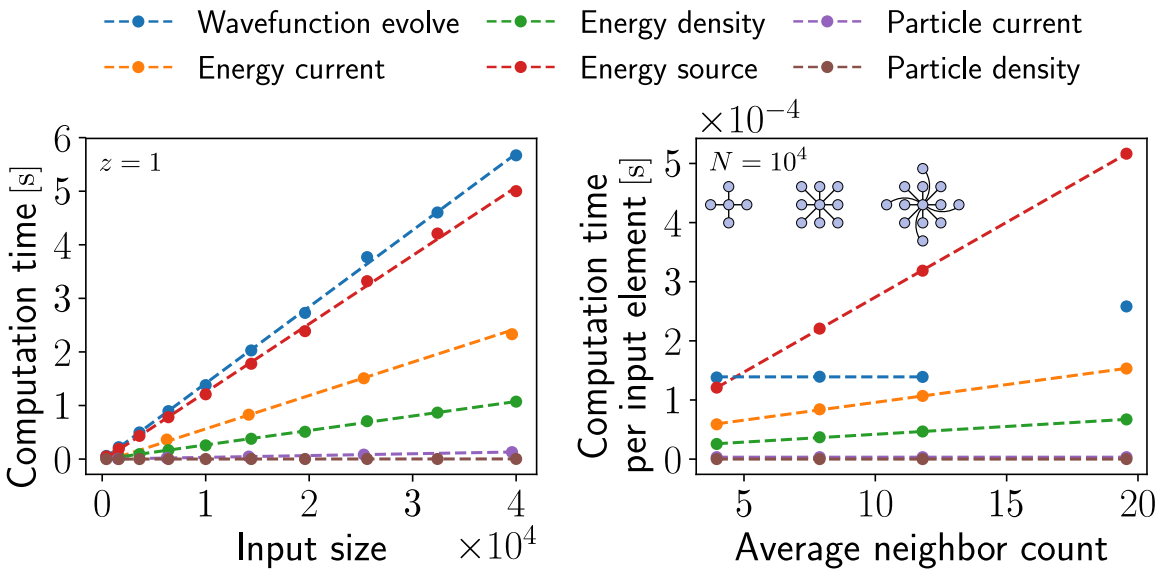

Figure 5.8. – Extracted from our published article [96]: Comparison of the computation times needed for the evolution of a single wave function by a time step and for the evaluation of its contribution to the particle and energy operators. Data (bullets) are shown for the square system made of $N = L^2$ sites defined in the text. Its Hamiltonian includes hopping terms up to the z-th nearest neighbors. Dashed lines are linear fits. (Left) CPU times for evaluating operators and evolving the wave function, as a function of the size of their input site/hopping tuples (varied by increasing L, for fixed $z = 1$). The input size equals $N = L^2$ for the wave function and the density/source operators, while it equals the number of hoppings $M_{[z=1]}/2 = L(L-1)$ for the current operators. (Right) CPU times divided by the input size N or $M_z/2$, as a function of the average number of neighbors per site M_z/N, varied by taking $z = 1, 2, 3$, and 4 at fixed $N = 10^4$ sites.

We check on the left panel of Fig.5.8 *(i)* that the CPU time used for evolving a wave function by a time step grows linearly with the number of sites N (as already reported in Refs.[66, 203]), and *(ii)* that the CPU times corresponding to the computation of the contributions to the various operators grow linearly with the size of the lists of sites or hoppings on which they are calculated. The relative positions of the straight lines in this panel (obtained for $z = 1$) show us that it takes (much) longer to calculate the energy operators than the particle ones (which is obvious in view of the mathematical expression of the operators) but that the global CPU time used by the simulation is nevertheless dominated by the calculation of the wave-function evolution. In the right panel of Fig. 5.8, we investigate how this picture is modified when second ($z = 2$), third ($z = 3$), and fourth ($z = 4$) nearest-neighbors are included. The CPU time used for the wave-function evolution is unaffected (except for $z = 4$ due to unknown – probably memory – reasons), as well as the CPU time corresponding to the particle density

and the CPU time per hopping corresponding to the particle current. On the contrary, the CPU times corresponding to the energy operators are much increased since their expressions involve a sum over neighboring sites.

It is to be noted at that stage that often, in practice, the operators only need to be calculated on a subsystem while the wave function must be calculated over the entire system. For instance, the lead (particle, energy, heat) currents are calculated at the interface between the leads and the scattering region which involves a negligible number of hoppings in comparison to the total number $M_z/2$ of hoppings in the system. For this reason, we conclude that evaluating operators has a low-to-negligible impact on the global `tkwant` computation time for most practical situations. For completeness, let us add that the CPU times needed for evaluating the operators and evolving the scattering states depend at a quantitative level on the simulated systems and on the hardware used. Additional (not shown) data indicate that this should not affect qualitatively the conclusion given above.

Extensive validation has been performed with various arbitrarily chosen systems (square and honeycomb lattice, with and without magnetic field) where gauge invariance, local energy conservation and Landauer-Büttiker static limits have been verified. The validation code and results is available at the `git` repository [4], in the `validation-params` branch, inside the `validation-scripts` folder.

In the following, we perform `tkwant` thermoelectric transport simulations (using our `tkwant-operator` module) in the paradigmatic time-dependent Resonant Level Model (RLM), in order to validate our approach and our numerical implementation. We also report on an exploratory investigation of time-dependent heat transport in a Quantum Point Contact (QPC) driven by voltage pulses. Without discussing deeply the physics involved, we illustrate the strong potential of `tkwant`, with our `tkwantoperator` module, in studying dynamical thermoelectricity and caloritronics.

5.3.2. Resonant Level Model as a benchmark

The (noninteracting) time-dependent RLM has been extensively studied in the literature to simulate dynamical charge transport (see *e.g.* Refs. [92, 149, 158]) and more recently dynamical energy transport [38, 116, 55, 121, 120, 219, 44, 215, 113, 37, 51] in a single level quantum dot or molecular junction connected to two electronic reservoirs. Hereafter we use this model, as described in the following section, as a test bed to benchmark our numerical approach described above. We consider two cases: *(i)* when (only) the dot onsite Hamiltonian coefficient $h_0(t)$ is varied in time as $h_0(t) = V_0 + \Delta V \Theta(t)$, Θ being the Heaviside function, and *(ii)* when the time-dependent step-like perturbation is performed in one of the two leads. We calculate the time-dependent energy and heat currents with our numerical approach and show that we reproduce in the expected limits the results obtained previously in the literature.

5.3.2.1. Model

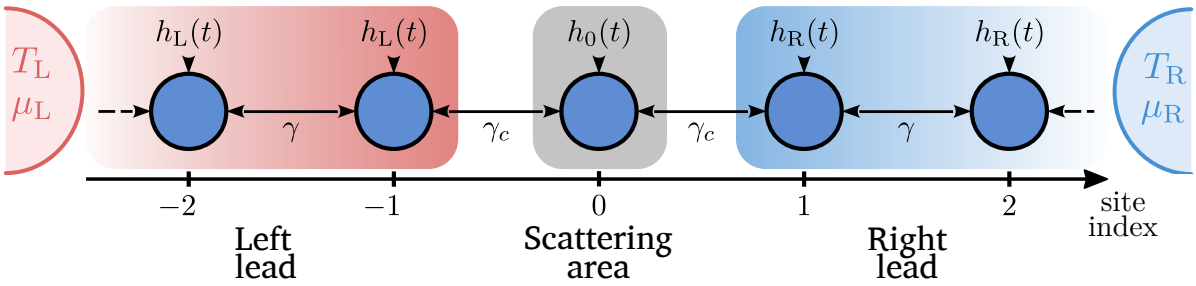

Figure 5.9. – Schematic representation of the Resonant Level Model: a one-dimensional (1D) chain made of a central site 0 connected through a nearest-neighbor hopping term γ_c to two semi-infinite left (L, on sites $i \leq -1$) and right (R, on sites $i \geq 1$) leads with uniform on-site Hamiltonian coefficients $h_{\mathrm{L}}(t)$ and $h_{\mathrm{R}}(t)$, and a nearest-neighbor hopping term γ. Each lead α is attached from the remote past to an electronic reservoir at equilibrium with static electrochemical potential μ_α and temperature T_α defined for $t \leq 0$. They remain at equilibrium for $t > 0$. The chemical potential and the temperature are supposed to remain constant.

We consider a one-dimensional (1D) infinite chain connected through nearest neighbor hoppings so that the Hamiltonian $\hat{H}$ writes

$$\hat{H} = \sum_i h_{ii}(t)\, \hat{c}_i^\dagger \hat{c}_i + h_{i,i+1}(t)\, \hat{c}_i^\dagger \hat{c}_{i+1} + h_{i+1,i}(t)\, \hat{c}_{i+1}^\dagger \hat{c}_i \tag{5.43}$$

The chain is separated into a central site 0 with an onsite Hamiltonian coefficient $h_{00}(t) = h_0(t)$, that acts as a 'dot', connected to it's neighbor sites through constant hoppings $h_{0,-1} = h_{0,1} = \gamma_c$. The sites on each side of the dot make up for the left and right lead. Each lead $\alpha = \mathrm{L}, \mathrm{R}$ has uniform onsite Hamiltonian coefficients terms $\forall i \in \mathcal{L}_\alpha \;\; h_{ii}(t) = h_\alpha(t)$ and uniform stationary hoppings $h_{i,i+1} = h_{i+1,i} = \gamma$. See Fig. 5.9. This enables us to separate spatially the Hamiltonian $\hat{H}$ as a sum of three subsystem Hamiltonians (each of them including half of the coupling Hamiltonian(s) with the neighboring subsystem(s))[7]

$$\hat{H} = \hat{H}_{\mathrm{L}} + \hat{H}_0 + \hat{H}_{\mathrm{R}} \tag{5.44}$$

where $\hat{H}_{\mathrm{L}}$ is the Hamiltonian of the left lead

$$\hat{H}_{\mathrm{L}}(t) = -\frac{1}{2}[\gamma_c \hat{c}_{-1}^\dagger \hat{c}_0 + \gamma_c^* \hat{c}_0^\dagger \hat{c}_{-1}] + \sum_{i \leq -1} h_{\mathrm{L}}(t)\, \hat{c}_i^\dagger \hat{c}_i - \gamma\, \hat{c}_{i-1}^\dagger \hat{c}_i - \gamma\, \hat{c}_i^\dagger \hat{c}_{i-1} \tag{5.45}$$

$\hat{H}_{\mathrm{R}}$ is the Hamiltonian of the right Lead

$$\hat{H}_{\mathrm{R}}(t) = -\frac{1}{2}[\gamma_c \hat{c}_1^\dagger \hat{c}_0 + \gamma_c^* \hat{c}_0^\dagger \hat{c}_1] + \sum_{i \geq 1} h_{\mathrm{R}}(t)\, \hat{c}_i^\dagger \hat{c}_i - \gamma\, \hat{c}_{i+1}^\dagger \hat{c}_i - \gamma\, \hat{c}_i^\dagger \hat{c}_{i+1} \tag{5.46}$$

And $\hat{H}_0$ is the Hamiltonian of the central dot

$$\hat{H}_0 = h_0(t)\, \hat{c}_0^\dagger \hat{c}_0 - \frac{1}{2}\gamma_c[\hat{c}_1^\dagger \hat{c}_0 + \hat{c}_{-1}^\dagger \hat{c}_0] - \frac{1}{2}\gamma_c^*[\hat{c}_0^\dagger \hat{c}_1 + \hat{c}_0^\dagger \hat{c}_{-1}] \tag{5.47}$$

The time dependence is allowed to begin only for $t \geq 0$. Note that within the `tkwant` approach, the time-dependent lead on-site terms terms $h_\alpha(t) = h_\alpha^0 + \phi_\alpha(t)$, with $\alpha = \mathrm{L}, \mathrm{R}$, are accounted for with a

[7] This is not the approach that is usually taken in the literature. See paragraph 'Local energy operator' in Sec. 4.3.3.4.

gauge transformation where the dot-lead hopping term γ_c acquires a dynamical phase (see Sec. 5.2.1) with the following gauge function $\Lambda_i(t)$

$$\begin{cases} \Lambda_0(t) = 0 \\ \Lambda_i(t) = -\int_{t_0}^{t} \mathrm{d}u\ \phi_{\mathrm{L}}(u) \ \text{ for } \ i < 0 \\ \Lambda_i(t) = -\int_{t_0}^{t} \mathrm{d}u\ \phi_{\mathrm{R}}(u) \ \text{ for } \ i > 0 \end{cases} \tag{5.48}$$

The onebody Hamiltonian matrix elements h_{ij}, used by `tkwant` to compute scattering states, is therefore the following

$$h_{ij} = \begin{cases} h_0(t) & \text{if} \quad i = j = 0 \\ -\gamma_c \exp\left(-\mathrm{i}\frac{q}{\hbar}\int_{t_0}^{t} \mathrm{d}u\ \phi_\alpha(u)\right) & \text{if} \quad i,j = 0,1 (\alpha = \mathrm{R}) \text{ or } 0,-1 (\alpha = \mathrm{L}) \\ -\gamma_c \exp\left(\mathrm{i}\frac{q}{\hbar}\int_{t_0}^{t} \mathrm{d}u\ \phi_\alpha(u)\right) & \text{if} \quad i,j = 1,0 (\alpha = \mathrm{R}) \text{ or } -1,0 (\alpha = \mathrm{L}) \\ -\gamma & \text{if} \quad i = j \pm 1 \\ 0 & \text{otherwise} \end{cases} \tag{5.49}$$

Finally, each lead α is attached from the remote past to an electronic reservoir at equilibrium with static electrochemical potential μ_α and temperature T_α defined for $t \leq 0$. They remain at equilibrium for $t > 0$. Only the electric part of the electrochemical potential may become time-dependent (depending on the gauge). The chemical potential and the temperature are supposed to remain constant.

5.3.2.2. Time-dependent dot energy level

Let us first consider the case where $h_\alpha(t) = 0$ for $\alpha = \mathrm{L}, \mathrm{R}$, while a step-like variation is applied to the dot energy level (see Inset of Fig.5.10(a))

$$h_0(t) = V_0 + \Delta V\, \Theta(t) \tag{5.50}$$

This configuration has the advantage of being analytically tractable with the NEGF technique in the so-called wide-band limit approximation. Moreover, since the time-dependent perturbations are restricted to the dot at $i = 0$: the lead's total energy operator $\hat{\mathcal{E}}^{\varepsilon}_{\alpha}$, given Eq. (4.207), coincides with the lead's Hamiltonian $\hat{H}_\alpha$ given in Eqs. (5.45)-(5.46)

Hereafter, we calculate with `tkwant` the time-dependent heat current in *e.g.* the left lead given by Eq. (4.211) (see Eqs. (4.206) and (4.204))

$$I^{\mathrm{Q}}_L(t) \equiv I^{\mathrm{Q},\varepsilon}_L(t) = I^{\mathrm{Q},h}_L(t) = -\partial_t \left\langle \hat{H}_L \right\rangle - \mu_L I^{\mathrm{N}}_L(t) \tag{5.51}$$

and compare it to the one obtained within the NEGF formalism under the wide-band limit approximation (see Appendix C.1). A similar comparison is done for the particle current $I^N_L(t)$ and for an alternative heat current $\tilde{I}^{\mathrm{Q}}_{\mathrm{L}}(t)$ with the Hamiltonian $\hat{\tilde{H}}_{\mathrm{L}}$ that does not include the contribution of the lead-dot tunneling Hamiltonian, as defined Eq. (4.162)

$$\tilde{I}^{\mathrm{Q}}_L(t) = -\partial_t \left\langle \hat{\tilde{H}}_{\mathrm{L}} \right\rangle - \mu_{\mathrm{L}} I^N_{\mathrm{L}}(t) \tag{5.52}$$

Such a definition of the heat current was considered in *e.g.* Refs.[38, 219]. Note that in the wave-function formalism, we have for the present model

$$\partial_t \left\langle \hat{\tilde{H}}_L \right\rangle = 2 \sum_{\lambda=\alpha,E,n} f_\alpha(E)\ \gamma\gamma_c\, \mathrm{Im}[\Psi^\lambda_{-2}(t)^*\, \Psi^\lambda_0(t)] \tag{5.53}$$

This allows us to compute $\tilde{I}_L^{\mathrm{Q}}(t)$ with `tkwant`. $I_L^N(t) = I_{-1,0}^N(t)$ and $I_L^{\mathrm{Q}}(t) = I_{-1,0}^{\varepsilon}(t) - S_{-1}^{\varepsilon}(t) - \mu_L I_{-1,0}^N(t)$ are calculated using Eqs. (5.30), (5.32) and (5.33).

Wideband approximation To make the comparison between the `tkwant` and the NEGF results in the wide-band limit, we follow the scaling approach used in Ref.[37]. We vary simultaneously the hopping terms in the chain by replacing the γ and γ_c parameters with

$$\bar{\gamma} = \lambda\gamma \tag{5.54a}$$

$$\bar{\gamma}_c = \sqrt{\lambda}\gamma_c \tag{5.54b}$$

where λ is a scaling factor. When λ is increased, the width $[-2\bar{\gamma}, 2\bar{\gamma}]$ of the (single) conduction band in the leads widens while the ratio Γ

$$\Gamma = 2\frac{\bar{\gamma}_c^2}{\bar{\gamma}} \tag{5.55}$$

remains fixed. In the limit $\lambda\gamma/\Gamma \to \infty$ (keeping γ finite), the retarded self-energy $\Sigma^R(E)$ of the (identical) time-independent left and right leads,

$$\text{For } \frac{|E|}{2|\bar{\gamma}|} \leq 1 \quad \Sigma^R(E) = \frac{\bar{\gamma}_c^2}{\bar{\gamma}}\left[\frac{E}{2\bar{\gamma}} - i\sqrt{1-\left(\frac{E}{2\bar{\gamma}}\right)^2}\right] \underset{\lambda\to\infty}{\longrightarrow} -\mathrm{i}\frac{\Gamma}{2} \tag{5.56}$$

converges to $-i\frac{\Gamma}{4}$ *i.e.* the real part of $\Sigma^R(E)$ becomes zero and its imaginary part becomes energy independent. This corresponds to the wide-band limit hypothesis.

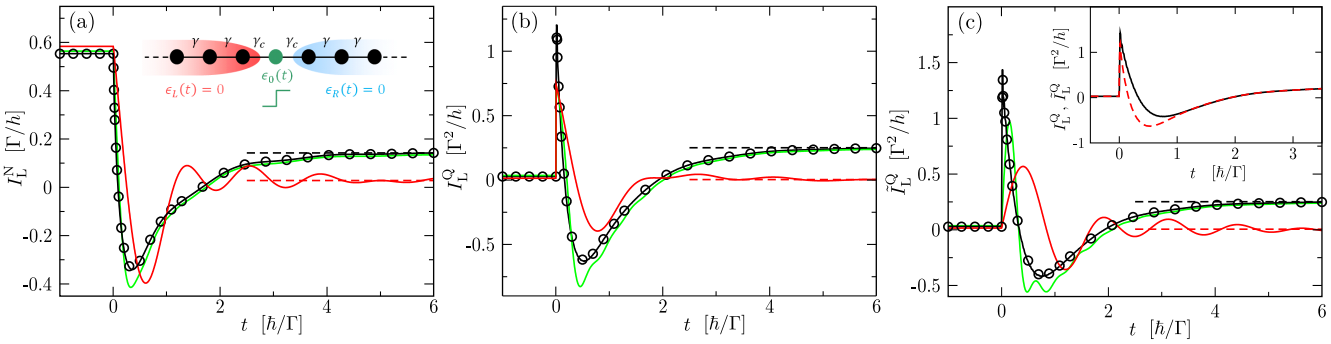

Figure 5.10. – Adapted from our published article [96]: Left particle current I_L^N (a) and left heat currents I_L^{Q} (b) and $\tilde{I}_L^{\mathrm{Q}}$ (c) as a function of time t, for the 1D RLM defined by Eq. (5.44), when the dot energy level is modified as $h_0(t) = V_0 + \Delta V\Theta(t)$ (inset of panel (a)). Units of the x and y axes are indicated in brackets. In all panels, data are computed numerically with `tkwant+tkwantoperator` for different values of $\lambda\gamma/\Gamma$ (1 (red lines), 6.25 (green lines), and 100 (black lines). The horizontal dashed lines plotted for $\lambda\gamma/\Gamma = 1$ (in red) and 100 (in black) correspond to the static limits at large times $\Gamma t/\hbar \gg 1$ given by the Landauer-Büttiker formulas (see Sec. 5.2.3.2). When $\lambda\gamma/\Gamma \gg 1$, the `tkwant` results converge to the NEGF results (circles) derived in the wide-band limit (Appendix C.1). Inset of panel (c): comparison of $I_L^Q(t)$ (red dashed line, given by Eq. (5.51)) and $\tilde{I}_L^Q(t)$ (black line, given by Eq. (5.52)) in the wide-band limit. In all panels, $V_0 = 0.5\Gamma$, $\Delta V = 2.5\Gamma$, $h_L(t) = h_R(t) = 0$, $T_L = \Gamma/k_B$, $T_R = 0$, $\mu_L = 0.5\Gamma$, and $\mu_R = -0.5\Gamma$. The NEGF curves are independent of Γ. The `tkwant` curves are functions of $\lambda\gamma/\Gamma$ and not of the three parameters λ, γ, and Γ taken separately.

In Fig.5.10, we plot $I_L^{\mathrm{N}}(t)$, $I_L^{\mathrm{Q}}(t)$, and $\tilde{I}_L^{\mathrm{Q}}(t)$ calculated with `tkwant` for various values of the ratio $\lambda\gamma/\Gamma = \lambda(\gamma/\gamma_c)^2/4$, keeping the other parameters fixed.[8] We check that in the wide-band limit

[8] The set of fixed parameters corresponds to the one used in Ref.[38].

$\lambda\gamma/\Gamma \gg 1$, the `tkwant` results (black lines in Fig.5.10) converge to the NEGF results[9] given in Appendix C.1 (circles in Fig.5.10). Moreover, in the inset of Fig.5.10(c), we compare $I_{\mathrm{L}}^{\mathrm{Q}}(t)$ and $\tilde{I}_{\mathrm{L}}^{\mathrm{Q}}(t)$ and show that both quantities coincide in the long time limit $\Gamma t/\hbar \to \infty$. This is illustrated in the wide-band limit $\lambda\gamma/\Gamma \to \infty$ but holds for any value of $\lambda\gamma/\Gamma$ (though the smaller $\lambda\gamma/\Gamma$, the slower the convergence). Such an equality between $I_{\mathrm{L}}^{\mathrm{Q}}(t)$ and $\tilde{I}_{\mathrm{L}}^{\mathrm{Q}}(t)$ at long times is expected as the energy may be stored only temporarily in the lead-dot coupling region. Finally, we also check that in the long time limit $\Gamma t/\hbar \to \infty$, the `tkwant` particle and heat currents converge to the static particle and heat currents $I_L^{\mathrm{N/Q,st}}$ given by the Landauer-Büttiker formulas (horizontal dashed lines in Fig.5.10), as expected from Eqs.(5.40a) and (5.41). Further development in the linear response regime enables us to recover the alleged efficiency boost reported by Zhou et al. [219], see Sec. 6.1.

5.3.2.3. Time-dependent voltage bias

We continue studying the RLM but now consider that a voltage bias is suddenly applied in the left lead, *i.e.* $h_{\mathrm{L}}(t) = V_L\Theta(t)$, while $h_0(t) = V_0$ and $h_{\mathrm{R}}(t) = 0$ (see Inset of Fig. 5.11). This model under the same configuration has been studied in Ref. [37] with an exact (partition-free) numerical approach [49] which is formally equivalent to the `tkwant` approach. The authors calculated the time-dependent particle currents $I_\alpha^{\mathrm{N}}(t)$ in the leads $\alpha = L$ and R, as well as the Hamiltonian based time-dependent heat currents $I_\alpha^{\mathrm{Q},h}$, *without* performing a gauge change to move the lead time-dependence to the lead-dot coupling Hamiltonian as we described in Eq. (5.49). Using Eq. (4.182), we connect the Hamiltonian based heat current $I_\alpha^{\mathrm{Q},h}(t)$, given by Eq. (4.210) and the gauge invariant 'total energy' based heat currents $I_\alpha^{\mathrm{Q}}(t) \equiv I_\alpha^{\mathrm{Q},\varepsilon}(t)$, given by Eq. (4.211)

$$I_{\mathrm{L}}^{\mathrm{Q}}(t) \equiv I_{\mathrm{L}}^{\mathrm{Q},\varepsilon}(t) = I_{\mathrm{L}}^{\mathrm{Q},h}(t) - V_L\left[I_L^N(t) + N_L(t)\delta(t)\right] \tag{5.57a}$$

$$I_{\mathrm{R}}^{\mathrm{Q}}(t) \equiv I_{\mathrm{R}}^{\mathrm{Q},\varepsilon}(t) = I_{\mathrm{R}}^{\mathrm{Q},h}(t) \tag{5.57b}$$

where $N_L = \sum_{i\in\mathcal{L}_\alpha}\rho_i$ is the particle number in the left lead, and ρ_i is the particle density given in Eq. (5.29). Using $I_\alpha^{\mathrm{N}}(t)$ and $I_\alpha^{\mathrm{Q},h}$ data [10] issued from Ref. [37], we compute the corresponding 'total energy' heat currents $I_\alpha^{\mathrm{Q},\varepsilon}$ data for $t > 0$ according to Eq. (5.57) and compare them to the ones calculated with `tkwant+twantoperator`. We find a perfect agreement (see Fig. 5.11). This provides an additional validity check of our approach and highlights the difference between the gauge invariant heat current $I_\alpha^{\mathrm{Q},\varepsilon}$ and the gauge dependent heat current $I_\alpha^{\mathrm{Q},h}$ when a time-dependent voltage is applied in the lead α.

5.3.3. Going further: Quantum Point Contact

To illustrate the potential of our `tkwant` based numerical approach, we simulate hereafter dynamical (electronic) heat transport in a QPC attached to two reservoirs held at different temperatures. We focus on the possibility of extracting heat from the cold reservoir by Peltier effect and ask whether or not Peltier cooling may be enhanced by applying time-resolved voltage pulses to one of the two electrodes attached to the QPC (instead of a constant voltage bias across the system).

[9] Note that we did not investigate in details the behavior of the NEGF data at small $t \gtrsim 0$. While the `tkwant` heat currents are observed to be continuous at $t = 0$, the NEGF heat currents calculated by integrating numerically Eq. (C.3) (with standard routines) turn out be numerically unstable in the vicinity of $t \gtrsim 0$. This is probably an (irrelevant) artifact of the wide-band limit approximation that leads in some cases to pathological singularities, as pointed out in Ref.[37].

[10] Data are courtesy of Florian Eich. They are the same data as the ones shown in Fig. 8 and in the lower panel of Fig. 9 of Ref.[37] (for $\lambda = 1$).

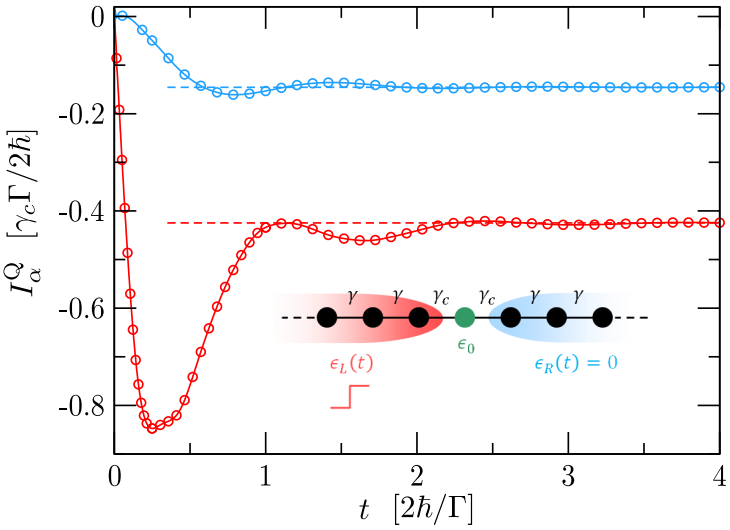

Figure 5.11 – Adapted from our published article [96]: Left heat current $I^{\mathrm{Q}}_{\mathrm{L}}$ (in red) and right heat current $I^{\mathrm{Q}}_{\mathrm{R}} \equiv I^{\mathrm{Q},\varepsilon}_{\mathrm{R}}$ (in blue) as a function of time t, as defined in Eq. (4.211) for the 1D RLM defined by Eq. (5.44), when a voltage step $h_L(t) = V_L\Theta(t)$ is applied in the left lead (sketch in inset). Units are indicated in brackets. The data issued from Ref.[37] (solid lines) and those calculated with `tkwant+tkwant-operator` (circles) are superimposed. The horizontal dashed lines show the static limits $I^{\mathrm{Q},st}_{\mathrm{L/R}}$ at large times given by the Landauer-Büttiker formula (see Sec.5.2.3.2). Parameters are fixed to $V_0 = 0.2\gamma_c$, $V_L = 2\gamma_c$, $h_R(t) = 0$, $\gamma = 5\gamma_c$ $T_L = T_R = 0.01\gamma_c/k_B$, and $\mu_L = \mu_R = 0$.

We consider a nanoribbon of length L and width W connected through semi-infinite leads to two left (L) and right (R) electronic reservoirs maintained at temperatures $T_L \lesssim T_R$ and electrochemical potentials $\mu_L \gtrsim \mu_R$ (see Fig.5.12 (a)). The system is discretized on a square lattice (with lattice spacing $a = 1$). For times $t \leq 0$, no time-dependent perturbation is applied and the system Hamiltonian $\hat{H}(t \leq 0) = \hat{H}^0$ reads

$$\hat{H}^0 = \sum_i (4\gamma + U_i)\hat{c}_i^\dagger \hat{c}_i - \gamma \sum_{\langle i,j \rangle} \hat{c}_i^\dagger \hat{c}_j \tag{5.58}$$

where γ is the nearest-neighbor hopping term and U_i is the QPC confining potential modeled by

$$U_i = \begin{cases} \left(\frac{y_i}{l_y}\right)^2 \left[1 - 3\left(\frac{2x_i}{l_x}\right)^2 + 2\left|\frac{2x_i}{l_x}\right|^3\right]^2 \text{ if } |x_i| < \frac{l_x}{2} \\ 0 \text{ if } |x_i| \geq \frac{l_x}{2}\,. \end{cases} \tag{5.59}$$

Here l_x and l_y are two parameters controlling the QPC shape and the site of coordinates $(x_i, y_i) = (0, 0)$ is taken at the center of the ribbon. The staircase-like transmission function $T(E)$ of the QPC in the static configuration (computed with `Kwant`) is plotted in Fig.5.12(b) for a given set of parameters used hereafter. We also fix $T_L \lesssim T_R$ and choose μ_R so as $T(E = \mu_R) \approx 0.6$ (guided by the fact that thermoelectric effects are to be sought near transmission steps in the adiabatic regime). The value of $\mu_L \gtrsim \mu_R$ is determined by the condition $I^{\mathrm{Q}}_{\mathrm{L}}(t \leq 0) = 0$.

From time $t = 0$, we apply in the left lead a Gaussian voltage pulse $V_L(t) = V_p \exp\left[-4\ln 2 \frac{(t-3\tau_p)^2}{\tau_p^2}\right]$ of width τ_p, amplitude V_p and center $3\tau_p$. Therefore, the system Hamiltonian becomes $\hat{H}(t > 0) = \hat{H}^0 + \sum_{i\in L} V_L(t)\hat{c}_i^\dagger \hat{c}_i$.

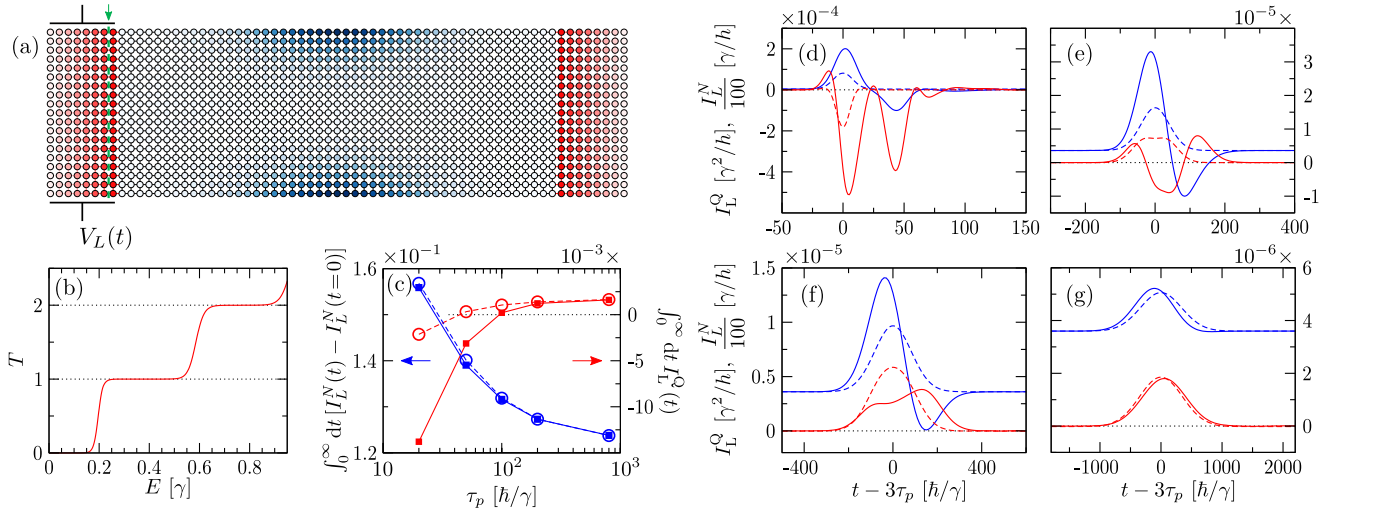

Figure 5.12. – (a) QPC discretized model. The site color in the central region encodes the value of the onsite potential U_i given by Eq. (5.59) (from 0 (white) to larger values (shades of blue)). A few layers of the left and right semi-infinite leads are shown in red. A voltage pulse $V_L(t)$ is applied in the left lead. Currents are evaluated at the (green dashed) interface indicated by the green arrow. (b) Transmission function $T(E)$ of the QPC defined by $\hat{H}^0$ (see Eq. (5.58)). (c) $\int_0^\infty \mathrm{d}t\,[I_L^N(t) - I_L^N(t=0)]$ (in blue, in units of $1/2\pi$) and $\int_0^\infty \mathrm{d}t\, I_\mathrm{L}^\mathrm{Q}(t)$ (in red, in units of $\gamma/2\pi$) as a function of the pulse width τ_p at fixed $n_p = 0.2$. Squares with full lines are `tkwant` results, circles with dashed lines are Landauer-Büttiker adiabatic results. Lines are guides to the eye. (d) to (g) Left particle currents I_L^N (in blue, in units of $100\gamma/h$) and left heat currents I_L^Q (in red, in units of γ^2/h) as a function of time t (in units of $\hbar/\gamma$), for different widths of the voltage pulse ($\tau_p = 20\,\hbar/\gamma$ (d), $100\,\hbar/\gamma$ (e), $200\,\hbar/\gamma$ (f), and $800\,\hbar/\gamma$ (g)) at fixed $n_p = 0.2$. Full lines are `tkwant` results, dashed lines are Landauer-Büttiker adiabatic results. In all panels, parameters are fixed to $W = 18$, $L = 48$, $l_x = 50$, $l_y = 5$, $\mu_L = 0.20607\gamma$, $\mu_R = 0.2\gamma$, $T_L = 0.018\gamma/k_B$, and $T_R = 0.02\gamma/k_B$.

Using `tkwant` along with our `tkwantoperator` extension [3] we compute the time-resolved particle (I_L^N) and heat (I_L^Q) currents in the left lead. Data are shown in panels (d) to (f) of Fig. 5.12 for different pulse parameters (τ_p, V_p) with fixed $n_p \equiv (e/h)\int V_L(t)\mathrm{d}t = (eV_p\tau_p)/(4\hbar\sqrt{\pi \ln 2})$ (total number of electrons injected by the voltage pulse in the left lead). To avoid spurious effects that appear when the edges of the system's conduction band are probed [66, 64] we consider relatively long pulses with $\hbar/\tau_p, V_p \lesssim \mu_L, \mu_R$ (but short enough to investigate the non-adiabatic regime). The `tkwant` currents are compared to the adiabatic currents $I_L^{N,\bar{st}}(V_L(t))$ and $I_L^{\mathrm{Q},\bar{st}}(V_L(t))$ given by the Landauer-Büttiker formulas (see Sec. 5.2.3.2). The latter depend parametrically on time through $V_L(t)$. They are computed for static systems by using `Kwant` and a numerical integrator over the energy. For small τ_p (short pulses, see panel (d)), the particle current $I_L^N(t)$ shows a first positive peak centered around $3\tau_p$ corresponding to the injected pulse and some time later, a second negative peak corresponding to the reflected part of the pulse. Both peaks are well resolved in this (non-adiabatic) regime. They contribute to two main negative peaks in the heat current $I_\mathrm{L}^\mathrm{Q}(t)$. For large τ_p (long pulses, see panel (g)), the `tkwant` currents converge to the adiabatic currents characterized by a single peak centered at $3\tau_p$. We note that the particle current converges more slowly to its adiabatic limit than the heat current. The crossover between the two regimes is shown in panels (e) and (f). Obviously, the time-resolved `tkwant` currents in the non-adiabatic regime depend on the position of the interface in the left lead at which they are calculated (green dashed line in Fig. 5.12 (a)). However, the currents integrated over time are independent of this position. In panel (c) of Fig. 5.12, we plot $\int \mathrm{d}t\,[I_L^N(t) - I_L^N(t=0)]$ and $\int \mathrm{d}t\, I_\mathrm{L}^\mathrm{Q}(t)$ as a function of τ_p ($I_\mathrm{L}^\mathrm{Q}(t=0) = 0$ by construction). We find that heat can be extracted from the cold reservoir ($\int \mathrm{d}t\, I_\mathrm{L}^\mathrm{Q}(t) > 0$) in the limit of long pulses only and for all τ_p, we have $\int \mathrm{d}t\, I_\mathrm{L}^\mathrm{Q}(t) \leq \int \mathrm{d}t\, I_\mathrm{L}^{\mathrm{Q},\bar{st}}(V_\mathrm{L}(t))$. Thus, the application of short voltage pulses involving a non-adiabatic response of

the quantum system turns out to be detrimental to Peltier cooling (at least for the set of parameters considered here). The present preliminary investigation shows the feasibility of further studies. Indeed, the set of `tkwant` curves shown in panels (d) to (g) of Fig. 5.12 required a few hours (d) to a few days (g) of computation time on a single CPU core.

The naive approach in trying to 'boost' the Peltier cooling of a QPC by simply adding the time-dependent ingredient is inconclusive and simply highlights that the effects at play are more complex to grasp. Therefore, in the next chapter, we go back to the Resonant Level Model where analytical expressions can be derived, in an effort to understand better the effects at play.

6. Application: Time-dependent Resonant Level Model

The Resonant Level Model (RLM) is a paradigmatic toy model extensively studied in the field of time-dependent theoretical thermodynamics and energy transport [52, 51, 38, 116, 219, 55, 54, 215, 142, 44, 121, 120, 24, 113, 37, 40, 143, 157, 79]. With a recent successful experiment in the stationary regime [93] (see Fig. 3.4 in Chapter 3), thermoelectric properties of this model have been predicted to be improved [38, 219] in the transient regime while under a time-dependent regime. *Zhou et al.* [219] predicted a 'boost' of the transient thermoelectric generation during the transient regime by a factor of 4 with respect to the stationary regime, when the dot's onsite Hamiltonian undergoes a step-like or square-like variations, and for a given set of parameters. In the following, we recover their results using `tKwant+tkwantoperator` and identify several shortcomings of their study. Then, we use an analytical wavefunction approach in the wide-band limit approximation to better understand energy transport in the time-dependent RLM. The results we obtain with our further work (and confirmed by our numerics) point instead towards a negative impact of time-dependence in the thermoelectric conversion, both in the transient regime and at long times.

In this chapter, we study the resonant level model described in Sec. 5.3.2.1 where we consider a time-dependent drive of the dot's onsite potential $h_0(t)$

$$h_0(t) = V_0 + V(t) \quad \text{with} \quad V(t < t_0) = 0 \tag{6.1}$$

while the leads are stationary with a zero onsite Hamiltonian. (see Fig. 6.1 for a sketch).

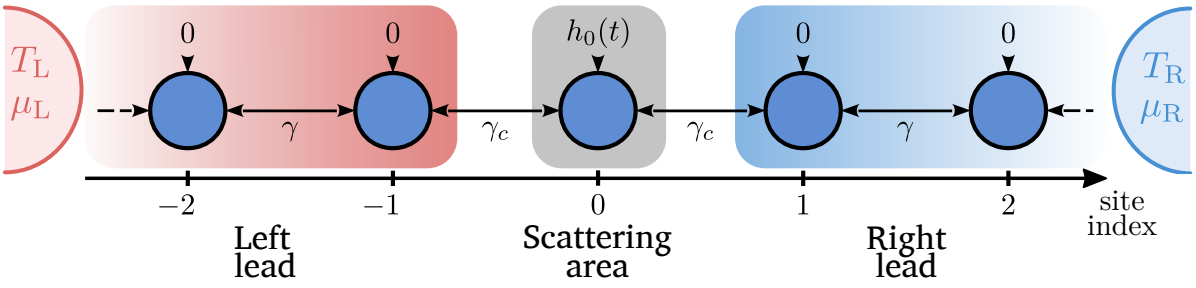

Figure 6.1. – Schematic representation of the Resonant Level Model: a one-dimensional (1D) chain made of a central site 0 connected through a nearest-neighbor hopping term γ_c to two semi-infinite left (L, on sites $i \leq -1$) and right (R, on sites $i \geq 1$) leads with uniform zero on-site Hamiltonian and a nearest-neighbor hopping term γ. Each lead α is attached from the remote past to an electronic reservoir at equilibrium, with an electrochemical potential μ_α and temperature T_α that are supposed remain constant.

The matrix elements h_{ij} of the Hamiltonian $\hat{H}$, given in Eq. (5.49), simplify to the following

$$h_{ij} = \begin{cases} V_0 + V(t) & \text{if} \quad i = j = 0 \\ -\gamma_c & \text{if} \quad i, j = 0, \pm 1 \text{ or } \pm 1, 0 \\ -\gamma & \text{if} \quad i = j \pm 1 \\ 0 & \text{otherwise} \end{cases} \tag{6.2}$$

We introduce the following notations, that we will adopt all along this Chapter

$$I_{\mathrm{L}} = I_{\text{-1,0}}(t) \qquad I_{\mathrm{L},x} = I_{-|x|,-|x|+1}(t) \;\text{ with }\; x \leq -2 \tag{6.3a}$$

$$I_{\mathrm{R}} = I_{1,0}(t) \qquad I_{\mathrm{R},x} = I_{|x|,|x|-1}(t) \;\text{ with }\; x \geq 2 \tag{6.3b}$$

where I_{ij} is a current flowing from i to j.

6.1. Linear-response regime

In this section, we attempt an extension of the Onsager matrix $\mathbf{L}$, whose definition in the stationary state is given in Sec. 3.3.2, to the time dependent regime of a driven dot and stationary leads (described by the Hamiltonian Eq. (6.2)). Such a generalization has been performed by *Zhou et al.* in their paper entitled "Boosting thermoelectric efficiency using time-dependent control" [219] where a heaviside drive of the dot is reported to improve the electric generator efficiency of the model, under a given set of parameters. However, we show that a time-dependent Onsager matrix that connects currents to ΔT and $\Delta\mu$ biases is not uniquely defined in the time-dependent regime. This matrix is therefore not physically interpretable though it can be blindly used to compute linear response quantities. We also highlight a few shortcomings in the definitions used by Ref. [219].

6.1.1. (Ill-defined) Onsager matrix

The heat I^{Q}_α and electric I^{N}_α currents, where $\alpha = \mathrm{L,R}$, vary in time due to the time dependent control but are also affected by the statically set bath temperatures (T_R, T_L) and electrochemical potentials (μ_R, μ_L). Thus, as functions, we have $I^{\mathrm{N}}_\alpha(t, \mu_R, \mu_L, T_R, T_L)$ and $I^{\mathrm{Q}}_\alpha(t, \mu_R, \mu_L, T_R, T_L)$, $\alpha = L, R$. Mathematically, these currents can be linearized for small $\Delta\mu = \mu_R - \mu_L$ and $\Delta T = T_R - T_L$, but that needs a change of variable from (μ_R, μ_L, T_R, T_L) to $(\mu, \Delta\mu, T, \Delta T)$. One can think of the following map, with $\chi \in [0, 1]$:

$$\begin{aligned} \mu &= \chi\mu_L + (1-\chi)\mu_R \\ T &= \chi T_L + (1-\chi)T_R \\ \Delta\mu &= \mu_R - \mu_L \\ \Delta T &= T_R - T_L \end{aligned} \tag{6.4}$$

We will note the currents after the change of variable with a bar, $\bar{I}$. Their first order linearization writes

$$\bar{I}^{\mathrm{N}}_\alpha(t,\mu,\Delta\mu,T,\Delta T) = \underbrace{\bar{I}^{\mathrm{N}}_\alpha(t,\mu,0,T,0)}_{\bar{I}^{\mathrm{N}}_{\alpha,0}} + \underbrace{\partial_{\Delta\mu}\bar{I}^{\mathrm{N}}_\alpha(t,\mu,0,T,0)}_{L^\alpha_{11}/q}\Delta\mu + \underbrace{\partial_{\Delta T}\bar{I}^{\mathrm{N}}_\alpha(t,\mu,0,T,0)}_{L^\alpha_{12}/T}\Delta T \tag{6.5a}$$

$$\bar{I}^{\mathrm{Q}}_\alpha(t,\mu,\Delta\mu,T,\Delta T) = \underbrace{\bar{I}^{\mathrm{Q}}_\alpha(t,\mu,0,T,0)}_{\bar{I}^{\mathrm{Q}}_{\alpha,0}} + \underbrace{\partial_{\Delta\mu}\bar{I}^{\mathrm{Q}}_\alpha(t,\mu,0,T,0)}_{L^\alpha_{21}/q}\Delta\mu + \underbrace{\partial_{\Delta T}\bar{I}^{\mathrm{Q}}_\alpha(t,\mu,0,T,0)}_{L^\alpha_{22}/T}\Delta T \tag{6.5b}$$

which can be rewritten in a Matrix equation, the connecting matrix $\mathbf{L}_\alpha(t)$ being called the Onsager Matrix:

$$\begin{bmatrix} \bar{I}^{\mathrm{N}}_\alpha(t) \\ \bar{I}^{\mathrm{Q}}_\alpha(t) \end{bmatrix} = \begin{bmatrix} \bar{I}^{\mathrm{N}}_{\alpha,0}(t) \\ \bar{I}^{\mathrm{Q}}_{\alpha,0}(t) \end{bmatrix} + \underbrace{\begin{bmatrix} L^\alpha_{11}(t) & L^\alpha_{12}(t) \\ L^\alpha_{21}(t) & L^\alpha_{22}(t) \end{bmatrix}}_{\mathbf{L}_\alpha(t)} \begin{bmatrix} \frac{\Delta\mu}{q} \\ \frac{\Delta T}{T} \end{bmatrix} \tag{6.6}$$

Note that in the time-*independent* regime, zero bias gives zero current, which implies that $\bar{I}^{\mathrm{N}}_{\alpha}(\mu, 0, T, 0) = 0$ and $\bar{I}^{\mathrm{Q}}_{\alpha}(\mu, 0, T, 0) = 0$, which simplifies the equation above. In the time-dependent case however, these un-biased currents are non-zero in general as the time-dependence can still cause energy and particle (displacement) currents in each lead.

Since we only have access to the original currents $I^{\mathrm{Q/N}}$ that depend on $(t, \mu_R, \mu_L, T_R, T_L)$, we need to write the relationship between the partial derivatives of $\bar{I}$ and I to compute the Onsager matrix:

$$\partial_{\Delta\mu}\bar{I}(\mu, \Delta\mu = 0) = \chi\, \partial_{\mu_R} I(\mu_R{=}\mu, \mu_L{=}\mu) - (1-\chi)\, \partial_{\mu_L} I(\mu_R{=}\mu, \mu_L{=}\mu) \tag{6.7}$$

This shows a dependence on χ, which can be arbitrarily chosen and hence calls into question the physical meaning of the Onsager matrix $\mathbf{L}_{\alpha}$. To answer this, let's consider, without loss in generality, the conservation equations of particles (given Eq. (4.157)) and energy (given Eq. (4.172)) with a dependence only with respect to (t, μ_L, μ_R):

$$-I^{\mathrm{N}}_{\mathrm{L}}(t, \mu_L, \mu_R) - I^{\mathrm{N}}_{\mathrm{R}}(t, \mu_L, \mu_R) + \partial_t \rho_0(t, \mu_L, \mu_R) = 0 \tag{6.8}$$

$$-I^{\epsilon}_{\mathrm{L}}(t, \mu_L, \mu_R) - I^{\epsilon}_{\mathrm{R}}(t, \mu_L, \mu_R) + \partial_t \rho^{\epsilon}_0(t, \mu_L, \mu_R) = S^{\epsilon}_0(t, \mu_L, \mu_R) \tag{6.9}$$

where ρ_0 is the particle density in the dot and ρ^{ϵ}_0 the energy density.

Stationary regime: In the static case, $\rho_0(t, \mu_L, \mu_R)$ is stationary and has a zero time-derivative:

$$I^{\mathrm{N}}_{\mathrm{L}}(\mu_L, \mu_R) + I^{\mathrm{N}}_{\mathrm{R}}(\mu_L, \mu_R) = 0 \quad \Longrightarrow \quad \partial_{\mu_R} I^{\mathrm{N}}_{L}(\mu_L, \mu_R) + \partial_{\mu_R} I^{\mathrm{N}}_{R}(\mu_L, \mu_R) = 0 \tag{6.10}$$

Given the central symmetry of the RLM with respect to the dot, we can swap L and R indices

$$\partial_{\mu_R} I^{\mathrm{N}}_{R}(\mu_L, \mu_R) = \partial_{\mu_L} I^{\mathrm{N}}_{L}(\mu_R, \mu_L) \tag{6.11}$$

and finally end up with

$$\partial_{\mu_R} I^{\mathrm{N}}_{L}(\mu_L, \mu_R) = -\partial_{\mu_L} I^{\mathrm{N}}_{L}(\mu_R, \mu_L) \tag{6.12}$$

On the other hand, using Eqs. (4.211) and (6.9) in the stationary regime (with a zero time-derivative of the dot density and zero source) leads to the following relationship between the heat currents I^{Q}_{α}

$$I^{\mathrm{Q}}_{L} + I^{\mathrm{Q}}_{R} = -\underbrace{\Delta\mu I^{\mathrm{N}}_{L}}_{\substack{\text{second order} \\ \text{in } \Delta\mu, \Delta T}} \approx 0 \tag{6.13}$$

This allows us to follow an analog derivation to the particle current and obtain

$$\partial_{\mu_R} I^{\mathrm{Q}}_{L}(\mu_L, \mu_R) = -\partial_{\mu_L} I^{\mathrm{Q}}_{L}(\mu_R, \mu_L) \tag{6.14}$$

This renders Eq. (6.7) χ independent for both the particle and heat currents: the Onsager matrix is unique in the stationary regime and is side independent (the left and right Onsager matrices differ only with a global sign, *i.e* $\mathbf{L}_{\mathrm{L}} = -\mathbf{L}_{\mathrm{R}}$).

Time dependent regime: The time derivatives of the dot densities are no longer zero and the derivation done in the stationary case no longer applies as we have

$$-I^{\mathrm{N}}_{L} - I^{\mathrm{N}}_{R} = -\partial_t \rho_0 \tag{6.15a}$$

$$-I^{\mathrm{Q}}_{L} - I^{\mathrm{Q}}_{R} = S^{\epsilon}_{\mathrm{tot}} - \partial_t \rho^{\epsilon}_0 + \cdots + \underset{\text{in } \Delta\mu, \Delta T}{\text{second order}} \tag{6.15b}$$

This implies that Eqs. (6.12) and (6.14) are no longer verified

$$\partial_{\mu_R} I_L^{\mathrm{N}}(t,\mu_L,\mu_R) \neq -\partial_{\mu_L} I_L^{\mathrm{N}}(t,\mu_R,\mu_L) \tag{6.16a}$$

$$\partial_{\mu_R} I_L^{\mathrm{Q}}(t,\mu_L,\mu_R) \neq -\partial_{\mu_L} I_L^{\mathrm{Q}}(t,\mu_R,\mu_L) \tag{6.16b}$$

and thus the Onsager coefficients L^{α}_{ab}, defined in Eqs. (6.5) are χ dependent (through Eq. (6.7)). This makes the time-resolved Onsager matrix ill-defined as it is no longer unique.

Another interesting equation can be obtained by writing equation (6.8) in the linear response regime. For that, we first need to linearize $\partial_t\bar{\rho}_0$ with respect to ΔT and $\Delta\mu$, like we did for $\bar{I}^{\mathrm{N}}_{\alpha}$ in equation (6.5a):

$$\partial_t\bar{\rho}_0(t,\mu,\Delta\mu,T,\Delta T) = \partial_t\bar{\rho}_0^0 + C_{11}\frac{\Delta\mu}{q} + C_{12}\frac{\Delta T}{T} \tag{6.17}$$

where $C_{11,12}(t,\mu,T) = q[\partial_{\Delta\mu,\Delta T}\partial_t\bar{\rho}_0]^{\Delta T=0}_{\Delta\mu=0}$ and the partial derivatives of $\partial_t\bar{\rho}_0$ and $\partial_t\rho_0$ are connected through an analog of equation (6.7). We can now write (6.8) in the (time-dependent) linear response regime

$$\partial_t\bar{\rho}_0^0 - I^{\mathrm{N}}_{\mathrm{L},0} - I^{\mathrm{N}}_{\mathrm{R},0} + \left(L^L_{11} + L^R_{11} + C_{11}\right)\frac{\Delta\mu}{q} + \left(L^L_{12} + L^R_{12} + C_{12}\right)\frac{\Delta T}{T} = 0 \tag{6.18}$$

This equation can be further simplified by noticing that $\partial_t\bar{\rho}_0^0 - I^{\mathrm{N}}_{\mathrm{L},0} - I^{\mathrm{N}}_{\mathrm{R},0} = 0$ since it is equation (6.8) with the following parameter values $(\mu, \Delta\mu = 0, T, \Delta T = 0)$. We finally obtain:

$$\forall_{\Delta\mu,\Delta T\text{ 'small enough'}}\quad \left(L^L_{11} + L^R_{11} + C_{11}\right)\frac{\Delta\mu}{q} + \left(L^L_{12} + L^R_{12} + C_{12}\right)\frac{\Delta T}{T} = 0 \tag{6.19}$$

from where we conclude the following, as $\Delta\mu$ and ΔT are independent

$$L^L_{11}(t) + L^R_{11}(t) + C_{11}(t) = 0 \quad \text{and} \quad L^L_{12}(t) + L^R_{12}(t) + C_{12}(t) = 0 \tag{6.20}$$

Equation (6.20), along with its heat current analog (involving L_{21} and L_{22}), yields the interesting result that the Onsager coefficients for the right and left side of the dot are in general not equal in the time dependent regime (while they are equal up to a minus sign, $L^L_{ij} = -L^R_{ij}$, in the stationary regime since $C_{11} = C_{12} = 0$ in that case).

To conclude, a time-resolved Onsager matrix, that links the currents to the temperature and electrochemical potential biases, is ill-defined since it depends on an arbitrary choice of the reference chemical potential μ and temperature T. No physical interpretation can be made based on this time-resolved matrix alone. On the other hand, time-averaged Onsager coefficients have been considered in Refs. [118, 153] in the periodic regime: it solves only partially the arbitrariness issue in the definition of the Onsager Matrix as *e.g.* the time-averaged total source term, over a period τ, $\frac{1}{\tau}\int_0^\tau \mathrm{d}t S_0^\epsilon$ from Eq. (6.15b) is still non-zero and will make the time-average of Eq. (6.7), for the heat current, still χ dependent. Ref. [118] performs a study to the first order over the adiabatic regime, on a two-terminal system, where the considerations over the change of variable (given Eq. (6.4)) are omitted ; whereas Ref. [153] uses a single reservoir and therefore the issue we highlight does not apply.

Numerical illustration

We compute the partial derivatives of the left particle current $I^{\mathrm{N}}_{\mathrm{L}}(t,\mu_R,\mu_L,T_R,T_L)$ and the left heat current $I^{\mathrm{Q}}_{\mathrm{L}}(t,\mu_R,\mu_L,T_R,T_L)$, with respect to (μ_R,μ_L,T_R,T_L), using the finite differences method:

$$\begin{cases} \partial\mu_\alpha I^{\mathrm{Q/N}}(\_,\mu_\alpha,\_) \approx \dfrac{1}{\varepsilon}\left[I^{\mathrm{Q/N}}(\_,\mu_\alpha+\dfrac{\varepsilon}{2},\_) - I^{\mathrm{Q/N}}(\_,\mu_\alpha-\dfrac{\varepsilon}{2},\_)\right] \\ \partial T_\alpha I^{\mathrm{Q/N}}(\_,T_\alpha,\_) \approx \dfrac{1}{\varepsilon}\left[I^{\mathrm{Q/N}}(\_,T_\alpha+\dfrac{\varepsilon}{2},\_) - I^{\mathrm{Q/N}}(\_,T_\alpha-\dfrac{\varepsilon}{2},\_)\right] \end{cases} \tag{6.21}$$

where ε is a small displacement: from a numerical point of view, it has to be small enough for Eq. (6.21) to be correct but not too small to guarantee that the limit of `tkwant`'s precision is not reached. In practice, we find that $\varepsilon = 0.01$ is a good choice. In Fig. 6.2 we plot the resulting partial derivatives of the electric and heat currents, for a given set of parameters, where we highlight numerically Eqs. (6.16)

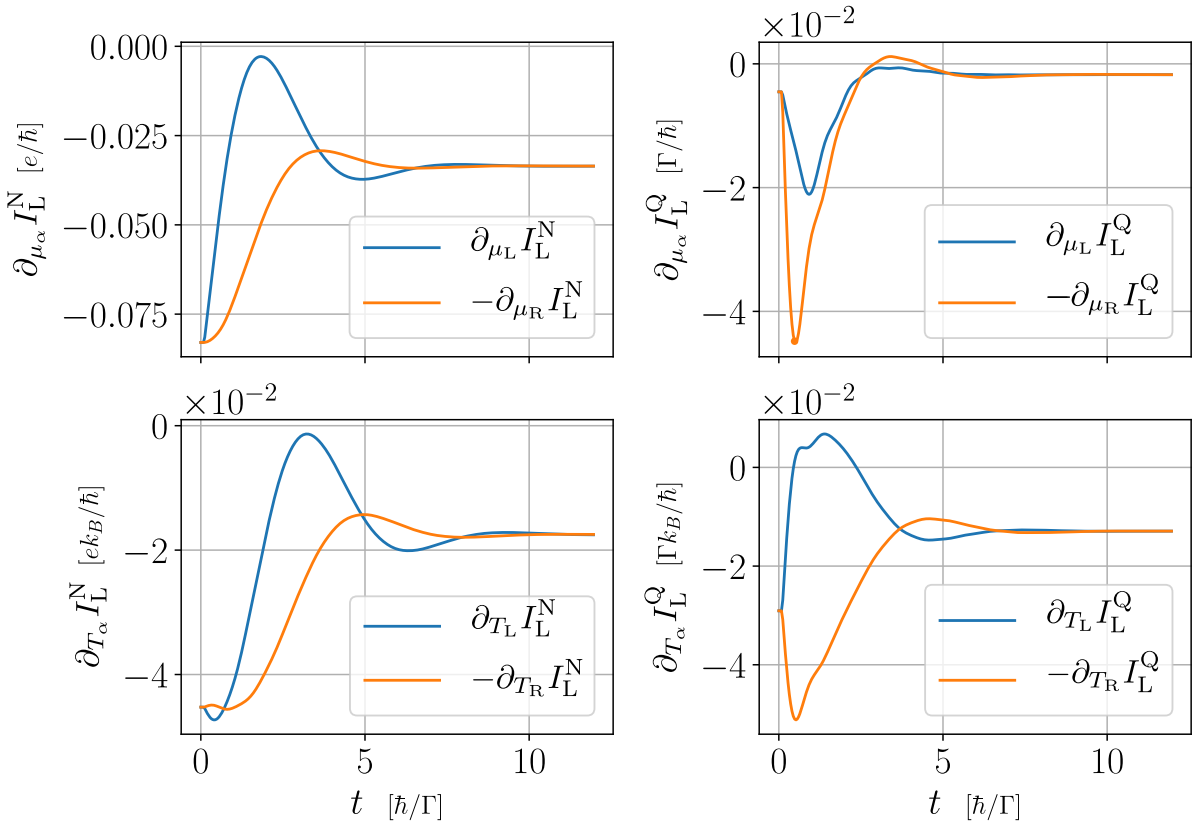

Figure 6.2. – Partial derivatives of the left electric ($I_L^N(t)$) and heat ($I_L^Q(t)$) currents, computed with the finite difference method (see Eq. (6.21)). In each panel, the blue and orange curves are clearly not superimposed : this illustrates Eqs. (6.16), which makes Eq. (6.7) χ dependent, and hence the Onsager matrix is in general ill-defined as it is not unique. Simulation values (in units of Γ): $t_0 = 0.1, \gamma = 4, \gamma_c = 1, \mu_L = \mu_R = 0, T_L = 0.1, T_R = 0.1, \lambda = 1, V_0 = 0.5, \Delta V = 0.5$, lead $= L, \varepsilon = 0.01$.

6.1.2. An alleged boost of the thermoelectric efficiency

In this subsection, we perform a numerical computation of the currents' partial derivatives using the parameters used by Zhou et al. in their article "Boosting thermoelectric efficiency using time-dependent control" [219]. We recover their results, including their reported 'boost' in the efficiency, then perform a critical analysis of their approach and highlight a few shortcomings. In our next section, we will raise some fundamental issues that make difficult defining a heat engine efficiency.

In Ref. [219], the onsite Hamiltonian matrix element $h_0(t)$ undergoes a step-like variation

$$h_0(t) = V_0 + \Delta V \Theta(t - t_0) \tag{6.22}$$

and transport quantities are computed within the wide-band limit, that we achieve in our numerical simulations with a parameter λ that we use the scale, according to Eq. (5.54), the hoppings γ and γ_c in the Hamiltonian $\hat{H}$ given Eq. (6.2). Note that we follow here Ref. [219] and calculate the left heat

current on the hopping $(-1, 0)$ *without* taking into account the coupling Hamiltonian H_{0L} (between the dot and the left lead) and using the Hamiltonian as energy operator[1] (see Sec. 4.3.4.2 for a more thorough discussion)

$$\tilde{I}_{\mathrm{L}}^{\mathrm{Q}} = -\partial_t \left\langle \hat{\tilde{H}}_L \right\rangle - \mu_L I_{\mathrm{L}}^{\mathrm{N}} \tag{6.23}$$

Ref. [219] presented some results involving the time-dependent Onsager matrix: the evolution of the ratio $L_{21}(t)/L_{12}(t)$ and its determinant $\det(L)$, within the wide band limit. The purpose was to point out that the thermodynamic constraints on the Onsager matrix in the stationary case (see Eq. (3.8)) are relaxed in the time-dependent regime. Our results are plotted in Figs. 6.3: we find a very good agreement with Ref. [219] for $\chi = 0.5$ while the results significantly differ for $\chi = 0$ (data not shown).

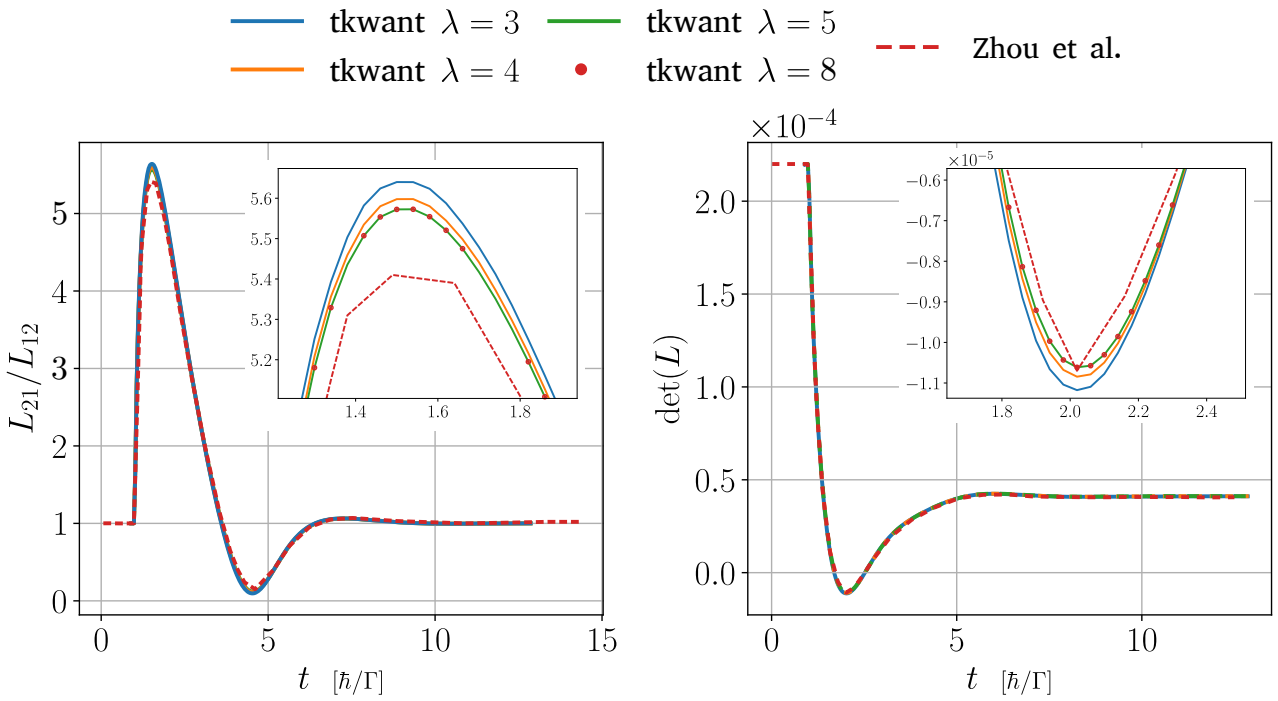

Figure 6.3. – Comparison between Zhou et al. [219] and `tkwant` in the calculated L_{21}/L_{12} and $\det(L)$. `tkwant` simulations have been performed for various λ values and with $\chi = 0.5$. In the limit of large λ (corresponding to the wide-band limit), `tkwant`'s data is in good agreement with the reported results (Data from [219] have been manually extracted using WebPlotDigitizer [161]. Uncertainty: $L_{21}/L_{12} \to \pm 0.1$, $\det(L) \to 10^{-6}$). Values (in units of Γ): $t_0 = 0.1, \gamma = 1, \gamma_c = 0.2, \chi = 0.5, \mu_L = \mu_R = 0, T_L = T_R = 0.1, V_0 = 0.5, \Delta V = 0.5$, lead $= L, \varepsilon = 0.01$.

To express the efficiency, Ref. [219] considered an additional virtual load resistance R_L put in series with the system so that a voltage bias $\Delta\mu(t)$ is created when the current goes through it. To take into account the time-dependent electrochemical potential bias $\Delta\mu(t)$ in our numerical approach, we use the computed partial derivatives of the currents: if the load resistance is small enough, the voltage bias it creates is small enough so the partial derivatives can be used to compute the new linear-response currents, taking into account the back-action of the load resistance. To match with Ref. [219] results, we make the hypothesis (although implicit in the reference) that the bias created by the load resistance is symmetric with respect to the left and right baths, *i.e.* $\chi = 0.5$, as other values do not match (data not shown).

[1] Computing quantities without the coupling term is not offered by `tkwantoperator` as we consider it to be non-physical. We used here our first implementation of the extension `tkwant` to energy, which offered it, it is available at [4] in the `energy-args-legacy` branch

To obtain the linear-response currents using the time-dependent Onsager matrix (for $\chi = 0.5$), one can first write that the voltage bias is due to the current going through the load resistance

$$\Delta\mu(t)/q = -R_L I^{\mathrm{N,load}}(t) \tag{6.24}$$

This relation can then be used along with the Onsager matrix, defined in Eq. (6.6), to give an expression for the electric current under the influence of the load resistance R_L

$$I^{\mathrm{N,load}} = I_0^{\mathrm{N}} - L_{11} R_L I^{\mathrm{N,load}} + L_{12}\frac{\Delta T}{T} \implies I^{\mathrm{N,load}} = \frac{I_0^{\mathrm{N}} + L_{12}\frac{\Delta T}{T}}{1 + L_{11}R_L} \tag{6.25}$$

The expression of $I^{\mathrm{N,load}}$ can then be used in the heat current's part of the Onsager matrix, so we obtain

$$I^{\mathrm{Q,load}} = I_0^{\mathrm{Q}} + \frac{L_{21}}{L_{11}} I^{\mathrm{N,load}} + \det(L)\frac{1}{L_{11}}\frac{\Delta T}{T} + [\det(L) - \frac{L_{22}}{L_{12}}]I_0^{\mathrm{N}} \tag{6.26}$$

Eqs. (6.25) and (6.26) are used by Ref. [219], with $I_0^{\mathrm{N}}(t) = 0$ and $I_0^{\mathrm{Q}}(t) = 0$ (even though they are not zero), to write the following thermoelectric efficiency of the heat-to-work conversion of the model

$$\eta = \frac{R_L \left(I^{\mathrm{N,load}}\right)^2}{I^{\mathrm{Q,load}} - \frac{1}{2}R_M \left(I^{\mathrm{N,load}}\right)^2} \quad \text{with} \quad R_M = 1/L_{11} \tag{6.27}$$

We implement this expression of the efficiency and compute it with our time-dependent Onsager matrix coefficients and finally recover the results of Ref. [219], see Fig 6.4.

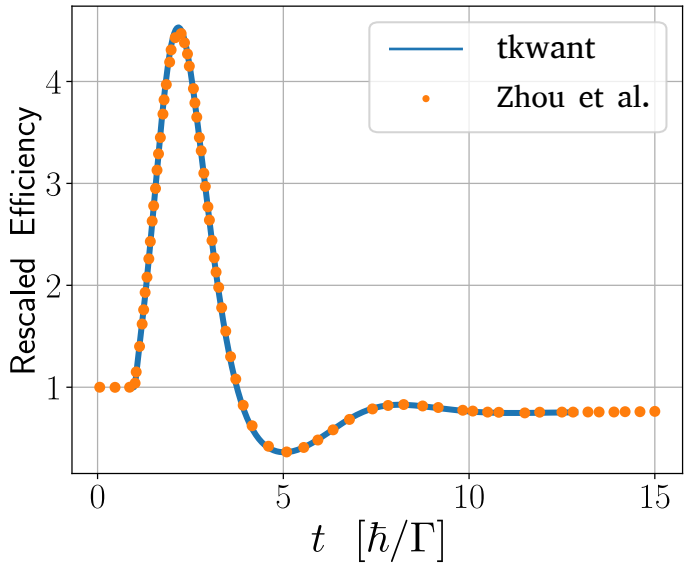

Figure 6.4 – Plot of Ref. [219] rescaled efficiency $\eta(t)/\eta(t=0)$, given by Eq. (6.27). We find a perfect match between their results and our `tkwant+tkwantoperator` simulation in the wideband limit (with $\lambda = 5$). The real efficiency starts at 2.2×10^{-4}. Values used (in units of Γ): $t_0 = 0.1, \gamma = 1, \gamma_c = 0.2, \chi = 0.5, \mu_L = \mu_R = 0, T_L = T_R = 0.1, V_0 = 0.5, \Delta V = 0.5$, lead $= L, \varepsilon = 0.01$

Critical analysis

The means used to recover Ref. [219]'s results puts into question the alleged 'boost' of the RLM as a generator, when the central dot is driven by step-like variation. Indeed, we raised a few issues while deriving the results:

- The calculated heat current $I_{\mathrm{L}}^{\mathrm{Q}}$, defined in Eq. (6.23) does not contain the coupling with the dot.

- When computing the efficiency η, given in Eq. (6.27), the electric current $I_0^{\mathrm{N}}(t) = \bar{I}^{\mathrm{N}}(t, \mu, 0, T, 0)$ and heat current $I_0^{\mathrm{Q}}(t) = \bar{I}^{\mathrm{Q}}(t, \mu, 0, T, 0)$ have been taken equal to zero, in this non-interacting model, while they are actually not.

- In the expression of the efficiency η, given in Eq. (6.27), an additional term in the denominator, $-\frac{1}{2}R_M \left(I^{\mathrm{N,load}}\right)^2$, is considered to take into account that 'half of the joule heating goes back the thermostats' and we do not understand this assertion as the calculated heat current is expected to be a 'net' heat current where no other contribution is to be added.

- The input power from the time-dependent drive has not been considered in the efficiency.

- The used definition for the efficiency involves time-resolved quantities in the ratio between work energy and spent energy. However, it is more physical to use finite-time integrated currents, $\int_0^\tau I^{\mathrm{Q}}(t)$ and $\int_0^\tau I^{\mathrm{N,load}}(t)^2$, in the ratio.

- The efficiency 'boost', shown Fig 6.4, actually jumps from a rather low initial efficiency (2.2×10^{-4}) and can be largely improved upon within the stationary regime, in the same model.

- The time resolved Onsager matrix in the time-dependent regime is ill-defined and its coefficients cannot a priori be physically interpreted or used in entropy considerations as more than a mathematical first order development (given in Eqs. (6.5)) with a specific (χ dependent) change of variables (given in Eqs. (6.4)).

Given these open questions, we have decided to further continue the study of the RLM model in the next section, for an arbitrary time-dependent variation of dot energy level. In Sec. 6.3.3, we attempt a definition of a heat engine efficiency and enumerate a number of fundamental challenges to consider and overcome. We will study in further detail the case of square-like variation of the dot level where some numerical curves will be presented.

6.2. Analytical treatment of the generic RLM in the wideband limit: deriving the scattering amplitudes

In this section and the next one, we consider the 1D Resonant Level Model sketched in Fig. 6.1 and keep arbitrary the time-dependent onsite potential $h_0(t) = V_0 + V(t)$ in the dot. We adopt a generic analytic approach and start in this section by calculating the scattering amplitudes d and r (defined in Eq. (5.11)). First, we give the self-consistent formulas d and r verify by solving the Schrödinger equation. Then, under the wideband limit, we give a simpler approach to compute them. In this section, we take $\hbar = 1$.

6.2.1. Scattering states

To express the scattering amplitudes r and d with Eq. (5.11), the scattering states need to be expressed then injected in the Schrödinger equation (4.79). The lead's eigenstates $\|_x^{\pm,E}$ have no transverse mode due the unidimensional nature of the model. They are plane waves that are solution to the discrete Schrödinger equation (spatially restricted to the leads)

$$\|_x^{\pm,E} = \frac{1}{\sqrt{|v_E|}} e^{\mathrm{i}k_E^{\pm}x - \mathrm{i}Et} \quad \text{where} \quad k_E^+ \geq 0 \text{ and } k_E^- = -k_E^+ \tag{6.28}$$

$k_E^\pm$ verify the following dispersion relation

$$E = -2\gamma\cos(k_E^\pm) \tag{6.29}$$

from which we can express the velocity $v_E = \partial_k E$

$$v_E^\pm = 2\gamma\sin(k_E^\pm) = \pm\sqrt{4\gamma^2 - E^2} \tag{6.30}$$

The previous two relations gives a useful additional relation

$$\mathrm{e}^{\mathrm{i}k_E^\pm} = -\frac{E}{2\gamma} + \mathrm{i}\frac{v_E^\pm}{2\gamma} = -\frac{E}{2\gamma} \pm \mathrm{i}\sqrt{1 - \left(\frac{E}{2\gamma}\right)^2} \tag{6.31}$$

that links $\mathrm{e}^{\mathrm{i}k_E^-}$ to the retarded lead self-energy $\Sigma^R(E)$ given in Eq. (5.56)

$$\Sigma^R(E) = \frac{\Gamma}{4}\mathrm{e}^{\mathrm{i}k_E^-} \tag{6.32}$$

The generic expression for a scattering state, given in Eq. (5.11), simplifies to the following for our 1D Resonant Level Model

$$\Psi_x^{\mathrm{L},E} = \begin{cases} \|_x^{+,E} + \displaystyle\int \frac{\mathrm{d}E'}{2\pi}\, \|_x^{-,E'}\, r(E',E) & \text{if } x < 0 \\ \displaystyle\int \frac{\mathrm{d}E'}{2\pi}\, \|_x^{+,E'}\, d(E',E) & \text{if } x > 0 \end{cases} \tag{6.33a}$$

$$\Psi_x^{\mathrm{R},E} = \begin{cases} \|_x^{-,E} + \displaystyle\int \frac{\mathrm{d}E'}{2\pi}\, \|_x^{-,E'}\, r'(E',E) & \text{if } x > 0 \\ \displaystyle\int \frac{\mathrm{d}E'}{2\pi}\, \|_x^{+,E'}\, d'(E',E) & \text{if } x < 0 \end{cases} \tag{6.33b}$$

where $r(E',E)$ and $d(E',E)$ are respectively the left-to-left reflection and left-to-right transmission amplitudes, from energy E to energy E', whereas the primed amplitudes are about the other side. Given that the system is symmetric with respect to the central site 0, the left and right amplitudes are equal

$$d'(E',E) = d(E',E) \qquad\qquad r'(E',E) = r(E',E) \tag{6.34}$$

Wide band approximation

To be able to explicitly express the scattering states without the energy integrals over E', we use the so called wide band approximation. Described in Sec. 5.3.2.2, it amounts to consider that the RLM's characteristic energies are negligible when compared to γ (characteristic band width in the leads) so that the transmission amplitude $d(E',E)$ and reflection amplitude $d(E',E)$ are relatively sharply peaked around E, as function of E'. Integrals of the type $\int \frac{\mathrm{d}E'}{2\pi}\, \|_x^{\pm,E'}\, l(E',E)$, where $l = r, d$ can therefore be approximated. One can think of two levels of approximation:

Approximation 1 [WBL1] γ is relatively big enough so we can consider the approximation done in Eq. (5.56) as valid. Using Eq. (6.32) and Eq. (6.30), it translates to the following

$$v_E^\pm = \pm 2\gamma \qquad\qquad \mathrm{e}^{\mathrm{i}k_E^\pm} = \pm i \tag{6.35}$$

The integrals $\int \frac{\mathrm{d}E'}{2\pi}\, \|_x^{\pm,E'}\, l(E',E)$ simplify to the following

$$\int \frac{\mathrm{d}E'}{2\pi}\, \|_x^{\pm,E'}\, l(E',E) \approx \pm\mathrm{i}\frac{1}{2\gamma}\int \frac{\mathrm{d}E'}{2\pi}\mathrm{e}^{-\mathrm{i}E't}\, l(E',E) = \pm\mathrm{i}\frac{1}{2\gamma}\,\tilde{l}(t,E) \tag{6.36}$$

where $\tilde{l}(t,E)$ is the inverse Fourier transform of $l(E',E)$ along E'.

Approximation 2 [WBL2] A more accurate approximation is to linearize the term $k^{\pm}_{E'}$ around E

$$k^{\pm}_{E'} = k^{\pm}_{E} + \frac{E' - E}{v^{\pm}_{E}} \tag{6.37}$$

While still considering the approximation $\left|v^{\pm}_{E'}\right| = |v_E| = 2\gamma$, we can write the following:

$$\begin{aligned}\int \frac{\mathrm{d}E'}{2\pi}\, \|^{\pm,E'}_{x}\, l(E',E) &\approx \frac{1}{2\gamma}\int \frac{\mathrm{d}E'}{2\pi} \mathrm{e}^{\mathrm{i}\left[k^{\pm}_{E}+\frac{E'-E}{\pm 2\gamma}\right]x} \mathrm{e}^{-\mathrm{i}E't}\, l(E',E) \\ &= \frac{1}{2\gamma}\mathrm{e}^{\mathrm{i}\left[k^{\pm}_{E}-\frac{E}{\pm 2\gamma}\right]x}\int \frac{\mathrm{d}E'}{2\pi}\mathrm{e}^{-\mathrm{i}E'\left(t-\frac{x}{\pm 2\gamma}\right)}\, l(E',E)\end{aligned}$$

Which finally gives:

$$\int \frac{\mathrm{d}E'}{2\pi}\, \|^{\pm,E'}_{x}\, l(E',E) \approx \frac{1}{2\gamma}\mathrm{e}^{\mathrm{i}\left[k^{\pm}_{E}-\frac{E}{\pm 2\gamma}\right]x}\, \tilde{l}(t-\frac{x}{\pm 2\gamma},E) \tag{6.38}$$

6.2.2. Solving the Schrödinger equation

We take here a first (unsuccessful) approach and obtain equations for the scattering amplitudes by solving the discrete Schrödinger equation (4.79), with the Hamiltonian matrix elements h_{ij} given in Eq. (6.2) and the scattering states $\Psi^{\mathrm{L},E}$ given in Eqs. (6.33)

$$i\partial_t \Psi_{-1} = -\gamma\ \Psi_{-2} - \gamma_c\, \Psi_0 \tag{6.39a}$$
$$i\partial_t \Psi_0 = -\gamma_c\, \Psi_{-1} + [V_0 + V(t)]\, \Psi_0 - \gamma_c\, \Psi_1 \tag{6.39b}$$
$$i\partial_t \Psi_1 = -\gamma_c\, \Psi_0 - \gamma\, \Psi_2 \tag{6.39c}$$

Further derivation leads to the following self-consistent equation involving the transmission and the reflection amplitudes

$$d(E,E') = \bar{d}(E)\, 2\pi\, \delta(E'-E) + \alpha(E') \int \frac{\mathrm{dU}}{2\pi}\, \tilde{v}(E'-U) d(U,E) \tag{6.40a}$$
$$r(E,E') = \bar{r}(E)\, 2\pi\, \delta(E'-E) + \alpha(E') \left[\tilde{v}(E'-E) + \int \frac{\mathrm{d}U}{2\pi}\, \tilde{v}(E'-U) r(U,E)\right] \tag{6.40b}$$

where $\bar{d}(U)$ and $\bar{r}(U)$ are the stationary, non-wideband limit, transmission and reflection amplitudes

$$\bar{d}(U) = \frac{2}{r}\, i\, \sin(k_U)\, \alpha(U) \tag{6.41a}$$
$$\bar{r}(U) = \left[(v_0 - u) - \frac{2}{r}\cos(k_U)\right]\, \alpha(U) \tag{6.41b}$$

with

$$\alpha(U) = r\left[r\,(u - v_0) + 2\exp(ik_U)\right]^{-1} \qquad \tilde{v}(U) = \int \mathrm{dt}\, v(t)\, e^{i\,Ut/\hbar} \tag{6.42}$$

and

$$r = \frac{\gamma}{\gamma_c} \qquad u = \frac{U}{\gamma_c} \qquad v_0 = \frac{V_0}{\gamma_c} \qquad v(t) = \frac{V(t)}{\gamma_c} \tag{6.43}$$

Solving Eqs. (6.40) has proven to be difficult. A more simple approach can be taken within the wide-band limit.

6.2.3. Composing subsystem scattering amplitudes in the wideband limit

We describe here a different route to obtain analytic expressions of the scattering amplitudes of the time-dependent RLM in the wide-band limit. We proceed in two steps: first, we do a gauge transformation to move the time-dependence in the dot to the hoppings connected to the dot ; second, we use the fact that the group velocity is infinite, within the wide band approximation, and move the time dependent hoppings (that come from the gauge transformation) one site away from the central dot. This enable us to separate the system into three subsystems so we can adopt the approach from Ref. [63]: we obtain the scattering amplitudes of the total system by composing the (known) subsystem scattering amplitudes.

Let us start with the first step. We perform a gauge change, according to Eq. (4.84), with the following gauge function Λ

$$\Lambda_i(t) = \begin{cases} \varphi(t) & \text{if} \quad i = 0 \\ 0 & \text{if} \quad i \neq 0 \end{cases} \quad \text{with} \quad \varphi(t) = -\int_{t_0}^{t} V(u)\mathrm{d}u \tag{6.44}$$

which leads to the following equivalent Hamiltonian (see Eq. (4.85)):

$$h_{ij} = \begin{cases} V_0 & \text{if} \quad i = j = 0 \\ 0 & \text{if} \quad i = j \neq 0 \\ -\gamma_c \mathrm{e}^{-\mathrm{i}\varphi(t)} & \text{if} \quad i,j = 0,1 \text{ or } 0,-1 \\ -\gamma_c \mathrm{e}^{\mathrm{i}\varphi(t)} & \text{if} \quad i,j = 1,0 \text{ or } -1,0 \\ -\gamma & \text{if} \quad i \neq j \end{cases} \tag{6.45}$$

Second, we use the fact that in the wide band approximation, the dispersion relation becomes linear and the group velocity is infinite. That means we can move the time-dependent hoppings one site away from the dot and still describe the same system, because the changes propagate fast/instantaneously (see Fig. 6.5): we will check numerically in Sec. 6.4 that this simplifying assumption is indeed justified and provides the correct results under the WBL approximation.

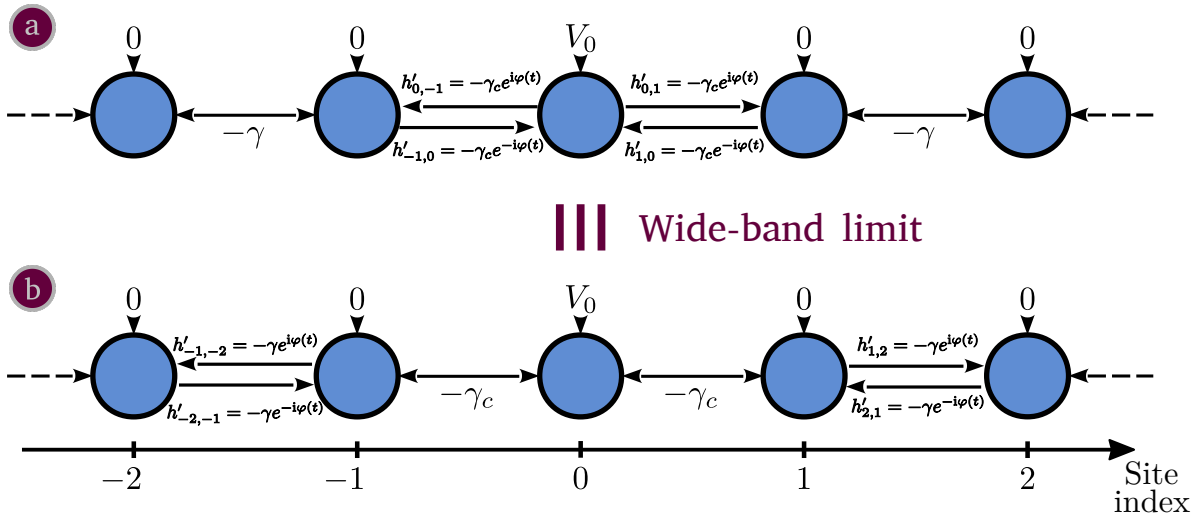

Figure 6.5. – Quantum dot approximation procedure. *(a)* Original tight-binding representation of the resonant level model, described Fig. 6.1, after the gauge change given in Eq. (6.44). *(b)* Thanks to the wide band approximation, moving the time-dependent hoppings (due to the gauge change) one site away from the central site will not affect the underlying described system as the changes propagate instantaneously.

This additional approximation enables us to subdivide the system then describe its transmission matrix using the matrices of each subsystem. The subsystems are (from left to right): 'Mirrored' heaviside

pulse in the (infinite) left lead, the stationary dot, and the heaviside pulse in the (infinite) right lead. electrons do not reflect against the abrupt heaviside voltage drops in the leads (see Appendix. C.2), a left incoming mode $\|_x^{+,E}$ will first be transmitted by the left pulse, with the transmission amplitude $d'_{\mathrm{p}}(\varepsilon, E)$, then transmitted or reflected by the stationary dot, whose scattering amplitudes are d_0 and r_0,

$$d_0(\varepsilon) = \frac{\Gamma}{\Gamma + \mathrm{i}(V_0 - \varepsilon)}\,, \qquad d_0 - r_0 = 1 \qquad \Longrightarrow \qquad |r_0(\varepsilon)|^2 + |d_0(\varepsilon)|^2 = 1 \tag{6.46}$$

with

$$\Gamma = 2\gamma_c^2/\gamma \tag{6.47}$$

to finally be transmitted by either of the pulses again. The scattering process between the subsystems is sketched in Fig. 6.6.

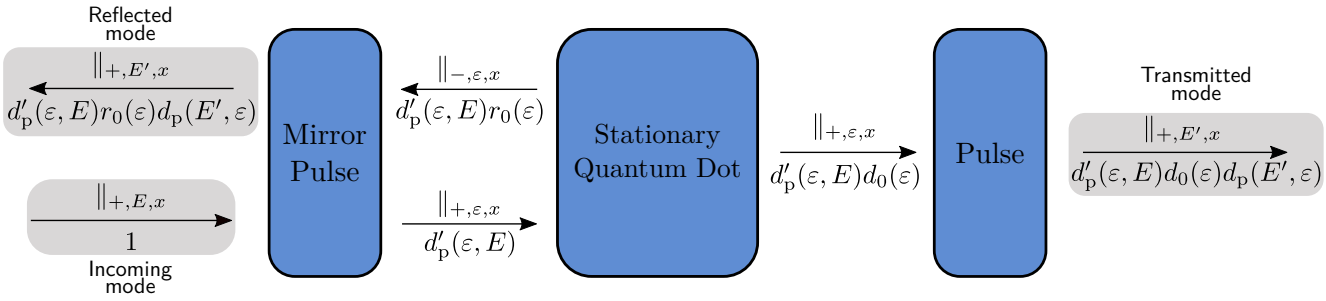

Figure 6.6. – Scattering process for the approximating model to the time-dependent quantum dot. d_{p} and d'_{p} are respectively the left-to-right and right-to-left transmissions of the pulse in the right lead (described in Appendix. C.2). Note that the pulse on the left of the stationary dot is its spatial mirror, which means its left-to-right transmission/reflection is the original pulse's right-to-left transmission/reflection. d_0 and r_0 are respectively the transmission and reflection amplitudes of the stationary quantum dot given in Eq. (6.46).

The transmission and the reflection amplitudes of the entire system can then be written as the sum over all the possible transmitted-to energies ε:

$$d(E', E) = \int \frac{\mathrm{d}\varepsilon}{2\pi}\, d'_{\mathrm{p}}(\varepsilon, E)\, d_0(\varepsilon)\, d_{\mathrm{p}}(E', \varepsilon) \tag{6.48a}$$

$$r(E', E) = \int \frac{\mathrm{d}\varepsilon}{2\pi}\, d'_{\mathrm{p}}(\varepsilon, E)\, r_0(\varepsilon)\, d_{\mathrm{p}}(E', \varepsilon) \tag{6.48b}$$

where the transmissions amplitudes d'_{p} and d_{p} are given by (See appendix. C.2)

$$d'_{\mathrm{p}}(\varepsilon, E) = K(\varepsilon - E) \qquad\qquad d_{\mathrm{p}}(E', \varepsilon) = K^*(\varepsilon - E') \tag{6.49}$$

with K being the Fourier transform of $\mathrm{e}^{-\mathrm{i}\varphi}$

$$K(U) = \int \mathrm{d}t\; \mathrm{e}^{iUt - i\varphi(t)} \tag{6.50}$$

Time domain To calculate the currents in the next section, we also need the fourier transformed transmission and reflection amplitudes along their first argument:

$$d(t, E) = \int \frac{\mathrm{d}E'}{2\pi}\, d(E', E)\, \mathrm{e}^{-\mathrm{i}E't} \qquad\qquad r(t, E) = \int \frac{\mathrm{d}E'}{2\pi}\, r(E', E)\, \mathrm{e}^{-\mathrm{i}E't} \tag{6.51}$$

Using Eqs. (6.48) and (6.50), along with the fourier transforms $(\tilde{d}_0, \tilde{r}_0)$ of (d_0, r_0), we obtain

$$d(t,E) = \mathrm{e}^{\mathrm{i}\varphi(t)} \int \mathrm{d}u\, \mathrm{e}^{-\mathrm{i}\varphi(u)-\mathrm{i}Eu}\, \tilde{d}_0(t-u) \tag{6.52a}$$

$$r(t,E) = \mathrm{e}^{\mathrm{i}\varphi(t)} \int \mathrm{d}u\, \mathrm{e}^{-\mathrm{i}\varphi(u)-\mathrm{i}Eu}\, \tilde{r}_0(t-u) \tag{6.52b}$$

where an analog derivation is made for the reflection amplitude. These can be seen as a convolution between $u \mapsto \mathrm{e}^{-\mathrm{i}\varphi(u)-\mathrm{i}Eu}$ and $\tilde{d}_0$ or $\tilde{r}_0$.

Useful relations Within the particular class of RLM system we are considering (stationary leads, time-dependent dot), one can use the Schrödinger equation (through Eqs. (6.39)) along with the wide-band limit (exposed Sec. 6.2.1) to prove the following relation between the scattering amplitudes (see Appendix. C.3)

$$r(t,E) = d(t,E) - \mathrm{e}^{-\mathrm{i}tE} \quad \Longrightarrow \quad |r|^2 = |d|^2 - 2\mathrm{Re}\big[d\,\mathrm{e}^{\mathrm{i}Et}\big] + 1 \tag{6.53}$$

Also, the following relations can be derived using Eqs. (6.52a) and (6.46)

$$-\left[V(t)+V_0\right]|d|^2 = \mathrm{Im}[d^*\partial_t d] + \Gamma\,\mathrm{Im}\big[\mathrm{e}^{itE}d\big] \tag{6.54a}$$

$$\Gamma\,\mathrm{Im}\big[\mathrm{e}^{\mathrm{i}Et}d\big] + \mathrm{Im}\big[\mathrm{e}^{\mathrm{i}Et}\partial_t d\big] = -\left(V(t)+V_0\right)\mathrm{Re}\big[\mathrm{e}^{\mathrm{i}Et}d\big] \tag{6.54b}$$

$$\partial_t |d|^2 = -2\Gamma\left(|d|^2 - \mathrm{Re}\big[\mathrm{e}^{\mathrm{i}Et}d\big]\right) \tag{6.54c}$$

6.3. Analytical treatment of the generic RLM in the wideband limit: deriving the transport quantities

In this section, we derive generic expressions for the time-resolved energy (and particle) currents and the time-resolved input driving power. Then, we expose their time-integrated counterpart to finally attempt a definition of an efficiency in the time-dependent regime.

6.3.1. Time-resolved currents and densities

Here, we write the expression of the time-resolved lead particle, energy and heat currents for the RLM, using a generic transmission amplitude $d(t,E)$ within the wide-band limit. Note that we make use of the system's left-right symmetry through Eq. (6.34). More thorough derivations are done in Appendix. C.4.

Particle current The wideband approximation is used to obtain simple expressions, as described in Sec. 6.2.1. The development done in Appendix. C.4.1 leads to the following expression for the lead particle currents within the `WBL1` approximation

$$I_\alpha^{\mathrm{N},1}(t) = I_{\alpha,x}^{\mathrm{N},1}(t) = \int \frac{\mathrm{d}E}{2\pi}\, f_\alpha(E)\,\left[1-|r(t,E)|^2\right] - f_{\bar{\alpha}}(E)\,|d(t,E)|^2 \tag{6.55}$$

where $\alpha = L, R$ is the considered lead, f_α is the Fermi distribution, and $\bar{\alpha}$ is the other lead. If the `WBL2` approximation is used, we find

$$I^{\mathrm{N},2}_{\alpha,x}(t) = \int \frac{\mathrm{d}E}{2\pi}\, f_\alpha(E)\, \left[1 - \left|r(t + \tfrac{x+0.5}{2\gamma}, E)\right|^2\right] - f_{\bar{\alpha}}(E)\, \left|d(t + \tfrac{x+0.5}{2\gamma}, E)\right|^2 \tag{6.56}$$

We notice that the strongest approximation `WBL1` leads to a position independent expression of the particle current, whereas `WBL2` enables taking into account that the group velocity is in practice finite: the particle current at further sites takes the same current as closer sites but shifted in time. `WBL2` is nevertheless still too coarse to describe the spreading of the electronic pulse due to the (nonlinear) dispersion relation in the leads (see Eq. (6.29)).

Dot's particle density In appendix C.4.2, we make a short derivation for the dot's particle density $\rho_0(t)$

$$\rho_0 = \int \frac{\mathrm{d}E}{2\pi}\, (f_R + f_L)\, \frac{1}{\Gamma}\, |d|^2 \tag{6.57}$$

This quantity is useful for understanding the transient regime. Indeed, electrons may be temporarily stored in the dot: they contribute to the displacement current but also receive input work from the external driving dot potential.

Input power Given its expression in (5.33), power is given to the system only on the sites $-1, 0$ and 1. We obtain the following expression for the input power in the right and left leads

$$S^\varepsilon_\alpha(t) = -\frac{1}{2} V(t) I^{\mathrm{N}}_\alpha(t) \tag{6.58}$$

The total input power $S^\varepsilon = S^\varepsilon_{-1} + S^\varepsilon_0 + S^\varepsilon_1$ in the system writes using the particle conservation equation (4.157)

$$S^\varepsilon(t) = -V(t)\, [I^{\mathrm{N}}_{\mathrm{L}} + I^{\mathrm{N}}_{\mathrm{R}}] = -V(t)\, \partial_t \rho_0 = -V(t) \int \frac{\mathrm{d}E}{2\pi}\, (f_R + f_L)\, \frac{1}{\Gamma} \partial_t\, |d|^2 \tag{6.59}$$

We can simply interpret this equation as: each electron leaving the site 0, at an instant t, takes an energy $V(t)$

Energy current In Appendix. C.4.3, we derive formulas for the energy currents using the `WBL1` approximation (see Sec. 6.2.1) in two special cases : far in the leads and for the hoppings that are connected to the central site 0. When far within the leads the expression for energy current is the generalization of the stationary Landauer-Buttiker formula (5.36b) with time-dependent transmission and reflection probabilities (and the Hamiltonian energy currents ($I^h_{\alpha,x}$) coincide with the "total energy" current ($I^\varepsilon_{\alpha,x}$) in these stationary leads)

$$I^{h,\varepsilon}_{\alpha,x}(t) = \int \frac{\mathrm{d}E}{2\pi}\, E\, \left[f_\alpha(E)\, \left[1 - |r(t,E)|^2\right] - f_{\bar{\alpha}}(E)\, |d(t,E)|^2\right] \tag{6.60}$$

Just like with the particle current, the above expressions are position independent. Note that in the time-dependent regime the transmission and reflection probabilities are not trivially connected

$$1 - |r(t,E)|^2 \neq |d(t,E)|^2 \quad \text{but} \quad \int \mathrm{d}t\, \left[1 - |r(t,E)|^2\right] = \int \mathrm{d}t\, \left[|d(t,E)|^2\right] \tag{6.61}$$

The expressions we obtain for the energy currents I^{ε}_{α}, evaluated on the hoppings $(-1,0)$ and $(0,1)$, are different as additional terms are non-zero when considering the expression (4.94) on those sites (see Appendix C.4.4)

$$I^{\varepsilon}_{\alpha}(t) = S^{\varepsilon}_{\alpha}(t) + \int \frac{\mathrm{d}E}{2\pi} \begin{bmatrix} E\left[f_{\alpha}\left(1-|r|^2\right) - f_{\bar{\alpha}}|d|^2\right] \\ -\left(f_{\alpha}+f_{\bar{\alpha}}\right)\mathrm{Im}[A\partial_t A^*] \\ -f_{\alpha}\,\mathrm{Re}[\partial_t A] \end{bmatrix} \tag{6.62}$$

where

$$A = -\mathrm{i}\,\mathrm{e}^{\mathrm{i}Et}d \tag{6.63}$$

The formula in Eq. (6.62), that applies on the neighboring hoppings of the central site 0 is different from the one in Eq. (6.60): we have observed (data not shown) that Eq. (6.60) yields results that do not match with tkwant simulations, for energy currents evaluated far in the leads[2]. Using `WBL2` instead of `WBL1` did not improve the mismatch. The reasons of the discrepancy are not yet clear but are (at least) related to the fact that Eq. (6.60) do not account properly for the source term S^{ε}_{α} i.e. the input driving power. The time integral should not depend on whether the currents are evaluated near the dot or far in the leads, this will become clearer in Eq. (6.70) where we express the time-integral of the 'dynamically injected' energy current in each lead. In the following, we will calculate the currents between the sites 0 and -1 (or 0 and 1) using WBL1 since our analytics in that case are confirmed by exact `tkwant` simulations, this will be illustrated in Sec. 6.4.1.

Heat current Writing the heat current, as defined by Eq. (4.211), is straightforward by using the energy current from Eqs. (6.62) and (6.58)

$$I^{\mathrm{Q}}_{\alpha}(t) = \int \frac{\mathrm{d}E}{2\pi} \begin{bmatrix} (E-\mu_{\alpha})\left[f_{\alpha}\left(1-|r|^2\right) - f_{\bar{\alpha}}|d|^2\right] \\ -\left(f_{\alpha}+f_{\bar{\alpha}}\right)\mathrm{Im}[A\partial_t A^*] \\ -f_{\alpha}\,\mathrm{Re}[\partial_t A] \end{bmatrix} \tag{6.64}$$

Note that if we do not take into account the coupling Hamiltonian $\hat{H}_{0\alpha}$ between the lead α and the central system, the resulting heat current $\tilde{I}^{\mathrm{Q}}_{\alpha}$ (defined in Eq. (6.23) in Sec. 6.1 in our linear response study) will have the same expression but without the $f_{\alpha}\,\mathrm{Re}[\partial_t A]$ term. This implies that, for a finite pulse $V(t)$, the time-integral of $I^{\mathrm{Q}}_{\alpha}(t) - \tilde{I}^{\mathrm{Q}}_{\alpha}(t)$ gives zero, given that the coupling Hamiltonian stores only temporarily some energy.

6.3.2. Time integrated currents and densities

The time-resolved formulas for the transport quantities we gave in the previous section are generic: they are valid under the `WBL1` approximation for any drive $V(t)$ of the dot. When $V(t)$ is finite in time, the contribution of the time-dependent drive can be assessed by computing 'time-integrated deltas over

[2] The comparison was done in the case where $V(t)$ is a square pulse. As shown later in Sec. 6.4, the scattering amplitudes $d(t,E)$ and $r(t,E)$ can be calculated exactly in that case, so that Eq. (6.60) can be evaluated independently from tKwant.

the stationary regime' (see proper definitions in the next paragraphs) for each quantity. For that purpose, we define T^{dyn} as the time-integral of the 'dynamical' – the time-dependent part – transmission probability $|d(t,E)|^2 - |d_0(E)|^2$

$$T^{\mathrm{dyn}}(E) = \int \mathrm{d}t \, \left[|d(t,E)|^2 - |d_0(E)|^2\right] \tag{6.65}$$

Using Eqs. (6.53), (6.54c) and (6.46), we show that

$$T^{\mathrm{dyn}}(E) = \int \mathrm{d}t \, \left[|r_0(E)|^2 - |r(t,E)|^2\right] \tag{6.66}$$

where d_0 and r_0 are the initial stationary scattering amplitudes of the RLM, given in Eq. (6.46). We show that the time-integrated currents have expressions that (partially) behave like stationary Landauer-Büttiker formulas with T^{dyn} as an *effective* stationary-like transmission probability, like the one defined in Eq. (5.37). An explicit expression for $T^{\mathrm{dyn}}(E)$ will be given for the specific case of a square drive of the dot in the next section. These 'dynamical' quantities are in general non-zero, which shows that the time dependent-drive leaves a signature even when a time-integration is performed. We will use these expressions (although with a finite-time integration) in the next section in our definition of electric generation efficiency.

Particle number The dynamically injected number of particles N_α^{dyn} throughout the pulse, in the lead α, is straightforward to write using T^{dyn}:

$$N_\alpha^{\mathrm{dyn}} \equiv \int \mathrm{d}t \, \left[I_\alpha^{\mathrm{N}}(t) - I_\alpha^{\mathrm{N}}|_{t=0}\right] = \int \frac{\mathrm{d}E}{2\pi} \, T^{\mathrm{dyn}}(E) \left[f_\alpha(E) - f_{\tilde{\alpha}}(E)\right] \tag{6.67}$$

This expression is a 1-to-1 analog to its stationary Landauer-Büttiker formula for particle currents in Eq. (5.36a): all the theoretical developments made in the stationary regime can apply to this expressions (*e.g.* linear response).

Input work The integration of the time resolved input power can be easily written from equation (6.59)

$$W^{\mathrm{ext}} = \int \mathrm{d}t \, S^\varepsilon = \int \frac{\mathrm{d}E}{2\pi} \, w(E) \left[f_R + f_L\right] \quad \text{with} \quad w(E) = -\frac{1}{\Gamma} \, V(t) \, \partial_t \, |d(t,E)|^2 \tag{6.68}$$

Energy In this paragraph we will highlight a subtlety that explains our choice in defining the heat current in Eq. (4.211). Let us write the energy conservation equation (4.172) at site -1, subtract the stationary energy current $I^\varepsilon_{\mathrm{L},-2}(t=0) = I^\varepsilon_{\mathrm{L}}(t=0)$ and time-integrate it

$$\int \mathrm{d}t \, \left[I^\varepsilon_{\mathrm{L},-2}(t) - I^\varepsilon_{\mathrm{L},-2}|_{t=0}\right] = \int \mathrm{d}t \, \left[I^\varepsilon_{\mathrm{L}}(t) - S^\varepsilon_L(t) - I^\varepsilon_{\mathrm{L}}|_{t=0}\right] + \underbrace{\left[\rho^\varepsilon_{-1}(t)\right]_{t=t_0}^{t=\infty}}_{=0} \tag{6.69}$$

where we used the convention expressed in Eq. (6.3). This conservation equation shows that the time-integral of the energy current on hopping $(-2,-1)$ differs from the one on hopping $(-1,0)$ by the source term $S^\varepsilon_{\mathrm{L}}$ on site -1. In other words, the total 'dynamically injected' energy $\mathcal{E}^{\mathrm{dyn}}_{\mathrm{L}}$ is given by the left-hand side of Eq. (6.69) if it is evaluated on hopping $(-2,-1)$ while it is given by the right-hand side of Eq. (6.69) – including the source term $S^\varepsilon_{\mathrm{L}}$ – if it is evaluated on hopping $(-1,0)$. The two definitions

coincide in virtue of energy conservation. Further derivation, done in Appendix. C.5.1, leads to the following interesting result

$$\mathcal{E}_\alpha^{\rm dyn} = \int \mathrm{d}t\ \left[I_{\rm L}^{\varepsilon}(t) - S_L^{\varepsilon}(t) - I_{\rm L}^{\varepsilon}|_{t=0}\right] = \int \frac{\mathrm{d}E}{2\pi}\ \left[E\, T_{\rm dyn}(E)\,(f_\alpha - f_{\bar\alpha})\right] - \frac{1}{2}W^{\rm ext} \tag{6.70}$$

where we see that the total dynamically injected energy in the lead α is a sum of two terms. The first term can be seen as an effective Landauer-Büttiker formula and translates the fact that the $N_\alpha^{\rm dyn}$ electrons dynamically injected in the lead α at different energies E carry with them that same energy. This term vanishes at equilibrium ($\mu_L = \mu_R$, $T_L = T_R$). The second term is half of the total input energy $W^{\rm ext}$, meaning that 50% of the input driving energy is dissipated as heat in the left lead and 50% in the right lead, regardless of the electrochemical potential and temperature of each lead. Note that this a consequence of the symmetry of the system, the dot being symmetrically coupled (with hopping term γ_c) to the left lead and to the right lead. Moreover, we notice that Eq. (6.70) coincides with Eq.(53) of Ref. [50] derived for a random telegraph process $V(t)$ modeled by a sum of square pulses of different widths in time, after averaging over the random processes. In that paper, the derivation is done with the NEGF formalism within the WBL approximation. On the contrary, we derived Eq. (6.70) with a wave-function approach valid (in the WBL approximation) for an arbitrary pulse $V(t)$ of finite duration.

Heat Writing the dynamically injected heat $Q_\alpha^{\rm dyn}$ in each lead is straightforward, using its definition in Eq. (4.211) and the expression of $\mathcal{E}_\alpha^{\rm dyn}$ given in Eq. (6.70)

$$Q_\alpha^{\rm dyn} = \int \mathrm{d}t\ \left[I_{\rm L}^{\rm Q}(t) - I_{\rm L}^{\rm Q}|_{t=0}\right] = \int \frac{\mathrm{d}E}{2\pi}\ \left[(E-\mu_\alpha)\, T_{\rm dyn}(E)\,(f_\alpha - f_{\bar\alpha})\right] - \frac{1}{2}W^{\rm ext} \tag{6.71}$$

With the plausible assumption that the input work is positive ($W^{\rm ext} > 0$, energy is given to the system), this term can bring some difficulties when trying to define a heat engine efficiency as it can be the dominant term and therefore heat *both* the reservoirs.

6.3.3. Electric generator efficiency

We try now to characterize the efficiency of the device when it operates as a heat engine. The electric heat engine efficiency is usually defined as the ratio between "useful power" and "spent power": identifying both terms is cumbersome in the time-dependent regime and several efficiencies may be a priori defined, depending on whether one wants to take into account the potential effect of finite-size baths, characterize the efficiency of the total process or only of the thermoelectric conversion.

In the stationary regime, the useful power is harvested from electrons climbing a chemical potential bias between the two reservoirs, and the spent power is the heat current leaving the hot reservoir. A necessary and sufficient condition to have a Seebeck effect is to have hot electrons climb a chemical potential bias: let us assume that and consider $T_{\rm L} > T_{\rm R}$ and $\mu_{\rm L} < \mu_{\rm R}$. The stationary efficiency writes:

$$\eta^{\rm st} = \frac{(\mu_{\rm R} - \mu_{\rm L}) I_{\rm L}^{\rm N,st}}{I_{\rm L}^{\rm Q,st}} \tag{6.72}$$

with $I_{\rm L}^{\rm N,st} > 0$ and $I_{\rm L}^{\rm Q,st} > 0$.

One could naively extend this stationary definition to the time-dependent regime by adding the (driving) input power while considering the time-dependence of each quantity

$$"\eta(t)" = \frac{(\mu_{\mathrm{R}} - \mu_{\mathrm{L}})\,[-I_{\mathrm{R}}^{\mathrm{N}}(t)]}{I_{\mathrm{L}}^{\mathrm{Q}}(t) + S^{\varepsilon}(t)} \tag{6.73}$$

Note that it would be important to pick $-I_{\mathrm{R}}^{\mathrm{N}}(t)$ instead of $I_{\mathrm{L}}^{\mathrm{N}}(t)$, and $I_{\mathrm{L}}^{\mathrm{Q}}(t)$ instead of $-I_{\mathrm{R}}^{\mathrm{Q}}(t)$, as they are not equal : work is done only when electrons have effectively climbed the chemical potential and reached the target lead ; and the spent heat is the one leaving the 'hot' reservoir. However, there are several fundamental issues that need to be considered before going any further in attempting to define an efficiency

1. The particle current $I_{\mathrm{R}}^{\mathrm{N}}$, the heat current $I_{\mathrm{L}}^{\mathrm{Q}}$ and also a priori the source term $S(t)$, can change sign in the time-dependent regime and the system will not always (at each time t) perform as an electric generator: $"\eta(t)"$ will not always be strictly positive nor smaller than the Carnot efficiency. There might also be some specific time intervals where $I_{\mathrm{R}}^{\mathrm{Q}}(t) > 0$ i.e. heat is extracted from the cold source even if $T_{\mathrm{L}} > T_{\mathrm{R}}$ and $\mu_{\mathrm{L}} < \mu_{\mathrm{R}}$.

2. The time-dependent drive on the dot has a symmetrical contribution on the electric currents that can blur out the notion of "useful energy". To illustrate this, one can think of the case where the time-dependent drive temporarily lowers the dot level up to the point where particle currents will flow towards the dot from both leads. And conversely, when the dot level may be increased high enough so that its particles will temporarily leave towards both leads where the potential is lower. The notion of electrons traveling from one bath to the other while 'climbing' an electrochemical potential bias would not apply in this considered transient regime.

3. The external time-dependent drive inputs energy W^{ext} in the system through the dot, that energy will eventually leave towards both leads through electron-carried, and outgoing, energy and heat currents. If the input power is high enough, it can even counterbalance the 'natural' hot to cold heat flow (see Eq. (6.71)) so that both the left and right reservoirs are heated at the same time ($I_{\mathrm{L}}^{\mathrm{Q}} < 0$, $I_{\mathrm{R}}^{\mathrm{Q}} < 0$). In this case, one needs to think about the heat's contribution to the "spent energy": the hot bath effectively would not lose but would win heat, which would naively indicate that this heat should be subtracted from the 'spent' energy, which would positively impact the efficiency. However, the cold bath does get heat nonetheless.

It is possible to define a more fitting, but still debatable, efficiency with some additional assumptions and restrictions. Inspired by periodic drive studies [44, 150], we use a time-resolved 'average behavior' of the system and account for 'net' quantities: the ratio between the net useful energy and the net spent energy, from $t = t_0$ and $t = \tau$

$$\eta(\tau) = \frac{[\mu_{\mathrm{R}} - \mu_{\mathrm{L}}](-N_{\mathrm{R}}(\tau))}{Q_{\mathrm{L}}(\tau) + W^{\mathrm{ext}}(\tau)} \tag{6.74}$$

where

$$\begin{vmatrix} N_\alpha(\tau) \\ Q_\alpha(\tau) \\ W^{\mathrm{ext}}(\tau) \end{vmatrix} = \int_{t_0}^{\tau} \mathrm{d}t \begin{vmatrix} I_\alpha^{\mathrm{N}}(t) \\ I_\alpha^{\mathrm{Q}}(t) \\ S^{\varepsilon}(t) \end{vmatrix} \tag{6.75}$$

For this heat engine efficiency to be interpretable, we make the following restrictions and hypotheses, on top of our initial setup where $T_{\mathrm{L}} > T_{\mathrm{R}}$ and $\mu_{\mathrm{L}} < \mu_{\mathrm{R}}$

- For periodic steady-state regime, or finite-time pulses where the stationary regime is a Seebeck regime, we consider that 'useful' energy is effectively harvested when there exists a time τ_η where we have

$$\forall \tau > \tau_\eta \;\; N_{\mathrm{R}}(\tau) < 0 \;\text{ and }\; N_{\mathrm{L}}(\tau) > 0 \tag{6.76}$$

  so that a net (positive) amount of electrons went from one lead to the other and 'climbed' an electrochemical bias.

- In the end, the efficiency is a matter of practical implementation of real life heat engines: in the usual case where the hot bath is obtained artificially and the cold bath is the outside environment, then it is physically understandable that the part of the input power that goes towards heating the artificial, and finite-size, hot bath should not be counted in "spent energy". We therefore make this assumption and the efficiency $\eta(\tau)$ defined right above properly accounts for this subtraction. Note that, within this hypothesis, the sign and value of $Q_{\mathrm{R}}(\tau)$ has no impact on the efficiency: heat can be lost to, or extracted from, the outside environment but the only energy we spend is the sum of heat that the artificial hot reservoir loses and the driving input power.

In the next section, we undergo a numerical study of the RLM in the specific case of rectangle drive of dot, using both `tkwant` and the analytical expressions derived previously. We will showcase the issues 1, 2 and 3 outlined above and study the efficiency $\eta(t)$ with the restrictions and considerations we exposed here.

6.4. Rectangle drive of the dot

In this section, we consider a specific drive $V(t)$ in the dot's onsite Hamiltonian $h_0(t)$ (see Eq. (6.2)) that is a rectangle function

$$V(t) = \Delta V\, \Theta(t)\Theta(\Delta t - t)$$

The phase $\varphi(t)$ from the gauge change in Eq. (6.44) writes:

$$\varphi(t) = -\int_0^t \mathrm{d}u\, V(u) = -t \times \Delta V\, \Theta(t)\, \Theta(\Delta t - t) - \Delta V \Delta t\, \Theta(t - \Delta t) \tag{6.77}$$

K, defined in (6.50), has the following expression in this case:

$$K(E) = \mathrm{i}\frac{\Delta V}{E(E+\Delta V)}\left(\mathrm{e}^{\mathrm{i}\Delta t(E+\Delta V)} - 1\right) + \pi\left(\mathrm{e}^{\mathrm{i}\Delta t \Delta V} + 1\right)\delta(E) \tag{6.78}$$

Given the expression of the scattering amplitudes of the stationary dot in (6.46), their Fourier transforms write as:

$$\tilde{d}_0(t) = \Gamma\, \mathrm{e}^{-t\Gamma}\mathrm{e}^{-\mathrm{i}tV_0}\,\Theta(t) \qquad\qquad \tilde{r}_0(t) = -\delta(t) + \tilde{d}_0(t) \tag{6.79}$$

This enables us to use (6.52a) to calculate the transmission amplitude $d(t, E)$. Using a CAS software (like Mathematica), or the residue theorem one can show that it simplifies to

$$d(t,E) = \begin{cases} d_0^E \mathrm{e}^{-\mathrm{i}tE} & \text{if } t \le 0 \\ d_1^E \mathrm{e}^{-\mathrm{i}tE} + \mathrm{e}^{-\Gamma t - \mathrm{i}t(V_0+\Delta V)}\left[d_0^E - d_1^E\right] & \text{if } 0 \le t \le \Delta t \\ d_0^E \mathrm{e}^{-\mathrm{i}tE} + \mathrm{e}^{-(\Gamma+\mathrm{i}V_0)(t-\Delta t)}\left[\mathrm{e}^{-\Delta t[\mathrm{i}(V_0+\Delta V)+\Gamma]} - \mathrm{e}^{-\mathrm{i}\Delta t E}\right]\left[d_0^E - d_1^E\right] & \text{if } \Delta t \le t \end{cases} \tag{6.80}$$

where d_0^E and d_1^E are shorthand notations for $d_0(E)$ and $d_1(E) = d_0(E - \Delta V)$ (transmission of the stationary dot after the ΔV jump) given in Eqs. (6.46). The reflection amplitude $r(t, E)$ can be expressed with $d(t, E)$ by using equation (6.53).

6.4.1. Comparing the analytical formulas to `tkwant`

We use the expressions derived in the WBL approximation for the time-resolved and time-integrated currents and densities (see Sec. 6.3) and numerically integrate them. On the other hand, we perform `tkwant`+`tkwantoperator` simulations using the scaling procedure described in Sec. 5.3.2.2, parametrized by the wide band parameter wb defined as

$$wb = \lambda\gamma/\Gamma \tag{6.81}$$

We compare our data obtained with both approaches in the limit of large $wb \gg 1$, where the WBL is reached.

First, we compute the time-resolved particle (I^{N}_α), energy (I^{ε}_α) and heat (I^{Q}_α) currents, as well as the energy input power/source (S^{ε}) and their finite time-integrals as defined in Eq. (6.75). We find good agreement in the WBL between `tkwant` simulations and the analytical expressions, over an example set of parameters (see Fig. 6.7) and showcase some interesting dynamics. The considered RLM is initially put in a stationary heat engine configuration then the dot level undergoes a rectangle function with an upward jump. The transient regime can be split into two phases: during the pulse and right after. During the pulse, electrons that were on the dot, win energy, then are expelled towards both leads. The energy they carry has a heat contribution that reduces the outgoing heat from the hot reservoir and increases the heat going to the cold reservoir.

Moreover, we perform another comparison between `tkwant`+`tkwantoperator` and our analytical formulas for the 'dynamical' time-integrated quantities exposed in Sec. 6.3.2. In Fig. 6.8, each point corresponds to the time-integrated response of the system to a single square pulse of width Δt. Data are plotted for various values of Δt, keeping constant the area $\Delta t \Delta V$ of the pulse (so that the limit of short pulses coincides with the Dirac pulse limit). Once again, the WBL is approached numerically with tKwant by increasing the parameter wb. We find perfect agreement between analytics and tKwant simulations for large Δt while larger and larger deviations appear when Δt is decreased (at fixed wb). This behavior can be understood after noticing that the time-dependent drive induces inelastic scattering processes in an energy range of width ΔV around $\mu_{\mathrm{L}}, \mu_{\mathrm{R}}$. When Δt decreases, ΔV increases and becomes comparable to the band width in the leads given by $2\lambda\gamma = 2wb\Gamma$. In that case, wb is not large enough to reach the WBL. However, increasing wb also increases the effective size of the leads in tKwant (see Sec. 5.1.3) so that treating large values of wb is computationally expensive.

Besides, we notice that all data shown in this section have been plotted after a proper scaling with Γ. Indeed, the previously used variables can be made dimensionless by expressing them in terms of Γ:

$$(V_0, \Delta V, \mu_\alpha, T_\alpha) = \Gamma\,(\bar{V}_0, \overline{\Delta V}, \bar{\mu}_\alpha, \bar{T}_\alpha) \qquad\qquad (t, \Delta t) = 1/\Gamma\,(\bar{t}, \overline{\Delta t}) \tag{6.82}$$

And these can be used to define dimensionless currents and powers as they do not depend on Γ anymore:

$$I^N \qquad (t, \Delta t, V_0, \Delta V, \mu_\alpha, T_\alpha, \Gamma) = \Gamma \qquad \bar{I}^N(\bar{t}, \overline{\Delta t}, \bar{V}_0, \overline{\Delta V}, \bar{\mu}_\alpha, \bar{T}_\alpha) \tag{6.83}$$

$$[I^{\varepsilon}, I^{\mathrm{h}}, S^{\varepsilon}](t, \Delta t, V_0, \Delta V, \mu_\alpha, T_\alpha, \Gamma) = \Gamma^2\,[\bar{I}^{\varepsilon}, \bar{I}^{\mathrm{h}}, \bar{S}^{\varepsilon}](\bar{t}, \overline{\Delta t}, \bar{V}_0, \overline{\Delta V}, \bar{\mu}_\alpha, \bar{T}_\alpha) \tag{6.84}$$

Using analytical formulas derived in Sec. 6.3.1, it is easy to show that the dimensionless (overlined) currents and powers are independent of Γ. This scaling has been tested numerically and is illustrated in Fig. 6.9 for two values of Γ, both for the analytical calculations and for the tKwant simulations in the WBL.

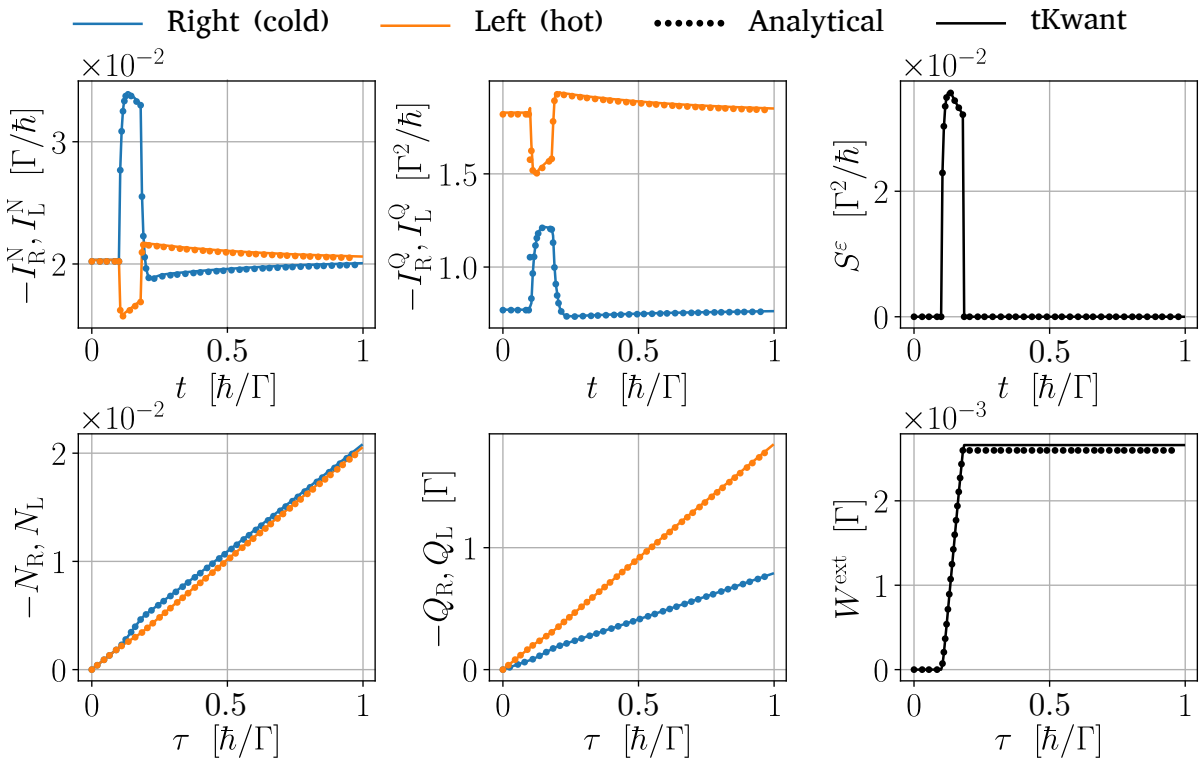

Figure 6.7. – Full `tkwant+tkwantoperator` (full lines) and analytical (dots) simulations of the RLM when its dot energy level $h_0(t)$ undergoes a rectangle drive $h_0(t) = V_0 + \Delta V \Theta(t)\Theta(\Delta t - t)$ while initially in a high efficiency ($> 0.8\eta_{\mathrm{C}}$) heat generator configuration. The time-resolved particle current I_α^{N}, energy current I_α^{ε}, heat current I_α^{Q} and total input power S^{ε} are computed (top panels), along with their finite-time integration (bottom panels), as defined in Eq. (6.75). In the transient regime, a sudden burst of electrons flow from the dot to both of the leads, while carrying energy and heat from the external drive. These additional energetic electrons contribute negatively (*i.e* reduce) to the heat leaving the hot left bath while they heat the cold bath more. This transient regime has a positive impact on the heat-engine efficiency $\eta(\tau)$, as defined in Eq. (6.74) (see Fig. 6.10), while noting that $W^{\mathrm{ext}}(\tau)$ has a negligible value with respect to the other terms. The dot's particle density is then slowly filled back by electrons from both reservoirs and the system goes back to its original stationary state. Simulation parameters (energies are in units of Γ and times in units of $1/\Gamma$): $T_{\mathrm{L}} = 87, T_{\mathrm{R}} = 25, \mu_{\mathrm{L}} = -26, \mu_{\mathrm{R}} = 26, V_0 = 55, \Delta V = 2, \Delta t = 0.08, t_0 = 0.1$. `tkwant` specific parameters: $wb = 400, \gamma = 1$

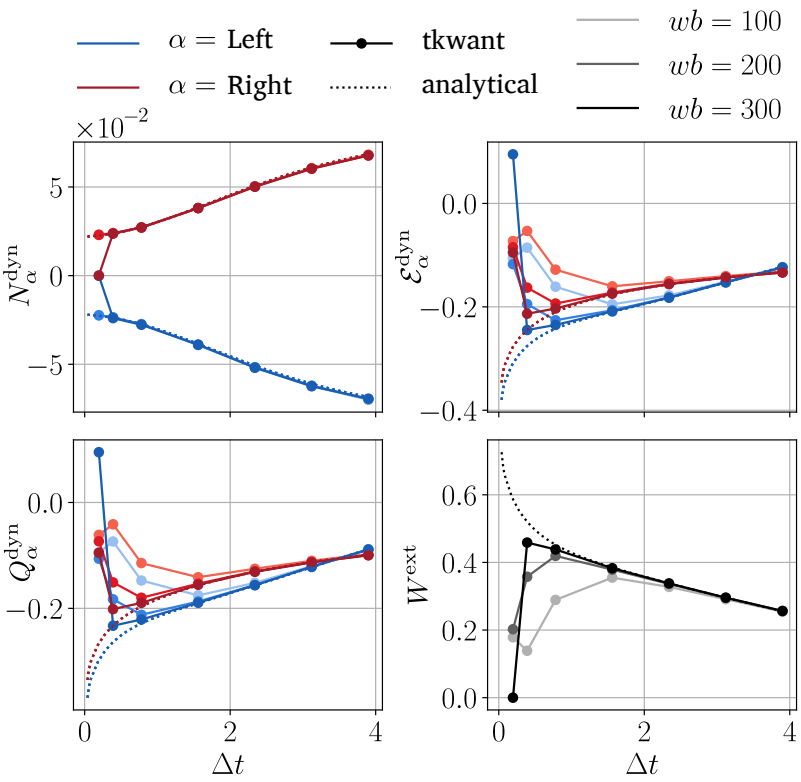

Figure 6.8 – Comparison between `tkwant+tkwantoperator` (dots connected with solid lines) and our analytical expressions (dotted lines) for the time-integrated 'dynamical' transport quantities, described in Sec. 6.3.2. `tkwant` simulations are run for three values of wb (shades of colors) to study the convergence towards the WBL. We test here the limit of short pulses with constant area. For that matter, we change simultaneously ΔV and Δt (see Eq. (6.77)) so their product is constant. We see here that higher values of wb enable `tkwant` to match analytical curves for shorter pulses (though the limit of very short pulses $\Delta t \lesssim 0.5$ – for which $\Delta V \gtrsim 20$ – is not reached even for $wb = 300$ – for which the band width $2wb\Gamma = 48$ is not big enough compared to ΔV). Values taken: $\Gamma = 0.08, \gamma = 1, t_0 = 0.1, V_0 = 0.5, \Delta V = 9.75/\Delta t, \mu_{\mathrm{L}} = 0.5, \mu_{\mathrm{R}} = -0.5, T_{\mathrm{L}} = 1, T_{\mathrm{R}} = 0$

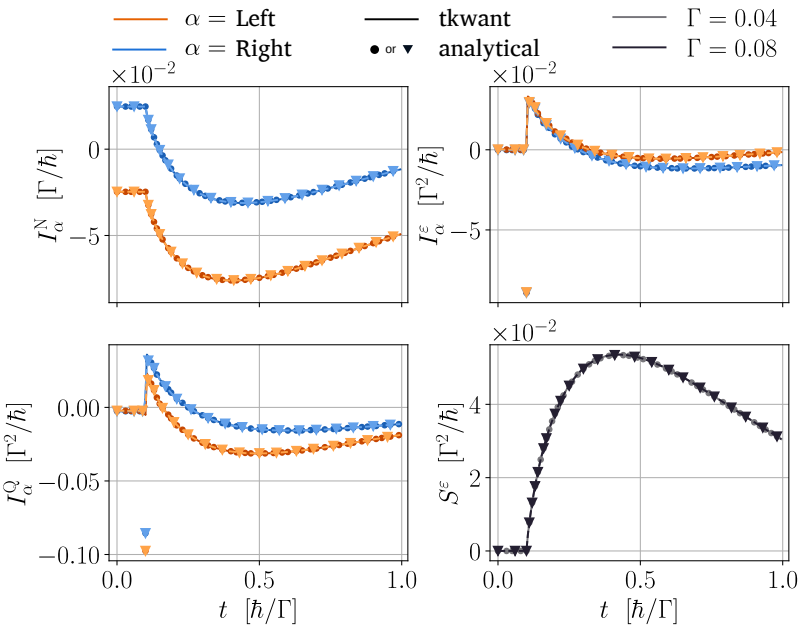

Figure 6.9 – Transport quantities as calculated from analytical formulas (symbols) and by tkwant (lines), for two values of Γ ($\Gamma = 0.04$ (circles and light colors) and $\Gamma = 0.08$ (triangles and dark colors)). The set of data for both values of Γ are perfectly superimposed. The discrepancy points between analytics and numerics for the energy and heat currents, at the time of jump $t = t_0$, is a signature of a singularity appearing in the WBL [37]. For $\Gamma = 0.04$ and $\Gamma = 0.08$, the other values being fixed to $\bar{t}_0 = 0.1, \overline{\Delta t} = 3.9, \bar{V}_0 = 0.5, \overline{\Delta V} = 0.5, \bar{\mu}_{\mathrm{L}} = -0.1, \bar{\mu}_{\mathrm{R}} = 0.1, \bar{T}_{\mathrm{L}} = 0.11, \bar{T}_{\mathrm{R}} = 0.09, wb = 500$

6.4.2. An improved, but unusable, efficiency in the transient regime

Our goal is to identify if there exist some regimes where the heat engine efficiency is improved by such time-dependent drive. For that, we derived analytical expressions for the finite-time integrated quantities[3], described in Eq. (6.75), and ran an algorithm that randomly explores various sets of parameters $(T_\alpha, \mu_\alpha, V_0, \Delta V, \Delta t)$ while still trying to make equidistant points with respect to the corresponding stationary efficiency (we used a Python package called `Adaptive` [140] to achieve that). The efficiency $\eta(\tau)$ we were monitoring is the one defined in Eq. (6.74) and discussed in Sec. 6.3.3. Various $(T_\alpha, \mu_\alpha, V_0, \Delta V, \Delta t)$ sets turn out to show an improved efficiency in the transient regime, including the one used in Fig. 6.7: its efficiency in the transient regime even exceeds the Carnot limit but decreases back to its stationary value at long times, one can also note that the input energy W^{ext} is negligible and does not affect the efficiency. One may think of cycling the drive, at a period τ_p that coincides with a high transient efficiency of the first pulse $\eta(\tau_P) > \eta^{\text{st}}$, but the efficiency $\eta(\tau)$ – that accounts for net (integrated) quantities between $t = 0$ and $t = \tau$ – also converges to a lower value (smaller than η_{C}), the steady state periodic value: further research (with *e.g.* a Floquet approach) is needed to assess the steady state value $\eta(\tau)$ is converging to, but we find empirically that this value is close to the initial stationary efficiency η^{st}. Cycling does although make the back-to-stationary convergence time of the efficiency longer (see Fig. 6.10). This transient improvement of the efficiency cannot be leveraged as-is in real world heat engines, as what is initially won eventually ends up being given back. A similar behaviour was observed in the classical experiment reported in Ref. [178] where a Peltier cooler has its cooling power temporarily improved when driven by a rectangular electric current pulse, see Fig. 6.11

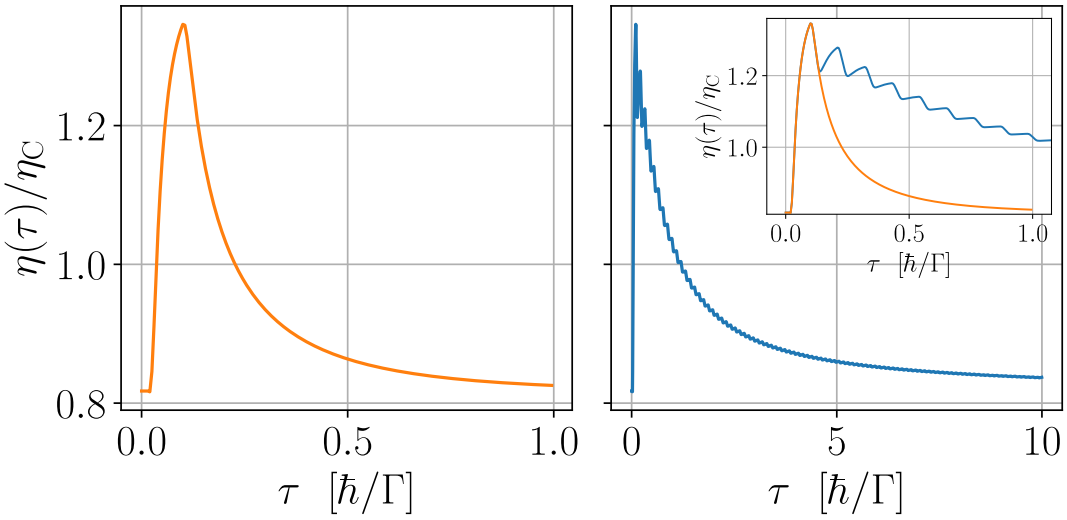

Figure 6.10. – An improved transient efficiency of the RLM. When the dot level is driven by a rectangle function, the particle and heat currents can behave in such a way (see Fig. 6.7 for a description) that the efficiency $\eta(\tau)$ (defined in Eq. (6.74), under the assumptions stated Sec. 6.3.3) is temporarily improved. The left panel is the resulting efficiency of a single pulse whereas the right panel is the resulting efficiency of the same pulse, periodically cycled with a period τ_p. Both curves are plotted in the inset of the right panel to show they coincide till $\tau = \tau_p$. We notice that this has the effect of delaying the return to a lower efficiency but does not seem to maintain a steady-state improvement. Both curves have been obtained through `tkwant+tkwantoperator` simulations. This result is reminiscent of the reported results of Ref. [178] on a Peltier cooler. Simulation parameters (energies are in units of Γ, times are in units of $1/\Gamma$): $T_{\text{L}} = 87, T_{\text{R}} = 25, \mu_{\text{L}} = -26, \mu_{\text{R}} = 26, V_0 = 55, \Delta V = 2, \Delta t = 0.08, t_0 = 0.1, \tau_p = 0.11, wb = 400, \gamma = 1$.

[3] They are not given in this thesis since each of them is heavy to write (i.e. is several lines long) and is hard to interpret. However, these analytical expressions make the numerical evaluation much faster. This allows us to perform a systematic and fine investigation of the parameter space.

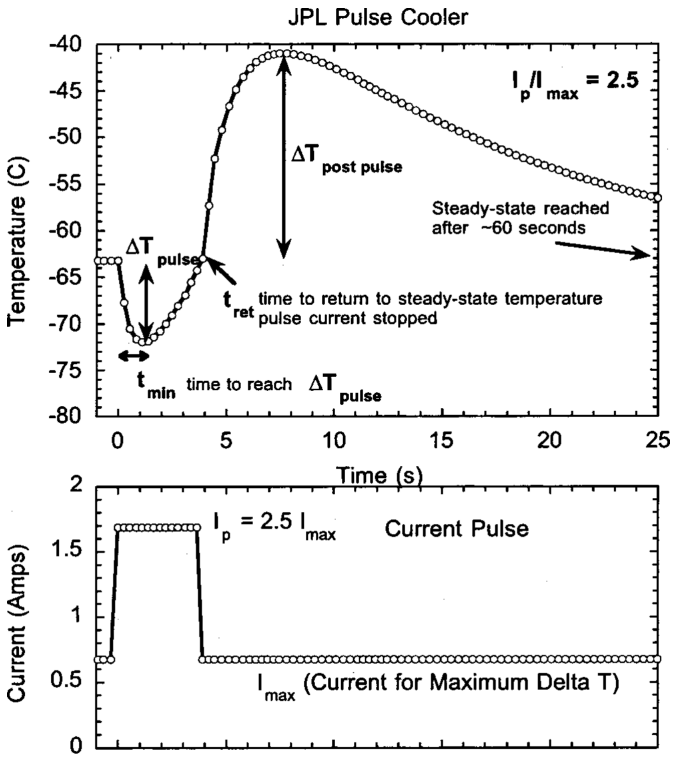

Figure 6.11 – Taken from Ref. [178]. Temporary 'super-cooling' of a real-life Peltier module when rectangle-driven by an electric current. The cold surface of the cooler gets abruptly cooled for a transient duration then undergoes a longer and stronger hot back action, after the end of the pulse.

6.5. Limitations of the model and perspectives

The time-dependent drive heats both the hot and cold reservoir, regardless of the electrochemical or temperature biases. One would want to not waste extra heat in the cold bath, both in a heat engine and cooler configuration, even more in the latter case. A possibility is the make the system not symmetrical with respect to the dot by making the lead-dot matrix element γ_c, defined in the Hamiltonian in Eq. (6.2) side-dependent

$$\gamma_c \to \gamma_{\rm L} \ \text{ or } \ \gamma_{\rm R} \tag{6.85}$$

We have explored this lead and re-derived the formulas expressed in this chapter: they simply get re-normalized according to a dimensionless asymmetry factor $a = (\Gamma_{\rm R} - \Gamma_{\rm L})/(\Gamma_{\rm R} + \Gamma_{\rm L})$ where $\Gamma_\alpha = 2\gamma_\alpha^2/\gamma$. This offers an extra knob in controlling the current flows between the left and right leads, it is however too 'global' as it plays on the coupling strengths Γ_α that affect all the transport quantities: *e.g.* lowering the coupling with cold bath indeed reduces the heat flow towards it but also the particle flow, which lowers the 'useful' power output. On the other hand, since the equations have the same (re-normalized) form, no extra effect will arise from this change.

Further models can be studied to attempt to work around the limitations of this simple RLM model. A few possibilities can already be considered

- Add stationary dots, for energy filtering purposes, around the central time-dependent dot. If the central dot's Hamiltonian matrix element $h_0(t)$ is driven between V_0 and $V_0 + \Delta V$, the stationary filter dots can be fine-tuned so that *(i)* the dot in contact with the hot bath $(T_{\rm L}, \mu_{\rm L})$ has a relatively narrow transmission window around $V_0 \approx \mu_{\rm L}$ whereas *(ii)* the dot in contact with cold bath $(T_{\rm R}, \mu_{\rm L})$, with $T_{\rm R} < T_{\rm L}$ and $\mu_{\rm R} > \mu_{\rm L}$, has its transmission window tuned around $V_0 + \Delta V \approx \mu_R$. This approach may offer better control on where the drive-generated heat goes, thanks to the filter dots.

- For cooling, one could consider using a third bath to redirect the extra generated heat to, and avoid "staining" the cold bath with the spurious heat that would come from the time-dependent drive. The means to achieve this have although to be thought through.

7. Conclusion

With the current progress in high frequency quantum experiments at low temperatures, theoretical and numerical tools have been developed jointly, and initially, for particle transport. Research in quantum thermodynamics and mesoscopic thermoelectricity (which is a subcategory of the former) have been led in parallel and the question of time-dependence is a central building-block for a consistent theory. This thesis work is one more contribution in these developments: it bridges the gap between one of the theoretical tools developed for time-dependent particle transport and time-dependent thermoelectric transport.

The objective was to bring new insights of the possible effects of time-dependence in quantum thermoelectrics. We started by going through the already developed scattering theory of non-interacting particle transport, the theoretical description in this thesis has nearly entirely avoided the use of the NEGF formalism thanks to the fruitful work behind the `tkwant` [1] simulation library, initiated during the PhD thesis of B. Gaury [63] (in X. Waintal's group at CEA Grenoble), that resulted into an intuitive and simple description through system-wide one-body wavefunctions. Then, we brought the pieces together from past literature to build upon the wavefunction particle transport: no new concept has been developed in this thesis, our work consisted in formulating properly and consistently a framework for time-dependent energy transport in arbitrary non-interacting systems. Our approach abode by two driving principles: electromagnetic gauge invariance and a specific form of local energy conservation where the source term recovers the quantum equivalent to the classical definition $\vec{j}(\vec{r},t)\cdot\vec{E}(\vec{r},t)$ – where $\vec{j}$ is the charge current density and $\vec{E}$ is the time-dependent part of the electric field – as the considered Hamiltonian $\hat{H}$ is semi-classical (light is not quantified). We derived the energy conservation equations in the one-body and many-body approaches, in both the continuous space and discrete spaces, the similarities between each approach were highlighted and understood. We then use this framework to extend `tkwant`, a powerful library that offers time-resolved simulations of realistic quantum tight-binding systems. A relatively substantial part of my work has been spent on understanding the inner workings of `tkwant` to extend it to energy transport and to a lesser extent, improve some functionalities ; a proper Python module, `tkwantoperator` has been written from scratch with extensive documentation and testing. `tkwantoperator` is open source and freely available at `gitlab.kwant-project.org/kwant/tkwantoperator`.

Once we finished developing and validating the module, we showcased the potential of the extended `tkwant` by simulating a Quantum Point Contact model, in the Peltier regime, made of more than thousand sites, and for long simulation times. The first results over the thermoelectric performance of such a model where difficult to grasp due do its complexity. To avoid blind exploration, we decided to go back to a simpler model, the Resonant Level model. Our goal was to better understand the reported predicted boost [219] of its thermoelectric efficiency: using exactly the model and definitions used in that reference, we reproduced within our own approach the reported results. The same comparison was done against other theoretical works. This allowed us to validate our approach and to better understand the hypotheses assumed in those papers. Then, we performed an analytical derivation of the transport quantities under an arbitrary drive of the dot, in the wideband limit, and obtained generic formulas for all the transport quantities where some general features were highlighted. We discussed the underlying

issues in defining a heat engine efficiency in the driven regime: the distinction between 'useful energy' and what is the 'spent energy' is a delicate subject ; and one must account for the driving input power, and its effect, in the energy bill. A joint semi-analytical (we integrate our analytical formulas) and numerical (using `tkwant`+`tkwantoperator`) study followed, with a rectangle-like drive of the dot, where the system-bath coupling has been taken into account (see Sec. 1.2.2). We found that the time-dependent drive can temporarily improve the heat generator efficiency of this model but does not seem to bring a lasting advantage. Other models, inspired by our understanding of the RLM, could be investigated for which our extension to `tkwant` comes in handy as it enables testing out ideas on any tight-binding system.

Perspectives

The `tkwant` + `tkwantoperator` platform offers is a first milestone towards the simulation of time-dependent (charge and energy) quantum transport in realistic nanodevices. The full potential of the numerical approach is yet to be leveraged by further studies as the only complex system we quickly explored is the Quantum Point Contact. On the other hand, our framework suffers from intrinsic limitations whose roles remain to be evaluated. The following points may be worth evaluating in additional studies:

Heat current There is no still no consensus in the literature about the proper definition of a time-resolved heat current. In this thesis, we have defined electronic heat currents in the leads at a given position and time, with the idea that electrons relax afterwards in the electronic reservoirs (a 'book-keeping procedure' also used in Ref. [47]). Far in the leads, we wrote time-resolved heat current $I^{\mathrm{Q}} = I^{\varepsilon} - \mu I^{\mathrm{N}}$, where I^{ε} is the total energy current and I^{N} the particle current and μ is the bath's chemical potential. This expression is based on the stationary hypothesis that electrons entering the bath at energy E bring in an $E - \mu$ heat contribution. This definition may need further studying from first principles while taking into account relaxation processes (*e.g.* with electron-electron or electron-phonon interaction) within a finite-size baths to fully understand the separation between the 'work' and 'heat' part of the incoming energy flux in the bath. Ref. [6] already led an initial study with 'Fermi mesoreservoir' with a finite number of energy levels that relax in turn in Lindblad baths. Having a clear understanding of the separation between 'work' and 'heat', especially in the time-dependent regime, will help bringing in more definite answers to the role of dynamical driving in thermoelectrics.

Electromagnetic back-action – electron-electron interaction In our approach, the considered electromagnetic control is externally imposed and electrons do not affect it. A first approach is to consider electrostatics and solve the Poisson equation self-consistently while the electrons are still described quantum mechanically

$$\vec{\nabla}^2 V_i(t) + \frac{\rho_i(t)}{\varepsilon_0} = 0 \tag{7.1}$$

where $\rho_i(t)$ is given Eq. (4.158), this problem is called the 'self-consistent Hartree' or the 'Poisson-Schrödinger problem'. X. Waintal's group is currently actively working on implementing this within `kwant` in the stationary regime [11] and `tkwant` in the time-dependent regime [100, 164]. One could take the development further by also treating the electron's radiation in the time-dependent regime

with the electromagnetic potentials' wave equations [91]

$$\frac{1}{c^2}\partial_t^2 \begin{bmatrix} \vec{A}(\vec{r},t) \\ \phi(\vec{r},t) \end{bmatrix} - \vec{\nabla}^2 \begin{bmatrix} \vec{A}(\vec{r},t) \\ \phi(\vec{r},t) \end{bmatrix} = 4\pi \begin{bmatrix} \vec{j}(\vec{r},t)/c \\ \rho(\vec{r},t) \end{bmatrix} \tag{7.2}$$

in the Lorentz gauge $\partial_t \phi/c + \vec{\nabla}\vec{A} = 0$. Although the conditions of applicability need to be studied too.

Spin and energy The development made in this thesis describes electrons without consideration for the spin. A first step towards considering spin is with the Zeeman coupling within the Pauli equation [172] for which it is straightforward to extend the energy quantities. In the basis that diagonalize $\hat{S}_z$, the Pauli equation writes

$$i\hbar\partial_t \begin{bmatrix} \psi_+ \\ \psi_- \end{bmatrix} = \left(\frac{1}{2m}(\vec{p} - q\vec{A})^2 + q\phi + V \right) \mathbb{1} \begin{bmatrix} \psi_+ \\ \psi_- \end{bmatrix} - \frac{\hbar q}{2m} \sum_{\alpha=x,y,z} B^\alpha \sigma_\alpha \begin{bmatrix} \psi_+ \\ \psi_- \end{bmatrix} \tag{7.3}$$

where $\mathbb{1}$ is the two-dimensional identity matrix and $(\sigma_x, \sigma_y, \sigma_z)$ are the 2×2 Pauli matrices. Given that the resulting Hamiltonian is diagonal with respect to the spin for the term $\frac{1}{2m}(\vec{p} - q\vec{A})^2 + q\phi + V$, the source term S_i^ε will still give rise to the classical term $(-\vec{\nabla}\phi_i - \partial_t \vec{A}_i) \cdot \vec{j}_i$ (as given in Eq. (4.188)), and an additional term

$$\sum_{\alpha=x,y,z} \sum_{\sigma\sigma'} (\partial_t B_i^\alpha) \sigma^\alpha_{\sigma\sigma'} G^<_{i\sigma' i\sigma} = \sum_{\alpha=x,y,z} (\partial_t B_i^\alpha) \operatorname{tr}\left[\sigma^\alpha \mathbf{G}^<_{ii}\right] \tag{7.4}$$

However, further research is needed when a Hamiltonian with relativistic corrections – such as spin-orbit coupling, the relativistic mass correction or the darwin term [171] – is considered : issues such as defining a proper energy operator, deriving a local energy conservation equation and figuring out regimes where the extra terms have non-negligible contribution need to be tackled.

Appendix A. First quantization derivations

In this appendix, we derive the main equations of Sec. 4.2, written for a single electron described by a wavefunction ψ.

A.1. Particle transport

In this section we expose the derivation of the particle conservation equation, both in its continuous and discrete version.

A.1.1. Continuous

We derive here the continuous one-body particle conservation equation expressed Eq. (4.56).

→ Current divergence Using the definition of the velocity operator $\vec{v}$ given in (4.44), the particle current writes

$$\vec{j} = \frac{\hbar}{m}\,\mathrm{Im}\left[\psi^*(\vec{\nabla}\psi)\right] - \frac{q}{m}\psi^*\psi\vec{A} \tag{A.1}$$

this enables us to write its divergence

$$\vec{\nabla}\cdot\vec{j} = \frac{1}{m}\left(\hbar\,\mathrm{Im}\Big[\underbrace{\vec{\nabla}\psi^*\cdot\vec{\nabla}\psi}_{\in\mathbb{R}\implies \mathrm{Im}[\cdots]=0} + \psi^*\Delta\psi\Big] - q\Big[\underbrace{\underbrace{\psi\left(\vec{\nabla}\psi^*\cdot\vec{A}\right) + \psi^*\left(\vec{\nabla}\psi\cdot\vec{A}\right)}_{=2\,\mathrm{Re}\left[\psi^*\left(\vec{\nabla}\psi\cdot\vec{A}\right)\right]=2\,\mathrm{Im}\left[\mathrm{i}\psi^*\left(\vec{\nabla}\psi\cdot\vec{A}\right)\right]} + \underbrace{\psi^*\psi\vec{\nabla}\cdot\vec{A}}_{\in\mathbb{R}}\Big]}_{=\mathrm{Im}[2\mathrm{i}\psi^*\left(\vec{\nabla}\psi\cdot\vec{A}\right)+\mathrm{i}\psi^*\psi\vec{\nabla}\cdot\vec{A}]}\right) \tag{A.2}$$

which finally gives

$$\vec{\nabla}\cdot\vec{j} = \frac{1}{m}\mathrm{Im}\left[\hbar\psi^*\Delta\psi - 2\mathrm{i}q\psi^*\left(\vec{\nabla}\psi\cdot\vec{A}\right) - \mathrm{i}q\psi^*\psi\vec{\nabla}\cdot\vec{A}\right] \tag{A.3}$$

→ Density time derivative The time derivative of the probability density is

$$\partial_t\rho = (\partial_t\psi^*)\psi + \psi^*(\partial_t\psi)$$

The Hamiltonian can be used to express the time derivative of the wavefunctions

$$\partial_t\psi = -\frac{\mathrm{i}}{\hbar}\hat{h}[\psi] \quad \text{and} \quad \partial_t\psi^* = \frac{\mathrm{i}}{\hbar}\hat{h}[\psi]^* \tag{A.4}$$

→ Conservation equation By writing the explicit expression of the effect of the Hamiltonian on a wavefunction:

$$\hat{h}[\psi] = \frac{1}{2m}\left[-\hbar^2\Delta\psi + \mathrm{i}\hbar q\left(2\vec{\nabla}\psi\cdot\vec{A} + \psi\vec{\nabla}\cdot\vec{A}\right) + q^2A^2\psi\right] + q\,\phi\,\psi + V\psi \tag{A.5}$$

we obtain an explicit expression for the density time derivative (A.6) . Given that $q^2A^2\psi^*\psi$ and $\psi^*\psi$ don't have an imaginary part, we obtain:

$$\partial_t\rho = \frac{1}{m}\mathrm{Im}\left[-\hbar\psi^*\Delta\psi + 2\mathrm{i}q\psi^*\left(\vec{\nabla}\psi\cdot\vec{A}\right) + \mathrm{i}q\psi^*\psi\vec{\nabla}\cdot\vec{A}\right] \tag{A.6}$$

By comparing (A.3) with (A.6), we verify (4.56).

→ Gauge invariance Lets write the expression of $\vec{v}'$ in the 'original' gauge:

$$\vec{v}' = -\mathrm{i}\frac{\hbar}{m}\vec{\nabla} - \frac{q}{m}(\vec{A} - \vec{\nabla}\Lambda) \tag{A.7}$$

Its action on the wave function $\psi' = \exp(-\mathrm{i}\frac{q}{\hbar}\Lambda)\psi$ is then:

$$\vec{v}'\psi' = \left[-\frac{q}{m}\vec{\nabla}\Lambda - \mathrm{i}\frac{\hbar}{m}\vec{\nabla}\psi\right]\exp\left(-\mathrm{i}\frac{q}{\hbar}\Lambda\right) - \frac{q}{m}(\vec{A} - \vec{\nabla}\Lambda)\exp\left(-\mathrm{i}\frac{q}{\hbar}\Lambda\right)\psi \tag{A.8}$$

$$= \left[-\mathrm{i}\frac{\hbar}{m}\vec{\nabla}\psi - \frac{q}{m}\vec{A}\psi\right]\exp\left(-\mathrm{i}\frac{q}{\hbar}\Lambda\right) = [\vec{v}\psi]\exp\left(-\mathrm{i}\frac{q}{\hbar}\Lambda\right) \tag{A.9}$$

Hence:

$$\vec{j}' = \mathrm{Re}[\psi'^*\vec{v}'\psi'] = \mathrm{Re}\left[\exp\left(\mathrm{i}\frac{q}{\hbar}\Lambda\right)\psi^*[\vec{v}\psi]\exp\left(-\mathrm{i}\frac{q}{\hbar}\Lambda\right)\right] = \mathrm{Re}[\psi^*\vec{v}\psi] = \vec{j} \tag{A.10}$$

A.1.2. Discrete

To derive here the particle conservation equation given Eq. (4.86), we use Eq. (4.87) and time derivate it

$$\partial_t\rho_i = [\mathrm{d}_t\psi_i^*]\,\psi_i + \psi_i^*\,[\mathrm{d}_t\psi_i]$$

then, by inserting the discrete Schrodinger equation (4.79), we find

$$\partial_t\rho_i = \frac{1}{\hbar}\sum_j -i\left[\psi_i^*h_{ij}\psi_j - \psi_ih_{ij}^*\psi_j^*\right] \tag{A.11}$$

which gives the conservation equation (4.86).

To derive relation Eq. (4.89) between the hopping particle current I_{ij}^{N} and the discrete particle current density vector $\vec{j}_i$, we use discretized version of the gradient operator Eq. (4.80) to write the current density vector from the continuum Eq. (A.1)

$$\vec{j}_i = \sum_{\alpha=x,y,z}\left[\frac{\hbar}{2ma}\mathrm{Im}\left[\psi_i^*\left(\psi_{n_\alpha(i)} - \psi_{p_\alpha(i)}\right)\right] - \frac{q}{m}\psi_i^*\psi_iA_i^\alpha\right]\vec{e}_\alpha \tag{A.12}$$

On the other hand, to express I^N_{ij} we use $\hat{h}[\psi]_i$ given in Eq. (4.81) to expand the discrete current density $\vec{j}_i$ given by Eq. (4.89)

$$\begin{aligned}
&\frac{a}{2}\left[I^N_{i,n_\alpha(i)} - I^N_{i,p_\alpha(i)}\right] \\
&= -\frac{a}{\hbar}\mathrm{Im}\left[\psi_i^* h_{i,n_\alpha(i)}\psi_{n_\alpha(i)} - \psi_i^* h_{i,p_\alpha(i)}\psi_{p_\alpha(i)}\right] \\
&= \mathrm{Im}\left[\psi_i^*\left(\left[\frac{\hbar}{2ma} - \mathrm{i}\frac{q}{2m}A_i^\alpha\right]\psi_{n_\alpha(i)} - \left[\frac{\hbar}{2ma} + \mathrm{i}\frac{q}{2m}A_i^\alpha\right]\psi_{p_\alpha(i)}\right)\right] \\
&= \frac{\hbar}{2ma}\mathrm{Im}\left[\psi_i^*\left(\psi_{n_\alpha(i)} - \psi_{p_\alpha(i)}\right)\right] - \frac{q}{m}A_i^\alpha \mathrm{Re}\left[\psi_i^*\frac{\psi_{n_\alpha(i)} + \psi_{p_\alpha(i)}}{2}\right]
\end{aligned}$$

The latter formula coincides with the α component j_i^α of $\vec{j}_i$ in equation (A.12) to the first order in the lattice spacing a[1] which concludes the derivation.

A.2. Energy transport

In this section we outline a more thorough derivation of the energy conservation equation, in the continuous and discrete space.

A.2.1. Expressing the current density vector with the hopping current

We will derive here the relation (4.96)

$$\vec{j}_i^\epsilon = \sum_{\alpha=x,y,z}\frac{a}{2}\left[I^\epsilon_{i,n_\alpha(i)} - I^\epsilon_{i,p_\alpha(i)}\right]\vec{e}_\alpha$$

that connects the hopping energy current I^ϵ_{ij} given by Eq. (4.94)

$$I^\epsilon_{ij} = -\frac{1}{\hbar}\sum_k \mathrm{Im}\left[\psi_k^*\epsilon_{ki}\epsilon_{ij}\psi_j - \psi_k^*\epsilon_{kj}\epsilon_{ji}\psi_i\right]$$

and the discretized energy current density vector $\vec{j}_i^\epsilon$ given by Eq. (4.95)

$$\vec{j}_i^\epsilon = \frac{1}{2}\mathrm{Re}\left[\hat{\epsilon}[\psi]_i^*\,\hat{\vec{v}}[\psi]_i + \psi_i^*\hat{\vec{v}}[\hat{\epsilon}[\psi]]_i\right]$$

where ϵ can either be the Hamiltonian h, given by Eq. (4.82), the kinetic energy operator κ given in Eq. (4.103) or the total energy operator ε given by Eq. (4.105). We will use the Hamiltonian as the base energy operator although the derivation still applies for kinetic and total energy operators as we have Eq. (4.173) : $h_{ij} = \kappa_{ij} = \varepsilon_{ij}$ for $i \neq j$

→ Expression of $\left[\hat{h}[\psi]_i^*\hat{\vec{v}}[\psi]_i^\alpha\right]$: Let us start by expressing $\hat{\vec{v}}[\psi]_i^\alpha$ by using the definition of $\vec{v}$ Eq. (4.44) and the discretized gradient operator Eq. (4.80):

$$\hat{\vec{v}}[\psi]_i^\alpha = \frac{-i\hbar}{2ma}\left(\psi_{n_\alpha(i)} - \psi_{p_\alpha(i)}\right) - \frac{q}{m}A_i^\alpha\psi_i \tag{A.13}$$

[1] $\psi_i \approx \left(\psi_{n_\alpha(i)} + \psi_{p_\alpha(i)}\right)/2$

We need to write the expression above using only Hamiltonian terms h_{ij} and the wave function and the wavefunction ψ_i. While having in mind the expression of h_{ij} Eq (4.82) that come from the discretization process with a being a small cubic lattice parameter, we can try the following:

$$\begin{aligned}
&h_{i,n_\alpha(i)}\psi_{n_\alpha(i)} - h_{i,p_\alpha(i)}\psi_{p_\alpha(i)} \\
&= \left[-\frac{\hbar^2}{2ma^2} + \mathrm{i}\frac{\hbar q}{2ma}A_i^\alpha\right]\psi_{n_\alpha(i)} - \left[-\frac{\hbar^2}{2ma^2} - \mathrm{i}\frac{\hbar q}{2ma}A_i^\alpha\right]\psi_{p_\alpha(i)} \\
&= -\frac{\hbar^2}{2ma^2}\left[\psi_{n_\alpha(i)} - \psi_{p_\alpha(i)}\right] + \mathrm{i}\frac{\hbar q}{ma}A_i^\alpha \underbrace{\left[\psi_{n_\alpha(i)} + \psi_{p_\alpha(i)}\right]/2}_{\approx\psi_i} \\
&= \frac{\hbar}{\mathrm{i}a}\left[-\frac{\mathrm{i}\hbar}{2ma}\left[\psi_{n_\alpha(i)} - \psi_{p_\alpha(i)}\right] - \frac{q}{m}A_i^\alpha\psi_i\right] = \frac{\hbar}{\mathrm{i}a}\hat{\vec{v}}[\psi]_i^\alpha
\end{aligned}$$

where we have used $\psi_i = \left[\psi_{n_\alpha(i)} + \psi_{p_\alpha(i)}\right]/2$, since a is a small lattice parameter. We have

$$\hat{h}[\psi]_i^*\hat{\vec{v}}[\psi]_i^\alpha = \frac{\mathrm{i}a}{\hbar}\hat{h}[\psi]_i^*\left[h_{i,n_\alpha(i)}\psi_{n_\alpha(i)} - h_{i,p_\alpha(i)}\psi_{p_\alpha(i)}\right] \tag{A.14}$$

→ Expression of $\left[\psi_i^*\hat{\vec{v}}[\hat{h}[\psi]]_i^\alpha\right]$: We express now the second term of the right hand side of Eq. (4.95)

$$\hat{\vec{v}}[\hat{h}[\psi]]_i^\alpha = \frac{-\mathrm{i}\hbar}{2ma}\left(\hat{h}[\psi]_{n_\alpha(i)} - \hat{h}[\psi]_{p_\alpha(i)}\right) - \frac{q}{m}A_i^\alpha\hat{h}[\psi]_i \tag{A.15}$$

From the matrix expression of the discrete Hamiltonian in equation (4.82), we can express the term $\frac{-\mathrm{i}\hbar}{2ma}$:

$$\frac{-\mathrm{i}\hbar}{2ma} = \frac{\mathrm{i}a}{\hbar}\left(H_{i,n_\alpha(i)} - \mathrm{i}\frac{\hbar q}{2ma}A_i^\alpha\right) \tag{A.16}$$

$$= \frac{\mathrm{i}a}{\hbar}\left(H_{i,p_\alpha(i)} + \mathrm{i}\frac{\hbar q}{2ma}A_i^\alpha\right) \tag{A.17}$$

Which enables us to further simplify the expression of $\hat{\vec{v}}[\hat{h}[\psi]]_i^\alpha$:

$$\begin{aligned}
\hat{\vec{v}}[\hat{h}[\psi]]_i^\alpha = &\left[\frac{\mathrm{i}a}{\hbar}h_{i,n_\alpha(i)} + \frac{q}{2m}A_i^\alpha\right]\hat{h}[\psi]_{n_\alpha(i)} \\
&- \left[\frac{\mathrm{i}a}{\hbar}h_{i,p_\alpha(i)} - \frac{q}{2m}A_i^\alpha\right]\hat{h}[\psi]_{p_\alpha(i)} \\
&- \frac{q}{m}A_i^\alpha\hat{h}[\psi]_i \\
= &\frac{\mathrm{i}a}{\hbar}\left[h_{i,n_\alpha(i)}\hat{h}[\psi]_{n_\alpha(i)} - h_{i,p_\alpha(i)}\hat{h}[\psi]_{p_\alpha(i)}\right] \\
&+ \frac{q}{m}A_i^\alpha\underbrace{\frac{1}{2}\left[\hat{h}[\psi]_{n_\alpha(i)} + \hat{h}[\psi]_{p_\alpha(i)}\right]}_{\approx\hat{h}[\psi]_i} - \frac{q}{m}A_i^\alpha\hat{h}[\psi]_i \\
= &\frac{\mathrm{i}a}{\hbar}\left[h_{i,n_\alpha(i)}\hat{h}[\psi]_{n_\alpha(i)} - h_{i,p_\alpha(i)}\hat{h}[\psi]_{p_\alpha(i)}\right]
\end{aligned} \tag{A.18}$$

→ Expression of $\vec{j}_i^{\mathrm{H}}$: Using Eq. (A.14) and Eq. (A.18), we can express the projection along the $\alpha = x, y, z$ direction of the energy current vector density

$$\begin{aligned} j_i^{\mathrm{H}} \cdot \vec{e}^{\alpha} &= \frac{1}{2}\mathrm{Re}\left[\hat{h}[\psi]_i^* [\vec{v}\psi]_i^{\alpha} + \psi_i^* \left[\vec{v}H\psi\right]_i^{\alpha}\right] \\ &= \frac{1}{2}\mathrm{Re}\Bigg[\frac{\mathrm{i}a}{\hbar}\Big[\hat{h}[\psi]_i^* \left[h_{i,n_\alpha(i)}\psi_{n_\alpha(i)} - h_{i,p_\alpha(i)}\psi_{p_\alpha(i)}\right] \\ &\qquad + \psi_i^* \left[h_{i,n_\alpha(i)}\hat{h}[\psi]_{n_\alpha(i)} - h_{i,p_\alpha(i)}\hat{h}[\psi]_{p_\alpha(i)}\right]\Big]\Bigg] \\ &= -\frac{a}{2\hbar}\mathrm{Im}\Bigg[\hat{h}[\psi]_i^* \left[h_{i,n_\alpha(i)}\psi_{n_\alpha(i)} - h_{i,p_\alpha(i)}\psi_{p_\alpha(i)}\right] \\ &\qquad + \psi_i^* \left[h_{i,n_\alpha(i)}\hat{h}[\psi]_{n_\alpha(i)} - h_{i,p_\alpha(i)}\hat{h}[\psi]_{p_\alpha(i)}\right]\Bigg] \end{aligned} \tag{A.19}$$

And in the other hand, we have:

$$\begin{aligned} I^E_{i,n_\alpha(i)} - I^E_{i,p_\alpha(i)} &= \frac{1}{\hbar}\mathrm{Im}\Big[- \hat{h}[\psi]_i^* h_{i,n_\alpha(i)}\psi_{n_\alpha(i)} - \psi_i^* h_{i,n_\alpha(i)}\hat{h}[\psi]_{n_\alpha(i)} \\ &\qquad + \hat{h}[\psi]_i^* h_{i,p_\alpha(i)}\psi_{p_\alpha(i)} + \psi_i^* h_{i,p_\alpha(i)}\hat{h}[\psi]_{p_\alpha(i)}\Big] \\ &= -\frac{1}{\hbar}\mathrm{Im}\Big[\hat{h}[\psi]_i^* \left[h_{i,n_\alpha(i)}\psi_{n_\alpha(i)} - h_{i,p_\alpha(i)}\psi_{p_\alpha(i)}\right] \\ &\qquad + \psi_i^* \left[h_{i,n_\alpha(i)}\hat{h}[\psi]_{n_\alpha(i)} - h_{i,p_\alpha(i)}\hat{h}[\psi]_{p_\alpha(i)}\right]\Big] \end{aligned} \tag{A.20}$$

→ Comment on the second term: One could have taken $\psi_i^*\hat{h}[\vec{v}[\psi]]_i^{\alpha}$ for the second term given that $[\vec{v}, H] = -\mathrm{i}[\hbar/m\vec{\nabla}, q\phi + V]$ is pure imaginary and the current's expression involves taking its real part

$$\begin{aligned} \psi_i^*\hat{h}[\vec{v}[\psi]]_i^{\alpha} &= \sum_j \psi_i^* h_{ij}\hat{\vec{v}}[\psi]_j^{\alpha} \\ &= \sum_j \frac{\mathrm{i}a}{\hbar}\psi_i^* h_{ij}\left[h_{j,n_\alpha(j)}\psi_{n_\alpha(j)} - h_{j,p_\alpha(j)}\psi_{p_\alpha(j)}\right] \end{aligned}$$

However, the resulting expression for the current vector density does not easily match with Eq. (A.20)

$$\begin{aligned} j_i^{\mathrm{H}} \cdot \vec{e}^{\alpha} &= \frac{1}{2}\mathrm{Re}\Bigg[\sum_j \frac{\mathrm{i}a}{\hbar}\Big(h_{ij}^*\psi_j^*\left[h_{i,n_\alpha(i)}\psi_{n_\alpha(i)} - h_{i,p_\alpha(i)}\psi_{p_\alpha(i)}\right] \\ &\qquad + \psi_i^* h_{ij}\left[h_{j,n_\alpha(j)}\psi_{n_\alpha(j)} - h_{j,p_\alpha(j)}\psi_{p_\alpha(j)}\right]\Big)\Bigg] \\ &= -\frac{a}{2\hbar}\mathrm{Im}\Bigg[\hat{h}[\psi]_i^*\left[h_{i,n_\alpha(i)}\psi_{n_\alpha(i)} - h_{i,p_\alpha(i)}\psi_{p_\alpha(i)}\right] \\ &\qquad + \sum_j \psi_i^* h_{ij}\left[h_{j,n_\alpha(j)}\psi_{n_\alpha(j)} - h_{j,p_\alpha(j)}\psi_{p_\alpha(j)}\right]\Bigg] \end{aligned}$$

A.2.2. Hamiltonian energy source: continuous

We derive the explicit expression of the Hamiltonian source term given in Eq. (4.74). Let's start by expressing the term $[\partial_t H]\psi$, we can derive it by taking the time partial time derivative of equation

(A.5) and keep only the terms that do not involve $\partial_t\psi$:

$$[\partial_t H]\,\psi = \frac{1}{2m}\left[\mathrm{i}\hbar q\left(2\partial_t\vec{A}\cdot\vec{\nabla}\psi + \psi\vec{\nabla}\cdot\vec{A}\right) + 2\psi q^2\,\partial_t\vec{A}\cdot\vec{A}\right] + \psi\partial_t V \tag{A.21}$$

And thus we get for $S = \mathrm{Re}[\psi^*[\partial_t H]\psi]$:

$$S = \frac{1}{2m}\mathrm{Re}\left[\mathrm{i}\hbar q\left(2\psi^*\partial_t\vec{A}\cdot\vec{\nabla}\psi + \psi^*\psi\vec{\nabla}\cdot\vec{A}\right) + 2\psi^*\psi q^2\,\partial_t\vec{A}\cdot\vec{A}\right] + \psi^*\psi\partial_t V \tag{A.22}$$

$$= \frac{1}{2m}\left[-2\hbar q\,\partial_t\vec{A}\cdot\mathrm{Im}[\psi^*\vec{\nabla}\psi] + 2\psi^*\psi\,q^2\,\partial_t\vec{A}\cdot\vec{A}\right] + \psi^*\psi\partial_t V \tag{A.23}$$

The term $\mathrm{Im}\left[\psi^*\vec{\nabla}\psi\right]$ being part of the expression of the particle current $\vec{j}$ (*c.f.* A.1), we can do the replacement:

$$S = \frac{1}{2m}\left[-2\hbar q\,\partial_t\vec{A}\cdot\left[\frac{m}{\hbar}\vec{j} + \frac{q}{\hbar}\cancel{\psi^*\psi\vec{A}}\right] + \cancel{2\psi^*\psi q^2\,\partial_t\vec{A}\cdot\vec{A}}\right] + \psi^*\psi\partial_t V \tag{A.24}$$

$$= q\vec{j}\cdot(-\partial_t\vec{A}) + \partial_t V\rho \tag{A.25}$$

A.2.3. Hamiltonian energy source: discrete

To give an expression for the source term $S_i = \mathrm{Re}\left[\psi_i^*\partial_t\hat{h}[\psi]_i\right]$, we need to express $\partial_t\hat{h}$ from (4.82):

$$h_{ij} = \begin{cases} q\,\partial_t\phi_i + \sum\limits_{\alpha=x,y,z}\mathrm{i}\frac{\hbar q}{4ma}\left(\partial_t A^\alpha_{n_\alpha(i)} - \partial_t A^\alpha_{p_\alpha(i)}\right) + \frac{q^2}{m}\left(\partial_t A^\alpha_i\right)A^\alpha_i & \text{for} \quad j = i \\ +\mathrm{i}\frac{\hbar q}{2ma}\partial_t A^\alpha_i & \text{for} \quad j = n_\alpha(i) \\ -\mathrm{i}\frac{\hbar q}{2ma}\partial_t A^\alpha_i & \text{for} \quad j = p_\alpha(i) \\ 0 & \text{otherwise} \end{cases} \tag{A.26}$$

The onsite term is:

$$\mathrm{Re}[\psi_i^*\partial_t h_{ii}\psi_i] = q\,\partial_t\phi_i\psi_i^*\psi_i + \sum_{\alpha=x,y,z}\frac{q^2}{m}\left(\partial_t A^\alpha_i\right)A^\alpha_i\psi_i^*\psi_i \tag{A.27}$$

The hopping terms are:

$$\sum_{j\neq i}\mathrm{Re}\left[\psi_i^*\partial_t h_{ij}\psi_j\right] = \sum_{\alpha=x,y,z}\mathrm{Re}\left[\mathrm{i}\frac{\hbar q}{2ma}\partial_t A^\alpha_i\psi_i^*\left[\psi_{n_\alpha(i)} - \psi_{p_\alpha(i)}\right]\right] \tag{A.28}$$

$$= \sum_{\alpha=x,y,z} -q\partial_t A^\alpha_i\,\frac{\hbar}{2ma}\mathrm{Im}\left[\psi_i^*\left[\psi_{n_\alpha(i)} - \psi_{p_\alpha(i)}\right]\right] \tag{A.29}$$

The source term is then:

$$S_i = q\,\partial_t\phi_i\,\psi_i^*\psi_i + \sum_{\alpha=x,y,z} -q\partial_t A^\alpha_i\,\frac{\hbar}{2ma}\mathrm{Im}\left[\psi_i^*\left[\psi_{n_\alpha(i)} - \psi_{p_\alpha(i)}\right]\right] + \frac{q^2}{m}\left(\partial_t A^\alpha_i\right)A^\alpha_i\psi_i^*\psi_i \tag{A.30}$$

$$= q\,\partial_t\phi_i\,\psi_i^*\psi_i + \sum_{\alpha=x,y,z} -\partial_t A^\alpha_i\,q\underbrace{\left(\frac{\hbar}{2ma}\mathrm{Im}\left[\psi_i^*\left[\psi_{n_\alpha(i)} - \psi_{p_\alpha(i)}\right]\right] - \frac{q}{m}A^\alpha_i\psi_i^*\psi_i\right)}_{j_i^\alpha} \tag{A.31}$$

Where we recognize the expression of the component along the α axis j_i^α of the particle current $\vec{j}$, from equation (A.12):

$$S_i = q\,\partial_t\phi_i\,\psi_i^*\psi_i + \sum_{\alpha=x,y,z} -\partial_t A^\alpha_i\,qj_i^\alpha = q\,\partial_t\phi_i\,\rho_i - \partial_t\vec{A}_i\cdot q\vec{j}_i \tag{A.32}$$

Appendix B. Second quantization tight-binding derivations

This appendix is reserved to derivations done with the lesser Green functions $G^<$ in a second quantization approach. We derive the particle and energy conservation equations in discrete/tightbinding systems.

B.1. Particle current

This appendix is dedicated to the derivations of the main equations of Sec. 4.3. The second quantization approach is used. In particular, we derive the particle and energy conservation equations in tight-binding systems as well as the expressions of the particle and energy currents and source power. They are expressed in terms of the lesser Green's function $G^<_{ji}(t,t)$. We also show the convergence of the currents to their static limits (when the external time-dependent electromagnetic field becomes stationary at long times) using the wavefunction approach introduced in Chapter 5.

B.1.1. Derivation of the particle current

We shortly derive here the expression of the particle current I^{N}_{ij}, given in Eq. (4.161), that flows from site i to site j, in second quantization.

We start by developing $\left[\hat{H},\hat{\rho}_i\right]$, the explicit time dependence of all terms is omitted for compactness:

$$\left[\hat{H},\hat{\rho}_i\right] = \sum_{j,k} h_{jk}\left[\hat{c}_j^\dagger\hat{c}_k, \hat{c}_i^\dagger\hat{c}_i\right] \tag{B.1}$$

A general relation between commutators helps us rewrite the commutator in the previous equation as the following:

$$\left[\hat{c}_1^\dagger\hat{c}_2, \hat{c}_3^\dagger\hat{c}_4\right] = \hat{c}_1^\dagger\left[\hat{c}_2,\hat{c}_3^\dagger\right]\hat{c}_4 + \left[\hat{c}_1^\dagger,\hat{c}_3^\dagger\right]\hat{c}_2\hat{c}_4 + \hat{c}_3^\dagger\hat{c}_1^\dagger\left[\hat{c}_2,\hat{c}_4\right] + \hat{c}_3^\dagger\left[\hat{c}_1^\dagger,\hat{c}_4\right]\hat{c}_2 \tag{B.2}$$

Using the commutation relations Eq. (4.122), the above equation simplifies to

$$\left[\hat{c}_1^\dagger\hat{c}_2, \hat{c}_3^\dagger\hat{c}_4\right] = \delta_{23}\hat{c}_1^\dagger\hat{c}_4 - \delta_{41}\hat{c}_3^\dagger\hat{c}_2 \tag{B.3}$$

from which we obtain

$$\left[\hat{H},\hat{\rho}_i\right] = \sum_j h_{ji}\hat{c}_j^\dagger\hat{c}_i - h_{ij}\hat{c}_i^\dagger\hat{c}_j \tag{B.4}$$

Taking its expectation value gives rise to the terms with the lesser Green functions $G^<$ in Eq. (4.142) and obtain Eq. (B.1)

B.1.2. Convergence to the static limit

Note: This section has been adapted from our published article [96].

We derive the connection, given in Eq. (5.40a), between the Landauer-Büttiker formula for the particle current and the generic lead particle current we give in Eq. (4.203), when the Hamiltonian $\hat{H}(t)$ defined in Sec. 5.2.1 converges to a static limit $\hat{H}(t \to \infty) = \hat{H}^{\bar{st}}$ at long times.

First, we focus first on the static problem defined by $\hat{H}^{\bar{st}}$ for all times. The local particle current for this static problem is given by Eq. (5.30)

$$I_{ji}^{\mathrm{N},\bar{\mathrm{st}}} = 2 \sum_{\lambda=\beta,m_\beta,E} f_{\mu_\beta+eV_\beta,T_\beta}(E)\,\mathrm{Im}\Big[\Big[\Psi_j^{\lambda,\bar{st}}\Big]^*\, h_{ji}^{\bar{st}}\, \Psi_i^{\lambda,\bar{st}}\Big] \tag{B.5}$$

where the shorthand notation $\sum_\lambda$ is defined in Eq. (5.27), $\Psi_j^{\lambda,\bar{st}}$ is the stationary scattering state, computed at site i, that corresponds to an incoming mode n in lead $\mathcal{L}_\beta$ with energy E, as defined in Eq. (5.8) (but here in discrete space). Note that the static electric potential V_β is included in the leads (*i.e* $h_{ii}^{\bar{st}} = h_{ii}^0 + qV_\beta$ if $i \in \mathcal{L}_\beta$) and in the reservoirs through the Fermi-Dirac distribution. We now make use of the periodic pattern of each semi-infinite lead built of identical unit cells, labeled $x = 1, 2, ...$ from the scattering region. In the stationary case, the total particle current $I_\beta^{N,\bar{st}}$ in the lead $\mathcal{L}_\beta$ (given by Eqs.(4.203) and (B.5)) is invariant along the lead axis and we have for any a

$$I_\beta^{\mathrm{N},\bar{\mathrm{st}}} = -2 \sum_{\lambda=\beta,m_\beta,E} f_{\mu_\beta+eV_\beta,T_\beta}(E)\,\mathrm{Im}\Big[\Big(\mathbf{\Psi}_{x-1}^{\lambda,\bar{st}}\Big)^\dagger \mathbf{W}_\beta\, \mathbf{\Psi}_x^{\lambda,\bar{st}}\Big] \tag{B.6}$$

$\mathbf{\Psi}_\beta^{\lambda,\bar{st}}$ being the vectorial value scattering state in the a-th cell of the lead $\mathcal{L}_\beta$ and $\mathbf{W}_\alpha$ the coupling matrix connecting neighboring unit cells in $\mathcal{L}_\alpha$ (see Fig. 5.5). Using the notations of Ref.[66], we write the scattering state $\mathbf{\Psi}_x^{\lambda,\bar{\mathrm{st}}}$ as a superposition of plane waves

$$\begin{aligned}\mathbf{\Psi}_{\alpha,x}^{m_\beta E,\bar{st}} =& \delta_{\alpha\beta}\frac{\boldsymbol{\xi}_{m_\beta}^{in}}{\sqrt{\hbar|v_{m_\beta}^{in}|}}e^{-ik_{m_\beta}^{in}x} \\ &+ \sum_{m_\alpha}\frac{\boldsymbol{\xi}_{m_\alpha}^{out}}{\sqrt{\hbar|v_{m_\alpha}^{out}|}}e^{ik_{m_\alpha}^{out}x}d_{m_\alpha m_\beta}^{\alpha\beta}\end{aligned} \tag{B.7}$$

where the sum runs over the modes m_α in lead $\mathcal{L}_\alpha$. The vectors $\boldsymbol{\xi}_{\alpha,m_\alpha}^{in}(E)$ and $\boldsymbol{\xi}_{\alpha,m_\alpha}^{out}(E)$ defined on one unit cell are the transverse parts of the incoming and outgoing modes m_α with energy E in lead $\mathcal{L}_\alpha$. $k_{m_\alpha}^{in}(E)$, $k_{m_\alpha}^{out}(E)$, and $v_{\alpha,m_\alpha}^{in}(E)$, $v_{\alpha,m_\alpha}^{out}(E)$ are the corresponding mode momenta and velocities. $d_{m_\alpha m_\beta}^{\alpha\beta}(E)$ is the scattering amplitude of an electron injected at energy E from the lead $\mathcal{L}_\beta$ in mode m_β into the mode m_α in lead $\mathcal{L}_\alpha$, as defined in Eq. (5.8) (with $d^{\alpha,\alpha} = r^\alpha$). By inserting Eq. (B.7) into Eq. (B.6) and by using the relations [206, 66]

$$i(\boldsymbol{\xi}_{m_\alpha}^{in})^\dagger[e^{-ik_{n_\alpha}^{in}}\mathbf{W}_\alpha - e^{ik_{m_\alpha}^{in}}\mathbf{W}_\alpha^\dagger]\boldsymbol{\xi}_{n_\alpha}^{in} = \delta_{n_\alpha m_\alpha}\hbar v_{m_\alpha}^{in} \tag{B.8}$$

$$i(\boldsymbol{\xi}_{m_\alpha}^{out})^\dagger[e^{ik_{n_\alpha}^{out}}\mathbf{W}_\alpha - e^{-ik_{m_\alpha}^{out}}\mathbf{W}_\alpha^\dagger]\boldsymbol{\xi}_{n_\alpha}^{out} = \delta_{n_\alpha m_\alpha}\hbar v_{m_\alpha}^{out} \tag{B.9}$$

$$i(\boldsymbol{\xi}_{m_\alpha}^{out})^\dagger[e^{-ik_{n_\alpha}^{in}}\mathbf{W}_\alpha - e^{-ik_{m_\alpha}^{out}}\mathbf{W}_\alpha^\dagger]\boldsymbol{\xi}_{n_\alpha}^{in} = 0 \tag{B.10}$$

it can be shown that $I_\alpha^{\mathrm{N},\bar{\mathrm{st}}}$ reduces to the standard Landauer-Büttiker formula

$$I_\alpha^{\mathrm{N},\bar{\mathrm{st}}} = \sum_{\beta\neq\alpha}\int\frac{\mathrm{d}E}{h}\,\bar{T}_{\alpha\beta}(E)[f_{\mu_\alpha+eV_\alpha,T_\alpha}(E) - f_{\mu_\beta+eV_\beta,T_\beta}(E)] \tag{B.11}$$

where $\bar{T}_{\alpha\beta} = \sum_{m_\alpha} \sum_{m_\beta} |d^{\alpha\beta}_{m_\alpha,m_\beta}|^2$.

Let us now consider the time-dependent problem defined by $\hat{H}(t)$. In that case, the local particle current $I^N_{ji}(t)$ given by Eq. (4.203) reads

$$I^{\mathrm{N}}_{ji}(t) = 2 \sum_{\lambda=\beta,m_\beta,E} f_{\mu_\beta,T_\beta}(E)\, \mathrm{Im}\left[\Psi^\lambda_j(t)^* h_{ji}(t) \Psi^\lambda_i(t)\right] . \tag{B.12}$$

To calculate $I^N_{ji}(t \to \infty)$ using $\hat{H}(t \to \infty) = \hat{H}^{\bar{st}}$, it is important to notice first that E in the equation above labels the energy of an incoming mode m_β in lead $\mathcal{L}_\beta$ in the remote past *i.e* for $t \leq t_0$. In that case, the on-site potential in $\mathcal{L}_\beta$ is $h_{ii}(t \leq t_0) = h^0_{ii}$ while $h^{\bar{st}}_{ii} = h^0_{ii} + qV_\beta$ (if $i \in \mathcal{L}_\beta$). For this reason the time-dependent scattering states converges to a stationary, energy shifted, scattering state

$$e^{i\theta_E(t)}\, \Psi_j^{\lambda=\beta,m_\beta,E}(t) \xrightarrow[t\to\infty]{} \Psi_j^{\lambda=(\beta,m_\beta,E+qV_\beta),\bar{st}} \tag{B.13}$$

where $\theta_E(t)$ is an (irrelevant) spatially constant phase. Doing the change of variable $E' = E + eV_\beta$ in Eq. (B.12) and comparing with Eq. (B.5), we find $I^N_{ji}(t \to \infty) = I^{N,\bar{st}}_{ji}$. We deduce Eq. (5.40a) by using Eqs. (4.203) and (B.11).

B.2. Total energy current

B.2.1. Deriving our definition

In Sec. 4.3.3.4 we have given the expression we chose for the total energy current. We give more details here on its derivation. We start from the continuity equation (4.186) and start from identification of the divergence of the energy current:

$$\sum_j I^\varepsilon_{ij}(t) = -\frac{\mathrm{i}}{\hbar} \left\langle [\hat{\mathcal{E}}(t), \hat{\mathcal{E}}_i(t)] \right\rangle \tag{B.14}$$

To come up with an expression for $I^\varepsilon_{ij}(t)$, we start by expanding $\left[\hat{\mathcal{E}}, \hat{\mathcal{E}}_i\right]$:

$$\left[\hat{\mathcal{E}}, \hat{\mathcal{E}}_i\right] = \left[\sum_{kl} \varepsilon_{kl} \hat{c}^\dagger_k \hat{c}_l \,,\, \frac{1}{2} \sum_j \varepsilon_{ij} \hat{c}^\dagger_i \hat{c}_j + \varepsilon_{ji} \hat{c}^\dagger_j \hat{c}_i \right] \tag{B.15}$$

$$= \frac{1}{2} \sum_{k,l,j} \varepsilon_{kl} \left(\varepsilon_{ij} [\hat{c}^\dagger_k \hat{c}_l, \hat{c}^\dagger_i \hat{c}_j] + \varepsilon_{ji} [\hat{c}^\dagger_k \hat{c}_l, \hat{c}^\dagger_j \hat{c}_i] \right) \tag{B.16}$$

then we use Eq. (B.3)

$$\begin{aligned}
\left[\hat{\mathcal{E}}, \hat{\mathcal{E}}_i\right] &= \frac{1}{2}\sum_{k,l,j} \varepsilon_{kl}\varepsilon_{ij}\delta_{li}\hat{c}_k^\dagger\hat{c}_j - \varepsilon_{kl}\varepsilon_{ij}\delta_{kj}\hat{c}_i^\dagger\hat{c}_l + \varepsilon_{kl}\varepsilon_{ji}\delta_{lj}\hat{c}_k^\dagger\hat{c}_i - \varepsilon_{kl}\varepsilon_{ji}\delta_{ki}\hat{c}_j^\dagger\hat{c}_l \\
&= \frac{1}{2}\sum_{k,l,j} \left[\varepsilon_{kl}\varepsilon_{ij}\delta_{li}\hat{c}_k^\dagger\hat{c}_j + \varepsilon_{kl}\varepsilon_{ji}\delta_{lj}\hat{c}_k^\dagger\hat{c}_i\right] - \frac{1}{2}\sum_{k,l,j} \left[\varepsilon_{kl}\varepsilon_{ij}\delta_{kj}\hat{c}_i^\dagger\hat{c}_l + \varepsilon_{kl}\varepsilon_{ji}\delta_{ki}\hat{c}_j^\dagger\hat{c}_l\right] \\
&= \frac{1}{2}\sum_{k,j} \left[\varepsilon_{ki}\varepsilon_{ij}\hat{c}_k^\dagger\hat{c}_j \quad + \varepsilon_{kj}\varepsilon_{ji}\hat{c}_k^\dagger\hat{c}_i \quad\right] - \frac{1}{2}\sum_{l,j} \left[\varepsilon_{jl}\varepsilon_{ij}\hat{c}_i^\dagger\hat{c}_l \quad + \varepsilon_{il}\varepsilon_{ji}\hat{c}_j^\dagger\hat{c}_l\right] \\
&= \frac{1}{2}\sum_{k,j} \left[\varepsilon_{ki}\varepsilon_{ij}\hat{c}_k^\dagger\hat{c}_j \quad + \varepsilon_{kj}\varepsilon_{ji}\hat{c}_k^\dagger\hat{c}_i \quad\right] - \frac{1}{2}\sum_{k,j} \left[\varepsilon_{jk}\varepsilon_{ij}\hat{c}_i^\dagger\hat{c}_k \quad + \varepsilon_{ik}\varepsilon_{ji}\hat{c}_j^\dagger\hat{c}_k\right] \\
&= \frac{1}{2}\sum_{k,j} \left(\varepsilon_{ki}\varepsilon_{ij}\hat{c}_k^\dagger\hat{c}_j - \varepsilon_{ik}\varepsilon_{ji}\hat{c}_j^\dagger\hat{c}_k\right) + \left(\varepsilon_{kj}\varepsilon_{ji}\hat{c}_k^\dagger\hat{c}_i - \varepsilon_{jk}\varepsilon_{ij}\hat{c}_i^\dagger\hat{c}_k\right)
\end{aligned} \tag{B.17}$$

The expectation value is

$$\begin{aligned}
\left\langle\left[\hat{\mathcal{E}}, \hat{\mathcal{E}}_i\right]\right\rangle &= -\mathrm{i}\frac{1}{2}\sum_{k,j} \left(\varepsilon_{ki}\varepsilon_{ij}G^<_{jk} - \varepsilon_{ik}\varepsilon_{ji}G^<_{kj}\right) + \left(\varepsilon_{kj}\varepsilon_{ji}G^<_{ik} - \varepsilon_{jk}\varepsilon_{ij}G^<_{ki}\right) \\
&= -\mathrm{i}\frac{1}{2}\sum_{k,j} \left(\varepsilon_{ki}\varepsilon_{ij}G^<_{jk} + \left[\varepsilon_{ki}\varepsilon_{ij}G^<_{jk}\right]^*\right) + \left(\varepsilon_{kj}\varepsilon_{ji}G^<_{ik} + \left[\varepsilon_{kj}\varepsilon_{ji}G^<_{ik}\right]^*\right) \\
&= -\mathrm{i}\sum_{k,j} \mathrm{Re}\left[\varepsilon_{ki}\varepsilon_{ij}G^<_{jk} + \varepsilon_{kj}\varepsilon_{ji}G^<_{ik}\right]
\end{aligned} \tag{B.18}$$

from which we finally obtain:

$$\frac{\mathrm{i}}{\hbar}\left\langle\left[\hat{\mathcal{E}}, \hat{\mathcal{E}}_i\right]\right\rangle = \frac{1}{\hbar}\sum_{kj} \mathrm{Re}\left[\varepsilon_{ki}\varepsilon_{ij}G^<_{jk} + \varepsilon_{kj}\varepsilon_{ji}G^<_{ik}\right] \tag{B.19}$$

Given the identification we made in Eq (B.14) between $\frac{\mathrm{i}}{\hbar}\left\langle\left[\hat{\mathcal{E}}, \hat{\mathcal{E}}_i\right]\right\rangle$ and the current divergence $\sum_j I^\varepsilon_{ij}(t)$, the sum on the right hand side of the equation (B.19) gives $\mathrm{Re}\left[\varepsilon_{ki}\varepsilon_{ij}G^<_{jk} + \varepsilon_{kj}\varepsilon_{ji}G^<_{ik}\right]$ as a first candidate for $I^\varepsilon_{ij}(t)$[1]. We notice that this first candidate is invariant when i and j are swapped, therefore we would not have $I^\varepsilon_{ij}(t) = -I^\varepsilon_{ji}(t)$ with this expression as-is. Swapping the sign of the first term, *i.e.* $\mathrm{Re}\left[-\varepsilon_{ki}\varepsilon_{ij}G^<_{jk} + \varepsilon_{kj}\varepsilon_{ji}G^<_{ik}\right]$, would fit that constraint. To prove that this term is also correct, we need to prove that the divergence of this new candidate gives the correct result

$$\frac{\mathrm{i}}{\hbar}\left\langle\left[\hat{\mathcal{E}}, \hat{\mathcal{E}}_i\right]\right\rangle \overset{?}{=} \frac{1}{\hbar}\sum_{kj} \mathrm{Re}\left[-\varepsilon_{ki}\varepsilon_{ij}G^<_{jk} + \varepsilon_{kj}\varepsilon_{ji}G^<_{ik}\right] \tag{B.20}$$

To prove the above equation, we will prove instead that $\sum_{kj} \varepsilon_{ki}\varepsilon_{ij}G^<_{jk} \in \mathrm{i}\mathbb{R}$ so its real part gives zero. Let's write its complex conjugate and prove it is equal to its opposite

$$\left[\sum_{kj} \varepsilon_{ki}\varepsilon_{ij}G^<_{jk}\right]^* = \sum_{kj} \varepsilon^*_{ki}\varepsilon^*_{ij}\left(G^<_{jk}\right)^* \tag{B.21}$$

[1] It is theoretically also possible to identify the j index in $\sum_j I^\varepsilon_{ij}(t)$ with the k index in $\sum_{jk} \mathrm{Re}\left[\varepsilon_{ki}\varepsilon_{ij}G^<_{jk} + \varepsilon_{kj}\varepsilon_{ji}G^<_{ik}\right]$

The total energy operator $\hat{\mathcal{E}}$ is hermitian thus it coefficients verify $\varepsilon^*_{ab} = \varepsilon_{ba}$ (Eq. (4.131)). The Lesser Green Function verifies $G^<_{jk}(t)^* = -G^<_{kj}(t)$ (Eq. (4.146))

$$\left[\sum_{kj} \varepsilon_{ki}\varepsilon_{ij}G^<_{jk}\right]^* = -\sum_{kj} \varepsilon_{ik}\varepsilon_{ji}G^<_{kj} \overset{k\leftrightarrow j}{=} -\sum_{jk} \varepsilon_{ij}\underbrace{\varepsilon_{ki}}_{\in\mathbb{C}} G^<_{jk} = -\sum_{jk} \varepsilon_{ki}\varepsilon_{ij}G^<_{jk} \tag{B.22}$$

Therefore the following equation is verified

$$\frac{\mathrm{i}}{\hbar}\left\langle\left[\hat{\mathcal{E}}, \hat{\mathcal{E}}_i\right]\right\rangle = \frac{1}{\hbar}\sum_{kj} \mathrm{Re}\left[-\varepsilon_{ki}\varepsilon_{ij}G^<_{jk} + \varepsilon_{kj}\varepsilon_{ji}G^<_{ik}\right] \tag{B.23}$$

and gives the expression for the total energy current Eq. (4.191)

$$I^{\varepsilon}_{ij} = -\frac{1}{\hbar}\sum_{k} \mathrm{Re}\left[-\varepsilon_{ki}\varepsilon_{ij}G^<_{jk} + \varepsilon_{kj}\varepsilon_{ji}G^<_{ik}\right] \tag{B.24}$$

B.2.2. Deriving the energy current of Ref. [129]

Ref. [210, 129] defines the energy current for the Hamiltonian operator as

$$\bar{I}^{\mathrm{H}}_{ij} = \frac{\mathrm{i}}{\hbar}\left\langle[\hat{H}_i, \hat{H}_j]\right\rangle \tag{B.25}$$

where $\hat{H}_i$ are onsite many-body Hamiltonian operators defined in Eq. (4.170) with $\epsilon \to h$. We can replace these onsite Hamiltonian operators $\hat{H}_i$ with the onsite total energy operators $\hat{\mathcal{E}}_i$ and define a total energy current analog

$$\bar{I}^{\varepsilon}_{ij} = \frac{\mathrm{i}}{\hbar}\left\langle[\hat{\mathcal{E}}_i, \hat{\mathcal{E}}_j]\right\rangle \tag{B.26}$$

Given that we have identified the energy current divergence expression in Eq. (4.186), this candidate also gives the correct divergence

$$\sum_j \bar{I}^{\varepsilon}_{ij}(t) = -\frac{\mathrm{i}}{\hbar}\left\langle[\hat{\mathcal{E}}(t), \hat{\mathcal{E}}_i(t)]\right\rangle \tag{B.27}$$

We will derive in what follows the explicit expression of this energy current candidate

$$\bar{I}^{\varepsilon}_{ij} = \frac{1}{2\hbar}\sum_{k} \mathrm{Re}\left[\varepsilon_{ik}\varepsilon_{kj}G^<_{ji} + \varepsilon_{ij}\varepsilon_{jk}G^<_{ki} + \varepsilon_{ki}\varepsilon_{ij}G^<_{jk}\right] \tag{B.28}$$

Note that we obtain the expression its Hamiltonian counterpart by simply replacing the total energy operator coefficients $\varepsilon_a b$ with the Hamiltonian coefficients h_{ab}. The following derivation proves the expression for both the Hamiltonian and Total energy operators.

Let's start by expanding the commutator $[\hat{\mathcal{E}}_j, \hat{\mathcal{E}}_i]$ by expressing the local onsite total energy operators from Eq. (4.170):

$$\begin{aligned}\left[\hat{\mathcal{E}}_j, \hat{\mathcal{E}}_i\right] &= \frac{1}{4}\left[\sum_k \varepsilon_{jk}\hat{c}^\dagger_j\hat{c}_k + \varepsilon_{kj}\hat{c}^\dagger_k\hat{c}_j\ ,\ \sum_l \varepsilon_{il}\hat{c}^\dagger_i\hat{c}_l + \varepsilon_{li}\hat{c}^\dagger_l\hat{c}_i\right] \\ &= \frac{1}{4}\sum_{kl} \varepsilon_{jk}\varepsilon_{il}\left[\hat{c}^\dagger_j\hat{c}_k, \hat{c}^\dagger_i\hat{c}_l\right] + \varepsilon_{jk}\varepsilon_{li}\left[\hat{c}^\dagger_j\hat{c}_k, \hat{c}^\dagger_l\hat{c}_i\right] \\ &\qquad + \varepsilon_{kj}\varepsilon_{il}\left[\hat{c}^\dagger_k\hat{c}_j, \hat{c}^\dagger_i\hat{c}_l\right] + \varepsilon_{kj}\varepsilon_{li}\left[\hat{c}^\dagger_k\hat{c}_j, \hat{c}^\dagger_l\hat{c}_i\right]\end{aligned} \tag{B.29}$$

Then we use the relation Eq. (4.124) to further simplify the commutator

$$\begin{aligned}\left[\hat{\mathcal{E}}_j, \hat{\mathcal{E}}_i\right] = \frac{1}{4}\sum_{kl} &\varepsilon_{jk}\varepsilon_{il}[\delta_{ki}\hat{c}_j^\dagger\hat{c}_l - \delta_{jl}\hat{c}_i^\dagger\hat{c}_k] + \varepsilon_{jk}\varepsilon_{li}[\delta_{kl}\hat{c}_j^\dagger\hat{c}_i - \delta_{ji}\hat{c}_l^\dagger\hat{c}_k] \\ &+ \varepsilon_{kj}\varepsilon_{il}[\delta_{ji}\hat{c}_k^\dagger\hat{c}_l - \delta_{kl}\hat{c}_i^\dagger\hat{c}_j] + \varepsilon_{kj}\varepsilon_{li}[\delta_{jl}\hat{c}_k^\dagger\hat{c}_i - \delta_{ki}\hat{c}_l^\dagger\hat{c}_j] \\ = \quad & \frac{1}{4}\sum_{k} -\varepsilon_{jk}\varepsilon_{ij}\hat{c}_i^\dagger\hat{c}_k + \varepsilon_{jk}\varepsilon_{ki}\hat{c}_j^\dagger\hat{c}_i - \varepsilon_{kj}\varepsilon_{ik}\hat{c}_i^\dagger\hat{c}_j + \varepsilon_{kj}\varepsilon_{ji}\hat{c}_k^\dagger\hat{c}_i \\ &+ \underbrace{\frac{1}{4}\sum_{l} \varepsilon_{ji}\varepsilon_{il}\hat{c}_j^\dagger\hat{c}_l - \varepsilon_{ij}\varepsilon_{li}\hat{c}_l^\dagger\hat{c}_j}_{Z} \\ &+ \underbrace{\frac{1}{4}\delta_{ji}\sum_{kl} \varepsilon_{kj}\varepsilon_{il}\hat{c}_k^\dagger\hat{c}_l - \varepsilon_{jk}\varepsilon_{li}\hat{c}_l^\dagger\hat{c}_k}_{\Omega}\end{aligned} \tag{B.30}$$

Let's show that $\Omega = 0$, let's first replace inside the sum j with i since it's zero when $i \neq j$:

$$\begin{aligned}\Omega &= \frac{1}{4}\delta_{ji}\sum_{kl} \varepsilon_{ki}\varepsilon_{il}\hat{c}_k^\dagger\hat{c}_l - \varepsilon_{ik}\varepsilon_{li}\hat{c}_l^\dagger\hat{c}_k \\ &= \frac{1}{4}\delta_{ji}\left[\sum_{kl} \varepsilon_{ki}\varepsilon_{il}\hat{c}_k^\dagger\hat{c}_l - \underbrace{\sum_{kl} \varepsilon_{ik}\varepsilon_{li}\hat{c}_l^\dagger\hat{c}_k}_{k\rightleftharpoons l}\right] \\ &= \frac{1}{4}\delta_{ji}\sum_{kl} \varepsilon_{ki}\varepsilon_{il}\hat{c}_k^\dagger\hat{c}_l - \varepsilon_{il}\varepsilon_{ki}\hat{c}_k^\dagger\hat{c}_l = 0\end{aligned} \tag{B.31}$$

We finally obtain, after replacing the dummy index l with k in the term Z

$$\begin{aligned}\left[\hat{\mathcal{E}}_j, \hat{\mathcal{E}}_i\right] = \frac{1}{4}\sum_{k} \quad &\varepsilon_{jk}\varepsilon_{ki}\hat{c}_j^\dagger\hat{c}_i - \varepsilon_{kj}\varepsilon_{ik}\hat{c}_i^\dagger\hat{c}_j \\ &+ \varepsilon_{kj}\varepsilon_{ji}\hat{c}_k^\dagger\hat{c}_i - \varepsilon_{jk}\varepsilon_{ij}\hat{c}_i^\dagger\hat{c}_k \\ &+ \varepsilon_{ji}\varepsilon_{ik}\hat{c}_j^\dagger\hat{c}_k - \varepsilon_{ij}\varepsilon_{ki}\hat{c}_k^\dagger\hat{c}_j\end{aligned} \tag{B.32}$$

This explicit expression of the commutator is then used to express the total energy current $\bar{I}_{ij}^{\varepsilon}$ given Eq. (B.26), with the help of the lesser green functions defined equation (4.145):

$$\begin{aligned}\bar{I}_{ij}^{\varepsilon} = \frac{1}{4\hbar}\sum_{k} \quad &\varepsilon_{kj}\varepsilon_{ik}G_{ji}^{<} - \varepsilon_{jk}\varepsilon_{ki}G_{ij}^{<} \\ &+ \varepsilon_{jk}\varepsilon_{ij}G_{ki}^{<} - \varepsilon_{kj}\varepsilon_{ji}G_{ik}^{<} \\ &+ \varepsilon_{ij}\varepsilon_{ki}G_{jk}^{<} - \varepsilon_{ji}\varepsilon_{ik}G_{kj}^{<}\end{aligned} \tag{B.33}$$

To further simplify the expression, we use Eq. (4.146) and Eq. (4.131) to swap indexes in some terms

$$\begin{aligned} I^{\varepsilon}_{ij} = \frac{1}{4\hbar}\sum_k \quad & \varepsilon_{kj}\varepsilon_{ik}G^{<}_{ji} + \left[\varepsilon_{kj}\varepsilon_{ik}G^{<}_{ji}\right]^* \\ & + \varepsilon_{jk}\varepsilon_{ij}G^{<}_{ki} + \left[\varepsilon_{jk}\varepsilon_{ij}G^{<}_{ki}\right]^* \\ & + \varepsilon_{ij}\varepsilon_{ki}G^{<}_{jk} + \left[\varepsilon_{ij}\varepsilon_{ki}G^{<}_{jk}\right]^* \end{aligned} \tag{B.34}$$

and we finally obtain the expression given (4.192)

$$I^{\varepsilon}_{ij} = \frac{1}{2\hbar}\sum_k \mathrm{Re}\left[\varepsilon_{kj}\varepsilon_{ik}G^{<}_{ji} + \varepsilon_{jk}\varepsilon_{ij}G^{<}_{ki} + \varepsilon_{ij}\varepsilon_{ki}G^{<}_{jk}\right] \tag{B.35}$$

B.2.3. Convergence to the static limit

Note: This section has been adapted from our published article [96].

We derive the connection, given in Eq. (5.40b), between the Landauer-Büttiker formula for the energy current and the generic lead energy current we give in Eq. (4.203), when the Hamiltonian $\hat{H}(t)$ defined in Sec. 5.2.1 converges to a static limit $\hat{H}(t\to\infty) = \hat{H}^{\bar{st}}$ at long times.

Let us consider first the static problem defined by $\hat{H}^{\bar{st}}$ for all times. For this static problem, we use the Hamiltonian based energy operator $\hat{\mathcal{E}}^h = \hat{H}^{\bar{st}}$. With this definition, the local energy current given by Eq. (5.32) simplifies to

$$I^{h,\bar{\mathrm{st}}}_{ji} = 2\sum_{\lambda=\beta,m_\beta,E} f_{\mu_\beta+eV_\beta,T_\beta}(E)\; E\;\mathrm{Im}\left[\left(\Psi^{\lambda,\bar{\mathrm{st}}}_j\right)^* h^{\bar{st}}_{ji}\,\Psi^{\lambda,\bar{\mathrm{st}}}_i\right] \tag{B.36}$$

after using the static eigenstate relation (5.6) that the stationary scattering states verify. To calculate the energy current $I^{h,\bar{st}}_{\alpha}$ in the lead $\mathcal{L}_\alpha$, it is convenient to go further away within the lead using Eq. (5.24). This does not change $I^{h,\bar{st}}_{\alpha}$ as static energy flow is constant throughout the lead. By using Eqs. (B.36) and (B.7)-(B.10), we find

$$I^{h,\bar{\mathrm{st}}}_{\alpha} = \sum_{\beta\neq\alpha}\int\frac{\mathrm{d}E}{h}\,E\,\bar{T}_{\alpha\beta}(E)[f_{\mu_\alpha+eV_\alpha,T_\alpha}(E) - f_{\mu_\beta+eV_\beta,T_\beta}(E)]\,. \tag{B.37}$$

Note that Eq. (B.37) is the usual Landauer-Büttiker formula for the lead energy current in the static case, which we recovered upon defining in this case the energy operator as the Hamiltonian $\hat{H}^{\bar{st}}$.

Let us consider on the other hand the time-dependent problem defined by $\hat{H}(t)$. We consider now the 'total energy' operator $\mathcal{E}^{\varepsilon}$, defined by Eq. (4.177). Using Eqs.(5.32), (B.13), and finally (5.6), we find for the local energy currents in the long time limit

$$I^{\varepsilon}_{ji}(t\to\infty) = I^{\varepsilon,\bar{st}}_{ji} - \frac{q}{2}(V_i+V_j)I^{\mathrm{N},\bar{\mathrm{st}}}_{ji} \tag{B.38}$$

where $V_i \equiv V_i(t\to\infty)$ is a shorthand notation for the long time limit of the external time-dependent scalar potentials $V_i(t)$. We deduce from Eq. (4.203)

$$I^{E}_{\alpha}(t\to\infty) = I^{E,\bar{st}}_{\alpha} - eV_\alpha I^{N,\bar{st}}_{\alpha} + S^{E}_{\alpha}(t\to\infty) \tag{B.39}$$

since $V_i = V_\alpha$ if $i\in\mathcal{L}_\alpha$ and $\partial_t\phi_{ij}\to 0$ (for a Hamiltonian given with a Peierls phase, given by Eq. (4.189)) in the static limit $t\to\infty$. This concludes the proof of Eq. (5.40a).

B.3. Total energy source term

In the total energy conservation equation (4.186), we defined the total energy source term as the following

$$S_i^{\varepsilon}(t) = \frac{\mathrm{i}}{\hbar}\left\langle [q\,\hat{\Phi}(t), \hat{\mathcal{E}}_i(t)]\right\rangle + \left\langle \partial_t \hat{\mathcal{E}}_i(t)\right\rangle \tag{B.40}$$

In this appendix section we further expand this expression to be able to identify the known classical form for the power $\vec{j}\cdot\vec{E}$, where $\vec{E} = -\nabla\phi - \partial_t\vec{A}$ is the electric field.

We start by expressing $[q\,\hat{\Phi}(t), \hat{\mathcal{E}}_i(t)]$ by replacing the scalar potential operator $\hat{\Phi}(t)$ with its expression Eq. (4.181) and the onsite total energy operator $\hat{\mathcal{E}}_i$ with its expression Eq. (4.170) (with $\epsilon \to \varepsilon$)

$$\begin{aligned}[q\,\hat{\Phi}(t), \hat{\mathcal{E}}_i(t)] &= \left[\sum_l q\phi_l\,\hat{c}_l^\dagger\hat{c}_l\ ,\ \frac{1}{2}\sum_j \varepsilon_{ij}\,\hat{c}_i^\dagger\hat{c}_j + \varepsilon_{ji}\,\hat{c}_j^\dagger\hat{c}_i\right] \\ &= \sum_{lj} q\phi_l\varepsilon_{ij}\,[\hat{c}_l^\dagger\hat{c}_l, \hat{c}_i^\dagger\hat{c}_j] + q\phi_l\varepsilon_{ji}\,[\hat{c}_l^\dagger\hat{c}_l, \hat{c}_j^\dagger\hat{c}_i]\end{aligned}$$

then we use Eq. (B.3)

$$\begin{aligned}[q\,\hat{\Phi}(t), \hat{\mathcal{E}}_i(t)] &= \frac{1}{2}\sum_{lj} q\phi_l\varepsilon_{ij}\,[\delta_{li}\hat{c}_l^\dagger\hat{c}_j - \delta_{jl}\hat{c}_i^\dagger\hat{c}_l] + q\phi_l\varepsilon_{ji}\,[\delta_{lj}\hat{c}_l^\dagger\hat{c}_i - \delta_{il}\hat{c}_j^\dagger\hat{c}_l] \\ &= \frac{1}{2}\sum_{j} q\varepsilon_{ij}\,[\phi_i\hat{c}_i^\dagger\hat{c}_j - \phi_j\hat{c}_i^\dagger\hat{c}_j] + q\varepsilon_{ji}\,[\phi_j\hat{c}_j^\dagger\hat{c}_i - \phi_i\hat{c}_j^\dagger\hat{c}_i] \\ &= \frac{1}{2}\sum_{j} q\phi_j[\varepsilon_{ji}\hat{c}_j^\dagger\hat{c}_i - \varepsilon_{ij}\hat{c}_i^\dagger\hat{c}_j] + q\phi_i[\varepsilon_{ij}\hat{c}_i^\dagger\hat{c}_j - \varepsilon_{ji}\hat{c}_j^\dagger\hat{c}_i]\end{aligned}$$

Its expectation value writes with the Lesser Green functions Eq. (4.145). We use directly Eq. (4.146) and Eq. (4.131) to swap indices and further simplify the result

$$\begin{aligned}\frac{\mathrm{i}}{\hbar}\left\langle [q\,\hat{\Phi}(t), \hat{\mathcal{E}}_i(t)]\right\rangle &= \frac{1}{2}\sum_{j} q\phi_j[\varepsilon_{ji}G^<_{ij} + [\varepsilon_{ji}G^<_{ij}]^*] + q\phi_i[\varepsilon_{ij}G^<_{ji} + [\varepsilon_{ij}G^<_{ji}]^*] \\ &= \sum_{j} q\phi_j \mathrm{Re}\left[\varepsilon_{ji}G^<_{ij}\right] + q\phi_i\mathrm{Re}\left[\varepsilon_{ij}G^<_{ji}\right] \\ &= \sum_{j} -q\phi_j \mathrm{Re}\left[\varepsilon_{ij}G^<_{ji}\right] + q\phi_i\mathrm{Re}\left[\varepsilon_{ij}G^<_{ji}\right]\end{aligned}$$

Given the expression of the particle current I^{N}_{ij} Eq. (4.161):

$$I^N_{ij} = 2\,\mathrm{Re}\left[h_{ij}G^<_{ji}\right] \tag{B.41}$$

we can identify particle current terms and obtain

$$\frac{\mathrm{i}}{\hbar}\left\langle [q\,\hat{\Phi}(t), \hat{\mathcal{E}}_i(t)]\right\rangle = \underbrace{\sum_j -\frac{1}{2}\left[\phi_j - \phi_i\right] qI^N_{ij}}_{-\vec{\nabla}\phi_i\,\cdot\,q\vec{j}_i}$$

where we can recover the discrete $-\vec{\nabla}\phi_i\cdot q\vec{j}_i$ if we interpret j as coming from the discretization process described Sec. 4.2.4.1 Eq. (4.76) where $j \in \{n_\alpha(i),\ \alpha = x, y, z\}$ and $\vec{j}_i$ is given by Eq. (4.89)

Now we show that $\left\langle \partial_t \hat{\mathcal{E}}_i(t) \right\rangle = -\partial_t \vec{A}_i \cdot q\vec{j}_i$. By expanding it using Eq. (4.170), Eq. (4.145) and Eq. (4.146) we obtain

$$\left\langle \partial_t \hat{\mathcal{E}}_i(t) \right\rangle = \sum_j \hbar \, \mathrm{Im}\left[\partial_t \varepsilon_{ij} G^<_{ji}\right]$$

To be able to go further, we need an explicit expression for $\partial_t \varepsilon_{ij}$. If we use the expression of h_{ij} in Eq. (4.82) derived by the discretization process Sec. 4.2.4.1, we can compute $\partial_t \varepsilon_{ij}$ by using its relation with h_{ij} given Eq. (4.105):

$$\partial_t \varepsilon_{ij} = \begin{cases} \sum\limits_{\alpha=x,y,z} \mathrm{i}\frac{\hbar q}{4ma}\left(\partial_t A^\alpha_{n_\alpha(i)} - \partial_t A^\alpha_{p_\alpha(i)}\right) + \frac{q^2}{m}(\partial_t A^\alpha_i)A^\alpha_i & \text{for} \quad j = i \\ +\mathrm{i}\frac{\hbar q}{2ma}\partial_t A^\alpha_i & \text{for} \quad j = n_\alpha(i) \\ -\mathrm{i}\frac{\hbar q}{2ma}\partial_t A^\alpha_i & \text{for} \quad j = p_\alpha(i) \\ 0 & \text{otherwise} \end{cases} \tag{B.42}$$

Given that $G^<_{ii}$ is a pure imaginary number, and that only the imaginary part of $\partial_t \varepsilon_{ii} G^<_{ii}$ gives rise to a non zero term, we get for $\mathrm{Im}[\partial_t \varepsilon_{ii} G^<_{ii}]$:

$$\mathrm{Im}[\partial_t \varepsilon_{ii} G^<_{ii}] = \sum_{\alpha=x,y,z} \mathrm{Im}\left[\frac{q^2}{m}(\partial_t A^\alpha_i)A^\alpha_i G^<_{ii}\right] \tag{B.43}$$

The hoppings terms are:

$$\sum_{j\neq i} \mathrm{Im}\left[\partial_t \varepsilon_{ij} G^<_{ji}\right] = \sum_{\alpha=x,y,z} \mathrm{Im}\left[\mathrm{i}\frac{\hbar q}{2ma}\partial_t A^\alpha_i \left(G^<_{n_\alpha(i),i} - G^<_{p_\alpha(i),i}\right)\right] \tag{B.44}$$

The sum of both is then:

$$\sum_{j} \mathrm{Im}\left[\partial_t \varepsilon_{ij} G^<_{ji}\right] = \sum_{\alpha=x,y,z} \mathrm{Im}\left[\frac{q^2}{m}(\partial_t A^\alpha_i)A^\alpha_i G^<_{ii} + \mathrm{i}\frac{\hbar q}{2ma}\partial_t A^\alpha_i \left(G^<_{n_\alpha(i),i} - G^<_{p_\alpha(i),i}\right)\right] \tag{B.45}$$

We now need to replace $G^<_{ii}$ with $\frac{1}{2}\left[G^<_{n_\alpha(i),i} + G^<_{p_\alpha(i),i}\right]$, which must be the case since a is the step taken to perform finite differences to define the operator $\vec{\nabla}$ Eq. (4.80):

$$\begin{aligned}\sum_{j} \mathrm{Im}\left[\partial_t \varepsilon_{ij} G^<_{ji}\right] = \sum_{\alpha=x,y,z} \mathrm{Im}\Bigg[&\frac{q^2}{2m}(\partial_t A^\alpha_i)A^\alpha_i \left[G^<_{n_\alpha(i),i} + G^<_{p_\alpha(i),i}\right] \\ &+ \mathrm{i}\frac{\hbar q}{2ma}\partial_t A^\alpha_i \left(G^<_{n_\alpha(i),i} - G^<_{p_\alpha(i),i}\right)\Bigg]\end{aligned}$$

$$\begin{aligned}\sum_{j} \mathrm{Im}\left[\partial_t \varepsilon_{ij} G^<_{ji}\right] = \sum_{\alpha=x,y,z} \partial_t A^\alpha_i q \mathrm{Im}\Bigg[&\mathrm{i}\left(\frac{\hbar}{2ma} - \mathrm{i}\frac{q}{2m}A^\alpha_i\right) G^<_{n_\alpha(i),i} \\ &- \mathrm{i}\left(\frac{\hbar}{2ma} + \mathrm{i}\frac{q}{2m}A^\alpha_i\right) G^<_{p_\alpha(i),i}\Bigg]\end{aligned}$$

h_{ab} terms given Eq. (4.82) can be identified

$$\sum_j \mathrm{Im}\left[\partial_t \varepsilon_{ij} G^<_{ji}\right] = \sum_{\alpha=x,y,z} \partial_t A^\alpha_i q \frac{a}{\hbar} \mathrm{Im}\Bigg[\mathrm{i} \underbrace{\left(\frac{\hbar^2}{2ma^2} - \mathrm{i}\frac{\hbar q}{2ma} A^\alpha_i\right)}_{h_{i,n_\alpha(i)}} G^<_{n_\alpha(i),i} - \mathrm{i} \underbrace{\left(\frac{\hbar^2}{2ma^2} + \mathrm{i}\frac{\hbar q}{2ma} A^\alpha_i\right)}_{h_{i,p_\alpha(i)}} G^<_{p_\alpha(i),i} \Bigg]$$

Particle current terms I^N_{ij} given Eq. (4.161) can be identified then replaced with the discrete particle current vector field $\vec{j}_i$ given Eq. (4.89)

$$\begin{aligned}
\sum_j \mathrm{Im}\left[\partial_t \varepsilon_{ij} G^<_{ji}\right] &= \sum_{\alpha=x,y,z} \partial_t A^\alpha_i q \frac{a}{\hbar} \mathrm{Im}\left[\mathrm{i} h_{i,n_\alpha(i)} G^<_{n_\alpha(i),i} - \mathrm{i} h_{i,p_\alpha(i)} G^<_{p_\alpha(i),i}\right] \\
&= \frac{1}{\hbar} \sum_{\alpha=x,y,z} -\partial_t A^\alpha_i q \frac{a}{2} \Bigg[\underbrace{2\,\mathrm{Re}\left[h_{i,n_\alpha(i)} G^<_{n_\alpha(i),i}\right]}_{I^N_{i,n_\alpha(i)}} - \underbrace{2\,\mathrm{Re}\left[h_{i,p_\alpha(i)} G^<_{p_\alpha(i),i}\right]}_{I^N_{i,p_\alpha(i)}} \Bigg] \\
&= \frac{1}{\hbar} \sum_{\alpha=x,y,z} -\partial_t A^\alpha_i q \underbrace{\frac{a}{2}\left[I^N_{i,n_\alpha(i)} - I^N_{i,p_\alpha(i)}\right]}_{j^\alpha_i} \\
&= \sum_{\alpha=x,y,z} -\partial_t A^\alpha_i \, q j^\alpha_i \\
&= -\partial_t \vec{A}_i \cdot q\vec{j}_i
\end{aligned}$$

We have show that the source term S^ε_i is equal to the discrete classical electromagnetic power $\vec{E}_i \cdot \vec{j}_i$

$$S^\varepsilon_i = -\vec{\nabla}\phi_i \cdot \, q\vec{j}_i - \partial_t \vec{A}_i \cdot q\vec{j}_i = \vec{E}_i \cdot q\vec{j}_i \tag{B.46}$$

Appendix C. Resonant level model derivations

We derive in this appendix the main equations pertaining to the Resonant Level Model studied in Sec. 5.3.2.1 and in Chapter 6.

C.1. Resonant Level Model within the NEGF formalism

In this appendix, we give the RLM formula for the lead particle current $I_\alpha^N(t)$ and the lead heat currents $I_\alpha^Q(t)$, $\tilde{I}_\alpha^Q(t)$ that are used in Fig. 5.10 to plot the NEGF curves. The model under consideration is the one introduced in Sec. 5.3.2.1 with $\epsilon_0(t) = \epsilon_0 + eV_0\Theta(t)$ and $\epsilon_L(t) = \epsilon_R(t) = 0$. The lead Hamiltonians $\hat{H}_\alpha$ and the tunneling Hamiltonians between the dot and the leads $\hat{H}_{0\alpha}$ are written in the reciprocal space, as

$$\hat{H}_\alpha = \sum_{k_\alpha} \epsilon_{k_\alpha} \hat{c}^\dagger_{k_\alpha} \hat{c}_{k_\alpha} \tag{C.1}$$

$$\hat{H}_{0\alpha} = \sum_{k_\alpha} V_{k_\alpha} \hat{c}^\dagger_{k_\alpha} \hat{c}_0 + h.c. \tag{C.2}$$

where $\hat{c}_{k_\alpha} = \sum_{j\in\alpha} e^{ijk_\alpha} \hat{c}_j$ is the annihilation operator of an electron with momentum k_α in lead $\alpha = L$ or R, $V_{k_\alpha} = \gamma_c \sin(k_\alpha)$ the hybridization term, and $\epsilon_{k_\alpha} = -2\gamma\cos(k_\alpha)$ the dispersion relation (with a lattice spacing fixed to unity). Then the currents are calculated within the NEGF formalism under the wide-band limit approximation, *i.e* assuming that $\Gamma_\alpha(E) \equiv -2\,\mathrm{Im}\Sigma^R(E) = 2\pi \sum_{k_\alpha} |V_{k_\alpha}|^2 \delta(E - \epsilon_{k_\alpha})$ is energy independent ($\Gamma_L = \Gamma_R = \Gamma/2$). This is true in the limit $\lambda\gamma/\Gamma \gg 1$ as noticed in Sec. 5.3.2.2. We refer to the seminal paper [92] of Jauho *et al.* for the derivation of the particle current and to Refs. [38, 219, 44, 121] for its extension to the energy and heat currents. We gather here the results. Introducing the notations $\hat{K}^N_\alpha = \hat{N}_\alpha = \sum_{i\in\alpha} \hat{c}^\dagger_i \hat{c}_i$, $\hat{K}^E_\alpha = \hat{H}_\alpha + \frac{1}{2}\hat{H}_{0\alpha}$, and $\hat{K}^{\tilde{E}}_\alpha = \hat{H}_\alpha$, we have for $\lambda = N$, E and $\tilde{E}$

$$\left\langle \frac{\mathrm{d}\hat{K}^\lambda_\alpha}{\mathrm{d}t} \right\rangle = \sum_\beta \int \frac{\mathrm{d}E}{2\pi} f_\beta(E)\, \mathcal{J}^\lambda_{\alpha\beta}(E,t) \tag{C.3}$$

where the sum over β is made over both leads L and R, and

$$\mathcal{J}^N_{\alpha\beta}(E,t) = \frac{\Gamma}{\hbar}\left[\frac{\Gamma}{4}|A(E,t)|^2 + \delta_{\alpha\beta}\mathrm{Im}[A(E,t)]\right] \tag{C.4}$$

$$\mathcal{J}^{\tilde{E}}_{\alpha\beta}(E,t) = E\,\mathcal{J}^N_{\alpha\beta}(E,t) + \frac{\Gamma^2}{4}\mathrm{Im}[A(E,t)\frac{\partial A^*}{\partial t}(E,t)] \tag{C.5}$$

$$\mathcal{J}^E_{\alpha\beta}(E,t) = \mathcal{J}^{\tilde{E}}_{\alpha\beta}(E,t) + \frac{\Gamma}{2}\delta_{\alpha\beta}\mathrm{Re}\left[\frac{\partial A}{\partial t}(E,t)\right] \tag{C.6}$$

while the spectral density $A(E,t)$ reads

$$A(E,t) = \frac{E - \epsilon_0 + i\frac{\Gamma}{2} - eV_0 e^{i(E-\epsilon_0 - eV_0 + i\frac{\Gamma}{2})t/\hbar}}{(E - \epsilon_0 + i\frac{\Gamma}{2})(E - \epsilon_0 - eV_0 + i\frac{\Gamma}{2})}\,. \tag{C.7}$$

We used the formula above to plot the NEGF particle current $I_\alpha^N(t) = -\langle\frac{\mathrm{d}\hat{N}_\alpha}{\mathrm{d}t}\rangle$ and the NEGF heat currents $I_\alpha^Q(t) = -[\langle\frac{\mathrm{d}\hat{K}_\alpha^E}{\mathrm{d}t}\rangle - \mu_\alpha\langle\frac{\mathrm{d}\hat{N}_\alpha}{\mathrm{d}t}\rangle]$ and $\tilde{I}_\alpha^Q(t) = -[\langle\frac{\mathrm{d}\hat{K}_\alpha^{\tilde{E}}}{\mathrm{d}t}\rangle - \mu_\alpha\langle\frac{\mathrm{d}\hat{N}_\alpha}{\mathrm{d}t}\rangle]$ in Fig.(5.10) (circles). The integrals over the energy were computed numerically.

C.2. Spatially semi-infinite uniform voltage pulse

In Sec. 6.2, the scattering amplitudes of the time-dependent RLM are evaluated in the wideband limit by combining the scattering amplitudes of three elementary building blocks: (i) an abrupt voltage pulse in a semi-infinite lead, (ii) the stationary dot, and (iii) a (reversed) abrupt voltage pulse in the other semi-infinite lead. In this section, we compute the scattering amplitudes associated to (i) and (iii). The system is defined by the following Hamiltonian

$$h_{ij} = \begin{cases} V(t) & \text{if} \quad i = j \text{ and } i \leq 0 \\ 0 & \text{if} \quad i = j \text{ and } i > 0 \\ -\gamma_c & \text{if} \quad i,j = 0,1 \text{ or } 1,0 \\ -\gamma & \text{if} \quad i \neq j \end{cases} \tag{C.8}$$

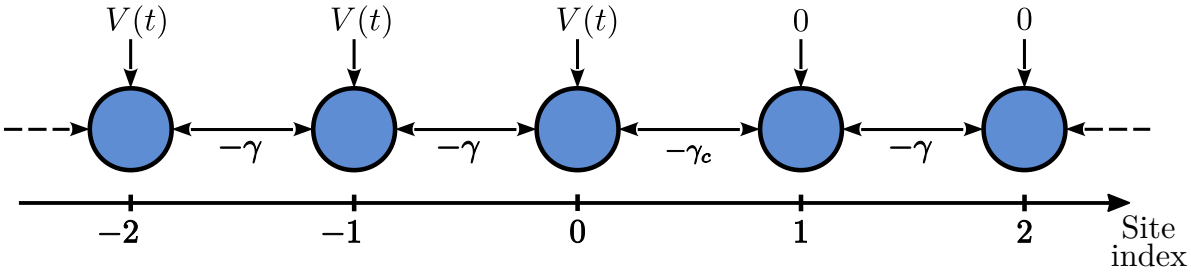

Figure C.1. – Homogenous chain with a semi infinite homogenous voltage pulse.

With the following gauge change:

$$\Lambda_i(t) = \begin{cases} \varphi(t) & \text{if} \quad i \leq 0 \\ 0 & \text{if} \quad i > 0 \end{cases} \tag{C.9}$$

where

$$\varphi(t) = -\int_{t_0}^{t} V(u)\mathrm{d}u \tag{C.10}$$

we can rewrite an equivalent gauge transformed Hamiltonian, according to Eq. (4.84)

$$h'_{ij} = \begin{cases} 0 & \text{if} \quad i = j \\ -\gamma_c e^{-\mathrm{i}\varphi(t)} & \text{if} \quad i,j = 0,1 \\ -\gamma_c e^{\mathrm{i}\varphi(t)} & \text{if} \quad i,j = 1,0 \end{cases} \tag{C.11}$$

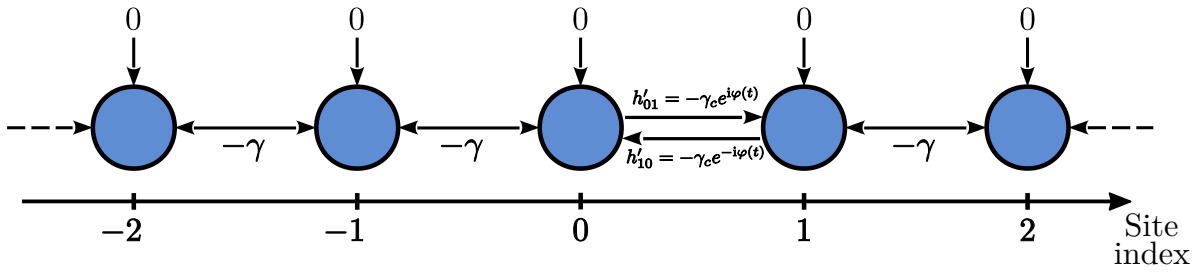

Figure C.2. – Gauge transformed system: homogenous chain with a semi infinite homogenous voltage pulse.

Transmission and reflection amplitudes

We use the gauge transformed Hamiltonian, given by the matrix elements h'_{ij} expressed in Eq. (C.11), to compute the scattering coefficients $r_{\mathrm{p}}(E', E)$ and $d_{\mathrm{p}}(E', E)$. An incoming mode $\|_{+,E,x}$ (defined in Sec 6.2.1) from the left at energy E creates a scattering state $\Psi_x^{\mathrm{L},E}$. It can be expressed in the following way, using the left-to-right transmission amplitude $d_{\mathrm{p}}(E', E)$ and the left reflection amplitude $r_{\mathrm{p}}(E', E)$

$$\Psi_x^{\mathrm{L},E} = \begin{cases} \Psi_x^{\mathrm{r,L},E} = \|_x^{+,E} + \displaystyle\int \frac{\mathrm{d}E'}{2\pi} \|_x^{-,E} \, r_{\mathrm{p}}(E', E) \text{ if } x \leq 0 \\ \Psi_x^{\mathrm{d,L},E} = \displaystyle\int \frac{\mathrm{d}E'}{2\pi} \|_{+,E',x} \, d_{\mathrm{p}}(E', E) \text{ if } x \geq 1 \end{cases} \tag{C.12}$$

We can now write the Schrödinger equation for $x = 0$ and $x = 1$ (we will omit the indexes L and E because not useful)

$$\mathrm{i}\partial_t \Psi_0^{\mathrm{r}} = -\gamma \Psi_{-1}^{\mathrm{r}} - \gamma_c \mathrm{e}^{-\mathrm{i}\varphi(t)} \Psi_1^{\mathrm{d}} \tag{C.13a}$$
$$\mathrm{i}\partial_t \Psi_1^{\mathrm{d}} = -\gamma_c \mathrm{e}^{\mathrm{i}\varphi(t)} \Psi_0^{\mathrm{r}} - \gamma \Psi_2^{\mathrm{d}} \tag{C.13b}$$

Given that Ψ_x^{r} and Ψ_x^{d} are a superposition of plane waves that satisfy the Schrödinger equation of the homogenous chain $\forall x$, Ψ_x^{r} and Ψ_x^{d} also satisfy it, in particular for $x = 0$ and $x = 1$:

$$\mathrm{i}\partial_t \Psi_0^{\mathrm{r}} = -\gamma \Psi_{-1}^{\mathrm{r}} - \gamma \Psi_1^{\mathrm{r}} \tag{C.14a}$$
$$\mathrm{i}\partial_t \Psi_1^{\mathrm{d}} = -\gamma \Psi_0^{\mathrm{d}} - \gamma \Psi_2^{\mathrm{d}} \tag{C.14b}$$

Taking the previous four equations together we obtain

$$\gamma \Psi_1^{\mathrm{r}} = \gamma_c e^{-\mathrm{i}\varphi(t)} \Psi_1^{\mathrm{d}} \tag{C.15a}$$
$$\gamma \Psi_0^{\mathrm{d}} = \gamma_c e^{\mathrm{i}\varphi(t)} \Psi_0^{\mathrm{r}} \tag{C.15b}$$

We can then replace each term by its respective expression:

$$\|_1^{+,E} + \int \frac{\mathrm{d}E'}{2\pi} \|_1^{-,E'} \, r_{\mathrm{p}}(E', E) = \frac{\gamma_c}{\gamma} e^{-\mathrm{i}\varphi(t)} \int \frac{\mathrm{d}E'}{2\pi} \|_{+,E',1} \, d_{\mathrm{p}}(E', E) \tag{C.16a}$$
$$\frac{\gamma}{\gamma_c} e^{-\mathrm{i}\varphi(t)} \int \frac{\mathrm{d}E'}{2\pi} \|_0^{+,E'} \, d_{\mathrm{p}}(E', E) = \|_0^{+,E} + \int \frac{\mathrm{d}E'}{2\pi} \|_0^{-,E'} \, r_{\mathrm{p}}(E', E) \tag{C.16b}$$

Wide band approximation To proceed further in the calculations, we will use the WBL1 approximation from the general considerations in Sec 6.2.1:

$$\mathrm{e}^{\mathrm{i}k_E^+ - \mathrm{i}Et} + \mathrm{e}^{\mathrm{i}k_E^-}\, r_\mathrm{p}(t,E) = \frac{\gamma_c}{\gamma} e^{-\mathrm{i}\varphi(t)} \mathrm{e}^{\mathrm{i}k_E^+} d_\mathrm{p}(t,E) \tag{C.17a}$$

$$\frac{\gamma}{\gamma_c} e^{-\mathrm{i}\varphi(t)} d_\mathrm{p}(t,E) = \mathrm{e}^{-\mathrm{i}Et} + r_\mathrm{p}(t,E) \tag{C.17b}$$

Using (C.17b) to replace $r_\mathrm{p}(t,E)$ in (C.17a), we get:

$$\mathrm{e}^{\mathrm{i}k_E^+ - \mathrm{i}Et} + \mathrm{e}^{\mathrm{i}k_E^-} \left(\frac{\gamma}{\gamma_c} e^{-\mathrm{i}\varphi(t)} d_\mathrm{p}(t,E) - \mathrm{e}^{-\mathrm{i}Et} \right) = \frac{\gamma_c}{\gamma} e^{-\mathrm{i}\varphi(t)} \mathrm{e}^{\mathrm{i}k_E^+} d_\mathrm{p}(t,E) \tag{C.18a}$$

$$\left[\frac{\gamma_c}{\gamma} e^{-\mathrm{i}\varphi(t)} \mathrm{e}^{\mathrm{i}k_E^+} - \mathrm{e}^{\mathrm{i}k_E^-} \frac{\gamma}{\gamma_c} e^{-\mathrm{i}\varphi(t)} \right] d_\mathrm{p}(t,E) = \mathrm{e}^{\mathrm{i}k_E^+ - \mathrm{i}Et} - \mathrm{e}^{\mathrm{i}k_E^-} \mathrm{e}^{-\mathrm{i}Et} \tag{C.18b}$$

$$e^{-\mathrm{i}\varphi(t)} \left[\frac{\gamma_c^2}{\gamma^2} \mathrm{e}^{2\mathrm{i}k_E^+} - 1 \right] d_\mathrm{p}(t,E) = \frac{\gamma_c}{\gamma} \left[\mathrm{e}^{2\mathrm{i}k_E^+} - 1 \right] \mathrm{e}^{-\mathrm{i}Et} \tag{C.18c}$$

$$d_\mathrm{p}(t,E) = \frac{\gamma_c}{\gamma} \frac{\mathrm{e}^{2\mathrm{i}k_E^+} - 1}{\frac{\gamma_c^2}{\gamma^2} \mathrm{e}^{2\mathrm{i}k_E^+} - 1} \mathrm{e}^{\mathrm{i}\varphi(t) - \mathrm{i}Et} \tag{C.18d}$$

$$\int \frac{\mathrm{d}E'}{2\pi}\, d_\mathrm{p}(t,E) \mathrm{e}^{\mathrm{i}E't} = \frac{\gamma_c}{\gamma} \frac{\mathrm{e}^{2\mathrm{i}k_E^+} - 1}{\frac{\gamma_c^2}{\gamma^2} \mathrm{e}^{2\mathrm{i}k_E^+} - 1} \int \frac{\mathrm{d}E'}{2\pi}\, \mathrm{e}^{\mathrm{i}\varphi(t) - \mathrm{i}(E-E')t} \tag{C.18e}$$

Which finally gives

$$d_\mathrm{p}(E',E) = \frac{\gamma_c}{\gamma} \frac{\mathrm{e}^{2\mathrm{i}k_E^+} - 1}{\frac{\gamma_c^2}{\gamma^2} \mathrm{e}^{2\mathrm{i}k_E^+} - 1} K^*(E - E') \tag{C.19}$$

where K is the fourier transform of $\mathrm{e}^{-\mathrm{i}\varphi}$

$$K(U) = \int \mathrm{d}t\, \mathrm{e}^{iUt - i\varphi(t)} \tag{C.20}$$

It is important to note that the calculations and results of this section have been done, and in a more general way, in [63, Chapter 4]. Given that that the previous approximation also implies that $\cos(k_E) = 0$ and $\sin(k_E) = 1$, the previous expression simplifies to:

$$d_\mathrm{p}(E',E) = K^*(E - E') \frac{2\gamma_c \gamma}{\gamma^2 + \gamma_c^2} \tag{C.21a}$$

$$r_\mathrm{p}(E',E) = \left[\frac{2\gamma_c \gamma}{\gamma^2 + \gamma_c^2} - 1 \right] 2\pi\delta(E - E') \tag{C.21b}$$

When $\gamma = \gamma_c$, we get:

$$d_\mathrm{p}(E',E) = K^*(E - E') \tag{C.22a}$$

$$r_\mathrm{p}(E',E) = 0 \tag{C.22b}$$

For the right incoming modes, the right transmission amplitude $d'_\mathrm{p}(E',E)$ is related to the left transmission amplitude $d_\mathrm{p}(E',E)$:

$$d'_\mathrm{p}(E',E) = d_\mathrm{p}(E,E')^* \tag{C.23}$$

C.3. A relation between the reflection and the transmission amplitudes

We now come back to the whole system and derive the relation (6.53) that links the transmission amplitude $d(E', E)$ and the reflection amplitude $r(E', E)$. Note that the scattering amplitudes are introduced in the scattering states $\Psi^{\lambda=\alpha,E}$ in Eq. (6.33) and their Fourier transform is defined in Eq. (6.51).

Let's write the Schrödinger equation on site -1 and site 1, for the left scattering state:

$$\begin{aligned} \mathrm{i}\partial_t \Psi_{\mathrm{L},E,-1} &= -\gamma\, \Psi^{\mathrm{L},E}_{-2} - \gamma_c\, \Psi^{\mathrm{L},E}_{0} \\ \mathrm{i}\partial_t \Psi^{\mathrm{L},E}_{1} &= -\gamma\, \Psi^{\mathrm{L},E}_{2} - \gamma_c\, \Psi^{\mathrm{L},E}_{0} \end{aligned}$$

Which gives the following relation:

$$\mathrm{i}\partial_t \Psi^{\mathrm{L},E}_{-1} + \gamma\, \Psi^{\mathrm{L},E}_{-2} = \mathrm{i}\partial_t \Psi^{\mathrm{L},E}_{1} + \gamma\, \Psi^{\mathrm{L},E}_{2}$$

Given that $\mathrm{i}\partial_t \ \|_{\pm,E,x} = E\ \|_{\pm,E,x}$, the previous relation writes, after expression the scattering state with plane waves and the scattering amplitudes:

$$\begin{aligned} E\ \|_{+,E,-1} - \gamma\ \|_{+,E,-2} + \int \frac{\mathrm{d}E'}{2\pi} \left[E'\ \|_{-,E',-1} - \gamma\ \|_{-,E',-2}\right] r(E', E) \\ = \int \frac{\mathrm{d}E'}{2\pi} \left[E'\ \|_{+,E',1} - \gamma\ \|_{+,E',2}\right] d(E', E) \end{aligned}$$

Plane waves satisfy the homogenous Schrödinger equation on the leads

$$\mathrm{i}\partial_t \ \|_{\pm,U,x} = -\gamma\, \partial_t \ \|_{\pm,U,x-1} - \gamma\, \partial_t \ \|_{\pm,U,x+1}$$

which means we have:

$$U\ \|_{\pm,U,x} + \gamma\, \partial_t \ \|_{\pm,U,x\pm1} = -\gamma\, \partial_t \ \|_{\pm,U,x\mp1}$$

Let's apply it to the equation involving the scattering coefficients:

$$-\gamma\ \|_0^{+,E} + \int \frac{\mathrm{d}E'}{2\pi} - \gamma\ \|_{-,E,0}\, r(E', E) = \int \frac{\mathrm{d}E'}{2\pi} - \gamma\ \|_0^{+,E}\, d(E', E)$$

Using equation (6.28), we have $\|_{\pm,E,0} = |v_E|^{-\frac{1}{2}}\, \mathrm{e}^{-\mathrm{i}Et}$:

$$|v_E|^{-\frac{1}{2}}\, \mathrm{e}^{-\mathrm{i}Et} + \int \frac{\mathrm{d}E'}{2\pi} |v_{E'}|^{-\frac{1}{2}}\, \mathrm{e}^{-\mathrm{i}Et} r(E', E) = \int \frac{\mathrm{d}E'}{2\pi} |v_{E'}|^{-\frac{1}{2}}\, \mathrm{e}^{-\mathrm{i}Et} d(E', E)$$

If we use the hypothesis that $r(E', E)$ is peaked around E, as a function of E', we can factor out the $|v_{E'}|^{-\frac{1}{2}}$ in the integrals and take it equal to $|v_E|^{-\frac{1}{2}}$. Which then we can remove entirely from the equation:

$$\mathrm{e}^{-\mathrm{i}Et} + \int \frac{\mathrm{d}E'}{2\pi} \mathrm{e}^{-\mathrm{i}Et} r(E', E) = \int \frac{\mathrm{d}E'}{2\pi} \mathrm{e}^{-\mathrm{i}Et} d(E', E)$$

Which lead to the result in the time domain:

$$\mathrm{e}^{-\mathrm{i}Et} + r(t, E) = d(t, E)$$

C.4. Expressing time-resolved transport quantities

Here, we write the expression of the time-resolved lead particle, energy and heat currents within the Resonant Level Model, using the scattering states expressed in Eqs. (6.33). As stated in the end of Sec. (5.2.3.1), the discrete one-body expressions for currents and densities that have been expressed in Sec. 4.2.4, can be used to compute the contribution of each scattering state Ψ^λ to the many-body expectation value to finally obtain Landauer-Büttiker formulas with the time-dependent transmission $d(t,E)$. The approach taken in our derivation consists in expressing first one-body contributions then integrating them over the scattering states with Fermi weights (following Eq. (5.26)).

C.4.1. Particle current

The contribution $I^{\mathrm{N},\lambda}_{x,x+1}$ of the scattering state $\Psi^{\lambda=\alpha,E}$ to the many-body particle current $I^{\mathrm{N}}_{x,x+1}$ flowing from site x to site $x+1$ can be expressed by jointly using the definition of the hopping particle current I^{N}_{ij}, defined Eq. (4.88), and the expression of the scattering state Ψ^λ using the scattering amplitudes $r(E',E)$ and $d(E',E)$, given by Eq. (6.33).

$$I^{\mathrm{N},\lambda}_{x,x+1} = I^{\mathrm{N},\lambda}_{x,x+1} = -2\,\mathrm{Im}\Big[\left(\Psi^\lambda_x\right)^* h_{x,x+1}\Psi^\lambda_{x+1}\Big] \tag{C.24}$$

For sites $x \notin \{-1,0\}$, we have $h_{x,x+1} = -\gamma$

$$I^{\mathrm{N},\lambda}_{x,x+1} = 2\gamma\,\mathrm{Im}\Big[\left(\Psi^\lambda_x\right)^* \Psi^\lambda_{x+1}\Big] \tag{C.25}$$

Let's consider first the current following through the left lead, *i.e.* $x \leq -2$. Let's start with $\lambda = (\mathrm{L},E)$, the scattering state generated by an incoming plane wave from the left (given in 6.33a):

$$x \leq -2, \quad \left(\Psi^{\mathrm{L},E}_x\right)^* \Psi^{\mathrm{L},E}_{x+1} = \left[\|^{+,E}_x + \int \frac{\mathrm{d}E'}{2\pi}\, \|^{-,E}_x\, r(E',E)\right]^* \left[\|_{+,E,x+1} + \int \frac{\mathrm{d}E'}{2\pi}\, \|_{-,E',x+1}\, r(E',E)\right]$$

for $\lambda = (R,E)$ (scattering state given in 6.33b):

$$x \leq -2, \quad \left(\Psi^{\mathrm{R},E}_x\right)^* \Psi^{\mathrm{R},E}_{x+1} = \left[\int \frac{\mathrm{d}E'}{2\pi}\, \|^{-,E}_x\, d'(E',E)\right]^* \left[\int \frac{\mathrm{d}E'}{2\pi}\, \|_{-,E',x+1}\, d'(E',E)\right]$$

Using WBL1 We use the approximation 1 from 6.2.1. After rewriting $k^-_E = -k^+_E$, we get for $\lambda = (L,E)$:

$$\begin{aligned}
x \leq -2, \quad \left(\Psi^{\mathrm{L},E}_x\right)^* \Psi^{\mathrm{L},E}_{x+1} &\approx |v_E|^{-1} \left[\mathrm{e}^{\mathrm{i}k^+_E x - \mathrm{i}Et} + \mathrm{e}^{-\mathrm{i}k^+_E x}\, r(t,E)\right]^* \left[\mathrm{e}^{\mathrm{i}k^+_E (x+1) - \mathrm{i}Et} + \mathrm{e}^{-\mathrm{i}k^+_E (x+1)}\, r(t,E)\right] \\
&= |v_E|^{-1} \left[\mathrm{e}^{-\mathrm{i}k^+_E x + \mathrm{i}Et} + \mathrm{e}^{\mathrm{i}k^+_E x}\, r(t,E)^*\right] \left[\mathrm{e}^{\mathrm{i}k^+_E (x+1) - \mathrm{i}Et} + \mathrm{e}^{-\mathrm{i}k^+_E (x+1)}\, r(t,E)\right] \\
&= |v_E|^{-1} \Big[\mathrm{e}^{\mathrm{i}k^+_E} + \mathrm{e}^{-\mathrm{i}k^+_E}\, |r(t,E)|^2 + \underbrace{\mathrm{e}^{-\mathrm{i}k^+_E(2x+1)+\mathrm{i}Et}\, r(t,E) + \mathrm{e}^{\mathrm{i}k^+_E(2x+1)-\mathrm{i}Et}\, r(t,E)^*}_{a+a^* \Longrightarrow \mathrm{Im}[a+a^*]=0}\Big]
\end{aligned}$$

And for $\lambda = (R, E)$:

$$x \leq -2, \quad \left(\Psi_x^{\mathrm{R},E}\right)^* \Psi_{x+1}^{\mathrm{R},E} \approx |v_E|^{-1} \, \mathrm{e}^{\mathrm{i}k_E^-} \left|d'(t,E)\right|^2$$

This approximation makes $I_{x,x+1}^{\mathrm{N},\lambda}$ position independent *but still side dependent*: the expressions written so far only apply to the left side (*i.e.* $x \leq -2$). It is to be noted the x independence can only be achieved if the group velocity is infinite: the approximation done thus implies considering an infinite group velocity $v_E \to \infty$.

$$\text{WBL1} \implies I_{x,x+1}^{\mathrm{N},\lambda} \text{ is } x \text{ independent} \implies v_E \equiv 2\gamma \implies \mathrm{e}^{\mathrm{i}k_E} = \mathrm{i} \tag{C.26}$$

Which enables us a to write a Landauer-Büttiker-like equation of the particle current, using Eq. (C.25)

$$x \leq -2, \;\; I_{x,x+1}^{\mathrm{N},\lambda=(\mathrm{L},E)}(t) = 2\gamma \left|v_E\right|^{-1} \mathrm{Im}\left[\mathrm{e}^{\mathrm{i}k_E^+} + \mathrm{e}^{-\mathrm{i}k_E^+} \left|r(t,E)\right|^2\right] = 1 - \left|r(t,E)\right|^2 \tag{C.27}$$

The same approach applies for $\lambda = (R, E)$ and results with the following:

$$I_{x,x+1}^{\mathrm{N},\lambda=(\mathrm{R},E)}(t) = -\left|d'(t,E)\right|^2 \tag{C.28}$$

Summing over the scattering states, as described in Eq. (5.27), gives the following for the particle current in the left lead $x \leq -2$

$$I_{\mathrm{L}}^{\mathrm{N}}(t) = \int \frac{\mathrm{d}E}{2\pi} f_L(E) \, I_{x,x+1}^{\mathrm{N},\lambda=(\mathrm{R},E)}(t) + f_R(E) \, I_{x,x+1}^{\mathrm{N},\lambda=(\mathrm{R},E)}(t) \tag{C.29}$$

where f_L and f_R are respectively the left reservoir and right reservoir Fermi distributions. And in our current `WBL1` approximation, it is position independent. A similar derivation calculation can be made in the right lead, resulting in the following expressions for the right and left lead particle current

$$I_{\mathrm{L}}^{\mathrm{N},1}(t) = I_{-1,0}^{\mathrm{N},1}(t) = \int \frac{\mathrm{d}E}{2\pi} \, f_L(E) \, \left[1 - \left|r(t,E)\right|^2\right] \, - f_R(E) \, \left|d'(t,E)\right|^2 \tag{C.30a}$$

$$I_{\mathrm{R}}^{\mathrm{N},1}(t) = I_{1,0}^{\mathrm{N},1}(t) \;\; = \int \frac{\mathrm{d}E}{2\pi} \, f_R(E) \, \left[1 - \left|r'(t,E)\right|^2\right] - f_L(E) \, \left|d(t,E)\right|^2 \tag{C.30b}$$

Using WBL2 We will use the approximation 2 from 6.2.1:

$$\begin{aligned}
\left(\Psi_x^{\mathrm{L},E}\right)^* \Psi_{x+1}^{\mathrm{L},E} &\approx |v_E|^{-1} \left[\mathrm{e}^{\mathrm{i}k_E^+ x - \mathrm{i}Et} + \mathrm{e}^{\mathrm{i}\left[k_E^- - \frac{E}{v_E^-}\right]x} \, r(t - \frac{x}{v_E^-}, E)\right]^* \\
&\qquad \left[\mathrm{e}^{\mathrm{i}k_E^+(x+1) - \mathrm{i}Et} + \mathrm{e}^{\mathrm{i}\left[k_E^- - \frac{E}{v_E^-}\right](x+1)} \, r(t - \frac{x+1}{v_E^-}, E)\right] \\
&= |v_E|^{-1} \left[\mathrm{e}^{-\mathrm{i}k_E^+ x + \mathrm{i}Et} + \mathrm{e}^{\mathrm{i}\left[k_E^+ - \frac{E}{v_E^+}\right]x} \, r(t + \frac{x}{v_E^+}, E)^*\right] \\
&\qquad \left[\mathrm{e}^{\mathrm{i}k_E^+(x+1) - \mathrm{i}Et} + \mathrm{e}^{-\mathrm{i}\left[k_E^+ - \frac{E}{v_E^+}\right](x+1)} \, r(t + \frac{x+1}{v_E^+}, E)\right] \\
&= |v_E|^{-1} \left[\mathrm{e}^{\mathrm{i}k_E^+} + \mathrm{e}^{-\mathrm{i}\left[k_E^+ - \frac{E}{v_E^+}\right]} r(t + \frac{x+1}{v_E^+}, E) r(t + \frac{x}{v_E^+}, E)^* + G\right]
\end{aligned}$$

Where

$$\begin{aligned}
G &= \mathrm{e}^{-\mathrm{i}k_E^+ x + \mathrm{i}Et} \mathrm{e}^{-\mathrm{i}\left[k_E^+ - \frac{E}{v_E^+}\right](x+1)} \, r(t + \frac{x+1}{v_E^+}, E) + \mathrm{e}^{\mathrm{i}k_E^+(x+1) - \mathrm{i}Et} \mathrm{e}^{\mathrm{i}\left[k_E^+ - \frac{E}{v_E^+}\right]x} \, r(t + \frac{x}{v_E^+}, E)^* \\
&= \mathrm{e}^{-\mathrm{i}k_E^+(2x+1) + \mathrm{i}\frac{E}{v_E^+}(x+1) + \mathrm{i}Et} \, r(t + \frac{x+1}{v_E^+}, E) + \mathrm{e}^{\mathrm{i}k_E^+(2x+1) - \mathrm{i}\frac{E}{v_E^+}x - \mathrm{i}Et} \, r(t + \frac{x}{v_E^+}, E)^*
\end{aligned}$$

We want to place ourselves in conditions where we can have $\mathrm{Im}[G] \approx 0$. To have that we need $\mathrm{e}^{\mathrm{i}E/v_E^+,E} r(t+\frac{x+1}{v_E}) \approx r(t+\frac{x}{v_E},E)$ Therefore we will make two additional hypotheses, that lead to two consecutive approximations that justify $\mathrm{Im}[G] \approx 0$:

1. $|l(t,E)|^2$ have negligible values around the edges of $]-2\gamma, 2\gamma[$, so we can do the approximation $v_E^+ \approx v_{E=0}^+ = 2\gamma$ in $l(t+x/v_E,E)$, where $l = r, d, r', d'$, and in $\mathrm{e}^{\mathrm{i}\frac{E}{v_E^+}}$.
2. γ is big enough to consider that $l(t+\frac{x+1}{2\gamma},E) \approx l(t+\frac{x}{2\gamma},E) \approx l(t+\frac{x+0.5}{2\gamma},E)$ where $l = r, d, r', d'$. And $\mathrm{e}^{\mathrm{i}\frac{E}{2\gamma}} \approx 1$

$I_{x,x+1}^{\mathrm{N},\lambda=(\mathrm{L},E)}(t)$ then writes:

$$\begin{aligned}
I_{x,x+1}^{\mathrm{N},\lambda=(\mathrm{L},E)}(t) &= 2\gamma\,|v_E|^{-1}\,\mathrm{Im}\left[\mathrm{e}^{\mathrm{i}k_E^+} + \mathrm{e}^{-\mathrm{i}\left[k_E^+ - \frac{E}{v_E^+}\right]}\left|r(t+\frac{x+0.5}{2\gamma},E)\right|^2\right] \\
&= |v_E|^{-1}\left[v_E^+ + 2\gamma\,\mathrm{Im}[\mathrm{e}^{-\mathrm{i}\left[k_E^+ - \frac{E}{v_E^+}\right]}]\left|r(t+\frac{x+0.5}{2\gamma},E)\right|^2\right] \\
&= 1 - 2\gamma\,|v_E|^{-1}\left[\frac{E}{2\gamma}\sin\frac{E}{v_E^+} + \frac{v_E^+}{2\gamma}\cos\frac{E}{v_E^+}\right]\left|r(t+\frac{x+0.5}{2\gamma},E)\right|^2 \\
&= 1 - \left[\frac{E}{v_E^+}\sin\frac{E}{v_E^+} + \cos\frac{E}{v_E^+}\right]\left|r(t+\frac{x+0.5}{2\gamma},E)\right|^2
\end{aligned} \tag{C.31}$$

A closer look at the pre-factor $\frac{E}{v_E^+}\sin\frac{E}{v_E^+} + \cos\frac{E}{v_E^+}$ (Fig C.3) shows that it's a mainly flat curve (equal to 1) on the interval $]-2\gamma, 2\gamma[$ and diverges at its edges. Given that this pre-factor comes as a multiplier of $\left|r(t+\frac{x+0.5}{2\gamma},E)\right|^2$ for which we made the hypothesis that it has negligible values on the edges of $]-2\gamma, 2\gamma[$, we can do the approximation pre-factor $= 1$ (The same result would have been achieved if we took $\mathrm{e}^{\mathrm{i}\frac{E}{2\gamma}} \approx 1$ for its other occurrences). This finally gives:

$$I_{x,x+1}^{\mathrm{N},\lambda=(\mathrm{L},E)}(t) = 1 - \left|r(t+\frac{x+0.5}{2\gamma},E)\right|^2 \tag{C.32}$$

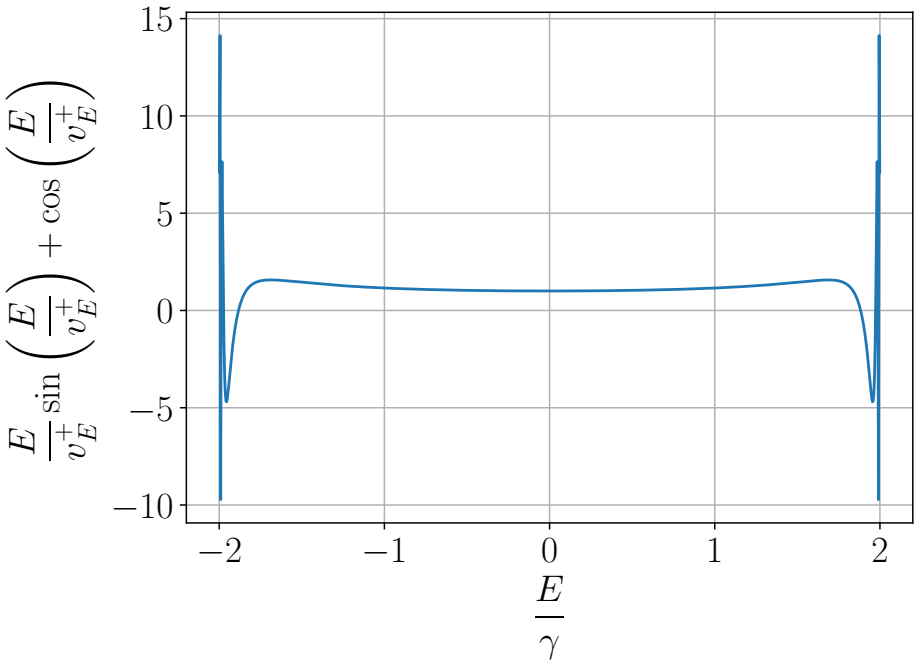

Figure C.3. – Representation of the pre-factor that appears in (C.31)

Now with $\lambda = (R, E)$, *i.e.* the scattering state $\Psi^{\lambda=\mathrm{R},E}$ created by the incoming right-to-left plane wave $\|_{-,E}$:

$$\begin{aligned}
\left(\Psi_x^{\mathrm{R},E}\right)^* \Psi_{x+1}^{\mathrm{R},E} &= \left[\int \frac{\mathrm{d}E'}{2\pi}\, \|_x^{-,E}\, d'(E',E)\right]^* \left[\int \frac{\mathrm{d}E'}{2\pi}\, \|_{-,E',x+1}\, d'(E',E)\right] \\
&\approx |v_E|^{-1} \left[\mathrm{e}^{\mathrm{i}\left[k_E^- - \frac{E}{v_E^-}\right]x}\, d'(t-\frac{x}{v_E^-},E)\right]^* \left[\mathrm{e}^{\mathrm{i}\left[k_E^- - \frac{E}{v_E^-}\right](x+1)}\, d'(t-\frac{x+1}{v_E^-},E)\right] \\
&= |v_E|^{-1} \left[\mathrm{e}^{\mathrm{i}\left[k_E^+ - \frac{E}{v_E^+}\right]x}\, d'(t+\frac{x}{v_E^+},E)^*\right] \left[\mathrm{e}^{-\mathrm{i}\left[k_E^+ - \frac{E}{v_E^+}\right](x+1)}\, d'(t+\frac{x+1}{v_E^+},E)\right] \\
&= |v_E|^{-1}\, \mathrm{e}^{-\mathrm{i}\left[k_E^+ - \frac{E}{v_E^+}\right]}\, d'(t+\frac{x+1}{v_E^+},E)\, d'(t+\frac{x}{v_E^+},E)^*
\end{aligned}$$

Where $d'(E', E)$ is the right-to-left transmission. We use the hypotheses made in the two bullet points above, along with the approximations they enable, to obtain:

$$I_{x,x+1}^{\mathrm{N},\lambda=(\mathrm{L},E)}(t) = -\left|d'(t+\frac{x+0.5}{2\gamma},E)\right|^2 \tag{C.33}$$

The total particle current writes:

$$I_{x,x+1}^{\mathrm{N}}(t) = \int \frac{\mathrm{d}E}{2\pi} f_L(E)\, I_{x,x+1}^{\mathrm{N},\lambda=(\mathrm{L},E)}(t) + f_R(E)\, I_{x,x+1}^{\mathrm{N},\lambda=(\mathrm{R},E)}(t) \tag{C.34}$$

where f_L and f_R are respectively the left reservoir and right reservoir Fermi distributions. And in our approximation, its expanded expression is (note that the $x, x+1$ index means from site x to site $x+1$):

$$I_{\mathrm{L},x,x+1}^{\mathrm{N},2}(t) = \int \frac{\mathrm{d}E}{2\pi}\, f_L(E) \left[1 - \left|r(t+\tfrac{x+0.5}{2\gamma},E)\right|^2\right] - f_R(E) \left|d'(t+\tfrac{x+0.5}{2\gamma},E)\right|^2 \tag{C.35a}$$

$$I_{\mathrm{R},x+1,x}^{\mathrm{N},2}(t) = \int \frac{\mathrm{d}E}{2\pi}\, f_R(E) \left[1 - \left|r'(t-\tfrac{x+0.5}{2\gamma},E)\right|^2\right] - f_R(E) \left|d(t-\tfrac{x+0.5}{2\gamma},E)\right|^2 \tag{C.35b}$$

which has the same form as Eqs. (C.30) with the benefit of taking into account the finite speed propagation in the leads, with a finite and fixed group velocity $v = 2\gamma$. Note that here x is negative in the left lead and positive in the right lead.

C.4.2. Dot's particle density

To obtain the value of the particle density on the dot (*i.e.* site 0), we need to express the scattering sates on that site. Let's express it starting off the Schrödinger equation:

$$\Phi_0 = -\mathrm{i}\tfrac{1}{\gamma_c}\partial_t\Phi_1 - \tfrac{\gamma}{\gamma_c}\Phi_2 \tag{C.36}$$

Given that the wave functions start with $v_E^{-\frac{1}{2}}$ where $v_E = 2\gamma$ in our current wideband approximation. If we express that prefactor out of the wavefunctions $\Phi = v_E^{-1/2}\Phi'$ we get that :

$$\begin{aligned}\Phi_0 &= -\mathrm{i}\frac{1}{\gamma_c\sqrt{2\gamma}}\partial_t\Phi_1' - \frac{\gamma}{\gamma_c\sqrt{2\gamma}}\Phi_2' \\ &= -\mathrm{i}\frac{1}{\gamma_c\sqrt{2\gamma}}\partial_t\Phi_1' - \frac{1}{\Gamma}\Phi_2'\end{aligned} \tag{C.37}$$

Another thing to consider from the wideband is that it symbolically amounts to taking $\gamma \to \infty$ and $\gamma_c \to \infty$ while keeping Γ (given in 5.55) constant. That means that $\frac{1}{\gamma_c\sqrt{2\gamma}} \to 0$ in the previous expression:

$$\Phi_0 = -\frac{1}{\sqrt{\Gamma}}\Phi_2' \tag{C.38}$$

We can now use the calculations carried in C.4.4 to express Φ_2' with $\mathrm{e}^{ik_E} = \mathrm{i}$ as a result of WBL1

$$\Phi'_{\mathrm{R},E,2} = -\left[\mathrm{e}^{-\mathrm{i}Et} + r'(t,E)\right] = -d'(t,E) \tag{C.39}$$

$$\Phi'_{\mathrm{L},E,2} = -d(t,E) \tag{C.40}$$

Therefore, the particle density ρ_0 writes:

$$\rho_0 = \int \frac{\mathrm{d}E}{2\pi}\left(f_R + f_L\right)\frac{1}{\Gamma}\left|d\right|^2 \tag{C.41}$$

Note: Eq. (C.38) implies that $\rho_0 \propto \rho_2$ but a tkwant simulation shows that it's not the case. The final expression of ρ_0, however, matches with simulation.

C.4.3. Energy current: far in the leads

The lead time-resolved energy current $I^{\varepsilon}_{\alpha,x}$ in an arbitrary position x of left $\alpha = \mathrm{L}$ and right $\alpha = \mathrm{R}$ lead can in theory computed using the scattering states defined in Eq. (6.33): by summing the contribution $I^{\varepsilon,\lambda}_{\alpha,x}$ of each scattering state Ψ^{λ}, given by Eq. (4.94) (with the total energy operator as the energy operator $\epsilon = \varepsilon$), according the Fermi distribution of each lead (see Eq. (5.27)), one obtains $I^{\varepsilon}_{\alpha,x}$. The contribution $I^{\varepsilon,\lambda}_{x,x+1}$ to the energy current flowing from x to $x+1$, of the scattering state Ψ^{λ}, writes (4.94):

$$I^{\varepsilon,\lambda}_{x,x+1} = \sum_k -\mathrm{Im}\left[\left(\Psi^{\lambda}_k\right)^* \varepsilon_{k,x}\varepsilon_{x,x+1}\Psi^{\lambda}_{x+1} - \left(\Psi^{\lambda}_k\right)^* \varepsilon_{k,x+1}\varepsilon_{x+1,x}\Psi^{\lambda}_{x}\right] \tag{C.42}$$

Let's develop this formula, knowing that in the leads we have $\varepsilon_{x,x} = 0$, $\varepsilon_{x,x\pm1} = -\gamma$:

$$I^{\varepsilon,\lambda}_{x,x+1} = -\mathrm{Im}\Big[\left(\Psi^\lambda_{x-1}\right)^* \varepsilon_{x-1,x}\varepsilon_{x,x+1}\Psi^\lambda_{x+1} + \left(\Psi^\lambda_x\right)^* \underbrace{\varepsilon_{x,x}}_{=0} \varepsilon_{x,x+1}\Psi^\lambda_{x+1} + \underbrace{\left(\Psi^\lambda_{x+1}\right)^* \varepsilon_{x+1,x}\varepsilon_{x,x+1}\Psi^\lambda_{x+1}}_{\in\mathbb{R}} \\ - \underbrace{\left(\Psi^\lambda_x\right)^* \varepsilon_{x,x+1}\varepsilon_{x+1,x}\Psi^\lambda_x}_{\in\mathbb{R}} - \left(\Psi^\lambda_{x+1}\right)^* \underbrace{\varepsilon_{x+1,x+1}}_{=0} \varepsilon_{x+1,x}\Psi^\lambda_x - \left(\Psi^\lambda_{x+2}\right)^* \varepsilon_{x+2,x+1}\varepsilon_{x+1,x}\Psi^\lambda_x \Big] \tag{C.43}$$

Which simplifies to:

$$I^{\varepsilon,\lambda}_{x,x+1} = -\gamma^2\,\mathrm{Im}\left[\left(\Psi^\lambda_{x-1}\right)^* \Psi^\lambda_{x+1} - {\Psi^\lambda_{x+2}}^* \Psi^\lambda_x\right] \tag{C.44}$$

Using WBL1 This approximation makes $I^{\varepsilon,\lambda}_{x,x+1}$ x independent *but still side dependent*. We will take $x = 0$ to simplify the notations. Same as with the particle current, we will consider the Left current (positive when flowing towards the central system). Let's start $\lambda = (\mathrm{L}, E)$:

$$\left(\Psi^{\mathrm{L},E}_{-1}\right)^* \Psi^{\mathrm{L},E}_1 = \left[\|_{+,E,-1} + \int \frac{\mathrm{d}E'}{2\pi}\, \|_{-,E',-1}\, r(E',E)\right]^* \left[\|^{+,E}_1 + \int \frac{\mathrm{d}E'}{2\pi}\, \|_{-,E',1}\, r(E',E)\right]$$

Using the approximation (6.36), we get:

$$\begin{aligned}
\left(\Psi^{\mathrm{L},E}_{-1}\right)^* \Psi^{\mathrm{L},E}_1 &\approx |v_E|^{-1} \left[\mathrm{e}^{-\mathrm{i}k^+_E - \mathrm{i}Et} + \mathrm{e}^{\mathrm{i}k^+_E}\, r(t,E)\right]^* \left[\mathrm{e}^{\mathrm{i}k^+_E - \mathrm{i}Et} + \mathrm{e}^{-\mathrm{i}k^+_E}\, r(t,E)\right] \\
&= |v_E|^{-1} \left[\mathrm{e}^{\mathrm{i}k^+_E + \mathrm{i}Et} + \mathrm{e}^{-\mathrm{i}k^+_E}\, r(t,E)^*\right] \left[\mathrm{e}^{\mathrm{i}k^+_E - \mathrm{i}Et} + \mathrm{e}^{-\mathrm{i}k^+_E}\, r(t,E)\right] \\
&= |v_E|^{-1} \big[\mathrm{e}^{2\mathrm{i}k^+_E} + \mathrm{e}^{-2\mathrm{i}k^+_E}\,|r(t,E)|^2 + \underbrace{\mathrm{e}^{\mathrm{i}Et} r(t,E) + \mathrm{e}^{-\mathrm{i}Et} r(t,E)^*}_{a+a^* \implies \mathrm{Im}[a+a^*]=0}\big]
\end{aligned}$$

Now we can use (6.31) to express $\mathrm{Im}\left[\mathrm{e}^{\pm 2\mathrm{i}k^+_E}\right] = \mp\frac{1}{2\gamma} v^+_E E$:

$$\mathrm{Im}\left[\left(\Psi^{\mathrm{L},E}_{-1}\right)^* \Psi^{\mathrm{L},E}_1\right] = -\mathrm{Im}\left[\left(\Psi^{\mathrm{L},E}_2\right)^* \Psi^{\mathrm{L},E}_0\right] = -\frac{E}{2\gamma^2}\left[1 - |r(t,E)|^2\right] \tag{C.45}$$

We finally get:

$$I^\varepsilon_{L,E} = E\left[1 - |r(t,E)|^2\right] \tag{C.46}$$

For $\lambda = (\mathrm{R}, E)$ we have similarly:

$$I^\varepsilon_{R,E} = -E\,|d'(t,E)|^2 \tag{C.47}$$

The total Left energy current, going towards the central system, writes:

$$I^\varepsilon(t) = \int \frac{\mathrm{d}E}{2\pi}\, E\left[f_L(E)\left[1 - |r(t,E)|^2\right] - f_R(E)\,|d'(t,E)|^2\right] \tag{C.48}$$

C.4.4. Energy current: hopping $(0,1)$

The contribution $I_{01}^{\varepsilon,\lambda}$ to the energy current flowing from site 0 to 1, of the scattering state Ψ^λ, can be expressed using Eq. (4.94):

$$I_{01}^{\varepsilon,\lambda} = \sum_k -\mathrm{Im}\Big[{\Psi_k^\lambda}^* \varepsilon_{k,0}\varepsilon_{0,1}\Psi_1^\lambda - {\Psi_k^\lambda}^* \varepsilon_{k,1}\varepsilon_{1,0}\Psi_0^\lambda\Big] \tag{C.49}$$

$$= -\mathrm{Im}\Big[{\Psi_{-1}^\lambda}^* \varepsilon_{-1,0}\varepsilon_{0,1}\Psi_1^\lambda + {\Psi_0^\lambda}^* \underbrace{\varepsilon_{0,0}}_{=V_0}\varepsilon_{0,1}\Psi_1^\lambda + \underbrace{{\Psi_1^\lambda}^*\varepsilon_{1,0}\varepsilon_{0,1}\Psi_1^\lambda}_{\in\mathbb{R}} \tag{C.50}$$

$$- \underbrace{{\Psi_0^\lambda}^*\varepsilon_{0,1}\varepsilon_{1,0}\Psi_0^\lambda}_{\in\mathbb{R}} - {\Psi_1^\lambda}^* \underbrace{\varepsilon_{1,1}}_{=0}\varepsilon_{1,0}\Psi_0^\lambda - {\Psi_2^\lambda}^*\varepsilon_{2,1}\varepsilon_{1,0}\Psi_0^\lambda\Big] \tag{C.51}$$

which simplifies to:

$$I_{01}^{\varepsilon,\lambda} = -\mathrm{Im}\Big[\gamma_c^2\Psi_{\lambda,-1}^*\Psi_1^\lambda - \gamma_c V_0 \Psi_{\lambda,0}^*\Psi_1^\lambda - \gamma\gamma_c {\Psi_2^\lambda}^*\Psi_0^\lambda\Big] \tag{C.52}$$

The contribution $I_{\lambda,01}^N$ of Ψ^λ to the particle current, from (4.88), writes:

$$I_{\lambda,01}^N = -2\mathrm{Im}\Big[{\Psi_0^\lambda}^* H_{01}\Psi_1^\lambda\Big] = 2\gamma_c \mathrm{Im}\Big[{\Psi_0^\lambda}^*\Psi_1^\lambda\Big]$$

We can replace in the previous equation:

$$I_{01}^{\varepsilon,\lambda} = \mathrm{Im}\Big[\gamma\gamma_c {\Psi_2^\lambda}^*\Psi_0^\lambda - \gamma_c^2\Psi_{\lambda,-1}^*\Psi_1^\lambda\Big] + \frac{1}{2}V_0 I_{\lambda,01}^N$$

Ψ_0 can't be expressed with the scattering coefficients, but can be with the Schrödinger equation:

$$\gamma_c\Psi_0 = -\mathrm{i}\partial_t\Psi_1 - \gamma\Psi_2$$

Thus we get:

$$\begin{aligned} I_{01}^{\varepsilon,\lambda} &= \mathrm{Im}\Big[-\gamma{\Psi_2^\lambda}^*(\mathrm{i}\partial_t\Psi_1^\lambda + \gamma\Psi_2^\lambda) - \gamma_c^2\Psi_{\lambda,-1}^*\Psi_1^\lambda\Big] + \frac{1}{2}V_0 I_{\lambda,01}^N \\ &= \mathrm{Im}\Big[-\gamma{\Psi_2^\lambda}^*\mathrm{i}\partial_t\Psi_1^\lambda - \gamma^2\underbrace{{\Psi_2^\lambda}^*\Psi_2^\lambda}_{\in\mathbb{R}} - \gamma_c^2\Psi_{\lambda,-1}^*\Psi_1^\lambda\Big] + \frac{1}{2}V_0 I_{\lambda,01}^N \end{aligned}$$

Which finally gives:

$$I_{01}^{\varepsilon,\lambda} = -\gamma\mathrm{Im}\Big[{\Psi_2^\lambda}^*\mathrm{i}\partial_t\Psi_1^\lambda\Big] - \gamma_c^2\mathrm{Im}\Big[\Psi_{\lambda,-1}^*\Psi_1^\lambda\Big] + \frac{1}{2}V_0 I_{\lambda,01}^N \tag{C.53}$$

→ WBL1 We will use here the approximation given in (6.36) for expressing the wave functions on all sites except 0.

$\lambda = (\mathbf{R}, E)$ Let's write the expression of the scattering state on each site (except 0), after remembering that sites at negative position bring a minus sign with them (*e.g.* for site -1 we will have $\mathrm{e}^{(-1)ik_E^-} = \mathrm{e}^{ik_E^+}$):

$$\begin{aligned} \Psi_{\mathrm{R},E,-1} &= |v_E|^{-\frac{1}{2}}\Big[\mathrm{e}^{\mathrm{i}k_E^+}\, d'(t,E)\Big] \\ \Psi_{\mathrm{R},E,1} &= |v_E|^{-\frac{1}{2}}\Big[\mathrm{e}^{-\mathrm{i}k_E^+ - \mathrm{i}Et} + \mathrm{e}^{\mathrm{i}k_E^+}\, r'(t,E)\Big] \\ \mathrm{i}\partial_t\Psi_{\mathrm{R},E,1} &= |v_E|^{-\frac{1}{2}}\Big[E\mathrm{e}^{-\mathrm{i}k_E^+ - \mathrm{i}Et} + \mathrm{e}^{\mathrm{i}k_E^+}\,\mathrm{i}\partial_t r'(t,E)\Big] \\ \Psi_{\mathrm{R},E,2} &= |v_E|^{-\frac{1}{2}}\Big[\mathrm{e}^{-2\mathrm{i}k_E^+ - \mathrm{i}Et} + \mathrm{e}^{2\mathrm{i}k_E^+}\, r'(t,E)\Big] \end{aligned}$$

Each term of (C.53) can now be expressed:

$$|v_E|\,\Psi^*_{\mathrm{R},E,2}\mathrm{i}\partial_t\Psi_{\mathrm{R},E,1} = \left[\mathrm{e}^{-2\mathrm{i}k_E^+ - \mathrm{i}Et} + \mathrm{e}^{2\mathrm{i}k_E^+}\,r'(t,E)\right]^* \left[E\mathrm{e}^{-\mathrm{i}k_E^+ - \mathrm{i}Et} + \mathrm{e}^{\mathrm{i}k_E^+}\,\mathrm{i}\partial_t r'(t,E)\right]$$
$$|v_E|\,\Psi^*_{\mathrm{R},E,-1}\Psi_{\mathrm{R},E,1} = \left[\mathrm{e}^{-\mathrm{i}k_E^+}\,d'(t,E)^*\right] \left[\mathrm{e}^{-\mathrm{i}k_E^+ - \mathrm{i}Et} + \mathrm{e}^{\mathrm{i}k_E^+}\,r'(t,E)\right]$$

The symmetry of the system enables using equation (6.34) that links left-to-right and right-to-left scattering amplitudes. Also, using the WBL1 approximation implies taking $\mathrm{e}^{\mathrm{i}k} = \mathrm{i}$ (see equation C.26) and $v_E = 2\gamma$. Therefore to two terms simplify to:

$$2\gamma\,\Psi^*_{\mathrm{R},E,2}\mathrm{i}\partial_t\Psi_{\mathrm{R},E,1} = \left[\mathrm{e}^{-\mathrm{i}Et} + r(t,E)\right]^* \left[\mathrm{i}E\mathrm{e}^{-\mathrm{i}Et} + \partial_t r(t,E)\right]$$
$$2\gamma\,\Psi^*_{\mathrm{R},E,-1}\Psi_{\mathrm{R},E,1} = d(t,E)^* \left[-\mathrm{e}^{-\mathrm{i}Et} + r(t,E)\right]$$

Now, using (6.53), we reach the following expressions:

$$2\gamma\,\Psi^*_{\mathrm{R},E,2}\mathrm{i}\partial_t\Psi_{\mathrm{R},E,1} = d(t,E)^* \left[2\mathrm{i}E\mathrm{e}^{-\mathrm{i}Et} + \partial_t d(t,E)\right]$$
$$2\gamma\,\Psi^*_{\mathrm{R},E,-1}\Psi_{\mathrm{R},E,1} = d(t,E)^* \left[-2\mathrm{e}^{-\mathrm{i}Et} + d(t,E)\right]$$

$\lambda = (\mathbf{L}, E)$ Let's write the expression of the scattering state on each site (except 0):

$$\Psi_{\mathrm{L},E,-1} = |v_E|^{-\frac{1}{2}} \left[\mathrm{e}^{-\mathrm{i}k_E^+ - \mathrm{i}Et} + \mathrm{e}^{\mathrm{i}k_E^+}\,r(t,E)\right]$$
$$\Psi_{\mathrm{L},E,1} = |v_E|^{-\frac{1}{2}} \left[\mathrm{e}^{\mathrm{i}k_E^+}\,d(t,E)\right]$$
$$\mathrm{i}\partial_t\Psi_{\mathrm{L},E,1} = |v_E|^{-\frac{1}{2}} \left[\mathrm{e}^{\mathrm{i}k_E^+}\,\mathrm{i}\partial_t d(t,E)\right]$$
$$\Psi_{\mathrm{L},E,2} = |v_E|^{-\frac{1}{2}} \left[\mathrm{e}^{2\mathrm{i}k_E^+}\,d(t,E)\right]$$

Each term of (C.53) can now be expressed:

$$|v_E|\,\Psi^*_{\mathrm{L},E,2}\,\mathrm{i}\partial_t\Psi_{\mathrm{L},E,1} = \mathrm{e}^{-\mathrm{i}k_E^+}\,d(t,E)^*\,\mathrm{i}\partial_t d(t,E)$$
$$|v_E|\,\Psi^*_{\mathrm{L},E,-1}\Psi_{\mathrm{L},E,1} = \left[\mathrm{e}^{-\mathrm{i}k_E^+ - \mathrm{i}Et} + \mathrm{e}^{\mathrm{i}k_E^+}\,r(t,E)\right]^* \mathrm{e}^{\mathrm{i}k_E^+}\,d(t,E)$$

Same as with $\lambda = (R, E)$, we can use $\mathrm{e}^{\mathrm{i}k} = 1$ and $v_E = 2\gamma$ due to the WBL1 approximation:

$$2\gamma\,\Psi^*_{\mathrm{L},E,2}\,\mathrm{i}\partial_t\Psi_{\mathrm{L},E,1} = d(t,E)^*\,\partial_t d(t,E)$$
$$2\gamma\,\Psi^*_{\mathrm{L},E,-1}\Psi_{\mathrm{L},E,1} = \left[-\mathrm{e}^{-\mathrm{i}Et} + r(t,E)\right]^* d(t,E)$$

Now, using (6.53), we reach the following expressions:

$$2\gamma\,\Psi^*_{\mathrm{L},E,2}\,\mathrm{i}\partial_t\Psi_{\mathrm{L},E,1} = d(t,E)^*\,\partial_t d(t,E)$$
$$2\gamma\,\Psi^*_{\mathrm{L},E,-1}\Psi_{\mathrm{L},E,1} = \left[-2\mathrm{e}^{-\mathrm{i}Et} + d(t,E)\right]^* d(t,E)$$

Total energy current The total energy current writes, knowing that $\mathrm{Im}[d^* d] = 0$:

$$I^{\varepsilon}_{0,-1} = \frac{1}{2}V_0 I^{\mathrm{N}}_{0,-1} - \int \frac{\mathrm{d}E}{2\pi} + \begin{matrix} f_{\mathrm{R}}\left[1/2\,\mathrm{Im}[d^*\partial_t d] - 1/2\,\Gamma\,\mathrm{Im}[\mathrm{e}^{\mathrm{i}Et}d]\right] \\ f_{\mathrm{L}}\left[1/2\,\mathrm{Im}[d^*\partial_t d] + 1/2\,\Gamma\,\mathrm{Im}[\mathrm{e}^{\mathrm{i}Et}d] + E\,\mathrm{Re}[\mathrm{e}^{\mathrm{i}Et}d]\right] \end{matrix} \tag{C.54a}$$

$$I^{\varepsilon}_{0,1} = \frac{1}{2}V_0 I^{\mathrm{N}}_{01} - \int \frac{\mathrm{d}E}{2\pi} + \begin{matrix} f_{\mathrm{L}}\left[1/2\,\mathrm{Im}[d^*\partial_t d] - 1/2\,\Gamma\,\mathrm{Im}[\mathrm{e}^{\mathrm{i}Et}d]\right] \\ f_{\mathrm{R}}\left[1/2\,\mathrm{Im}[d^*\partial_t d] + 1/2\,\Gamma\,\mathrm{Im}[\mathrm{e}^{\mathrm{i}Et}d] + E\,\mathrm{Re}[\mathrm{e}^{\mathrm{i}Et}d]\right] \end{matrix} \tag{C.54b}$$

With $\Gamma = 2\gamma_c^2/\gamma$. These formulas can already be used as-is for numerical integration, although it is more useful to make the source terms S^ε_{-1} and S^ε_1 appear so the heat current can easily computed. To achieve this goal, let's use the relation (6.54a) to replace $\mathrm{Im}[d^*\partial_t d]$:

$$I^\varepsilon_{01} = \frac{1}{2}V_0 I^{\mathrm{N}}_{01} - \int \frac{\mathrm{d}E}{2\pi} \begin{matrix} f_{\mathrm{L}}\left[-1/2\,\left[V(t)+V_0\right]|d|^2 - \Gamma\,\mathrm{Im}\left[\mathrm{e}^{itE}d\right]\right] \\ f_{\mathrm{R}}\left[-1/2\,\left[V(t)+V_0\right]|d|^2 + E\,\mathrm{Re}\left[\mathrm{e}^{\mathrm{i}Et}d\right]\right] \end{matrix} \tag{C.55}$$

We can now try to factor out S^E_1, whose expression is given by Eq. (4.106):

$$S^E_1 = \frac{1}{2}\Big[0 - V(t)\Big] I^{\mathrm{N}}_{10} = \frac{1}{2}V(t) I^{\mathrm{N}}_{01} \tag{C.56}$$

With I^{N}_{01} given by (C.30) with a minus sign:

$$I^{\mathrm{N}}_{01} = \int \frac{\mathrm{d}E}{2\pi}\, f_L\,|d|^2 - f_R(E)\,\left[1-|r|^2\right] \tag{C.57}$$

Then we can use (6.53) to express everything in terms of d:

$$S^E_1 = \int \frac{\mathrm{d}E}{2\pi} \begin{matrix} f_L\ \ 1/2 V(t)\,|d|^2 \\ f_R\Big[1/2 V(t)\,|d|^2 - V(t)\mathrm{Re}\left[d\,\mathrm{e}^{\mathrm{i}Et}\right]\Big] \end{matrix} \tag{C.58}$$

which gives the following for the energy current

$$I^\varepsilon_{01} = \frac{1}{2}V_0 I^{\mathrm{N}}_{01} + S^E_1 - \int \frac{\mathrm{d}E}{2\pi} \begin{matrix} f_{\mathrm{L}}\left[-1/2 V_0\,|d|^2 - \Gamma\,\mathrm{Im}\left[\mathrm{e}^{itE}d\right]\right] \\ f_{\mathrm{R}}\left[-1/2 V_0\,|d|^2 + \left[E-V(t)\right]\,\mathrm{Re}\left[\mathrm{e}^{\mathrm{i}Et}d\right]\right] \end{matrix} \tag{C.59}$$

We can factor out another I^{N}_{01} term:

$$1/2 V_0 I^{\mathrm{N}}_{01} = \int \frac{\mathrm{d}E}{2\pi} \begin{matrix} f_L\ \ 1/2 V_0\,|d|^2 \\ f_R\Big[1/2 V_0\,|d|^2 - V_0\mathrm{Re}\left[d\,\mathrm{e}^{\mathrm{i}Et}\right]\Big] \end{matrix} \tag{C.60}$$

and obtain the following for I^ε_{01}:

$$I^\varepsilon_{01} = V_0 I^{\mathrm{N}}_{01} + S^E_1 - \int \frac{\mathrm{d}E}{2\pi} \begin{matrix} f_{\mathrm{L}}\left[-\Gamma\,\mathrm{Im}\left[\mathrm{e}^{itE}d\right]\right] \\ f_{\mathrm{R}}\left[E-V(t)-V_0\right]\,\mathrm{Re}\left[\mathrm{e}^{\mathrm{i}Et}d\right] \end{matrix} \tag{C.61}$$

When squashing all the terms together, we get:

$$I^\varepsilon_{01} = -\int \frac{\mathrm{d}E}{2\pi} \begin{matrix} f_L\left[-\left[1/2 V(t)+V_0\right]|d|^2 - \Gamma\,\mathrm{Im}\left[\mathrm{e}^{\mathrm{i}Et}d\right]\right] \\ f_R\left[-\left[1/2 V(t)+V_0\right]|d|^2 + \left[V_0+E\right]\mathrm{Re}\left[\mathrm{e}^{\mathrm{i}Et}d\right]\right] \end{matrix} \tag{C.62}$$

$$I^\varepsilon_{0,-1} = -\int \frac{\mathrm{d}E}{2\pi} \begin{matrix} f_R\left[-\left[1/2 V(t)+V_0\right]|d|^2 - \Gamma\,\mathrm{Im}\left[\mathrm{e}^{\mathrm{i}Et}d\right]\right] \\ f_L\left[-\left[1/2 V(t)+V_0\right]|d|^2 + \left[V_0+E\right]\mathrm{Re}\left[\mathrm{e}^{\mathrm{i}Et}d\right]\right] \end{matrix} \tag{C.63}$$

The energy current plus the source term writes

$$I^\varepsilon_{01} + S^E_1 = -\int \frac{\mathrm{d}E}{2\pi} \begin{matrix} f_L\left[-\left[V(t)+V_0\right]|d|^2 - \Gamma\,\mathrm{Im}\left[\mathrm{e}^{\mathrm{i}Et}d\right]\right] \\ f_R\left[-\left[V(t)+V_0\right]|d|^2 + \left[V_0+V(t)+E\right]\mathrm{Re}\left[\mathrm{e}^{\mathrm{i}Et}d\right]\right] \end{matrix} \tag{C.64a}$$

$$I^\varepsilon_{0,-1} + S^E_{-1} = -\int \frac{\mathrm{d}E}{2\pi} \begin{matrix} f_R\left[-\left[V(t)+V_0\right]|d|^2 - \Gamma\,\mathrm{Im}\left[\mathrm{e}^{\mathrm{i}Et}d\right]\right] \\ f_L\left[-\left[V(t)+V_0\right]|d|^2 + \left[V_0+V(t)+E\right]\mathrm{Re}\left[\mathrm{e}^{\mathrm{i}Et}d\right]\right] \end{matrix} \tag{C.64b}$$

which is useful for the heat current $I^{\mathrm{Q}}_{1,0}$ and $I^{\mathrm{Q}}_{-1,0}$, that are defined using Eq. (4.211) as the following:

$$I^{\mathrm{Q}}_{\mathrm{R}} = I^\varepsilon_{1,0} - S^\varepsilon_1 - \mu_{\mathrm{R}} I^{\mathrm{N}}_{1,0} \tag{C.65}$$

$$I^{\mathrm{Q}}_{\mathrm{L}} = I^\varepsilon_{-1,0} - S^\varepsilon_{-1} - \mu_{\mathrm{L}} I^{\mathrm{N}}_{-1,0} \tag{C.66}$$

C.5. Time-integrated quantities

C.5.1. Energy

We are interested in the dynamically injected energy throughout the pulse (*i.e.* finite in time) in lead α:

$$\varepsilon_\alpha^{\text{dyn}} = \int \mathrm{d}t\, I_\alpha^\varepsilon(t) - I_\alpha^{\text{E}}(t=0) \tag{C.67}$$

Where $I_{0,\alpha}^{\text{E}}$ is the stationary energy current before the start of the pulse, given by the standard Landauer-Buttiker formula:

$$I_{01}^{\text{E}}(t=0) = \int \frac{\mathrm{d}E}{2\pi}\, E\left[D_0 f_L - [1-R_0]\, f_R\right] \tag{C.68}$$

$$I_{0,-1}^{\text{E}}(t=0) = \int \frac{\mathrm{d}E}{2\pi}\, E\left[D_0 f_R - [1-R_0]\, f_L\right] \tag{C.69}$$

Given that $\int \mathrm{d}t\, I_{01}^E \neq \int \mathrm{d}t\, I_{12}^E$ (because of $S_1^E \neq 0$) and also that $\forall x \geq 1 \int dt\, I_{12}^E = \int \mathrm{d}t\, I_{x,x+1}^E$, and since we are interested in the currents far in the lead, it is more fitting to consider $I_{01}^E + S_1^E$ because of the following :

$$\partial_t \varepsilon_1 + I_{10}^E + I_{12}^E = S_1^E \implies \partial_t \varepsilon_1 + I_{12}^E = I_{01}^E + S_1^E \implies \int \mathrm{d}t\, I_{12}^E = \int \mathrm{d}t\, I_{01}^E + S_1^E \tag{C.70}$$

To proceed further, we will use the following equivalent expression for the energy current:

$$I_{01}^E + S_1^E = \int \frac{\mathrm{d}E}{2\pi} + \begin{array}{l} f_R\Big[E[\,|r|^2 - 1\,] + \mathrm{Im}[A\partial_t A^*] + \mathrm{Re}[\partial_t A]\Big] \\ f_L\Big[E\ \ |d|^2 \qquad\quad + \mathrm{Im}[A\partial_t A^*]\Big] \end{array} \tag{C.71}$$

$$I_{0,-1}^E + S_{-1}^E = \int \frac{\mathrm{d}E}{2\pi} + \begin{array}{l} f_L\Big[E[\,|r|^2 - 1\,] + \mathrm{Im}[A\partial_t A^*] + \mathrm{Re}[\partial_t A]\Big] \\ f_R\Big[E\ \ |d|^2 \qquad\quad + \mathrm{Im}[A\partial_t A^*]\Big] \end{array} \tag{C.72}$$

Where

$$A = -\mathrm{i}\,\mathrm{e}^{\mathrm{i}Et} d \tag{C.73}$$

The above expressions can be split like the following:

$$I_{01}^E + S_1^E = \int \frac{\mathrm{d}E}{2\pi}\, E\left[f_L\,|d|^2 - f_R\left(1-|r|^2\right)\right] + (f_L+f_R)\,\mathrm{Im}[A\partial_t A^*] + f_R\,\mathrm{Re}[\partial_t A] \tag{C.74}$$

$$I_{0,-1}^E + S_{-1}^E = \int \frac{\mathrm{d}E}{2\pi}\, E\left[f_R\,|d|^2 - f_L\left(1-|r|^2\right)\right] + (f_L+f_R)\,\mathrm{Im}[A\partial_t A^*] + f_L\,\mathrm{Re}[\partial_t A] \tag{C.75}$$

Now we subtract the initial stationary current (given in C.69 and C.68), knowing that $S^E\big|_{t=0} = 0$:

$$I_{01}^E + S_1^E - I_{01}^E\big|_{t=0} = \int \frac{\mathrm{d}E}{2\pi} \begin{bmatrix} E\left[f_L\left(|d|^2 - D_0\right) - f_R\left(R_0 - |r|^2\right)\right] \\ +\,(f_L+f_R)\,\mathrm{Im}[A\partial_t A^*] \\ +\,f_R\,\mathrm{Re}[\partial_t A] \end{bmatrix} \tag{C.76}$$

$$I_{0,-1}^E + S_{-1}^E - I_{0,-1}^E\big|_{t=0} = \int \frac{\mathrm{d}E}{2\pi} \begin{bmatrix} E\left[f_R\left(|d|^2 - D_0\right) - f_L\left(R_0 - |r|^2\right)\right] \\ +\,(f_L+f_R)\,\mathrm{Im}[A\partial_t A^*] \\ +\,f_L\,\mathrm{Re}[\partial_t A] \end{bmatrix} \tag{C.77}$$

Now we can calculate the time integral from $t = 0$ to $t = \infty$, let's start with $\partial_t A$, while having in mind (6.79) and (6.63):

$$\int_0^\infty \mathrm{d}t\, \mathrm{Re}[\partial_t A] = \mathrm{Re}\Big[\underbrace{A|_{t=\infty}}_{=-\mathrm{i}d_0} - \underbrace{A|_{t=0}}_{=-\mathrm{i}d_0} \Big] = 0 \tag{C.78}$$

using the definition of T_{dyn} in (6.65):

$$\int \mathrm{d}t \left[I^E_{01} \quad + S^E_1 - I^E_{01}\big|_{t=0} \right] \quad = \quad \left[\begin{array}{l} + \displaystyle\int \frac{\mathrm{d}E}{2\pi}\, E\,(f_L - f_R)\, T_{\mathrm{dyn}} \\ \displaystyle\int \frac{\mathrm{d}E}{2\pi}\, \mathrm{d}t\ \ (f_L + f_R)\, \mathrm{Im}[A\partial_t A^*] \end{array} \right. \tag{C.79}$$

$$\int \mathrm{d}t \left[I^E_{0,-1} + S^E_{-1} - I^E_{0,-1}\big|_{t=0} \right] = \quad \left[\begin{array}{l} + \displaystyle\int \frac{\mathrm{d}E}{2\pi}\, E\,(f_R - f_L)\, T_{\mathrm{dyn}} \\ \displaystyle\int \frac{\mathrm{d}E}{2\pi}\, \mathrm{d}t\ \ (f_L + f_R)\, \mathrm{Im}[A\partial_t A^*] \end{array} \right. \tag{C.80}$$

Given the relation (C.70) and that $\forall x\ I^E_{x,x+1}\big|_{t=0} = I^E_{0,1}\big|_{t=0}$, we have:

$$\begin{aligned} \int \mathrm{d}t \left[I^\varepsilon_{0,1} \quad + S^{\mathrm{E}}_1 \ - I^\varepsilon_{0,1}\big|_{t=0} \right] \ &= \int \mathrm{d}t \left[I^\varepsilon_{1,2} \quad - I^\varepsilon_{1,2}\big|_{t=0} \right] \\ \int \mathrm{d}t \left[I^\varepsilon_{0,-1} + S^{\mathrm{E}}_{-1} - I^\varepsilon_{0,-1}\big|_{t=0} \right] &= \int \mathrm{d}t \left[I^\varepsilon_{-1,-2} - \ I^\varepsilon_{-1,-2}\big|_{t=0} \right] \end{aligned} \tag{C.81}$$

To further simplify the equations above, one can write the conservation equation on the group of sites $-1, 0$ and 1:

$$\partial_t[\varepsilon_{-1} + \varepsilon_0 + \varepsilon_1] + I^E_{-1,-2} + I^E_{1,2} = S^E \tag{C.82}$$

where S^E is given by (6.59). The time integral of this relation gives:

$$\underbrace{[\varepsilon_{-1} + \varepsilon_0 + \varepsilon_1]^{t=\infty}_{t=0}}_{=0 \text{ (back to initial state)}} + \int \mathrm{d}t\ \left[I^E_{-1,-2} + I^E_{1,2} \right] = \int \mathrm{d}t\, S^E \tag{C.83}$$

The term $\int \mathrm{d}t\ \left[I^E_{-1,-2} + I^E_{1,2} \right]$ can be expressed by summing (C.80) and (C.79). With (C.81) in mind and $I^E_{1,2}\big|_{t=0} + I^E_{-1,-2}\big|_{t=0} = 0$:

$$\int \mathrm{d}t\ \left[I^E_{-1,-2} + I^E_{1,2} \right] = \int \mathrm{d}t\, S^E = \int \frac{\mathrm{d}E}{2\pi}\, \mathrm{d}t\ 2\ (f_L + f_R)\, \mathrm{Im}[A\partial_t A^*] \tag{C.84}$$

And this enables writing a simple formula for $\varepsilon^{\mathrm{dyn}}_\alpha$:

$$\begin{aligned} \varepsilon^{\mathrm{dyn}}_R &= \int \mathrm{d}t \left[I^\varepsilon_{1,2} \quad - I^\varepsilon_{1,2}\big|_{t=0} \right] \quad = \int \frac{\mathrm{d}E}{2\pi}\, E\,(f_R - f_L)\, T_{\mathrm{dyn}} + \frac{1}{2} \int \mathrm{d}t\, S^\varepsilon \\ \varepsilon^{\mathrm{dyn}}_L &= \int \mathrm{d}t \left[I^\varepsilon_{-1,-2} - \ I^\varepsilon_{-1,-2}\big|_{t=0} \right] = \int \frac{\mathrm{d}E}{2\pi}\, E\,(f_L - f_R)\, T_{\mathrm{dyn}} + \frac{1}{2} \int \mathrm{d}t\, S^\varepsilon \end{aligned} \tag{C.85}$$

Bibliography

[1] The t-Kwant package is free, open-source, and available online at https://tkwant.kwant-project.org.

[2] The Kwant package is a free (open-source) software available at https://kwant-project.org/.

[3] The `tkwantoperator` Python extensions to `tkwant` is free and open-source. It is available online at https://gitlab.kwant-project.org/kwant/tkwantoperator.

[4] The development history of `tkwantoperator` code is available at following deprecated repository https://gitlab.kwant-project.org/spec-gmt/tkwant-energy-transport.

[5] Adel Abbout et al. "Cooperative Charge Pumping and Enhanced Skyrmion Mobility." In: *Physical Review Letters* 121.25 (Dec. 19, 2018). Publisher: American Physical Society, p. 257203. DOI: 10.1103/PhysRevLett.121.257203.

[6] Shigeru Ajisaka et al. "Nonequlibrium particle and energy currents in quantum chains connected to mesoscopic Fermi reservoirs." In: *Physical Review B* 86.12 (Sept. 7, 2012). DOI: 10.1103/PhysRevB.86.125111.

[7] AE Allahverdyan and Th M Nieuwenhuizen. "Extraction of work from a single thermal bath in the quantum regime." In: *Physical Review Letters* 85.9 (2000), p. 1799.

[8] Philip B. Allen and Joseph L. Feldman. "Thermal conductivity of disordered harmonic solids." In: *Physical Review B* 48.17 (Nov. 1, 1993). Publisher: American Physical Society, pp. 12581–12588. DOI: 10.1103/PhysRevB.48.12581.

[9] Bjarne Andresen. "Current Trends in Finite-Time Thermodynamics." In: *Angewandte Chemie International Edition* 50.12 (2011), pp. 2690–2704. ISSN: 1521-3773. DOI: 10.1002/anie.201001411.

[10] Bjarne Andresen, Peter Salamon, and R Stephen Berry. "Thermodynamics in finite fille." In: *Physics today* (1984), p. 63.

[11] Pacome Armagnat et al. "The self-consistent quantum-electrostatic problem in strongly nonlinear regime." In: *SciPost Physics* 7.3 (Sept. 11, 2019), p. 031. ISSN: 2542-4653. DOI: 10.21468/SciPostPhys.7.3.031.

[12] Liliana Arrachea, Michael Moskalets, and Luis Martin-Moreno. "Heat production and energy balance in nanoscale engines driven by time-dependent fields." In: *Phys. Rev. B* 75 (24 June 2007), p. 245420. DOI: 10.1103/PhysRevB.75.245420.

[13] Francesca Battista, Federica Haupt, and Janine Splettstoesser. "Energy and power fluctuations in ac-driven coherent conductors." In: *Phys. Rev. B* 90 (8 Aug. 2014), p. 085418. DOI: 10.1103/PhysRevB.90.085418.

[14] Christopher Bäuerle et al. "Coherent control of single electrons: a review of current progress." In: *Reports on Progress in Physics* 81.5 (Apr. 2018), p. 056503. ISSN: 0034-4885. DOI: 10.1088/1361-6633/aaa98a.

[15] C. W. J. Beenakker and A. A. M. Staring. "Theory of the thermopower of a quantum dot." In: *Phys. Rev. B* 46 (15 Oct. 1992), pp. 9667–9676. DOI: 10.1103/PhysRevB.46.9667.

[16] Giuliano Benenti et al. "Fundamental aspects of steady-state conversion of heat to work at the nanoscale." In: *Physics Reports*. Fundamental aspects of steady-state conversion of heat to work at the nanoscale 694 (June 9, 2017), pp. 1–124. ISSN: 0370-1573. DOI: 10.1016/j.physrep.2017.05.008.

[17] Bibek Bhandari et al. "Geometric properties of adiabatic quantum thermal machines." In: *Phys. Rev. B* 102 (15 Oct. 2020), p. 155407. DOI: 10.1103/PhysRevB.102.155407.

[18] Dinesh Bhatia et al. "Pacemakers charging using body energy." In: *Journal of Pharmacy and Bioallied Sciences* 2.1 (2010), pp. 51–54. ISSN: 0976-4879. DOI: 10.4103/0975-7406.62713.

[19] Robert Biele, Roberto D'Agosta, and Angel Rubio. "Time-Dependent Thermal Transport Theory." In: *Phys. Rev. Lett.* 115 (5 July 2015), p. 056801. DOI: 10.1103/PhysRevLett.115.056801.

[20] Ya. M. Blanter and M. Büttiker. "Shot noise in mesoscopic conductors." In: *Physics Reports* 336.1 (Sept. 1, 2000), pp. 1–166. ISSN: 0370-1573. DOI: 10.1016/S0370-1573(99)00123-4.

[21] Alisa Bokulich. "Reexamining the quantum-classical relation." In: *Reexamining the Quantum-Classical Relation* (2008).

[22] Olivier Bourgeois et al. "Reduction of phonon mean free path: From low-temperature physics to room temperature applications in thermoelectricity." In: *Comptes Rendus Physique*. Mesoscopic thermoelectric phenomena / Phénomènes thermoélectriques mésoscopiques 17.10 (Dec. 1, 2016), pp. 1154–1160. ISSN: 1631-0705. DOI: 10.1016/j.crhy.2016.08.008.

[23] Heinz-Peter Breuer et al. *The Theory of Open Quantum Systems*. Oxford University Press, 2002. 648 pp. ISBN: 978-0-19-852063-4.

[24] Anton Bruch, Caio Lewenkopf, and Felix von Oppen. "Landauer-Büttiker Approach to Strongly Coupled Quantum Thermodynamics: Inside-Outside Duality of Entropy Evolution." In: *Phys. Rev. Lett.* 120 (10 Mar. 2018), p. 107701. DOI: 10.1103/PhysRevLett.120.107701.

[25] Anton Bruch et al. "Quantum thermodynamics of the driven resonant level model." In: *Phys. Rev. B* 93 (11 Mar. 2016), p. 115318. DOI: 10.1103/PhysRevB.93.115318.

[26] P. N. Butcher. "Thermal and electrical transport formalism for electronic microstructures with many terminals." In: *J. Phys.: Condens. Matter* 2.22 (June 1990), pp. 4869–4878. DOI: 10.1088/0953-8984/2/22/008.

[27] Jeremy Butterfield and John Earman. *Philosophy of physics*. Vol. 2. Elsevier, 2007.

[28] M. Büttiker. "Scattering theory of current and intensity noise correlations in conductors and wave guides." In: *Physical Review B* 46.19 (Nov. 15, 1992), pp. 12485–12507. DOI: 10.1103/PhysRevB.46.12485.

[29] Herbert B. Callen. *Thermodynamics and an Introduction to Thermostatistics, 2nd Edition*. Wiley, 1985. 512 pp. ISBN: 978-0-471-86256-7.

[30] Patrice A Camati et al. "Experimental rectification of entropy production by Maxwell's demon in a quantum system." In: *Physical review letters* 117.24 (2016), p. 240502.

[31] Michele Campisi, Peter Hänggi, and Peter Talkner. "Colloquium: Quantum fluctuation relations: Foundations and applications." In: *Reviews of Modern Physics* 83.3 (July 6, 2011). Publisher: American Physical Society, pp. 771–791. DOI: 10.1103/RevModPhys.83.771.

[32] Sadi Carnot. *Réflections sur la Puissance Motrice du Feu et sur les Machines propres à développer cette Puissance*. Bachelier: Paris, France, 1824.

[33] Anffany Chen et al. "Quantum Holography in a Graphene Flake with an Irregular Boundary." In: *Physical Review Letters* 121.3 (July 18, 2018). Publisher: American Physical Society, p. 036403. DOI: 10.1103/PhysRevLett.121.036403.

[34] J. Chen, M. ShangGuan, and J. Wang. "A gauge invariant theory for time dependent heat current." In: *New J. Phys.* 17 (2015), p. 053034. DOI: 10.1088/1367-2630/17/5/053034.

[35] R. Chirla and C. P. Moca. "Finite-frequency thermoelectric response in strongly correlated quantum dots." In: *Phys. Rev. B* 89 (4 Jan. 2014), p. 045132. DOI: 10.1103/PhysRevB.89.045132.

[36] Nathanaël Cottet et al. "Observing a quantum Maxwell demon at work." In: *Proceedings of the National Academy of Sciences* 114.29 (July 18, 2017), pp. 7561–7564. ISSN: 0027-8424, 1091-6490. DOI: 10.1073/pnas.1704827114.

[37] F. Covito et al. "Transient Charge and Energy Flow in the Wide-Band Limit." In: *J. Chem. Theory Comput.* 14.5 (2018), pp. 2495–2504. DOI: 10.1021/acs.jctc.8b00077.

[38] Adeline Crépieux et al. "Enhanced thermopower under a time-dependent gate voltage." In: *Phys. Rev. B* 83 (15 Apr. 2011). and Phys. Rev. B **89**, 239907 (2014), p. 153417. DOI: 10.1103/PhysRevB.83.153417.

[39] Alexander Croy and Ulf Saalmann. "Propagation scheme for nonequilibrium dynamics of electron transport in nanoscale devices." In: *Phys. Rev. B* 80 (24 Dec. 2009), p. 245311. DOI: 10.1103/PhysRevB.80.245311.

[40] Eduardo C. Cuansing, Jian-Sheng Wang, and Juzar Thingna. "Nonadiabatic particle and energy pump at strong system-reservoir coupling." In: *arXiv:2003.04589 [cond-mat]* (Mar. 10, 2020). arXiv: 2003.04589.

[41] Longji Cui et al. "Perspective: Thermal and thermoelectric transport in molecular junctions." In: *The Journal of Chemical Physics* 146 (2017), p. 092201. DOI: 10.1063/1.4976982.

[42] Frank L Curzon and B Ahlborn. "Efficiency of a Carnot engine at maximum power output." In: *American Journal of Physics* 43.1 (1975), pp. 22–24.

[43] Simone Dalola et al. "Characterization of Thermoelectric Modules for Powering Autonomous Sensors." In: *IEEE Transactions on Instrumentation and Measurement* 58.1 (Jan. 2009). Conference Name: IEEE Transactions on Instrumentation and Measurement, pp. 99–107. ISSN: 1557-9662. DOI: 10.1109/TIM.2008.928405.

[44] A.-M. Daré and P. Lombardo. "Time-dependent thermoelectric transport for nanoscale thermal machines." In: *Phys. Rev. B* 93 (3 Jan. 2016), p. 035303. DOI: 10.1103/PhysRevB.93.035303.

[45] Nastaran Dashti et al. "Minimal excitation single-particle emitters: Comparison of charge-transport and energy-transport properties." In: *Phys. Rev. B* 100 (3 July 2019), p. 035405. DOI: 10.1103/PhysRevB.100.035405.

[46] Supriyo Datta. *Electronic Transport in Mesoscopic Systems*. Cambridge Studies in Semiconductor Physics and Microelectronic Engineering. Cambridge University Press, 1995. DOI: 10.1017/CBO9780511805776.

[47] Wenjie Dou et al. "Universal approach to quantum thermodynamics in the strong coupling regime." In: *Phys. Rev. B* 98 (13 Oct. 2018), p. 134306. DOI: 10.1103/PhysRevB.98.134306.

[48] B. Dutta et al. "Single-Quantum-Dot Heat Valve." In: *Phys. Rev. Lett.* 125 (23 Dec. 2020), p. 237701. DOI: 10.1103/PhysRevLett.125.237701.

[49] F. G. Eich, M. Di Ventra, and G. Vignale. "Temperature-driven transient charge and heat currents in nanoscale conductors." In: *Phys. Rev. B* 93 (13 Apr. 2016), p. 134309. DOI: 10.1103/PhysRevB.93.134309.

[50] O. Entin-Wohlman et al. "Heat currents in electronic junctions driven by telegraph noise." In: *Physical Review B* 96.19 (Nov. 28, 2017), p. 195435. DOI: 10.1103/PhysRevB.96.195435.

[51] M. Esposito et al. "Finite-time thermodynamics for a single-level quantum dot." In: *EPL (Europhysics Letters)* 89.2 (Jan. 2010), p. 20003. ISSN: 0295-5075. DOI: 10.1209/0295-5075/89/20003.

[52] Massimiliano Esposito, Upendra Harbola, and Shaul Mukamel. "Nonequilibrium fluctuations, fluctuation theorems, and counting statistics in quantum systems." In: *Reviews of Modern Physics* 81.4 (Dec. 2, 2009). Publisher: American Physical Society, pp. 1665–1702. DOI: 10.1103/RevModPhys.81.1665.

[53] Massimiliano Esposito, Katja Lindenberg, and Christian Van den Broeck. "Thermoelectric efficiency at maximum power in a quantum dot." In: *EPL (Europhysics Letters)* 85.6 (2009), p. 60010.

[54] Massimiliano Esposito, Maicol A. Ochoa, and Michael Galperin. "Nature of heat in strongly coupled open quantum systems." In: *Phys. Rev. B* 92 (23 Dec. 2015), p. 235440. DOI: 10.1103/PhysRevB.92.235440.

[55] Massimiliano Esposito, Maicol A. Ochoa, and Michael Galperin. "Quantum Thermodynamics: A Nonequilibrium Green's Function Approach." In: *Phys. Rev. Lett.* 114 (8 Feb. 2015), p. 080602. DOI: 10.1103/PhysRevLett.114.080602.

[56] Richard P. Feynman. *The Feynman Lectures on Physics: Quantum Mechanics*. New millenium edition for tablets. Vol. 3. Basic Books, 2013. ISBN: 978-0-465-07294-1.

[57] Leslie L. Foldy and Siegfried A. Wouthuysen. "On the Dirac Theory of Spin 1/2 Particles and Its Non-Relativistic Limit." In: *Physical Review* 78.1 (Apr. 1, 1950). Publisher: American Physical Society, pp. 29–36. DOI: 10.1103/PhysRev.78.29.

[58] GW Ford and RF O'Connell. "A quantum violation of the second law?" In: *Physical review letters* 96.2 (2006), p. 020402.

[59] Antonio Fornieri et al. "Evidence of topological superconductivity in planar Josephson junctions." In: *Nature* 569.7754 (May 2019), pp. 89–92. ISSN: 1476-4687. DOI: 10.1038/s41586-019-1068-8.

[60] M. Fruchart et al. "Probing (topological) Floquet states through DC transport." In: *Physica E: Low-dimensional Systems and Nanostructures* 75 (Jan. 1, 2016), pp. 287–294. ISSN: 1386-9477. DOI: 10.1016/j.physe.2015.09.035.

[61] F. Gallego-Marcos and G. Platero. "Coherent long-range thermoelectrics in nonadiabatic driven quantum systems." In: *Phys. Rev. B* 95 (7 Feb. 2017), p. 075301. DOI: 10.1103/PhysRevB.95.075301.

[62] S. Gattenlöhner et al. "L\'evy Flights due to Anisotropic Disorder in Graphene." In: *Physical Review Letters* 117.4 (July 22, 2016). Publisher: American Physical Society, p. 046603. DOI: 10.1103/PhysRevLett.117.046603.

[63] Benoit Gaury. "Emerging concepts in time-resolved quantum nanoelectronics." en. PhD thesis. Université de Grenoble, Oct. 2014.

[64] Benoit Gaury and Xavier Waintal. "Dynamical control of interference using voltage pulses in the quantum regime." In: *Nat. Commun.* 5 (Apr. 2014), p. 3844. DOI: 10.1038/ncomms4844.

[65] Benoit Gaury, Joseph Weston, and Xavier Waintal. "Stopping electrons with radio-frequency pulses in the quantum Hall regime." In: *Physical Review B* 90.16 (Oct. 22, 2014). Publisher: American Physical Society, p. 161305. DOI: 10.1103/PhysRevB.90.161305.

[66] Benoit Gaury et al. "Numerical simulations of time-resolved quantum electronics." In: *Physics Reports* 534.1 (Jan. 2014), pp. 1–37. ISSN: 03701573. DOI: 10.1016/j.physrep.2013.09.001.

[67] Max Geier et al. "Second-order topological insulators and superconductors with an order-two crystalline symmetry." In: *Physical Review B* 97.20 (May 25, 2018). Publisher: American Physical Society, p. 205135. DOI: 10.1103/PhysRevB.97.205135.

[68] David Gelbwaser-Klimovsky, Wolfgang Niedenzu, and Gershon Kurizki. "Chapter Twelve - Thermodynamics of Quantum Systems Under Dynamical Control." In: *Advances In Atomic, Molecular, and Optical Physics*. Ed. by Ennio Arimondo, Chun C. Lin, and Susanne F. Yelin. Vol. 64. Academic Press, Jan. 1, 2015, pp. 329–407. DOI: 10.1016/bs.aamop.2015.07.002.

[69] JE Geusic, EO Schulz-DuBios, and HED Scovil. "Quantum equivalent of the carnot cycle." In: *Physical Review* 156.2 (1967), p. 343.

[70] Eitan Geva and Ronnie Kosloff. "A quantum-mechanical heat engine operating in finite time. A model consisting of spin-1/2 systems as the working fluid." In: *The Journal of chemical physics* 96.4 (1992), pp. 3054–3067.

[71] Eitan Geva and Ronnie Kosloff. "On the classical limit of quantum thermodynamics in finite time." In: *The Journal of chemical physics* 97.6 (1992), pp. 4398–4412.

[72] Eitan Geva, Ronnie Kosloff, and JL Skinner. "On the relaxation of a two-level system driven by a strong electromagnetic field." In: *The Journal of chemical physics* 102.21 (1995), pp. 8541–8561.

[73] H J Goldsmid and R W Douglas. "The use of semiconductors in thermoelectric refrigeration." In: *British Journal of Applied Physics* 5.11 (Nov. 1954), pp. 386–390. DOI: 10.1088/0508-3443/5/11/303.

[74] H. Julian Goldsmid. *Introduction to Thermoelectricity*. 2nd ed. Springer Series in Materials Science. Berlin Heidelberg: Springer-Verlag, 2016. ISBN: 978-3-662-49255-0. DOI: 10.1007/978-3-662-49256-7.

[75] Christophe Goupil. *Continuum Theory and Modeling of Thermoelectric Elements*. Weinheim: Wiley VCH, Jan. 13, 2016. 400 pp. ISBN: 978-3-527-41337-9.

[76] S. R. De Groot and P. Mazur. *Non-Equilibrium Thermodynamics*. Dover ed edition. New York: Dover Publications, Feb. 17, 2011. 528 pp. ISBN: 978-0-486-64741-8.

[77] Christoph W Groth et al. "Kwant: a software package for quantum transport." In: *New Journal of Physics* 16.6 (June 27, 2014), p. 063065. ISSN: 1367-2630. DOI: 10.1088/1367-2630/16/6/063065.

[78] Shmuel Gurvitz. "Single-electron approach for time-dependent electron transport." en. In: *Physica Scripta* T165 (Oct. 2015). Publisher: IOP Publishing, p. 014013. ISSN: 1402-4896. DOI: 10.1088/0031-8949/2015/T165/014013.

[79] Shmuel Gurvitz. "Zero-bias current induced by periodic drive of arbitrary shape." In: *The European Physical Journal Special Topics* 230.4 (June 1, 2021), pp. 827–835. ISSN: 1951-6401. DOI: 10.1140/epjs/s11734-021-00086-0.

[80] Pedro E. Harunari et al. "Maximal power for heat engines: Role of asymmetric interaction times." In: *Phys. Rev. Research* 3 (2 June 2021), p. 023194. DOI: 10.1103/PhysRevResearch.3.023194.

[81] Patrick Haughian, Massimiliano Esposito, and Thomas L. Schmidt. "Quantum thermodynamics of the resonant-level model with driven system-bath coupling." In: *Phys. Rev. B* 97 (8 Feb. 2018), p. 085435. DOI: 10.1103/PhysRevB.97.085435.

[82] F. Haupt et al. "Heat, molecular vibrations, and adiabatic driving in non-equilibrium transport through interacting quantum dots." In: *physica status solidi (b)* 250.11 (2013), pp. 2315–2329. DOI: 10.1002/pssb.201349219.

[83] P. Havu et al. "Nonequilibrium electron transport in two-dimensional nanostructures modeled using Green's functions and the finite-element method." In: *Phys. Rev. B* 69 (11 Mar. 2004), p. 115325. DOI: 10.1103/PhysRevB.69.115325.

[84] Wenke He et al. "High thermoelectric performance in low-cost SnS0.91Se0.09 crystals." In: *Science* 365.6460 (Sept. 27, 2019). Publisher: American Association for the Advancement of Science Section: Research Article, pp. 1418–1424. ISSN: 0036-8075, 1095-9203. DOI: 10.1126/science.aax5123.

[85] Joseph P. Heremans et al. "When thermoelectrics reached the nanoscale." In: *Nature Nanotechnology* 8.7 (July 2013), pp. 471–473. ISSN: 1748-3395. DOI: 10.1038/nnano.2013.129.

[86] L. D. Hicks and M. S. Dresselhaus. "Thermoelectric figure of merit of a one-dimensional conductor." In: *Physical Review B* 47.24 (June 15, 1993). Publisher: American Physical Society, pp. 16631–16634. DOI: 10.1103/PhysRevB.47.16631.

[87] B. Hinterleitner et al. "Thermoelectric performance of a metastable thin-film Heusler alloy." In: *Nature* 576.7785 (Dec. 2019), pp. 85–90. ISSN: 1476-4687. DOI: 10.1038/s41586-019-1751-9.

[88] Douglas R. Hofstadter. "Energy levels and wave functions of Bloch electrons in rational and irrational magnetic fields." In: *Phys. Rev. B* 14 (6 Sept. 1976), pp. 2239–2249. DOI: 10.1103/PhysRevB.14.2239.

[89] Zhong-Yue Huang et al. "Achieving high thermoelectric performance of Ni/Cu modified Bi0.5Sb1.5Te3 composites by a facile electroless plating." In: *Materials Today Energy* 9 (Sept. 1, 2018), pp. 383–390. ISSN: 2468-6069. DOI: 10.1016/j.mtener.2018.06.011.

[90] A. F. Ioffe et al. "Semiconductor Thermoelements and Thermoelectric Cooling." In: *Physics Today* 12.5 (May 1, 1959). Publisher: American Institute of Physics, pp. 42–42. ISSN: 0031-9228. DOI: 10.1063/1.3060810.

[91] John David Jackson. *Classical electrodynamics*. American Association of Physics Teachers, 1999.

[92] Antti-Pekka Jauho, Ned S. Wingreen, and Yigal Meir. "Time-dependent transport in interacting and noninteracting resonant-tunneling systems." In: *Phys. Rev. B* 50 (8 Aug. 1994), pp. 5528–5544. DOI: 10.1103/PhysRevB.50.5528.

[93] Martin Josefsson et al. "A quantum-dot heat engine operating close to the thermodynamic efficiency limits." In: *Nature Nanotechnology* 13.10 (Oct. 2018), pp. 920–924. ISSN: 1748-3387, 1748-3395. DOI: 10.1038/s41565-018-0200-5.

[94] Martin Josefsson et al. "Optimal power and efficiency of single quantum dot heat engines: Theory and experiment." In: *Phys. Rev. B* 99 (23 June 2019), p. 235432. DOI: 10.1103/PhysRevB.99.235432.

[95] Mercouri G. Kanatzidis. "Nanostructured Thermoelectrics: The New Paradigm?" In: *Chemistry of Materials* 22.3 (Feb. 9, 2010). Publisher: American Chemical Society, pp. 648–659. ISSN: 0897-4756. DOI: 10.1021/cm902195j.

[96] Adel Kara Slimane, Phillipp Reck, and Geneviève Fleury. "Simulating time-dependent thermoelectric transport in quantum systems." In: *Physical Review B* 101.23 (June 8, 2020). Publisher: American Physical Society, p. 235413. DOI: 10.1103/PhysRevB.101.235413.

[97] Bayan Karimi et al. "Reaching the ultimate energy resolution of a quantum detector." In: *Nat. Commun.* 11 (2020), p. 367. DOI: 10.1038/s41467-019-14247-2.

[98] Shubhash C Kaushik, Sudhir K Tyagi, and Pramod Kumar. *Finite time thermodynamics of power and refrigeration cycles*. Springer, 2017.

[99] GE Kimball and GH Shortley. "The numerical solution of Schrödinger's equation." In: *Physical Review* 45.11 (1934), p. 815.

[100] Thomas Kloss, Joseph Weston, and Xavier Waintal. "Transient and Sharvin resistances of Luttinger liquids." In: *Physical Review B* 97.16 (Apr. 23, 2018), p. 165134. DOI: 10.1103/PhysRevB.97.165134.

[101] Thomas Kloss et al. "Tkwant: a software package for time-dependent quantum transport." In: *New Journal of Physics* 23.2 (Feb. 2021). Publisher: IOP Publishing, p. 023025. ISSN: 1367-2630. DOI: 10.1088/1367-2630/abddf7.

[102] D H Kobe and E C -T Wen. "Gauge invariance in quantum mechanics: charged harmonic oscillator in an electromagnetic field." In: *Journal of Physics A: Mathematical and General* 15.3 (Mar. 1982), pp. 787–803. DOI: 10.1088/0305-4470/15/3/018.

[103] D H Kobe and Kuo-Ho Yang. "Energy of a classical charged particle in an external electromagnetic field." en. In: *European Journal of Physics* 8.4 (Oct. 1987), pp. 236–244. ISSN: 0143-0807, 1361-6404. DOI: 10.1088/0143-0807/8/4/002.

[104] Donald H. Kobe. "Gauge invariance in second quantization: Applications to Hartree-Fock and generalized random-phase approximations." In: *Phys. Rev. A* 19 (5 May 1979), p. 1876. DOI: 10.1103/PhysRevA.19.1876.

[105] Jonne V Koski et al. "Experimental observation of the role of mutual information in the nonequilibrium dynamics of a Maxwell demon." In: *Physical review letters* 113.3 (2014), p. 030601.

[106] Jonne V. Koski and Jukka P. Pekola. "Maxwell's demons realized in electronic circuits." In: *Comptes Rendus Physique* 17.10 (Dec. 2016), pp. 1130–1138. ISSN: 16310705. DOI: 10.1016/j.crhy.2016.08.011.

[107] Ronnie Kosloff. "Quantum Thermodynamics: A Dynamical Viewpoint." In: *Entropy* 15.6 (2013), p. 2100. ISSN: 1099-4300. DOI: 10.3390/e15062100.

[108] M. Krawiec and K. I. Wysoki ński. "Thermoelectric effects in strongly interacting quantum dot coupled to ferromagnetic leads." In: *Phys. Rev. B* 73 (7 Feb. 2006), p. 075307. DOI: 10.1103/PhysRevB.73.075307.

[109] S. Kurth et al. "Time-dependent quantum transport: A practical scheme using density functional theory." In: *Phys. Rev. B* 72 (3 July 2005), p. 035308. DOI: 10.1103/PhysRevB.72.035308.

[110] S. Kurth et al. "Time-dependent quantum transport: A practical scheme using density functional theory." In: *Phys. Rev. B* 72 (3 July 2005), p. 035308. DOI: 10.1103/PhysRevB.72.035308.

[111] Michel Le Bellac. *Physique Quantique - Fondements - Tome I*. fr. 3rd ed. CNRS Editions. ISBN: 978-2-271-07736-3.

[112] Soochan Lee et al. "Thermoelectric-based sustainable self-cooling for fine-grained processor hot spots." In: *2016 15th IEEE Intersociety Conference on Thermal and Thermomechanical Phenomena in Electronic Systems (ITherm)*. 2016, pp. 847–856. DOI: 10.1109/ITHERM.2016.7517635.

[113] Thomas Lehmann et al. "Time-dependent framework for energy and charge currents in nanoscale systems." In: *Chem. Phys.* 514 (2018), p. 176. ISSN: 0301-0104. DOI: https://doi.org/10.1016/j.chemphys.2018.01.011.

[114] Johannes Liebl et al. "The thermoelectric generator from BMW is making use of waste heat." In: *MTZ worldwide* 70.4 (Apr. 1, 2009), pp. 4–11. ISSN: 2192-9114. DOI: 10.1007/BF03226939.

[115] Jong Soo Lim, Rosa López, and David Sánchez. "Dynamic thermoelectric and heat transport in mesoscopic capacitors." In: *Phys. Rev. B* 88 (20 Nov. 2013), 201304(R). DOI: 10.1103/PhysRevB.88.201304.

[116] Wei Liu et al. "Elastic Transient Energy Transport and Energy Balance in a Single-Level Quantum Dot System." In: *Jpn. J. Appl. Phys.* 51 (Aug. 2012), p. 094303. DOI: 10.1143/jjap.51.094303.

[117] C Lozej and T. Rejec. "Time-dependent thermoelectric transport in nanosystems: Reflectionless Luttinger field approach." In: *Phys. Rev. B* 98 (7 Aug. 2018), p. 075427. DOI: 10.1103/PhysRevB.98.075427.

[118] María Florencia Ludovico et al. "Adiabatic response and quantum thermoelectrics for ac-driven quantum systems." In: *Physical Review B* 93.7 (Feb. 18, 2016), p. 075136. DOI: 10.1103/PhysRevB.93.075136.

[119] María Florencia Ludovico et al. "Dynamical energy transfer in ac-driven quantum systems." In: *Physical Review B* 89.16 (Apr. 21, 2014), p. 161306. ISSN: 1098-0121, 1550-235X. DOI: 10.1103/PhysRevB.89.161306.

[120] María Florencia Ludovico et al. "Periodic Energy Transport and Entropy Production in Quantum Electronics." In: *Entropy* 18.11 (Nov. 2016), p. 419. DOI: 10.3390/e18110419.

[121] María Florencia Ludovico et al. "Dynamics of energy transport and entropy production in ac-driven quantum electron systems." In: *Phys. Rev. B* 94 (3 July 2016), p. 035436. DOI: 10.1103/PhysRevB.94.035436.

[122] J. M. Luttinger. "The Effect of a Magnetic Field on Electrons in a Periodic Potential." In: *Phys. Rev.* 84 (4 Nov. 1951), p. 814. DOI: 10.1103/PhysRev.84.814.

[123] Zhong-Shui Ma and Lothar Schülke. "ac thermoelectric response in the nanostructure and corresponding nonlinear kinetic coefficients." In: *Phys. Rev. B* 59 (20 May 1999), pp. 13209–13220. DOI: 10.1103/PhysRevB.59.13209.

[124] G. D. Mahan and M. Bartkowiak. "Wiedemann–Franz law at boundaries." In: *Applied Physics Letters* 74.7 (Feb. 1999). Publisher: American Institute of Physics, pp. 953–954. ISSN: 0003-6951. DOI: 10.1063/1.123420.

[125] Sreenath K. Manikandan, Étienne Jussiau, and Andrew N. Jordan. "Autonomous quantum absorption refrigerators." In: *Phys. Rev. B* 102 (23 Dec. 2020), p. 235427. DOI: 10.1103/PhysRevB.102.235427.

[126] Richard M. Martin. *Electronic Structure: Basic Theory and Practical Methods*. Cambridge University Press, 2004. DOI: 10.1017/CBO9780511805769.

[127] W. N. Mathews. "Energy Density and Current in Quantum Theory." In: *American Journal of Physics* 42.3 (1974), pp. 214–219. DOI: 10.1119/1.1987650.

[128] R. David Mayrhofer et al. "Stochastic thermodynamic cycles of a mesoscopic thermoelectric engine." In: *Phys. Rev. B* 103 (7 Feb. 2021), p. 075404. DOI: 10.1103/PhysRevB.103.075404.

[129] Fabienne Michelini and Katawoura Beltako. "Asymmetry induces long-lasting energy current transients inside molecular loop circuits." In: *Phys. Rev. B* 100 (2 July 2019), p. 024308. DOI: 10.1103/PhysRevB.100.024308.

[130] Kristof Moors et al. "Magnetotransport signatures of three-dimensional topological insulator nanostructures." In: *Physical Review B* 97.24 (June 29, 2018). Publisher: American Physical Society, p. 245429. DOI: 10.1103/PhysRevB.97.245429.

[131] Christophe Mora and Karyn Le Hur. "Universal resistances of the quantum resistance–capacitance circuit." In: *Nature Physics* 6.9 (Sept. 2010), pp. 697–701. ISSN: 1745-2481. DOI: 10.1038/nphys1690.

[132] M. Moskalets and M. Büttiker. "Dissipation and noise in adiabatic quantum pumps." In: *Phys. Rev. B* 66 (3 July 2002), p. 035306. DOI: 10.1103/PhysRevB.66.035306.

[133] M. Moskalets and M. Büttiker. "Floquet scattering theory of quantum pumps." In: *Physical Review B* 66.20 (Nov. 26, 2002). Publisher: American Physical Society, p. 205320. DOI: 10.1103/PhysRevB.66.205320.

[134] Michael Moskalets. "Floquet Scattering Matrix Theory of Heat Fluctuations in Dynamical Quantum Conductors." In: *Phys. Rev. Lett.* 112 (20 May 2014), p. 206801. DOI: 10.1103/PhysRevLett.112.206801.

[135] Michael V. Moskalets. *Scattering Matrix Approach To Non-stationary Quantum Transport*. World Scientific, Sept. 16, 2011. 297 pp. ISBN: 978-1-908977-65-6.

[136] Fumiya Nagasawa et al. "Gate-controlled anisotropy in Aharonov-Casher spin interference: Signatures of Dresselhaus spin-orbit inversion and spin phases." In: *Physical Review B* 98.24 (Dec. 4, 2018). Publisher: American Physical Society, p. 245301. DOI: 10.1103/PhysRevB.98.245301.

[137] Natthapon Nakpathomkun, H. Q. Xu, and Heiner Linke. "Thermoelectric efficiency at maximum power in low-dimensional systems." In: *Physical Review B* 82.23 (Dec. 15, 2010). Publisher: American Physical Society, p. 235428. DOI: 10.1103/PhysRevB.82.235428.

[138] Frederik Nathan and Mark S. Rudner. "Universal Lindblad equation for open quantum systems." In: *Phys. Rev. B* 102 (11 Sept. 2020), p. 115109. DOI: 10.1103/PhysRevB.102.115109.

[139] Yuli V. Nazarov. *Quantum Transport: Introduction to Nanoscience*. 1st edition. Cambridge, UK ; New York: Cambridge University Press, May 1, 2009. 590 pp. ISBN: 978-0-521-83246-5.

[140] Bas Nijholt et al. *Adaptive: parallel active learning of mathematical functions*. 2019. DOI: 10.5281/zenodo.1182437.

[141] Wolfgang Nolting. *Theoretical Physics 2: Analytical Mechanics*. 2016. ISBN: 978-3-319-40128-7. DOI: 10.1007/978-3-319-40129-4.

[142] Maicol A. Ochoa, Anton Bruch, and Abraham Nitzan. "Energy distribution and local fluctuations in strongly coupled open quantum systems: The extended resonant level model." In: *Phys. Rev. B* 94 (3 July 2016), p. 035420. DOI: 10.1103/PhysRevB.94.035420.

[143] Annabelle Oz, Oded Hod, and Abraham Nitzan. "Numerical Approach to Nonequilibrium Quantum Thermodynamics: Nonperturbative Treatment of the Driven Resonant Level Model Based on the Driven Liouville von-Neumann Formalism." In: *Journal of Chemical Theory and Computation* 16.2 (Feb. 11, 2020). Publisher: American Chemical Society, pp. 1232–1248. ISSN: 1549-9618. DOI: 10.1021/acs.jctc.9b00999.

[144] Michał Papaj and Liang Fu. "Magnus Hall Effect." In: *Physical Review Letters* 123.21 (Nov. 22, 2019). Publisher: American Physical Society, p. 216802. DOI: 10.1103/PhysRevLett.123.216802.

[145] Yanzhong Pei et al. "Low effective mass leading to high thermoelectric performance." In: *Energy & Environmental Science* 5.7 (June 20, 2012). Publisher: The Royal Society of Chemistry, pp. 7963–7969. ISSN: 1754-5706. DOI: 10.1039/C2EE21536E.

[146] Jukka P. Pekola. "Towards quantum thermodynamics in electronic circuits." In: *Nat. Phys.* 11 (2015), p. 118.

[147] Jukka P. Pekola, Francesco Giazotto, and Olli-Pentti Saira. "Radio-Frequency Single-Electron Refrigerator." In: *Phys. Rev. Lett.* 98 (3 Jan. 2007), p. 037201. doi: 10.1103/PhysRevLett.98.037201.

[148] JL Pichard and RS Whitney. "Mesoscopic thermoelectric phenomena/Phénomènes thermoélectriques mésoscopiques." In: *Comptes Rendus Physique* 17 (2016), pp. 1039–1046. url: https://www.sciencedirect.com/journal/comptes-rendus-physique/vol/17/issue/10.

[149] G. Platero and R. Aguado. "Photon-assisted transport in semiconductor nanostructures." In: *Physics Reports* 395.1 (2004), pp. 1–157. issn: 0370-1573. doi: https://doi.org/10.1016/j.physrep.2004.01.004.

[150] G. Platero and R. Aguado. "Photon-assisted transport in semiconductor nanostructures." In: *Physics Reports* 395.1 (2004), pp. 1–157. issn: 0370-1573. doi: https://doi.org/10.1016/j.physrep.2004.01.004.

[151] Matthias A. Popp, André Erpenbeck, and Heiko B. Weber. "Thermoelectricity of near-resonant tunnel junctions and their relation to Carnot efficiency." In: *Scientific Reports* 11 (2020), p. 2031. doi: 10.1038/s41598-021-81466-3.

[152] J. R. Prance et al. "Electronic Refrigeration of a Two-Dimensional Electron Gas." In: *Phys. Rev. Lett.* 102 (14 Apr. 2009), p. 146602. doi: 10.1103/PhysRevLett.102.146602.

[153] Karel Proesmans, Bart Cleuren, and Christian Van den Broeck. "Linear stochastic thermodynamics for periodically driven systems." In: *Journal of Statistical Mechanics: Theory and Experiment* 2016.2 (Feb. 2016), p. 023202. issn: 1742-5468. doi: 10.1088/1742-5468/2016/02/023202.

[154] Hechen Ren et al. "Topological superconductivity in a phase-controlled Josephson junction." In: *Nature* 569.7754 (May 2019), pp. 93–98. issn: 1476-4687. doi: 10.1038/s41586-019-1148-9.

[155] Miguel Rey et al. "Nonadiabatic electron heat pump." In: *Phys. Rev. B* 76 (8 Aug. 2007), p. 085337. doi: 10.1103/PhysRevB.76.085337.

[156] Yair Rezek and Ronnie Kosloff. "Irreversible performance of a quantum harmonic heat engine." In: *New Journal of Physics* 8.5 (2006), p. 83.

[157] Federico D. Ribetto, Raúl A. Bustos-Marún, and Hernán L. Calvo. "Role of coherence in quantum-dot-based nanomachines within the Coulomb blockade regime." In: *Physical Review B* 103.15 (Apr. 30, 2021). Publisher: American Physical Society, p. 155435. doi: 10.1103/PhysRevB.103.155435.

[158] Michael Ridley, Angus MacKinnon, and Lev Kantorovich. "Current through a multilead nanojunction in response to an arbitrary time-dependent bias." In: *Phys. Rev. B* 91 (12 Mar. 2015), p. 125433. doi: 10.1103/PhysRevB.91.125433.

[159] Laura Rincón-García et al. "Thermopower measurements in molecular junctions." In: *Chem. Soc. Rev.* 45 (15 2016), p. 4285. doi: 10.1039/C6CS00141F.

[160] Robert A. Robinson et al. "Large violation of the Wiedemann–Franz law in Heusler, ferromagnetic, weyl semimetal Co2MnAl." en. In: *Journal of Physics D: Applied Physics* (2021). issn: 0022-3727. doi: 10.1088/1361-6463/ac1cb6.

[161] Ankit Rohatgi. *Webplotdigitizer: Version 4.5*. 2021. url: https://automeris.io/WebPlotDigit

[162] É Roldán et al. "Universal features in the energetics of symmetry breaking." In: *Nature Physics* 10.6 (2014), pp. 457–461.

[163] Javier I. Romero et al. "Nonlinear charge and energy dynamics of an adiabatically driven interacting quantum dot." In: *Phys. Rev. B* 95 (23 June 2017), p. 235117. DOI: 10.1103/PhysRevB.95.235117.

[164] Benoît Rossignol, Thomas Kloss, and Xavier Waintal. "Role of Quasiparticles in an Electric Circuit with Josephson Junctions." In: *Phys. Rev. Lett.* 122 (20 May 2019), p. 207702. DOI: 10.1103/PhysRevLett.122.207702.

[165] Dmitry A. Ryndyk. *Theory of Quantum Transport at Nanoscale*. Springer, Cham, 2016. ISBN: 978-3-319-24086-2. DOI: 10.1007/978-3-319-24088-6.

[166] Peter Salamon et al. "Principles of control thermodynamics." In: *Energy* 26.3 (2001), pp. 307–319.

[167] Cristián G. Sánchez et al. "Molecular conduction: Do time-dependent simulations tell you more than the Landauer approach?" In: *The Journal of Chemical Physics* 124.21 (June 7, 2006), p. 214708. ISSN: 0021-9606. DOI: 10.1063/1.2202329.

[168] Tatiane P. Santos, Leandro R. F. Lima, and Caio H. Lewenkopf. "An order N numerical method to efficiently calculate the transport properties of large systems: An algorithm optimized for sparse linear solvers." In: *Journal of Computational Physics* 394 (Oct. 1, 2019), pp. 440–455. ISSN: 0021-9991. DOI: 10.1016/j.jcp.2019.05.034.

[169] Björn Sbierski et al. "Criticality of Two-Dimensional Disordered Dirac Fermions in the Unitary Class and Universality of the Integer Quantum Hall Transition." In: *Physical Review Letters* 126.7 (Feb. 18, 2021). Publisher: American Physical Society, p. 076801. DOI: 10.1103/PhysRevLett.126.076801.

[170] R. Schmidt et al. "Work and heat for two-level systems in dissipative environments: Strong driving and non-Markovian dynamics." In: *Phys. Rev. B* 91 (22 June 2015), p. 224303. DOI: 10.1103/PhysRevB.91.224303.

[171] Franz Schwabl. *Advanced Quantum Mechanics*. Springer-Verlag Berlin Heidelberg, 2008. ISBN: 978-3-540-85062-5. DOI: 10.1007/978-3-540-85062-5.

[172] Franz Schwabl. *Quantum Mechanics*. Springer-Verlag Berlin Heidelberg, 2007. ISBN: 978-3-540-71933-5. DOI: 10.1007/978-3-540-71933-5.

[173] Stefano Scopa et al. "Exact solution of time-dependent Lindblad equations with closed algebras." In: *Phys. Rev. A* 99 (2 Feb. 2019), p. 022105. DOI: 10.1103/PhysRevA.99.022105.

[174] Henry ED Scovil and Erich O Schulz-DuBois. "Three-level masers as heat engines." In: *Physical Review Letters* 2.6 (1959), p. 262.

[175] Alexander Semenov and Abraham Nitzan. "Transport and thermodynamics in quantum junctions: A scattering approach." In: *J. Chem. Phys.* 152 (2020), p. 244126. DOI: 10.1063/5.0010127.

[176] Xiao-Lei Shi, Jin Zou, and Zhi-Gang Chen. "Advanced Thermoelectric Design: From Materials and Structures to Devices." In: *Chemical Reviews* 120.15 (Aug. 12, 2020). Publisher: American Chemical Society, pp. 7399–7515. ISSN: 0009-2665. DOI: 10.1021/acs.chemrev.0c00026.

[177] G. Jeffrey Snyder and Eric S. Toberer. "Complex thermoelectric materials." In: *Nature Materials* 7.2 (Feb. 2008), pp. 105–114. ISSN: 1476-4660. DOI: 10.1038/nmat2090.

[178] G. Jeffrey Snyder et al. "Supercooling of Peltier cooler using a current pulse." In: *Journal of Applied Physics* 92.3 (July 18, 2002). Publisher: American Institute of Physics, pp. 1564–1569. ISSN: 0021-8979. DOI: 10.1063/1.1489713.

[179] Paolo Solinas, Dmitri V Averin, and Jukka P Pekola. "Work and its fluctuations in a driven quantum system." In: *Physical Review B* 87.6 (2013), p. 060508.

[180] Paolo Solinas, Riccardo Bosisio, and Francesco Giazotto. "Microwave quantum refrigeration based on the Josephson effect." In: *Phys. Rev. B* 93 (22 June 2016), p. 224521. DOI: 10.1103/PhysRevB.93.224521.

[181] AAM Staring et al. "Coulomb-blockade oscillations in the thermopower of a quantum dot." In: *EPL (Europhysics Letters)* 22.1 (1993), p. 57.

[182] G. Stefanucci et al. "Time-dependent approach to electron pumping in open quantum systems." In: *Physical Review B* 77.7 (Feb. 29, 2008). Publisher: American Physical Society, p. 075339. DOI: 10.1103/PhysRevB.77.075339.

[183] Gianluca Stefanucci and Robert van Leeuwen. *Nonequilibrium Many-Body Theory of Quantum Systems: A Modern Introduction*. Cambridge University Press, Mar. 7, 2013. 620 pp. ISBN: 978-0-521-76617-3.

[184] Mallat Stephane. *A wavelet tour of signal processing*. Elsevier, 1999.

[185] A M Stewart. "Why semiclassical electrodynamics is not gauge invariant." en. In: *Journal of Physics A: Mathematical and General* 33.50 (Dec. 2000), pp. 9165–9176. ISSN: 0305-4470, 1361-6447. DOI: 10.1088/0305-4470/33/50/303.

[186] Philipp Strasberg et al. "Quantum and Information Thermodynamics: A Unifying Framework Based on Repeated Interactions." In: *Phys. Rev. X* 7 (2 Apr. 2017), p. 021003. DOI: 10.1103/PhysRevX.7.021003.

[187] Y. Suba ş ı et al. "Equilibrium states of open quantum systems in the strong coupling regime." In: *Phys. Rev. E* 86 (6 Dec. 2012), p. 061132. DOI: 10.1103/PhysRevE.86.061132.

[188] Artis Svilans, Martin Leijnse, and Heiner Linke. "Experiments on the thermoelectric properties of quantum dots." In: *Comptes Rendus Physique*. Mesoscopic thermoelectric phenomena / Phénomènes thermoélectriques mésoscopiques 17.10 (Dec. 1, 2016), pp. 1096–1108. ISSN: 1631-0705. DOI: 10.1016/j.crhy.2016.08.002.

[189] Makariy A. Tanatar et al. "Anisotropic Violation of the Wiedemann-Franz Law at a Quantum Critical Point." In: *Science* 316.5829 (June 1, 2007), pp. 1320–1322. ISSN: 0036-8075, 1095-9203. DOI: 10.1126/science.1140762.

[190] Kristinn Torfason et al. "Thermoelectric current and Coulomb-blockade plateaus in a quantum dot." In: *Physica E: Low-dimensional Systems and Nanostructures* 53 (2013), p. 178. ISSN: 1386-9477. DOI: 10.1016/j.physe.2013.05.005.

[191] Terry M. Tritt, Harald Böttner, and Lidong Chen. "Thermoelectrics: Direct Solar Thermal Energy Conversion." In: *MRS Bulletin* 33.4 (Apr. 2008). Publisher: Cambridge University Press, pp. 366–368. ISSN: 1938-1425, 0883-7694. DOI: 10.1557/mrs2008.73.

[192] Piotr Trocha and Józef Barna ś. "Large enhancement of thermoelectric effects in a double quantum dot system due to interference and Coulomb correlation phenomena." In: *Phys. Rev. B* 85 (8 Feb. 2012), p. 085408. DOI: 10.1103/PhysRevB.85.085408.

[193] S. Vaitiekėnas et al. "Flux-induced topological superconductivity in full-shell nanowires." In: *Science* 367.6485 (Mar. 27, 2020). Publisher: American Association for the Advancement of Science Section: Research Article. ISSN: 0036-8075, 1095-9203. DOI: 10.1126/science.aav3392.

[194] M.V. Vedernikov and E.K. Iordanishvili. "A.F. Ioffe and origin of modern semiconductor thermoelectric energy conversion." In: *Seventeenth International Conference on Thermoelectrics. Proceedings ICT98 (Cat. No.98TH8365)*. Seventeenth International Conference on Thermoelectrics. Proceedings ICT98 (Cat. No.98TH8365). ISSN: 1094-2734. May 1998, pp. 37–42. DOI: 10.1109/ICT.1998.740313.

[195] C. Vega et al. "Heat capacity of water: A signature of nuclear quantum effects." In: *The Journal of Chemical Physics* 132.4 (Jan. 28, 2010), p. 046101. ISSN: 0021-9606. DOI: 10.1063/1.3298879.

[196] Mihai D Vidrighin et al. "Photonic Maxwell's demon." In: *Physical review letters* 116.5 (2016), p. 050401.

[197] Cronin B. Vining. "An inconvenient truth about thermoelectrics." In: *Nature Materials* 8.2 (Feb. 2009), pp. 83–85. ISSN: 1476-4660. DOI: 10.1038/nmat2361.

[198] Sai Vinjanampathy and Janet Anders. "Quantum thermodynamics." In: *Contemporary Physics* 57.4 (Oct. 1, 2016), pp. 545–579. ISSN: 0010-7514. DOI: 10.1080/00107514.2016.1201896.

[199] P. Virtanen, P. Solinas, and F. Giazotto. "Spectral representation of the heat current in a driven Josephson junction." In: *Phys. Rev. B* 95 (14 Apr. 2017), p. 144512. DOI: 10.1103/PhysRevB.95.144512.

[200] Nicholas Wakeham et al. "Gross violation of the Wiedemann–Franz law in a quasi-one-dimensional conductor." In: *Nature Communications* 2.1 (July 19, 2011), p. 396. ISSN: 2041-1723. DOI: 10.1038/ncomms1406.

[201] L. B. Wang, O.-P. Saira, and J. P. Pekola. "Fast thermometry with a proximity Josephson junction." In: *Applied Physics Letters* 112.1 (Jan. 1, 2018). Publisher: American Institute of Physics, p. 013105. ISSN: 0003-6951. DOI: 10.1063/1.5010236.

[202] Joseph Weston, Benoit Gaury, and Xavier Waintal. "Manipulating Andreev and Majorana bound states with microwaves." In: *Physical Review B* 92.2 (July 28, 2015). Publisher: American Physical Society, p. 020513. DOI: 10.1103/PhysRevB.92.020513.

[203] Joseph Weston and Xavier Waintal. "Linear-scaling source-sink algorithm for simulating time-resolved quantum transport and superconductivity." In: *Phys. Rev. B* 93 (13 Apr. 2016), p. 134506. DOI: 10.1103/PhysRevB.93.134506.

[204] Joseph Weston and Xavier Waintal. "Towards realistic time-resolved simulations of quantum devices." In: *Journal of Computational Electronics* 15.4 (Dec. 2016), pp. 1148–1157. ISSN: 1572-8137. DOI: 10.1007/s10825-016-0855-9.

[205] Robert S. Whitney. "Non-Markovian quantum thermodynamics: Laws and fluctuation theorems." In: *Phys. Rev. B* 98 (8 Aug. 2018), p. 085415. DOI: 10.1103/PhysRevB.98.085415.

[206] Michael Wimmer. "Quantum transport in nanostructures: From computational concepts to spintronics in graphene and magnetic tunnel junctions." PhD thesis. Regensburg University, 2009.

[207] Michael Wimmer. "Quantum transport in nanostructures: from computational concepts to spintronics in graphene and magnetic tunnel junctions." OCLC: 551979435. PhD thesis. Regensburg, 2009. 250 pp. ISBN: 978-3-86845-025-5.

[208] Alexandra Witze. "Nuclear power: Desperately seeking plutonium." In: *Nature* 515.7528 (Nov. 1, 2014), pp. 484–486. ISSN: 1476-4687. DOI: 10.1038/515484a.

[209] *World Energy Consumption Statistics | Enerdata.* URL: https://yearbook.enerdata.net/total-energy/world-consumption-statistics.html (visited on 09/06/2021).

[210] Lian-Ao Wu and Dvira Segal. "Energy flux operator, current conservation and the formal Fourier law." en. In: *J. Phys. A: Math. Theor.* 42.2 (Nov. 2008). Publisher: IOP Publishing, p. 025302. ISSN: 1751-8121. DOI: 10.1088/1751-8113/42/2/025302.

[211] Shiyun Xiong and Sebastian Volz. "Nanostructuration for thermoelectricity: The path to an unlimited reduction of phonon transport." In: *Comptes Rendus Physique.* Mesoscopic thermoelectric phenomena / Phénomènes thermoélectriques mésoscopiques 17.10 (Dec. 1, 2016), pp. 1146–1153. ISSN: 1631-0705. DOI: 10.1016/j.crhy.2016.08.009.

[212] Yangyang Xu, Veerabhadran Ramanathan, and David G. Victor. "Global warming will happen faster than we think." In: *Nature* 564.7734 (Dec. 2018), pp. 30–32. DOI: 10.1038/d41586-018-07586-5.

[213] Kuo-Ho Yang. "Gauge transformations and quantum mechanics I. Gauge invariant interpretation of quantum mechanics." In: *Annals of Physics* 101.1 (Sept. 1976), pp. 62–96. ISSN: 0003-4916. DOI: 10.1016/0003-4916(76)90275-X.

[214] Lei Yang et al. "High Performance Thermoelectric Materials: Progress and Their Applications." In: *Advanced Energy Materials* 8.6 (2018), p. 1701797. ISSN: 1614-6840. DOI: 10.1002/aenm.201701797.

[215] Zhizhou Yu, Gao-Min Tang, and Jian Wang. "Full-counting statistics of transient energy current in mesoscopic systems." In: *Phys. Rev. B* 93 (19 May 2016), p. 195419. DOI: 10.1103/PhysRevB.93.195419.

[216] Tamar Zelovich, Leeor Kronik, and Oded Hod. "Driven Liouville von Neumann approach for time-dependent electronic transport calculations in a nonorthogonal basis-set representation." In: *The Journal of Physical Chemistry C* 120.28 (2016), pp. 15052–15062. DOI: 10.1021/acs.jpcc.6b03838.

[217] Tamar Zelovich, Leeor Kronik, and Oded Hod. "Molecule–Lead Coupling at Molecular Junctions: Relation between the Real-and State-Space Perspectives." In: *Journal of chemical theory and computation* 11.10 (2015), pp. 4861–4869.

[218] Tamar Zelovich, Leeor Kronik, and Oded Hod. "State representation approach for atomistic time-dependent transport calculations in molecular junctions." In: *Journal of chemical theory and computation* 10.8 (2014), pp. 2927–2941.

[219] Hangbo Zhou et al. "Boosting thermoelectric efficiency using time-dependent control." In: *Scientific Reports* 5 (2015), p. 14870. DOI: 10.1038/srep14870.

[220] Natalya A Zimbovskaya. "Thermoelectric properties of a double-dot system in serial configuration within the Coulomb blockade regime." In: *The Journal of Chemical Physics* 153.12 (2020), p. 124712.

université PARIS-SACLAY

ÉCOLE DOCTORALE
Physique en Île-de-France (PIF)

Titre: Transport thermoélectrique dépendant du temps dans des systèmes quantiques

Mots-clés: contrôle temporel, transport quantique, thermoélectricité, simulation quantique, théorie de la diffusion

Résumé: Ce dernier siècle est marqué par l'évolution alarmante du phénomène de réchauffement climatique. À son cœur repose la continuelle augmentation des besoins en énergie « utile » pour nos activités. Ainsi, une grande pression repose sur la recherche pour réaliser des usines de production électriques plus efficaces et plus respectueuses de l'environnement. Dans ce contexte, la thermoélectricité offre une façon différente et prometteuse de réaliser des machines thermiques et réfrigérateurs. Les dispositifs se basant sur cet effet sont cependant peu démocratisés car ils souffrent d'un rendement relativement bas par rapport aux machines traditionnelles. Durant ces dernières années, de nouvelles pistes prometteuses ont été explorées pour améliorer la performance des dispositifs thermoélectriques, en s'appuyant notamment sur une meilleure compréhension du comportement quantique de la matière et sur les progrès technologiques en miniaturisation. Une de ces pistes propose de s'intéresser aux (nano)dispositifs mis hors-équilibre, en particulier dans un régime dépendant du temps. Bien que la grande majorité des études en thermoélectricité ont été motivées par des arguments uniquement valides dans le régime stationnaire proche de l'équilibre, des développements théoriques récents prédisent une forte amélioration du rendement dans le régime quantique dépendant du temps, loin de l'équilibre. D'autre part, les progrès en nanoélectronique haute fréquence permettent aujourd'hui de mesurer le transport quantique à de courtes échelles temporelles et spatiales, remettant en question les lois classiques de la thermodynamique.

L'objectif de cette thèse est d'explorer les opportunités offertes par le transport thermoélectrique dynamique à l'échelle mésoscopique. Pour ce faire, nous construisons dans un premier temps une approche invariante de jauge décrivant (outre le transport de charge déjà traité dans la littérature) le transport d'énergie dépendant du temps dans un système quantique ouvert sous l'influence d'un champ électromagnétique dynamique. Cette approche est basée sur une description semi-classique où le champ électromagnétique est décrit par les équations (classiques) de Maxwell, tandis que les électrons sont décrits par l'équation (quantique) de Schrödinger. Puis, nous utilisons ce formalisme pour étendre tkwant, une bibliothèque de simulation quantique de systèmes modélisés en liaisons-fortes, au transport énergétique : cette bibliothèque étendue permet alors de simuler la thermoélectricité, avec dépendance temporelle, dans de larges systèmes mésoscopiques, au-delà des modèles jouets. On illustre ensuite la puissance de cette bibliothèque en investiguant l'effet Peltier dynamique dans un « Contact Ponctuel Quantique » bidimensionnel. Enfin, nous nous intéressons au très étudié modèle jouet du niveau résonnant pour avoir une meilleure compréhension fondamentale des phénomènes en jeux : une étude numérique et semi-analytique nous permet d'apporter un nouvel éclairage sur le potentiel de la thermoélectricité dépendante du temps dans les points quantiques.

Université Paris-Saclay
Espace Technologique / Immeuble Discovery
Route de l'Orme aux Merisiers RD 128 / 91190 Saint-Aubin, France

université PARIS-SACLAY

ÉCOLE DOCTORALE
Physique en Île-de-France (PIF)

Title: Time-dependent thermoelectric transport in quantum systems

Keywords: time-dependent, quantum transport, thermoelectricity, quantum simulation, scattering theory

Abstract: This past century has seen a very quick rise to the prominent issue of global warming. At its root is the ever growing need for "work" energy in our activities, this pressures research into making energy production facilities more efficient and more environmentally friendly. Thermoelectricity in this context offers a different and promising way to make or complement traditional heat engines and coolers. Devices leveraging this effect are however still not broadly used as they suffer from a relatively low efficiency when compared to traditional coolers and heat engines. In the recent years, new waves of ideas came from technological progress in miniaturization from the semi-conductor industry and further understanding of the quantum behavior of matter. A new research avenue in thermoelectricity suggests investigating (nano)devices far from equilibrium, in particular in the time-dependent regime. While the vast majority of studies in thermoelectrics have been motivated by arguments valid in the stationary, near equilibrium regime, recent theoretical literature predicts a boost of thermoelectric efficiency in the far from equilibrium, dynamical quantum regime. On the other hand, progress in experimentation at mesoscopic scales with high frequency control enables probing quantum transport at short length and time scales and bring into question the (classical) laws of thermodymanics.

Research is ongoing in building a consistent theory of quantum thermodynamics in all regimes and this thesis intervenes in this context: we build a gauge-invariant framework for describing energy transport, on top of the currently published research on time-dependent charge transport, in an open electronic quantum system under the influence of a time-dependent electromagnetic field. This framework is based on the semi-classical approach where light is described by the (classical) Maxwell equations and electrons are non-interacting and described by the (quantum) Schrödinger equation. We then use this framework to extend tkwant, a tight-binding time-resolved quantum simulation library, to energy transport: this extended package makes possible the simulation of time-dependent thermoelectric transport in large scale systems that can model a broad class of mesoscopic devices beyond toy models. We illustrate our numerical approach by investigating briefly the dynamical Peltier effect in a two-dimensional Quantum Point Contact then go back to the extensively studied Resonant Level (toy) Model to be able to grasp a more fundamental understanding of the effects at play : we use our approach, in both its numerical and analytical adaptations, and obtain new insights on the potential of time-dependent thermoelectricity in quantum dots.

Université Paris-Saclay
Espace Technologique / Immeuble Discovery
Route de l'Orme aux Merisiers RD 128 / 91190 Saint-Aubin, France